



EVERGLADES COALITION

May 2, 2023

Brooke P. Clark
Secretary, U.S. Nuclear Regulatory Commission
Washington, D.C. 20555-001

ATTN: Rulemaking and Adjudications Staff

Sent Via Email: Rulemaking.Comments@nrc.gov

RE: Proposed Rule Amending Environmental Protection Regulations Pursuant to Revision 2 to NUREG-1437 “Generic Environmental Impact Statement for License Renewal of Nuclear Plants” (LR GEIS)

Dear Secretary Clark,

On behalf of nearly 60 state, local and national organizations which make up the Everglades Coalition and its many individual members and supporters, we thank you for the opportunity to provide the following comments. Please include this letter as part of the responsive comments to the Federal Register notice issued March 10, 2023, at 88 FR 14958 regarding the agency’s revision of its Generic Environmental Impact Statement for License Renewal of Nuclear Plants rule (LR GEIS). In the interest of protecting the health and integrity of the greater Everglades ecosystem, Florida’s valuable natural resources, fresh-water supplies, and national parks, we strongly urge you to revise the LR GEIS in a way that incorporates the need for site-specific evaluations of unique and significant environmental impacts related to the Cooling Canal System (CCS) at the Turkey Point plant.

The CCS poses unique and significant geologic, hydrological, water, and aquatic issues that should require site-specific environmental assessments at the Turkey Point plant. We trust the following information will inform the revision of your rule.

Geologic Environment; Geology and soils: This is a unique and site-specific environmental consideration at the Turkey Point plant. For example, the CCS is carved into oolitic limestone and the porous nature of the limestone allows water to move freely in all directions. Research and understanding of the interaction of the CCS water budget and connectivity with the model lands region, L-31 E, and surrounding Biscayne National Park should be considered an important site-specific review.

Surface Water Resources: This is a unique, significant, and site-specific consideration. The plant and CCS are vulnerable to sea level rise and storm surge and discharge of biocides, sanitary wastes, and various chemicals. Turkey Point sits inside the boundaries of Biscayne National Park and is surrounded by wetlands earmarked for Everglades restoration activities, any discharges will have significant adverse

The Everglades Coalition is a 501(c)3 alliance of local, state, and national conservation organizations dedicated to the full protection and restoration of America's Everglades.

evergladescoalition.org

impacts on the environment, as well as any usage of surrounding surface waters. Surface to surface water interactions happen regularly, especially during King Tides, storm events, heavy rains; there is an overflow of the CCS on a regular basis and this interacts with the surrounding resources. Biscayne Bay is a designated Outstanding Florida Water Body, National Park and Aquatic Preserve and therefore deserves a site specific level of review. In addition to contamination, the CCS evaporates away 40 MGD and regularly uses between 3-5 MGD of freshwater otherwise earmarked for restoration and drinking water. The use of surface waters from the model lands region have been recorded by Miami Dade County DERM up to 90 MGD. The current operations are exacerbating saltwater intrusion to the west, while restoration efforts from Biscayne Bay Southeastern Everglades Restoration (BBSEER) are working to slow this process and restore coastal wetlands.

Groundwater Resources: Groundwater contamination and use (non-cooling system impacts) are unique, significant site-specific considerations. Is site-specific because Turkey Point is adjacent to the boundary of Biscayne National Park, local geology allows rapid lateral drift of groundwater in all directions, and discharges have significant adverse effects on the adjacent environment, including but not limited to the degradation of nearshore seagrass meadows. Groundwater quality degradation resulting from the concentration of salt and other contaminants in a plume that is about 10 miles wide which is under 1 mile of the Newton wellfield to the west, and is under Biscayne National Park. Additionally, it is site-specific because water withdrawals at Turkey Point alter freshwater flows into the Southeast Coastal Everglades and interfere with some of the goals and objectives of Everglades restoration (BBSEER). Specifically, by blocking all freshwater groundwater and surface water that would otherwise be reaching the nearshore of Biscayne National Park. One of the primary goals in this area is to reestablish mesohaline conditions in the nearshore. This will be nearly impossible to achieve along this section of coastline as long as the CCS is in operation.

Terrestrial Resources: Exposure of terrestrial organisms to radionuclides are unique, site-specific considerations. It is site-specific because Turkey Point lies between two national parks, Everglades National Park, and Biscayne National Park, both of which are home to numerous endangered and threatened organisms. We are especially concerned about these radionuclide effects on these organisms, many of which are terrestrial, because FPL does not measure radionuclide release during refueling of the reactors at Turkey Point and prevailing winds half the year push air from Turkey Point into Everglades National Park. This area is on the Atlantic Flyway and Bird collisions with plant structures and transmission lines is a site-specific issue, as well as impacts to bird food sources by degrading the ecosystem in the nearshore of Biscayne National Park. The Florida 3rd DCA, in ruling against FPL's request for transmission lines on the edge of the Everglades, made it clear that risk of bird collisions is site specific. The court's opinion specifically mentioned the risk of transmission lines to young Wood Storks. Since Turkey Point is unique in being adjacent to wading bird nesting areas, the assessments of risk have been legally determined to be site specific. See 3rd Florida DCA Miami-Dade County, et al., vs. In Re: Florida Power & Light Co., etc., et al., 2016.

Aquatic Resources: Effects of non-radiological contaminants on aquatic organisms are unique, site-specific considerations because the leaching of hypersaline, phosphorus, and nitrogen-laden water from the cooling canals at Turkey Point has damaged adjacent seagrass meadows in Biscayne National Park. This has occurred first by fertilization and then by replacement with more nutrient-loving species of

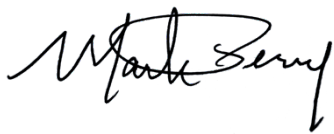
The Everglades Coalition is a 501(c)3 alliance of local, state, and national conservation organizations dedicated to the full protection and restoration of America's Everglades.

evergladescoalition.org

seagrasses and finally macroalgae. This in turn impacts fish and wildlife by degrading ecosystem function impacting community structure, abundance, and diversity of fish and their prey opportunity.

South Florida is a highly transmissive area due to its unique geology and Turkey Point has a CCS that, at the time of licensing, was an experimental design, it has never been replicated anywhere else in the world. It is not a closed-loop system as determined recently by the Department of Environmental Protection in its new operating license. This coalition's concern is that we protect the investments of Everglades Restoration activities by ensuring there are no conflicts with our restoration efforts. We ask that you not use a one size fits all generic EIS process for this unique area and circumstance, but instead consider the uniqueness of this area and ensure you are taking into account all of this site-specific information and data that has been collected by various agencies, nonprofits, and governments.

Sincerely,



Mark Perry
Co-Chair



Kelly Cox
Co-Chair

Appendix:

[Previous letter](#) submitted August 1, 2018 (also attached below)

https://www.evergladescoalition.org/_files/ugd/599879_bab58bb0e061457ab80131f688c2923f.pdf

CC:

- USACE April Patterson; April.N.Patterson@usace.army.mil
- USACE Brad Foster; Bradley.A.Foster@usace.army.mil
- SFWMD Executive Director, Drew Bartlett; DBartlett@sfwmd.gov
- BBSEER Project Manager Nicole Niemeyer; nniemeye@sfwmd.gov
- FDEP Secretary, Shawn Hamilton; shawn.hamilton@floridadep.gov
- Monroe County Mayor, Craig Cates; boccdis1@monroecounty-fl.gov
- Miami Dade County Mayor, Daniella Levine Cava; mayor@miamidade.gov
- DERM director, Lisa Spadafina; Lisa.Spadafina@miamidade.gov

The Everglades Coalition is a 501(c)3 alliance of local, state, and national conservation organizations dedicated to the full protection and restoration of America's Everglades.

evergladescoalition.org



Everglades Coalition

August 1, 2018

Eric R. Oesterle

Chief, License Renewal Project Branch

Office of Nuclear Reactor Regulation

U.S. Nuclear Regulatory Commission

Washington, DC 20555

RE: Docket ID NRC-2018-0101, Turkey Point Nuclear Plant, Units 3 & 4 – Subsequent License Renewal Application

Dear Mr. Oesterle,

On behalf of the 62 state, local and national organizations which make up the Everglades Coalition and the many individual members and supporters thereof, we thank you for the opportunity to provide comments. We hope you will consider and include the following letter as part of the National Environmental Policy Act (NEPA) scoping process and information gathering process for the Turkey Point Nuclear Plant Units 3 & 4 Subsequent License Renewal application, identified under Nuclear Regulatory Commission (NRC) Docket ID NRC-2018-0101.

In the interest of protecting the health and integrity of Florida's valuable natural resources, fresh-water supplies, and national parks, we strongly urge you to thoroughly analyze the environmental impacts from the Cooling Canal System at Turkey Point as part of the NEPA review process as further described herein.

Background

The Turkey Point Nuclear Generating Station's negative impact on the surrounding ecology and natural resources is largely a result of its unique and outdated Cooling Canal System (CCS). This unlined and open system interacts directly with the underlying groundwater including the federally protected G II aquifer to the west as well as the surface waters of the L-31 E canal and Biscayne National Park and National Marine Sanctuary to the east.

Committed to full protection and restoration of America's Everglades

1000 Friends of Florida
Arthur R. Marshall Foundation
Audubon Florida
Audubon of Southwest Florida
Audubon of the Western Everglades
Audubon Society of the Everglades
Backcountry Fly Fishers of Naples
Bullsugar Alliance
Calusa Waterkeeper
Center for Biological Diversity
Clean Water Action
Conservancy of Southwest Florida
Defenders of Wildlife
"Ding" Darling Wildlife Society
Earthjustice
Environment Florida
Everglades Foundation
Everglades Law Center
Everglades Trust
Florida Conservation Voters Education Fund
Florida Defenders of the Environment
Florida Keys Environmental Fund
Florida Native Plant Society
Florida Oceanographic Society
Friends of the Arthur R. Marshall
Loxahatchee National Wildlife Refuge
Friends of the Everglades
Hendry-Glades Audubon Society
International Dark-Sky Association,
FL Chapter
Izaak Walton League of America
Izaak Walton League Florida Division
Izaak Walton League Florida Keys Chapter
Izaak Walton League Mangrove Chapter
Lake Worth Waterkeeper
Last Stand
League of Women Voters of Florida
Martin County Conservation Alliance
Miami Pine Rocklands Coalition
Miami Waterkeeper
National Audubon Society
National Parks Conservation Association
National Wildlife Refuge Association
Natural Resources Defense Council
North Carolina Outward Bound School
Ocean Research & Conservation Association
Reef Relief
Sanibel-Captiva Conservation Foundation
Save It Now, Glades!
Sierra Club
Sierra Club Florida Chapter
Sierra Club Broward Group
Sierra Club Calusa Group
Sierra Club Central Florida Group
Sierra Club Loxahatchee Group
Sierra Club Miami Group
Snook and Gamefish Foundation
South Florida Audubon Society
Southern Alliance for Clean Energy
The Florida Wildlife Federation
The Institute for Regional Conservation
The National Wildlife Federation
The Urban Environment League of
Greater Miami
Theodore Roosevelt Conservation
Partnership
Tropical Audubon Society

Multiple agencies, including the National Park Service, the Miami Dade County Department of Environmental Resources Management,¹ and the Florida Department of Environmental Protection² have found that hyper-saline, nutrient enriched, and tritiated effluent from the CCS has seeped into the underlying protected Biscayne Aquifer, generating a pollution plume that is spreading west towards Miami Dade and Monroe County drinking water wellfields and the surface waters of the L-31 E canal and east under and into the surface waters of Biscayne National Park.³

The excess salt that has concentrated in the plume and the excessive water use nuclear power generation requires is in conflict with Everglades restoration efforts underway in adjacent wetlands called the ‘model lands basin’.⁴ The addition of excess nutrients into the nutrient-limited waters of Biscayne Bay and Biscayne National Park has the potential to foment the death of seagrass communities and encourage their displacement by fast growing noxious seaweed, as well as stimulate algal growth, which could lead to persistent algal blooms and wildlife impacts.⁵ Maintaining the health of South Florida’s waters is critical to ensuring the future of our communities, viable water supply, and the species that depend on these waters for critical habitat.

Before considering a new license for continued operations until 2053 this nuclear facility must come into compliance with all administrative orders and permits that govern this facility. The pollution that has been identified must be immediately corrected and a better operations procedure must be established and required as a condition to certification. Accordingly, we strongly urge you to include an in-depth analysis of the environmental impacts of the continued operation of Units 3 & 4 and the CCS in the NEPA review process.

Everglades Restoration

Units 3&4 as operated today are a major competitor for vital freshwater resources that could otherwise go towards Everglades Restoration projects and raising the freshwater head of coastal wetlands in the surrounding model lands basin to combat saltwater intrusion. There are several critical Everglades restoration projects which are influenced by the CCS, including the Biscayne Bay Coastal Wetlands project and the C-111 Spreader Canal Project which are currently in conflict ⁶ with the operations of the CCS. Conditions to certification should be considered to resolve these conflicts. For example, operational changes to the CCS should be considered that end the use of the interceptor ditch pumps and simultaneously raise stages of water in the model lands basin to meet the goals of the C-111 project and help provide water in the dry season to the Biscayne Bay Coastal Wetlands Project and C-111 spreader project. Ending the use of the failing Interceptor Ditch pumps will save the system on average 3 million

¹ Miami Dade County Department of Environmental Resources Management, Notice of Violation and Orders for Corrective Action dated October 2, 2015, attached hereto and incorporated herein.

² Director Frederick L. Aschauer, Jr. Florida Department of Environmental Protection, Warning Letter to Florida Power and Light Company, April 25, 2016, attached hereto and incorporated herein.

³ Biscayne National Park Correspondence with the U.S. Environmental Protection Agency, Florida Department of Environmental Protection, and Miami Dade County. May 13, 2016, attached hereto and incorporated herein.

⁴ National Parks Service. Estimates of flows to meet salinity targets for western Biscayne National Park. Resource Evaluation Report. SFNRC Technical Series 2008:2. June, 2008, attached hereto and incorporated herein.

⁵ Expert Report of J.W Fourqurean. United States District Court, Southern District Court of Florida, Miami Division. Case No.: 1:16-cv-23017-DPG, attached hereto and incorporated herein.

⁶ Central & Southern Florida Project Comprehensive Everglades Restoration Plan C-111 Spreader Canal Western Project, Final Environmental Impact Statement, Table D-3. July 2009, attached hereto and incorporated herein.

Committed to full protection and restoration of America’s Everglades

gallons of water each day⁷. In addition, all of the land inholdings that have been identified for CERP and are owned by FPL should be placed into public ownership in fee simple to help reduce the cost of the overall restoration to the tax payer and speed the restoration efforts in the area.

Endangered Species

Turkey Point is located proximal to a number of highly ecologically valuable protected areas, including the Biscayne Bay Aquatic Preserve, Crocodile Lake National Wildlife Refuge, Florida Keys National Marine Sanctuary, Everglades National Park to the west and Biscayne National Park directly to the east. The ecological value and sensitivity of this area is massive in scope. Everglades National Park is recognized internationally as a UNESCO world heritage site, a Ramsar wetland of international importance, and an international biosphere reserve. Biscayne National Park is similarly important to the ecology of southern Florida and its residents and is home to over 600 native fish, neo-tropical water birds and over 20 threatened and endangered species.⁸ The area affected by the operations of the Turkey Point Nuclear Generating Station serves as crucial habitat for a number of threatened and endangered species, including the American Saltwater Crocodile, Florida Manatee, Florida Panther, Wood stork, Least tern, Piping plover, Southeastern American kestrel, White-crowned pigeon, Miami blue butterfly, Schaus swallowtail butterfly, Smalltooth sawfish, Staghorn coral, Elkhorn coral, Pillar coral, five species of sea turtles, as well as many other protected species.⁹ These species depend on the natural conditions of regular freshwater flow into Biscayne Bay, and healthy mangrove and seagrass communities which this regular flow helps to preserve. We ask you to consider the continued operations of Turkey Point and the CCS on threatened and endangered species, based on the impacts that have already occurred, particularly to the American Crocodile.

Economics

The health and well-being of the Greater Everglades ecosystem is of vital importance to the vitality of South Florida's economy. Visitors to Everglades National Park in 2014 spent over \$104 million in communities near the park. This spending supported 1,552 jobs in the local area and had a cumulative benefit to the local economy of over \$155 million.¹⁰ Over 1.4 million visitors visited Everglades and Biscayne National Parks in 2017.¹¹ This massive direct economic contribution is dwarfed by the importance of the ecological resources provided by the Everglades watershed. This watershed is essential to maintaining the regional fresh-water supply of South Florida (including drinking water supplies through its role in recharging the Biscayne aquifer), the viability of south Florida's commercial and recreational fishing industries, and the strength of South Florida's real estate market. According to research conducted by the Bonefish & Tarpon Trust, recreational fishing alone accounts for \$1.2 billion in economic activity annually throughout South Florida,¹² and the value of the fresh-water provided by the Everglades system is virtually incalculable.

⁷ William K Nuttle. Review of the Water Budget for the FPL Turkey Point Cooling Canal System: Regional Impacts and Discharge to Groundwater. Southern Alliance for Clean Energy. June 7, 2017, attached hereto and incorporated herein.

⁸ National Park Service, Biscayne National Park, Animals, *available at*: <https://www.nps.gov/bisc/learn/nature/animals.htm>.

⁹ National Park Service, Biscayne National Park, Protected Animals, *available at*: <https://www.nps.gov/bisc/learn/nature/threatened-and-endangered-animals.htm>

¹⁰ Tourism to Everglades National Park creates \$104.5 Million in Economic Benefits' National Park Service. April 24, 2015, <https://www.nps.gov/ever/learn/news/tourism-to-everglades-national-park-creates-104-million-in-economic-benefits.htm>.

¹¹ National Park Service, National Park Service Visitor Use Statistics, *available at*: <https://irma.nps.gov/Stats/>.

¹²Fedler, T. The Economic Impact of Recreational Fishing in the Everglades Region. Bonefish and Tarpon trust-Everglades Foundation. December, 2009, attached hereto and incorporated herein.

Committed to full protection and restoration of America's Everglades

Sea Level Rise

Turkey Point's geographic location and underlying porous limestone topography make it uniquely susceptible to sea level rise and the impacts of storm events. The facility lies only 20 feet above sea level at its highest point, and most of the CCS lies at sea level. Under even the most optimistic scenarios provided by the National Parks Service,¹³ and the National Oceanographic and Atmospheric Administration,¹⁴ much of the Turkey Point facility and the CCS will be inundated well before the end of the proposed license extension. During Hurricane Irma, the berm separating the CCS from the waters of Biscayne Bay was breached by storm surge in several locations, leading to additional mixing of chloride, nutrient, tritium and potentially heavy metal polluted industrial wastewater from the facility with waters of the U.S. We urge you to consider the sea level rise projections provided by the U.S. Army Corps of Engineers and the National Oceanic and Atmospheric Administration and to analyze both best- and worst-case scenarios for sea level rise impacts on the facility through 2053. Furthermore, we ask that you evaluate the cumulative environmental impacts of sea level rise projections and CCS hydrologic connectivity with the Biscayne Aquifer and Biscayne Bay at sea-level.

Finally, in consideration of the Subsequent License Renewal, we urge you to analyze increased vulnerability of Units 3 & 4 and ancillary facilities to storm surge resulting from sea level rise. Additionally, NRC must include conditions to certification requiring alternative technologies necessary to adapt to sea level rise, such as cooling towers that could be raised well above sea-level to make the facility less vulnerable to rising seas, and to minimize the other environmental impacts described herein.

Thank you in advance for your consideration.

Sincerely,



Mark Perry
Co-Chair



Marisa Carrozzo
Co-Chair

Cc:

William "Butch" Burton, NRC, Turkey Point Relicensing Environmental Project Manager via email to:

william.burton@nrc.gov

May Ma, NRC, Chief, Program Management, Announcements and Editing Branch

Office of Administration via email to: TurkeyPoint34SLREIS@nrc.gov

Lois James, NRC, Senior Project Manager, License Renewal Projects Branch

Division of Materials and License Renewal via email to: Lois.James@nrc.gov

Appendix attached includes all referenced material within this letter

¹³ Park, J., E. Stabenau, and K. Kotun. 2017. Sea-level rise and inundation scenarios for national parks in South Florida. *Park Science* 33(1):63–73, attached hereto and incorporated herein.

¹⁴ Sweet, W. Dusek, G. Obeysekera, J. Marra, J. Patterns and Projections of High Tide Flooding Along the U.S. Coastline Using a Common Impact Threshold. National Oceanographic and Atmospheric Administration. February 2018, attached hereto and incorporated herein.

Committed to full protection and restoration of America's Everglades

APPENDIX

Committed to full protection and restoration of America's Everglades

450 N. Park Road # 301, Hollywood FL 33021 | www.evergladescoalition.org | info@evergladescoalition.org

Review of the Water Budget for the FPL Turkey Point Cooling Canal System: Regional Impacts and Discharge to Groundwater

Prepared by:
William K. Nuttle, PhD, PEng

For:
Southern Alliance for Clean Energy

7 June 2017

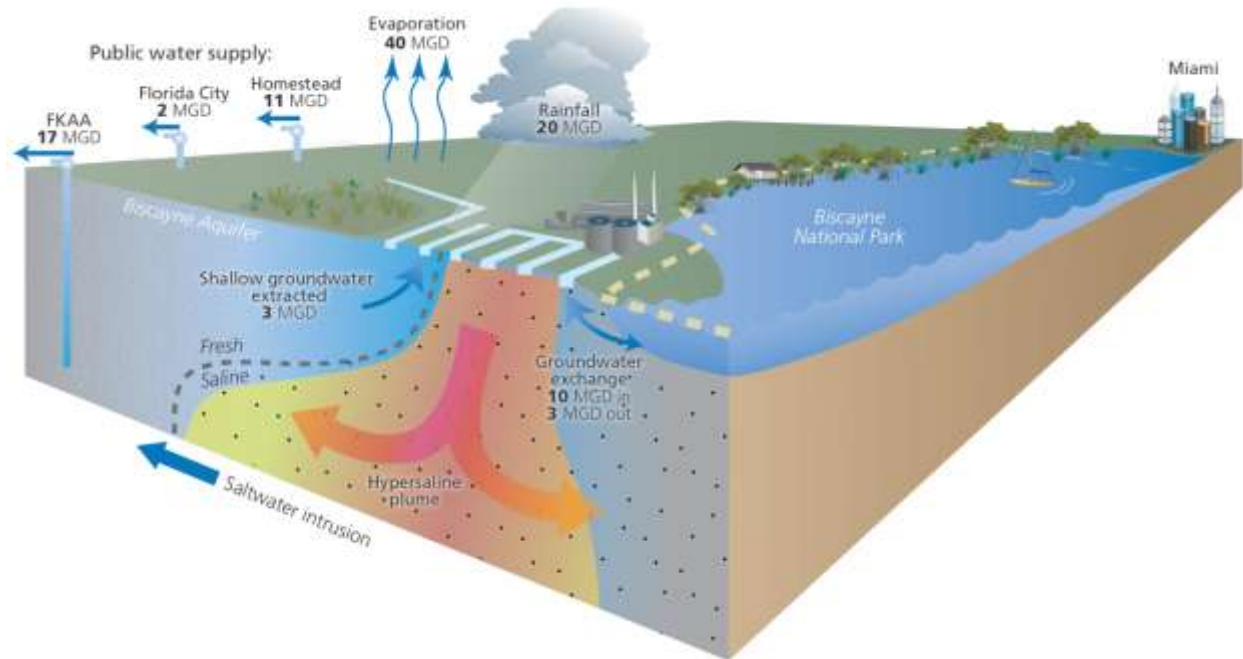
Table of Contents

Findings.....	3
General.....	3
CCS Discharge to Groundwater.....	4
Impact to Regional Water Resources.....	4
Introduction.....	5
Review and Analysis of Water Budget Data	7
Inconsistencies in Reported Seepage Fluxes	7
Overview of CCS Water Budget.....	12
Effect of Hydrologic Variability on the Water Budget.....	14
CCS Discharge to the Aquifer	15
Factors that Affect Discharge to Biscayne Bay	15
Magnitude of Seepage into the Aquifer	21
Impact on Regional Water Resources.....	23
Freshwater Withdrawal by ID pumping	23
Hypersaline Groundwater Plume.....	25

Findings

General

Generally, water lost from the CCS by evaporation is balanced by rainfall, seepage into the CCS from the Biscayne aquifer, and other inputs. Average input provided by seepage is small compared with rainfall and other inputs over the long-term, but day-to-day seepage fluxes are comparable in magnitude to the other components of the water budget.



Evaporation - 40 MGD

Evaporation from the CCS removes waste heat produced by the power plants, and because of this evaporation from the CCS is 10 mgd greater than would occur under natural conditions. This function is essential both for generating electricity and for safe operation of the nuclear power plants.

Rainfall - 20 MGD

Rainfall is the major source of fresh water available to the CCS to replace water removed by evaporation. On average, rainfall provides enough water to replace only about half of the water removed by evaporation. But, on days with heavy rainfall can add over half a billion gallons of water to the CCS, causing water levels to rise rapidly.

Net Seepage Input from Biscayne Bay – 8 MGD

Seepage from Biscayne Bay balances the water lost by evaporation. Water moves freely through the porous limestone that separates the CCS from Biscayne Bay. Day-to-day seepage flows both into and out of the CCS in response to fluctuations in water levels in the CCS and in Biscayne Bay.

Other Inputs of Water - 20 MGD

Other inputs of water for the CCS include water discharges by the power plants other than cooling water, water pumped from the ID, and new inputs of water added after the fall of 2014. New inputs of water include fresh water pumped from the L-31E canal, water from shallow saline wells, and brackish water pumped from the deep Floridan aquifer.

CCS Discharge to Groundwater

Periods during which seepage adds water to the CCS alternate with periods in which the CCS discharges water to groundwater. The average net seepage out of the CCS is about 9 mgd. At this rate the entire contents of the CCS empty into the aquifer every 1.5 years.

Seepage is an important component of the mass budgets for salt and other dissolved substances. The only mechanism for controlling the accumulation of salt and other solutes in the CCS is through seepage discharge to groundwater.

The period high seepage out of the CCS into Biscayne Bay that occurred during December 2015 and January 2016 is the longest and most intense event captured by the monitoring program, but it is not unique. Periods of seepage out of the CCS toward Biscayne Bay have occurred regularly in the period September 2010 through November 2016.

Impact to Regional Water Resources

Continued operation of the CCS impacts regional fresh water resources in two ways:

- First, the CCS competes with other users to obtain freshwater from the Biscayne aquifer, an increasingly scarce resource. Operation of the ID withdraws an amount of fresh water from the aquifer that is comparable to water withdrawal by nearby public water supply wells.
- Second, seepage of salty water from the CCS into the underlying aquifer feeds the growth of a large plume of hypersaline water that is moving to the west. This plume accelerates the intrusion of saltwater toward well fields used for public water supply.

Pumping 14 mgd of contaminated water from the aquifer, to remediate the plume, is barely adequate to counter the rate at which seepage from the CCS adds water to the plume, allowing for uncertainties in estimating this rate of seepage.

Introduction

The Cooling Canal System (CCS) at the Turkey Point Power Station provides cooling for two nuclear-powered thermo-electric generating units, Units 3 and 4, operated by Florida Power and Light (FPL). The Turkey Point plant is located on the shore of Biscayne Bay, immediately adjacent to Biscayne National Park and about 25 miles southwest of Miami. The CCS consists of a system of shallow canals that cover an area approximately 6,100 acres, two miles wide by five miles long. The CCS is underlain by the Biscayne aquifer. The Biscayne aquifer is a surficial, i.e. watertable, aquifer comprised of very porous limestone that extends to about 100 feet beneath the CCS. The surrounding landscape is extremely flat. Inland of the CCS, wetlands occupy much of the area between the Turkey Point plant and Homestead, Florida, located 4.5 miles northwest of the site.

The CCS functions as a “closed-loop” system for the purposes of providing cooling for the power plants at Turkey Point, its primary function. Water is recycled continuously within the system of canals and through the power plants to cool steam condensers. Heated water discharged from the power plants enters the CCS through a canal running east-west along its north boundary. From this canal, the water enters and flows south through a series of shallow, parallel canals. At the south boundary of the CCS, the circulating water is collected in a single, large canal that carries it east and into a smaller set of parallel canals, which then carry the cooled water north, back to the intake bay of the circulating water pumps at the power plants. More details of the construction, operation, and cooling characteristics of the CCS are provided in a recent technical report¹ by Dr. David Chin (University of Miami).

However, hydrologically the CCS functions as an open system. Water in the canals is directly connected to, and actively exchanges with, the atmosphere and groundwater in the underlying Biscayne aquifer. This report assesses the impact of the CCS on the regional water resources and through the discharge of pollutants by seepage into the aquifer. This assessment is based on data collected in the pre- and post-uprate monitoring program² that FPL has conducted at the Turkey Point site since 2010. This report summarizes the major fluxes of water between the CCS and the Biscayne aquifer, identifies the factors that influence discharge through seepage into Biscayne Bay, and evaluates the undocumented withdrawal of freshwater from the Biscayne aquifer as a result of the operation of the Interceptor Ditch (ID).

Of particular interest is the discharge of water from the CCS into Biscayne Bay through a groundwater pathway. There is no direct surface water connection between the CCS and Biscayne Bay, but high levels of tritium were detected in Biscayne Bay surface waters soon after the CCS was put into service.³ Recently, in January 2016, high levels of tritium and ammonium were detected in Biscayne Bay immediately adjacent to the CCS, Figure 1. This occurred during

¹ Chin, D.A., 2016. The Cooling-Canal System at the FPL Turkey Point Power Station. Final Report prepared for Miami-Dade County, May 2016.

² SFWMD, 2009. FPL Turkey Point Power Plant Groundwater, Surface Water, and Ecological Monitoring Plan. October 14, 2009.

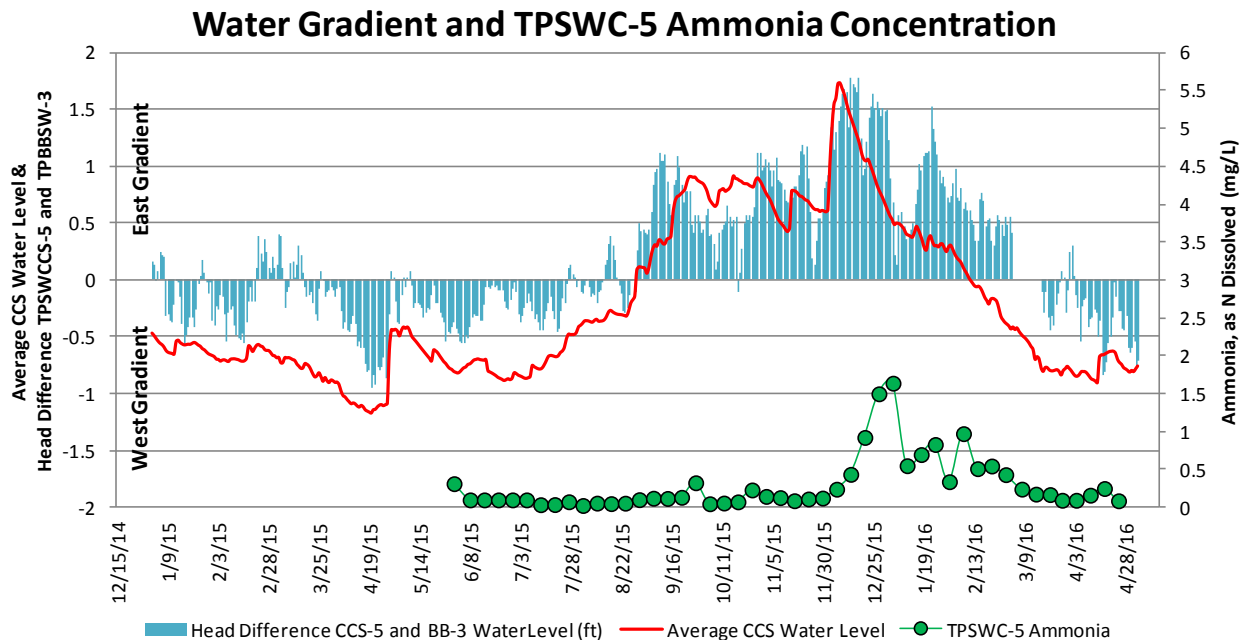
³ Ostlund, H.G., and Dorsey, H.G., 1976. Turkey Point Tritium. Progress Report to Energy Research and Development Administration, Contract E-(40-1)-3944. UM-RSMAS-#76005, April 20, 1976.

a period in which the usual pattern of water levels was reversed, and water level⁴ in the return canals of the CCS was higher than water the water level in Biscayne Bay. On average, water level in the eastern, north-flowing return canals is drawn down below water level in Biscayne Bay under the influence of the circulating water pumps at the power plants, and the direction of groundwater movement is from Biscayne Bay into the CCS. The event in January 2016 indicates that groundwater movement out of the CCS toward Biscayne Bay can occur episodically.

The objectives of this report are:

1. Review available data on components of the CCS water budget to characterize the both the average, long-term impacts on regional water resources and the discharge of pollutants from the CCS into the surrounding aquifer that may occur episodically;
2. Quantify the level of pollution loading from the CCS into the aquifer; and
3. Quantify the impacts of CCS operations on regional water resources.

Figure 1⁵: A reversal of the usual difference in water level (i.e. hydraulic head; in blue), supporting the discharge of water from the CCS toward Biscayne Bay, occurred prior to and during a period in which high ammonium concentrations (green) were detected in the surface water of Biscayne Bay adjacent to the CCS. Water levels in the CCS are plotted in red.



⁴ “Water level” refers to daily-average level, so the effect of diurnal tidal fluctuation in Biscayne Bay water level has been removed.

⁵ This figure is taken from a spreadsheet obtained from Miami-Dade DERM. The author of the spreadsheet is indicated as Sara Mechtensimer. A LinkedIn profile for Sara Mechtensimer identifies her as an employee of FPL. [accessed 25 May 2017].

Review and Analysis of Water Budget Data

The data reviewed are from annual reports on the CCS water and salt budgets that FPL provides as part of the pre- and post-uprate monitoring program. The data that relate to the water and salt budgets include pumping rates, water levels, salinity, rainfall, water temperature, and meteorological parameters related to evaporation. These data are used to calculate fluxes of water and salt entering and leaving the CCS and changes in water volume and salt mass contained in the CCS.

The calculated water fluxes include rainfall, evaporation, and the exchange of water by seepage between the CCS and the Biscayne aquifer. The calculated rainfall input into the canals also accounts for runoff from the land surface around the canals. These calculations involve a number of adjustable parameters. The parameter values are determined by calibration, i.e. by selecting values so that the changes in CCS volume, calculated as the net result of all the water inflows and outflows, match the measured changes in volume.

The analysis in this report focuses on water levels measured in the CCS at locations CCS-1, CCS-5 and CCS-6, water level measured in Biscayne Bay at BBSW-3, salinity values measured in the ID and in the L-31E canal, the rate at which water is pumped from the ID into the CCS, and shallow horizontal seepage between the CCS and Biscayne Bay along the Return Canal and Intake Canal, Figure 2.

Inconsistencies in Reported Seepage Fluxes

Daily values for components of the water were obtained from two spreadsheet files that cover separate but overlapping periods of time: **Sep 2010 to Nov 2015**⁶ and **Jun 2015 to Nov 2016**.⁷ Both files contain data from the monitoring program for the period September 2010 through November 2015, but the later file calculates water budget fluxes only for the period June 2015 through November 2016.

⁶ File contents are identified by this title on the “README” tab, “Water and Salt Balance Model of the Florida Power & light Cooling Canal System (CCS),” and this statement on the “Key” tab: “This model is based on the previously calibrated balance model (September 2010 through May2015) saved with filename Water&Salt_Balance_Thru_May2015_report.xlsx.” The author of the file is identified as James Ross.

⁷ File contents are identified by this title on the “README” tab, “Water and Salt Balance Model of the Florida Power & light Cooling Canal System (CCS),” and this statement on the “Key” tab: “This model is based on the previously calibrated balance model (September 2010 through May 2016) saved with filename Balance_Model_May2016_draftfinal_v2.xlsx.” The author of the file is identified as James Ross.

Figure 2: Location of monitoring data and seepage fluxes referenced in this report



The two files report different values for the calculated water budget fluxes for the overlapping period June 2015 through November 2015, Figure 3. I found no explanation for this difference; evidently the difference reflects a recalibration of the parameters used in calculating the component fluxes of the water balance. The discrepancy is greatest for the calculated seepage fluxes across the south and east (Return and Intake canals) boundaries of the CCS. Values of rainfall and evaporation are different in the overlapping period, but not markedly so. It appears that the calculation of evaporation in the later spreadsheet corrects for some missing or bad data present in the earlier spreadsheet. The total water input from other water inputs includes blowdown from the power plants, pumping from the ID, and water inputs from the L-31E and various wells. These data are similar for the two spreadsheets in the overlapping period.

Differences in average values of components of the water budget between the two data sets reflect differences in weather (rainfall), thermal loading by the power plants (evaporation) and actions taken to remediate problems of high temperature and salinity (other water inputs). Averages are computed for component fluxes of the water budget based on the daily fluxes reported in each spreadsheet, Table 1. Rainfall (including runoff), evaporation, and inputs from other inputs are unidirectional.

Differences in the seepage fluxes reflect the influence of all these factors plus one more. Seepage fluxes fluctuate in both magnitude and direction; therefore averages are computed separately for additions to (positive) and losses from (negative) the CCS. Large changes were made in the adjustable parameters used in the seepage flux calculations. The input of water from other inputs, on average, increased in the later period, and this is reflected in an increase in the net discharge of water by seepage out of the bottom of the CCS, Table 1.

The effect of recalibration on the seepage flux calculation is seen in the comparison of daily seepage fluxes for the Return Canal and Intake Canal, shown in Figure 3. The magnitude of the seepage flux calculated for the same time period, June 2015 through November 2015, is decreased by about a factor of seven.⁸ A difference of this magnitude resulting from recalibration of the flux calculations indicates that the calculated seepage fluxes must be taken as highly uncertain.

⁸ Based on the reduction in variation measured by the standard deviation.

Figure 3: Comparison of calculated water budget fluxes obtained from two data reports covering the periods Sep 2010 to Nov 2015 and Jun 2015 to Nov 2016. Both reports were produced by FPL based on the pre- and post-uprate monitoring program. Data in the uppermost plot are calculated values of seepage east (positive for water leaving the CCS) along the Return and Intake Canals.

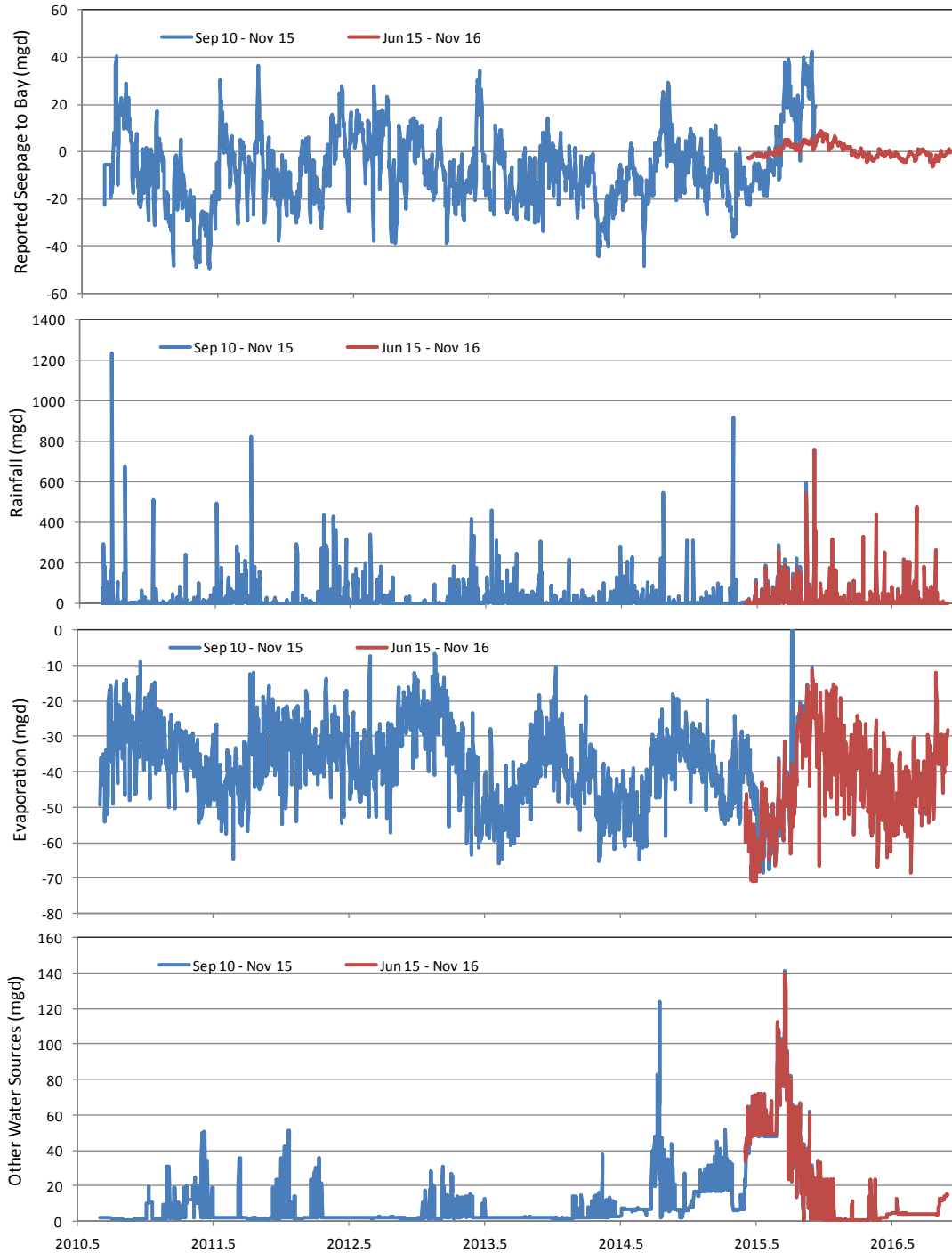


Table 1: Average of daily water budget fluxes (mgd) reported in FPL spreadsheets. Seepage fluxes (+) are the average over the entire period of daily fluxes into the CCS; seepage fluxes (-) are the average of fluxes out of the CCS. Average seepage fluxes are not calculated for the period of the combined data sets because of inconsistencies in the calculations reported in the two spreadsheets.

	Sep10 to Nov15	Jun15 to Nov16	Sep10 to Nov16
Rainfall (including runoff)	20.76	25.88	21.33
Evaporation	-37.58	-42.21	-38.22
Bottom (+)	6.24	1.76	-
Bottom (-)	-10.54	-11.99	-
L31-E (+)	0.79	0.35	-
L-31E (-)	0.00	0.00	-
South Canal (+)	1.87	9.68	-
South Canal (-)	-0.06	-2.43	-
Return and Intake canal (in)	10.70	1.01	-
Return and Intake canal (out)	-3.74	-1.31	-
North Canal (+)	0.01	0.02	-
North Canal (-)	-0.01	-0.01	-
Net seepage	5.26	-2.92	-
ID Pumping	4.02	4.32	3.76
Blowdown	1.54	0.82	1.31
Additional Units 3,4	0.50	0.57	0.51
L-31E Input	1.93	5.08	1.62
PTF Well #3	0.62	0.40	0.62
PW-1	1.27	2.15	1.07
SW-1, SW-2	1.89	6.74	1.62
Floridan Wells	0.00	1.07	1.07
Sum of other water inputs	11.77	21.15	10.76
Change in volume	-0.53	1.55	-0.03

Overview of CCS Water Budget

Water budget is a daily accounting of all the ways that water enters or leaves the CCS. If the accounting is complete, then the sum of all inflows minus all the outflows must equal the change in the amount of water contained in the CCS, Equation 1. Changes in the volume of water in the CCS are reflected in changes in water level. The volume of the CCS fluctuates generally between four and seven and a half billion gallons. Large changes in volume occur from week to week and month to month. Over longer time periods, such as in Table 1, the average flux due to a change in storage (in terms of millions of gallons per day) is small, and the water budget can be roughly stated as the sum of inflows must equal the sum outflows.

$$\boxed{\text{Rainfall}} + \boxed{\text{Other inputs}} - \boxed{\text{Evap}} - \boxed{\text{Net seepage}} = \boxed{\text{Change in volume}} \quad \text{Eq. 1}$$

I combined the data reported in the two spreadsheets in order to construct a water budget for the entire period September 2010 through November 2016. Daily values for the period September 2010 through May 2015, from the **Sep 2010 to Nov 2015** spreadsheet, are appended to the daily values for the entire period reported in the **Jun 2015 to Nov 2016** spreadsheet. Average fluxes are calculate for rainfall, evaporation and other inputs for the period September 2010 through November 2016 are based on a combined data set, Table 1. Average seepage fluxes are not calculated for the period of the combined data sets because of inconsistencies in the seepage flux calculations reported in the two spreadsheets.

These results provide the following picture of the long-term average CCS water budget:

Overall Water Balance

Over the long-term, water losses from evaporation are balanced by rainfall, other inputs and seepage into the CCS from the Biscayne aquifer. The input provided by seepage is small compared with rainfall and other inputs over the long-term, but daily seepage fluxes are comparable in magnitude to other water budget components.

Seepage fluxes vary spatially in the direction and magnitude of the net flux. Most of the inflow by seepage occurs as shallow, horizontal flow across the east and south boundaries of the CCS, carrying water with salinity near seawater (34 mg/l) into the CCS. Most seepage outflow occurs down through the bottom of the CCS, carrying hypersaline water (typically 60 mg/l) into the aquifer, Table 1.

Evaporation - 40 MGD⁹

Evaporation from the CCS removes waste heat produced by the power plants, and due to this evaporation from the CCS is 10 mgd greater than would occur under natural conditions.¹⁰ This

⁹ Average evaporation for September 2010 through November 2016, rounded to the nearest 10 mgd.

function is essential both for generating electricity and for safe operation of the nuclear power plants.

Rainfall - 20 MGD¹¹

Rainfall is the major source of freshwater available to the CCS to replace evaporation. On average, rainfall provides enough water to replace only about half of the water removed by evaporation. The rest is provided by the input of water from other inputs and groundwater seepage, mostly from Biscayne Bay. Periods of heavy rainfall can add over a billion gallons of water to the CCS. When this happens, water levels in the CCS rise rapidly, and this increases seepage that flushed the contents of the CCS into the underlying porous limestone Biscayne Aquifer.

Net Seepage Input from Biscayne Bay – 8 MGD¹²

Saline water from Biscayne Bay seeps into the CCS to replace some of the water removed by evaporation. Water moves freely through the porous limestone that underlies the shoreline. Seepage occurs both into and out of the CCS in response to fluctuations in water levels in the CCS and in Biscayne Bay. Water levels in Biscayne Bay fluctuate in response to daily tides, storm tides, and the seasonal fluctuation in sea level. Water levels in the CCS fluctuate in response to rainfall events and the operation of the power plant's circulating water pumps.

Other Inputs of Water - 20 MGD¹³

Other inputs of water for the CCS includes blowdown, i.e. water discharged by the power plants in addition to cooling water, water pumped from the ID and new inputs of water added after the fall of 2014. New inputs of water include fresh water pumped from the L-31E canal, water from shallow saline wells, and brackish water pumped from the deep Floridan aquifer.

¹⁰ “The estimate of potential evapotranspiration (ETp) from open water and wetlands in the LEC Planning Area is 53 inches” (page 187; 2011–2014 Water Supply Plan Support Document September 2014), which is equivalent to a flux of 28 mgd over the total CCS area of 6100 acres when the potential evapotranspiration rate is applied to the water surface area within the CCS.

¹¹ Average rainfall for the period September 2010 through November 2016, rounded to the nearest 10 mgd. Rainfall includes both the rain falling directly onto the surface of the water in the canals plus runoff from the land surface within the CCS boundary.

¹² 8 mgd is the net inflow to the CCS by seepage fluxes calculated for the South Canal and the Return and Intake Canals for both time periods, taken together, Table 1. The recalibration of the seepage calculations between the earlier and later time periods has the effect of shifting the position of the major seepage inflow from the Return and Intake Canals to the South Canal. The salinity of seepage inflow at both locations is around 30 mg/l, making Biscayne Bay the likely source of this water.

¹³ Average flux of water from other inputs for the period June 2015 through November 2016, rounded to the nearest 10 mgd, Table 1. This figure best represents current conditions. Pumping from the L-31E canal, from shallow saline wells, and from the deep Floridan aquifer began in the fall of 2014 and continues to the present.

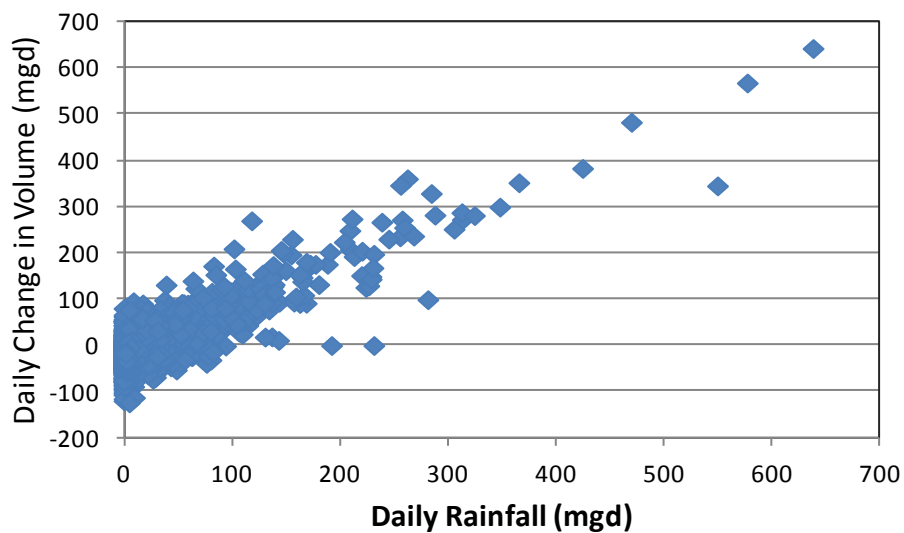
Effect of Hydrologic Variability on the Water Budget

On a daily timescale the CCS water budget can look quite different than the long-term average. This occurs principally because daily rainfall is highly variable, Table 2. The average influx due to rainfall is the same order of magnitude as the rate of water removal by evaporation. However, daily rainfall ranges from zero, on most days, to days in which rainfall far exceeds other fluxes in the water budget. On days with high rainfall the canals of the CCS simply fill up, Figure 4. Rainfall on the day with the maximum rainfall in the period September 2010 through November 2016 added a volume equal to one quarter of the average volume of the CCS.

Table 2: Variability of the water budget component fluxes computed daily

	Average	Standard Dev.	Maximum	Minimum
Rainfall	21.33	70.20	1236.46	0.00
Evaporation	-38.22	11.58	-6.73	-70.90
Net seepage	-	-	-	-
Other water inputs	10.76	17.27	139.82	0.70
Change in volume	-0.03	67.12	686.25	-177.70

Figure 4: Influx of water on days of high rainfall is absorbed by an increase in water storage



CCS Discharge to the Aquifer

The evidence of CCS discharge to Biscayne Bay, Figure 1, indicates that such discharge occurs as discrete events. To assess their impact one needs to know how frequently these events occur, the quantity of water involved, and what factors contribute to their occurrence.

I investigated the frequency and magnitude of these discharge events by plotting the difference in daily-average water level¹⁴ measured in the Return Canal (CCS-5) minus the level in Biscayne Bay (BBSW-3), Figure 5; this is the same statistic as plotted in Figure 1. This difference is used by FPL to calculate horizontal seepage in the upper ~20 feet of the limestone aquifer; 20 feet is the depth of the Return Canal.

The discharge event that occurred during December 2015 and January 2016 is the longest and most intense event captured by the monitoring program, but it is not unique. Over the long-term, the net flow of water is from Biscayne Bay into the Return Canal (negative values for the difference in water levels). Periods of several days during which the difference in water levels drove seepage out of the CCS toward Biscayne Bay have occurred regularly in the period September 2010 through November 2016.

Factors that Affect Discharge to Biscayne Bay

In general, three factors contribute to the variation in the seepage flux along the eastern boundary of the CCS:

1. non-tidal variation in water level in *Biscayne Bay*;
2. changes in the *drawdown* of water level in the Return and Intake Canals, as a result of changes in the rate at which water is pumped through the power plants; and
3. changes in the *net exchange* of water between the CCS and the Biscayne aquifer resulting from variation in the CCS water budget leading.

I conducted a correlation analysis to determine which of these factors has the greatest influence on the difference in water levels, as a proxy for the seepage flux. The data used are daily average water level measured in Biscayne Bay (BBSW-3; for *Biscayne Bay* water level), the difference in daily average water level CCS-1 minus CCS-6 (for *drawdown*), and the daily net seepage flux between the CCS and the Biscayne aquifer calculated from the water budget (for *net exchange*), Figures 6 and 7.

¹⁴ Note that the use of daily-average water levels removes the transient influence of diurnal tides on the seepage flux.

Figure 5: Upper panel: water level difference driving seepage out of the CCS toward Biscayne Bay (+ values) along the Return Canal. The difference is water level at CCS-5 minus water level at BBSW-3 (ft). Lower panel: water level in the CCS and daily inflow from rainfall and other inputs (mgd). The red box marks off the time period that is the first quarter of 2016.

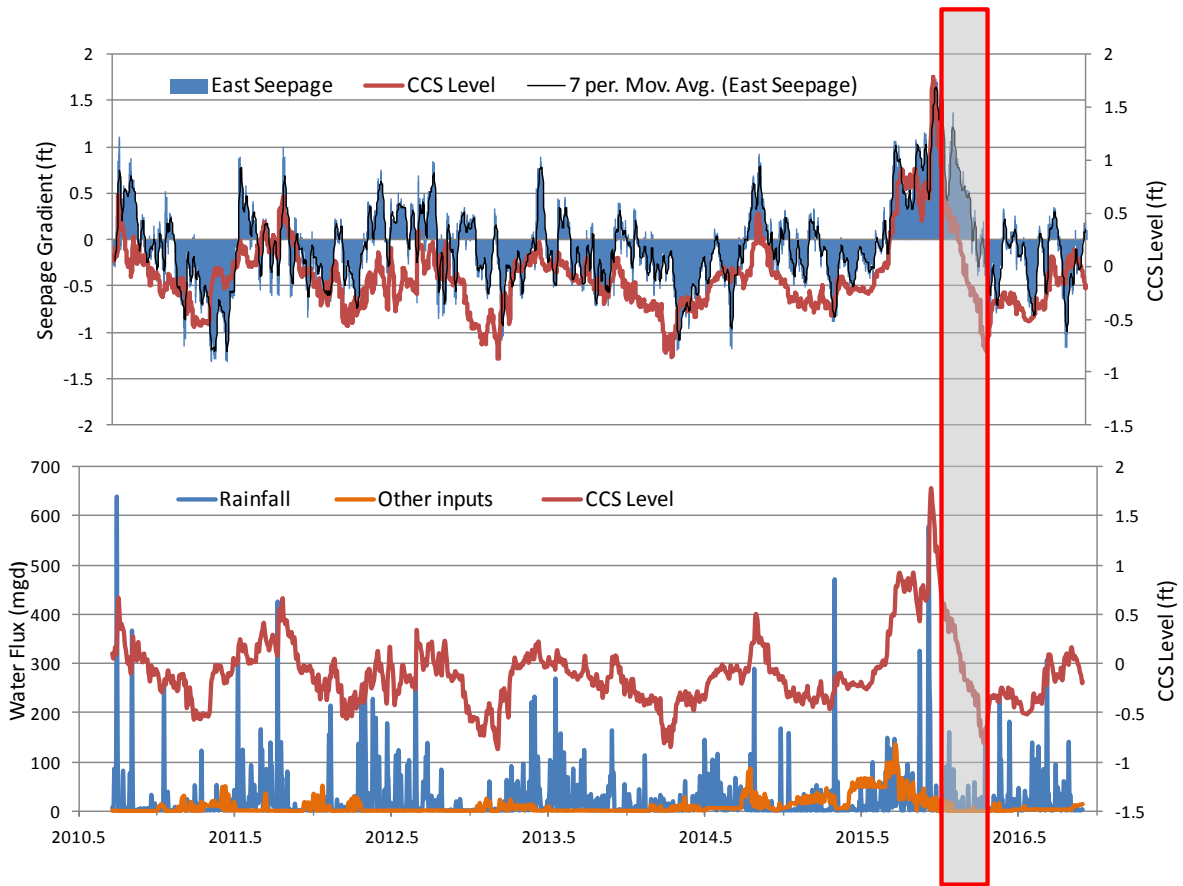


Figure 6: Upper panel: Water levels (ft) in the CCS (CCS-1, CCS-5, CCS-6), in Biscayne Bay (BBSW-3), and the drawdown in water level related to pumping at the plant (level at CCS-1 minus CCS-6). Higher values for drawdown correspond to higher pumping. Lower panel: Daily fluctuations in water level in the CCS (CCS-1, ft) and the resulting change in water volume (mgd)

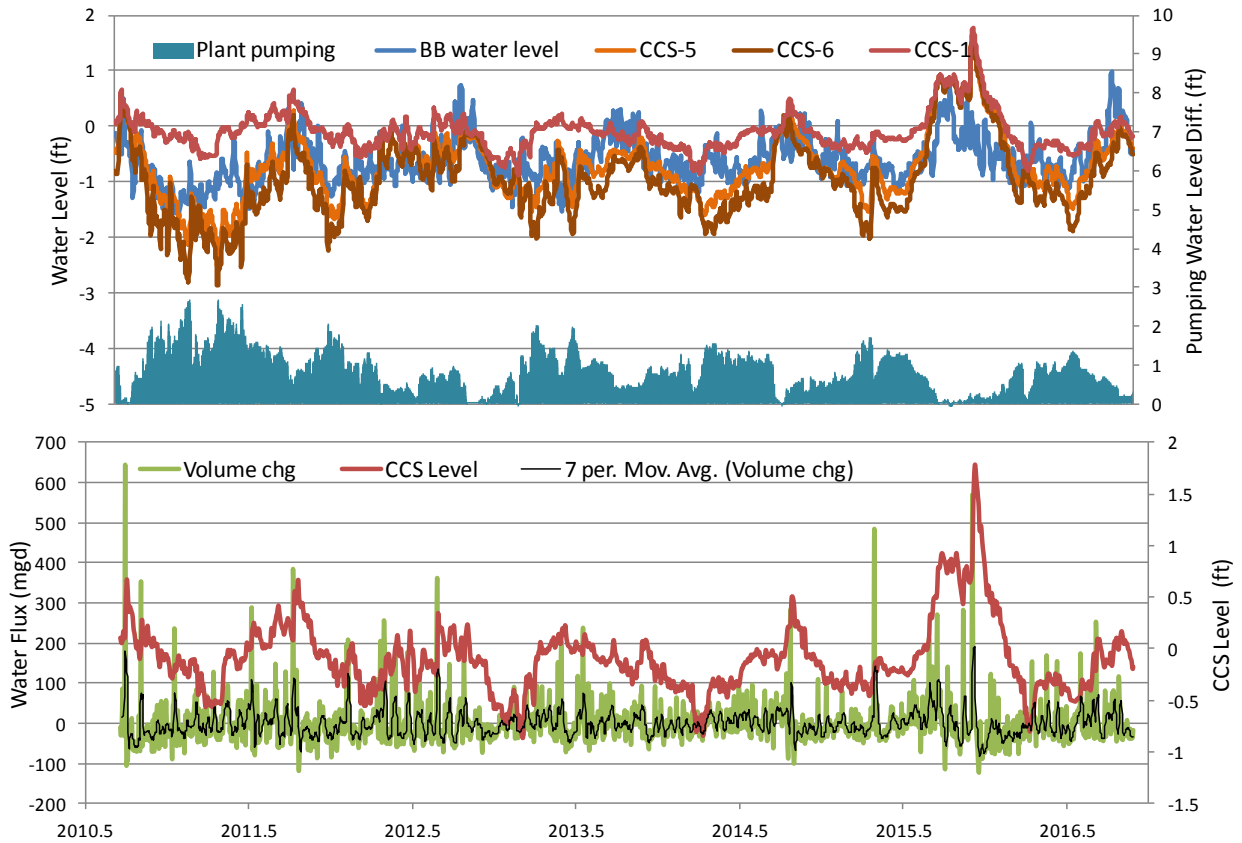
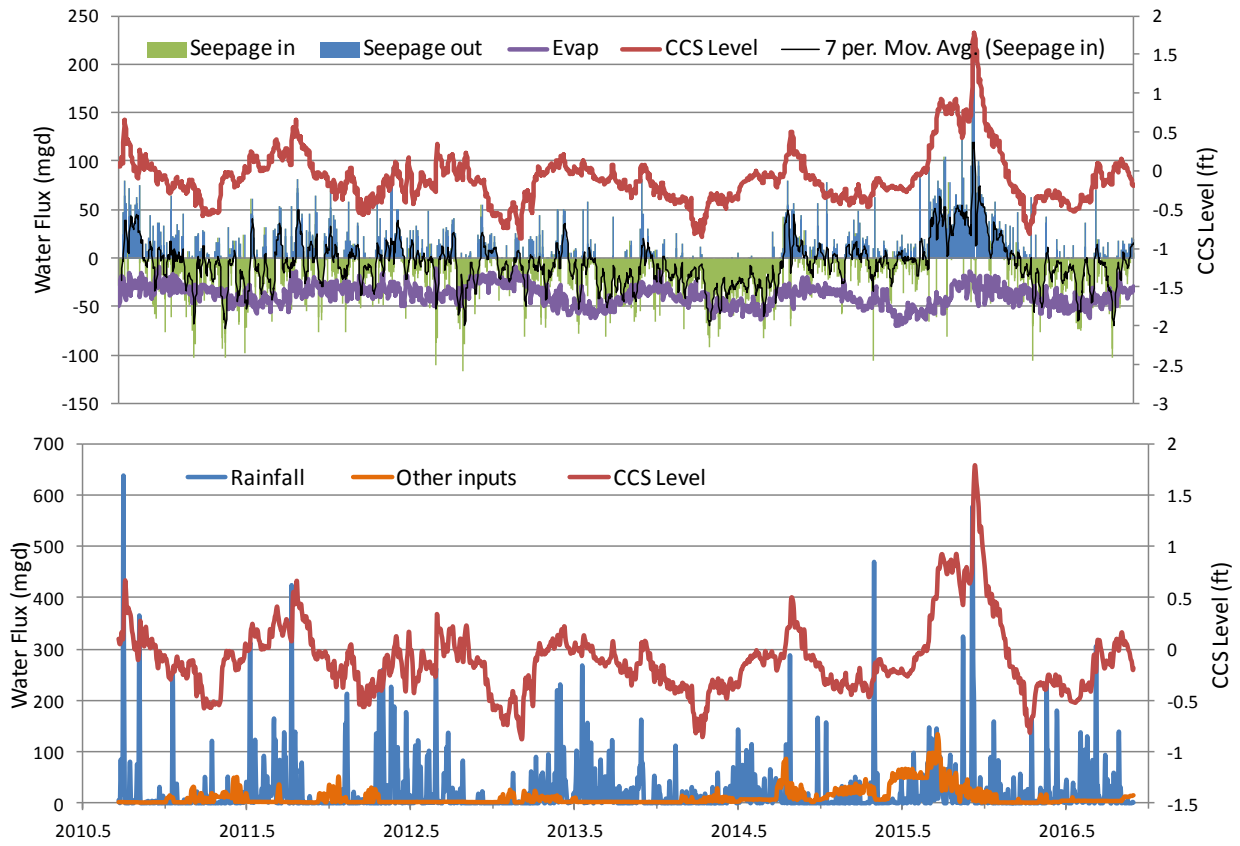


Figure 7: Upper panel: computed daily net seepage exchange (mgd) with the aquifer (+ into the aquifer), CCS water level (CCS-1, ft), and water loss from evaporation (mgd). Lower panel: water level in the CCS and daily inflow from rainfall and other inputs (mgd).



Daily values of net seepage, Figure 7, are calculated from the water budget equation, Equation 2. All the other fluxes and the change in the volume of water in the CCS are either measured directly or calculated. This approach to estimating the net seepage does not rely on the calculated seepage fluxes reported by FPL.

$$\boxed{\text{Net seepage}} = \boxed{\text{Rainfall}} + \boxed{\text{Other inputs}} - \boxed{\text{Evap}} - \boxed{\text{Change in volume}} \quad \text{Eq. 2}$$

Results of the correlation analysis show that the net seepage flux is the most important factor that affects the direction and magnitude of groundwater seepage between the CCS and Biscayne Bay, Table 3. In turn, the variation in the seepage flux reflects the influence of hydrologic variation on the daily water budget, Equation 1 and 2. The daily variation in rainfall is of particular importance, because it is a significant component of the water budget and it is by far the most variable component. Similar results are obtained when the correlation analysis is conducted separately on data from the two FPL spreadsheets, Table 4.

Correlation results also show that variation in the drawdown of water levels in the Return and Intake Canals due to the operation of the pumps at the power plants is nearly as important as net seepage flux. Both net seepage and drawdown contributed to the discharge event during December 2015 and January 2016. Water levels in the CCS were high, due to the accumulation of rainfall and other inputs in the preceding months, and drawdown from the circulating pumps was low, which further raised water levels in the Return and Intake Canals.

Biscayne Bay water level is not found to be an important factor affecting seepage toward Biscayne Bay generally, but it appears that high water levels Biscayne Bay played a role in the discharge event during December 2015 and January 2016. Water level in Biscayne Bay rose to its seasonal high in October and then remained higher than normal through November and December, Figure 6. (Monthly mean sea level attained its highest value for the period September 2010 through November 2016 in October 2015, Figure 8.¹⁵) The sustained high stand of water levels in Biscayne Bay would have raised the water table in the Biscayne aquifer, impeding seepage out of the CCS and thus contributing to the accumulation of water in the CCS. Then, water level in Biscayne Bay fell rapidly during January and February 2016, contributing to maintaining the head difference driving seepage into Biscayne Bay even while water levels in the CCS also dropped.

¹⁵

<https://tidesandcurrents.noaa.gov/waterlevels.html?id=8723214&units=standard&bdate=20100901&edate=20161130&timezone=GMT&datum=MLLW&interval=m&action=> [accessed 1 Jun 2017]

Table 3: Correlation matrix for the period September 2010 through November 2016. East seepage is the difference in water levels CCS-5 minus BBSW-3. Plant pump is the drawdown at the plant intake, CCS-1 minus CCS-6. BB Level is Biscayne Bay water level, BBSW-3. Net seepage is the daily net exchange flux between the CCS and the aquifer.

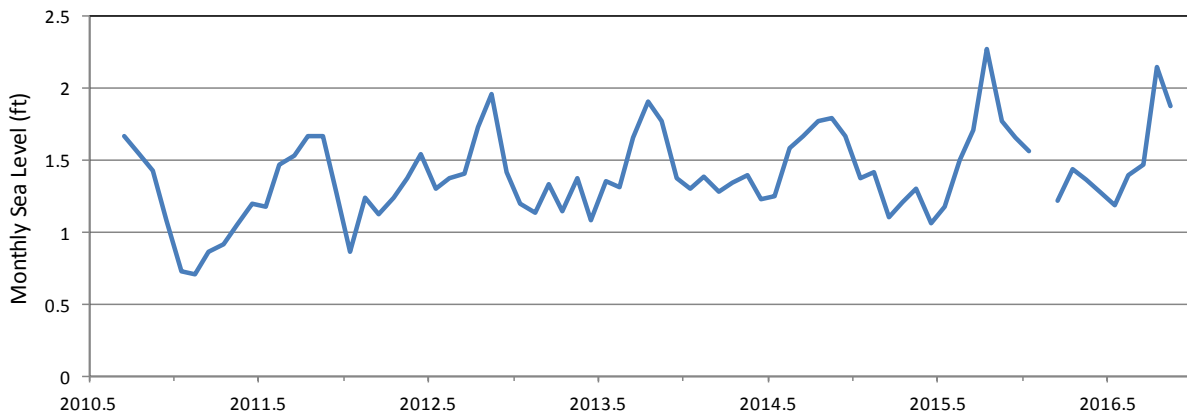
	East seepage	Plant pump	BB Level	Net seepage
East seepage (ft)	1.000			
Plant pumps (ft)	-0.546	1.000		
BB Level (ft)	-0.054	-0.521	1.000	
Net seepage (mgd)	0.658	-0.324	-0.111	1.000

Table 4: Correlation matrices as in Table 3 but for periods (A) September 2010 through November 2015 and (B) June 2015 through November 2016.

(A)	East seepage	Plant pump	BB Level	Net seepage
East seepage (ft)	1.000			
Plant pumps (ft)	-0.497	1.000		
BB Level (ft)	-0.185	-0.464	1.000	
Net seepage (mgd)	0.603	-0.248	-0.258	1.000

(B)	East seepage	Plant pump	BB Level	Net seepage
East seepage (ft)	1.000			
Plant pumps (ft)	-0.631	1.000		
BB Level (ft)	0.012	-0.628	1.000	
Net seepage (mgd)	0.713	-0.465	0.059	1.000

Figure 8: Monthly mean sea level measured at the tide gage on Virginia Key



Magnitude of Seepage into the Aquifer

Daily net seepage rates provide insight into the magnitude and dynamics of exchange between the CCS and the Biscayne aquifer, Table 5. Over the long-term, net seepage is a source of water for the CCS. Periods of net seepage into the CCS alternate with periods of net seepage out, Figure 7. The cumulative impact of the average net seepage out of the CCS, ~9 mgd, is that the entire contents of the CCS empty into the aquifer every 1.5 years.¹⁶

Daily net seepage rates tell only part of the story of exchange between the CCS and the aquifer. Frequently, the estimated seepage fluxes calculated and reported by FPL include days on which seepage inflow occurs into one part of the CCS at the same time that seepage outflow occurs in another part. This “flow-through” exchange is not reflected in the daily net seepage calculation.

To illustrate the role that net seepage to the aquifer can play in the water budget and solute budgets, consider the cumulative water budget fluxes for the period January 2016 through March 2016, Figures 5 and 9. This corresponds with the later part of the discharge event shown in Figure 1. During this period the discharge of water from the CCS into the aquifer accounted for 40 percent of the net change in volume of water in the CCS. Seepage also accounted for 100 percent of the reduction in salt content.

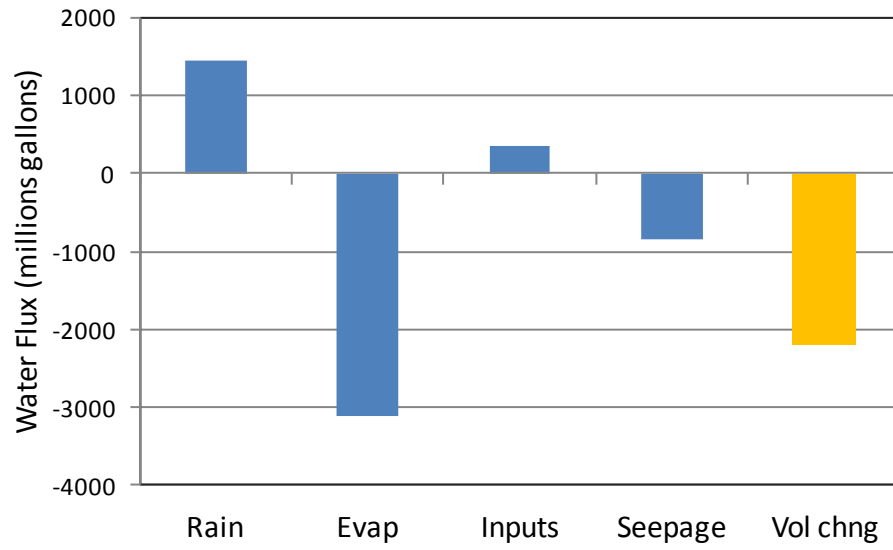
Seepage is an important component of the mass budgets for salt and other dissolved substances that might be of interest. Evaporation removes only water from the CCS, leaving solutes behind, and rainfall and other inputs of water only add solutes. Seepage out of the CCS is the only mechanism for controlling the accumulation of salt and other solutes in the CCS. Reducing salinity is one of the justifications that FPL provided in its applications for permits to add water from the L-31E canal and the Floridan aquifer as new input to the CCS. However, the mechanism that removes salt from the CCS is through seepage discharge into the aquifer.

Table 5: Magnitude of the daily net seepage flux calculated from the water budget (mgd); positive values denote fluxes out of the CCS into the aquifer. Statistics are reported for the entire period Sep 2010 through Nov 2016 in terms of the net flux and fluxes out of and into the CCS taken separately.

	Net Seepage	Seepage out	Seepage in
Average	-6.11	9.06	-15.17
Standard deviation	31.46	18.26	19.53
Maximum	223.31	223.31	0.00
Minimum	-117.19	0.00	-117.19

¹⁶ The volume of water in the CCS ranges between 3.7 to 7.8 billion gallons, with an average of 4.9 billion gallons.

Figure 9: Cumulative water budget fluxes for the period January through March 2016.



Impact on Regional Water Resources

Continued operation of the CCS impacts regional fresh water resources in two ways. First, the CCS competes with other users, such as the public water utilities of the FCAA, Florida City and Homestead, for the limited resources of the surficial aquifer system in south Miami-Dade County. Operations of the ID withdraw fresh water from the Biscayne aquifer at rates comparable to pumping from nearby public water supply wells. Second, hypersaline conditions created in the CCS and active exchange between the CCS and the underlying aquifer feeds the growth of a plume of hypersaline water in the Biscayne aquifer. The movement of this plume westward and to the northwest accelerates the intrusion of saltwater into the Biscayne aquifer toward well fields used for public water supply.

Freshwater Withdrawal by ID pumping

The purpose of the ID is to create a barrier to prevent westward movement of CCS water by seepage through the aquifer. Water is pumped out of the canal to maintain water levels in the ID lower than water levels in the L-31E canal, which runs parallel to the ID, Figure 2. In theory, this assures that the direction of groundwater seepage is always from the L-31E canal into the ID, thus creating a hydraulic barrier to the westward movement of seepage from the CCS. In practice, the ID has failed to prevent the westward movement of the dense hypersaline plume along the bottom of the aquifer, ~ 100 feet below the land surface. The ID is too shallow, ~20 feet deep, to influence the movement of water deep in the aquifer, especially under the conditions where flow in the aquifer is stratified.

Water pumped from the ID is a mixture of saline water that seeps in from the CCS and fresh groundwater seepage from the west. Water pumped out of the CCS is discharged into the CCS, where it contributes to the water budget as a portion of the “other inputs,” Equation 1. The results below are based on daily data on ID pumping and salinity for the ID pumping for period Sep 2010 through Nov 2016.

On any day, the amount of water pumped from the ID, Q_{ID} , is the sum of an amount of water that has seeped into the ID from the west, from Q_{L31} , and an amount of water recycled from the CCS, Q_{RW} ,

$$Q_{ID} = Q_{L31} + Q_{RW}. \quad \text{Eq. 3}$$

Similarly, the amount of salt in the water pumped from the ID is the sum of an amount carried into the ID in seepage from the west and in seepage of recycled water from the CCS;

$$Q_{ID}S_{ID} = Q_{RW}S_{CCS} + Q_{L31}S_{L31}. \quad \text{Eq. 4}$$

From these two equations, one can derive the following formula to calculate the portion of the total daily ID pumping that is fed by seepage from the west:

$$Q_{L31} = Q_{ID}[(S_{CCS} - S_{ID}) / (S_{CCS} - S_{L31})] \quad \text{Eq. 5}$$

The daily rate of pumping from the ID, Q_{ID} , and the salinity of water in the ID, S_{ID} , are measured, Table 6. The salinity measured in the L-31E canal can be taken as representative of the salinity of water seeping into the ID from the west. Shallow groundwater west of the CCS is not totally fresh, as a consequence of infrequent flooding of the wetlands there by water from Biscayne Bay. The salinity of water below the CCS is taken to be 60 gm/l, which reflects the long-term, stable average of salinity measured in a shallow well in the center of the CCS, Figure 10.

Based on these data, calculations reveal that ID pumping removes about 3 mgd of mostly fresh groundwater from the Biscayne aquifer west of the CCS. This is the average of the amount of freshwater extracted calculated using Equation 5 applied with daily values of pumping rate and salinity, Table 6. The pumping rate varies from day to day, and salinity in the ID tends to be higher on days with higher rates of pumping.

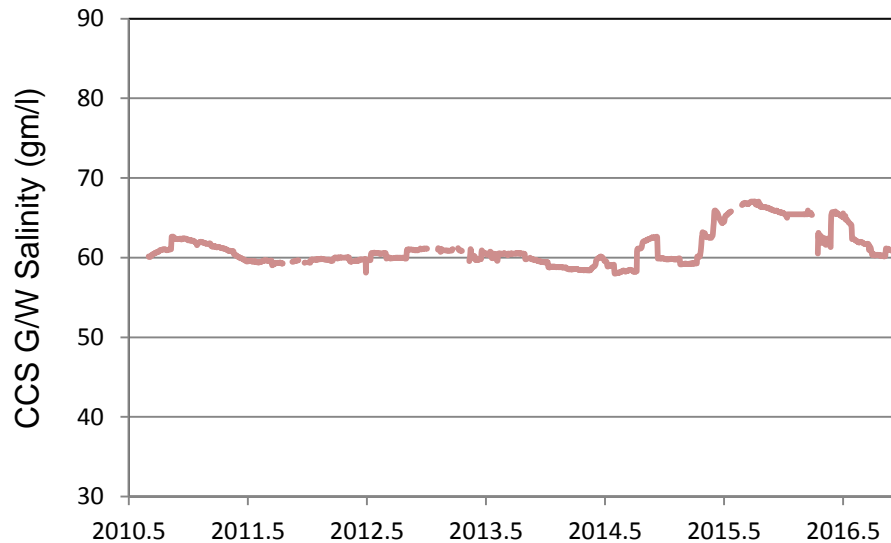
This rate of extraction of freshwater from the Biscayne aquifer is large relative to other withdrawals from the aquifer. Nearby well fields operated by public water utilities¹⁷ withdraw 2 mgd (Florida City), 11 mgd (Homestead), and 17 mgd (FKAA). The withdrawal of freshwater as a consequence of ID operations is not documented in current regional water supply plans. Regional water supply plans include data on water use by power plants. The Lower East Coast water supply plan notes the water withdrawn from the Floridan aquifer for cooling for the gas-fired Unit 5 at Turkey Point, but it does not account for the extraction of water from the Biscayne aquifer to supply water for the CCS.¹⁸ Since the latest update to the Lower East Coast plan, FPL has obtained permits to withdraw additional water for the CCS from the L-31E and from the Floridan aquifer.

Table 6: Calculated rate of freshwater extraction from the Biscayne aquifer by pumping the Interceptor Ditch. Data are for the period June 2015 through November 2016.

	Calculated fresh water flow (mgd)	Measured ID Pump Rate (mgd)	ID salinity	L31E salinity
Average	3.10	3.76	6.15	1.02
Standard deviation	6.51	8.10	5.88	0.88
Maximum	42.78	49.57	38.23	4.86
Minimum	0.00	0.00	1.11	0.18

¹⁷ Water use figures from Table A-8, 2013 LEC Water Supply Plan Update: Appendices, October 10, 2013.

¹⁸ “FPL increased its power generation capacity at the existing Turkey Point plant by adding combined cycle generating technology to respond to significant population growth in South Florida. Unit 5 is a natural gas-fired combined-cycle unit that uses groundwater drawn from the Floridan aquifer while the other four units, Units 1–4, use water from the closed cycle recirculation canal system.”

Figure 10: Salinity of groundwater beneath the CCS (TPGW-13)

Hypersaline Groundwater Plume

High salinity values and elevated water levels in the CCS drive the seepage of hypersaline water through the bottom of the CCS into the porous limestone aquifer. The salinity in the CCS has increased over the 40 years of its operations due to the continual seepage of saline water (~30 mg/l) from Biscayne Bay into the CCS and the concentration of salts by evaporation. By 2010, average salinity values were about 60 parts per thousand, about twice the salinity of seawater. Salinity remained near that value until the summer of 2014, when it began to increase rapidly. Salinity values peaked at around 100 mg/l in June 2015 before declining to around 60 mg/l at the end of 2016.

The continuing seepage of hypersaline water into the aquifer feeds the growth of a dense, hypersaline groundwater plume. Hypersaline water seeping out of the bottom of the CCS accumulates at the bottom of the Biscayne Aquifer in a dense plume. The plume's higher density and the higher water levels in the CCS, maintained by the power plant's circulating pumps, combine to drive lateral movement in the plume toward the west. Lateral movement of the plume occurs near the bottom of the aquifer, below the influence of the interceptor ditch. Over the 40 years of operation of the CCS, the plume of water from the CCS has moved 4 to 5 miles to the west, increasing the intrusion of saltwater into the Biscayne Aquifer.¹⁹ It has been

¹⁹ Simulations with a 2-D groundwater model show that the present location of the salt-fresh interface is about 1.5 miles further west of the position it would have attained if the salinity in the CCS had been held at 35 mg/l for its 40-year operating lifetime. (Giddings, J., 2013. FPL Turkey Point Cooling Canal System Salinity Reduction Proposal Review. South Florida Water Management District, October 2013)

estimated that the plume is driving the westward intrusion of the salt-fresh interface by 600 feet per year.²⁰

In 2013 it was estimated that the aquifer contained more than 120 billion gallons of CCS water.²¹ This figure is based on a GIS analysis to estimate that 17 billion cubic feet (124 billion gallons) of water from the CCS that remained accumulated in the aquifer in the mapped area of the plume. The mapped area includes the area beneath the CCS and the area to the west. Results of a model used by FPL to simulate the plume's development suggest that the plume extends roughly the same distance east, beneath Biscayne Bay. The estimated volume of CCS water in the aquifer is consistent with a long-term average rate of seepage of 8 mgd over the 40-year life of CCS operations. This figure compares favorably with the long-term average discharge by net seepage (9 mgd) and the calculated seepage outflow through the bottom of the CCS reported by FPL (11 mgd for the period September 2010 through November 2015 and 12 mgd for the period June 2015 through November 2016).

The volume of water contained within the plume's mapped boundaries, i.e. the volume that ultimately must be remediated, is considerably larger than the cumulative seepage from the CCS due to mixing in the aquifer with ambient water. The plan to remediate the plume is based on withdrawing 14 mgd of contaminated water for disposal by deep-well injection. However, this rate of withdrawal barely exceeds the rate at which seepage from the CCS currently adds water to the plume, allowing for the uncertainty in the seepage estimates.

²⁰ "According to the DEP's own 2014 management plan, it has advanced at a rate of 525 to 660 feet per year with up to 600,000 pounds of salt escaping daily from the canals." According to 2011 technical report commissioned by FPL: "the study found that canal water had moved 3.5 miles west of the plant and was spreading at a relatively brisk pace of 500 feet a year." [online:

<http://www.miamiherald.com/news/local/environment/article73233802.html#storylink=cpy> ; accessed 4 Jun 2017]

²¹ This figure is based on calculations by SFWMD staff in 2013 of the total volume of CCS water in the mapped portion of the hypersaline groundwater plume, reported in Nuttle, W.K., 2013. Review of CCS Water and Salt Budgets Reported in the 2012 FPL Turkey Point Pre-Uprate Report and Supporting Data. Report to the South Florida Water Management District, 5 April 2013. The mapped portion of the plume includes only the western portion and the portion beneath the CCS. Including the unmapped portion that extends under Biscayne Bay could increase this number by a factor 1.5 to 2.



Sea-level rise and inundation scenarios for national parks in South Florida

Big Cypress National Preserve, Biscayne National Park, Dry Tortugas National Park, Everglades National Park

By Joseph Park, Erik Stabenau, and Kevin Koutun

Abstract

National parks in South Florida are intimately connected to the sea. As sea levels rise, coastal regions of these parks experience both physical and ecological changes. Based on a state-of-the-art sea-level rise projection we propose two sea-level rise trajectories for South Florida, a low projection for general planning purposes and a high projection for risk assessment of sensitive ecological or physical systems. Sea-level rise projections only consider long time horizons; on shorter time scales the growth of recurrent coastal inundation events and storm surges have immediate ecological and physical impacts and we provide quantitative assessments of these processes.

Key words

inundation, sea-level rise, South Florida

The National Park Service (NPS) is tasked with the unimpaired preservation of the natural and cultural resources of the National Park System for the enjoyment, education, and inspiration of current and future generations. This mission and perspective positions the National Park Service as a leader in the recognition of and adaptation to changes in Earth's climate. It is now unequivocal that the climate is warming, and since the 1950s many of the observed changes are unprecedented over decades to millennia. The atmosphere and oceans have warmed, snow and ice have diminished, sea level has risen, and concentrations of greenhouse gases have increased (Steffan et al. 2015; IPCC 2013).

One of the most robust indicators of climate change is rising sea level driven by thermal expansion of ocean water and addition of land-based ice-melt to oceans. Sea-level rise is not evenly distributed around the globe, and the response of a regional coastline is highly dependent on local natural and human settings (Cazenave and Le Cozannet 2014). Nowhere is this more evident than in the national parks and national preserve located at the southern end of the Florida peninsula—Dry Tortugas, Biscayne, and Everglades National Parks and Big Cypress National Preserve—where low elevations and exceedingly flat topography provide an ideal setting for encroachment of the sea.

The physical and ecological impacts of sea-level rise on these parks will be pronounced, and in some cases, such as the distribution of mangrove forests, change

has already been observed (Krauss et al. 2011). The natural ecological capacity for adaptation and resilience to these changes will be enhanced through the timely implementation of the Comprehensive Everglades Restoration Plan (CERP), simultaneously protecting the regional water supply for both natural and urban needs (NRC 2014).

Given these current and anticipated changes, it is prudent to define expectations for sea-level rise and the associated physical responses over the coming decades. This article is intended to inform the current state of science regarding these expectations.

Sea-level rise

The Intergovernmental Panel on Climate Change (IPCC) is composed of leading scientists from around the world whose mission is to review and assess the most recent scientific, technical, and socioeconomic information relevant to the understanding of climate change. Its most recent assessment, published in 2013, is the Fifth Assessment Report (AR5), which includes projections of global sea-level rise based on different representation concentration pathway (RCP) scenarios reflecting possible scenarios for future concentrations of greenhouse gases. RCP 8.5 is the highest emission and warming scenario under which greenhouse gas concentrations continue to rise throughout the 21st century, while RCP 6 and RCP 4.5 expect substantial emission declines to begin near 2080 and 2040, respectively.

The IPCC sea-level rise scenarios are comprehensive, but do not include contributions from a potential collapse of Antarctic ice sheets. However, recent evidence suggests that such a collapse may be under way (Holland et al. 2015; Wouters et al. 2015). In addition, the IPCC projections do not account for local processes such as land uplift or subsidence and ocean currents, and do not provide precise estimates of the probabilities associated with specific sea-level rise scenarios, which are a crucial decision support metric in the development and assessment of risk.

A contemporary estimate of local effects and comprehensive probabilities for the RCP scenarios is provided by Kopp et al. (2014). This work is based on a synthesis of tide gauge data, global climate models, and expert elicitation, and includes consideration of the Greenland ice sheet, West and East Antarctic ice sheets, glaciers, thermal expansion, regional ocean dynamic effects, land water storage, and long-term, local, nonclimatic factors such as glacial isostatic adjustment, sediment compaction, and tectonics. Following a review of scientific literature, we have adopted the work of Kopp et al. (2014) as the basis for sea-level rise scenarios at the four South Florida national parks.

Datums and mean sea level

A tidal datum provides a geodetic link between ocean water level and a land-based elevation reference such as the North American Vertical Datum of 1988 (NAVD88). The National Tidal Datum Epoch (NTDE) in the United States is a 19-year period over which

tidal datums specific to each tide gauge are determined. The current NTDE for the United States is 1983–2001 and sea-level rise projections are referenced to the midpoint of this period (1992), consistent with procedures for sea-level rise design determined by the U.S. Army Corps of Engineers (USACE) and the National Oceanic and Atmospheric Administration’s (NOAA) National Climate Assessment (USACE 2014). Common tidal datums include mean sea level (MSL), mean high-higher water (MHHW), and mean low-lower water (MLLW) as defined by NOAA (Center for Operational Oceanographic Products and Services 2013). As sea level rises, tidal datum elevations also rise, and a new tidal datum is established every 20 to 25 years to account for sea-level change and vertical adjustment of the local landmass (Center for Operational Oceanographic Products and Services 2000).

Kopp et al. (2014) use a local mean sea-level reference starting in the year 2000 instead of the NTDE MSL datum centered on 1992. To convert these projections to NTDE we estimate mean sea-level rise over the 1992 to 2000 period at Vaca Key with a nonlinear trend analysis and add the resulting value of 1.4 cm (0.6 in) to their projections. All projected water levels are then converted to NAVD88 by subtraction of the 25.3 cm (10.0 in) NAVD88 to NTDE MSL offset at the Vaca Key tide station.

Projection

Examination of local sea-level rise projections around South Florida finds small differences among Naples, Virginia Key, Vaca Key, and Key West, which are geographically closest to Big Cypress National Preserve, Biscayne National Park, Everglades National Park, and Dry Tortugas National Park, respectively. We chose the Vaca Key station sea-level data as representative of all four natural areas since it best reflects local oceanographic processes that influence coastal sea levels around South Florida.

Regarding selection of greenhouse gas emission scenarios, we employ RCP 8.5, also known as the “business-as-usual” scenario in which greenhouse gas emissions continue to rise. Although significant rhetoric is aimed at global emissions reduction, emissions continue to escalate and presently there is no clear socioeconomic driver to depart from a carbon-based energy infrastructure. More specifically, recent assessments of global energy production and population conclude that the RCP 4.5 emission scenario is unobtainable, and there is significant uncertainty as to whether the RCP 6.0 scenario can be realized (Jones and Warner 2016).

Each emission scenario and geographic location will have a spectrum of projections that span the possible ranges of sea-level rise, and this range is expressed as a probability of occurrence. A probability is commonly understood as the chance or likelihood of an event happening out of a large pool of possible events, and in this case the probability refers to occurrence of a specific sea-level rise curve out of the many possible curves under a particular climate scenario. Many different curves are possible for each scenario since there are uncertainties in the observable data (e.g., ice sheets and thermal expansion) as well as limitations in the models from which the projections are

derived. The median projection (50th percentile) is in the middle of the projections (one-half of the projections are lower, one-half are higher) and can be considered a likely scenario given the current state of knowledge. A high percentile projection such as the 99th percentile is one with only a 1% chance that sea levels would exceed it, and is considered a worst-case scenario.

Since this projection is intended to inform authorities of sea-level rise for adaptation and planning purposes, and in light of the significant uncertainties inherent in generation of the projections and future dynamics of the climate, it is prudent to consider the upper percentile range of projections. In evaluating these factors we select the RCP 8.5 median (50th percentile) as the lower boundary of the projection, and the 99th percentile as the upper boundary. We are therefore conservatively biasing the projections to lie between a lower bound of likely sea-level rise and a high projection representing an upper limit to be considered in risk assessments for highly vulnerable, costly, or risk-averse applications. We emphasize that the high projection is deemed to have only a 1% chance of occurrence under current climate conditions, but in the event of Antarctic ice sheet collapse, its projected sea-level rise is consistent with estimates that include Antarctic ice melt contribution (DeConto and Pollard 2016).

The sea-level rise projection for South Florida referenced to the NAVD88 datum for the RCP 8.5 emission scenario and occurrence probabilities of 50% and 99% is shown in figure 1, and is tabulated in tables 1A and 1B. These projections have been offset to match currently observed mean sea level in Florida Bay over the period 2008–2015 shown in figure 2 and tabulated in [appendix 1](#). These projections do not include tides or storm surges. Water levels will be both higher and lower than mean sea level depending on the tidal, weather, and storm conditions.

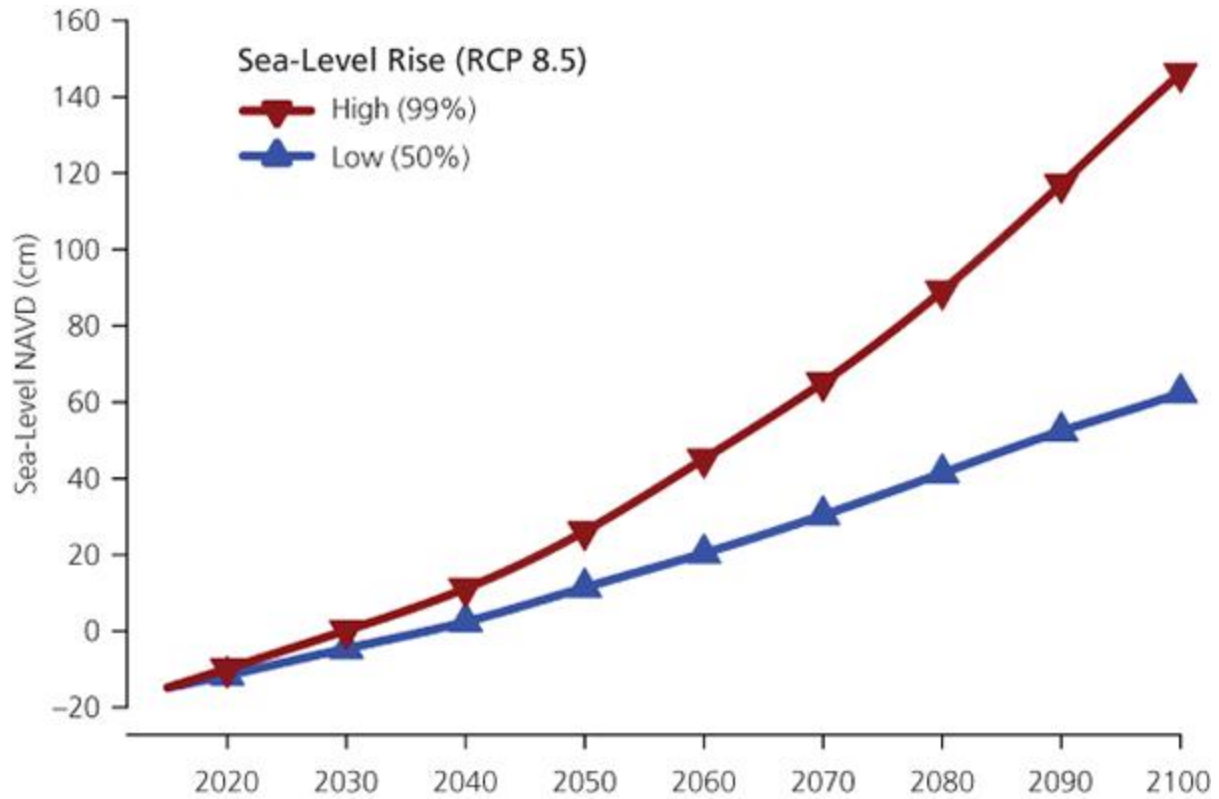


Figure 1. South Florida sea-level rise projection in centimeters NAVD for the RCP 8.5 greenhouse gas emission scenario. Low projection in blue is the median (50th percentile), high projection in red (99th percentile). Tides and storm surges are not included in this projection. Full values are tabulated in tables 1A and 1B below.

MSL 6-30-2008 to 6-30-2015: -14.8 (cm) NAVD

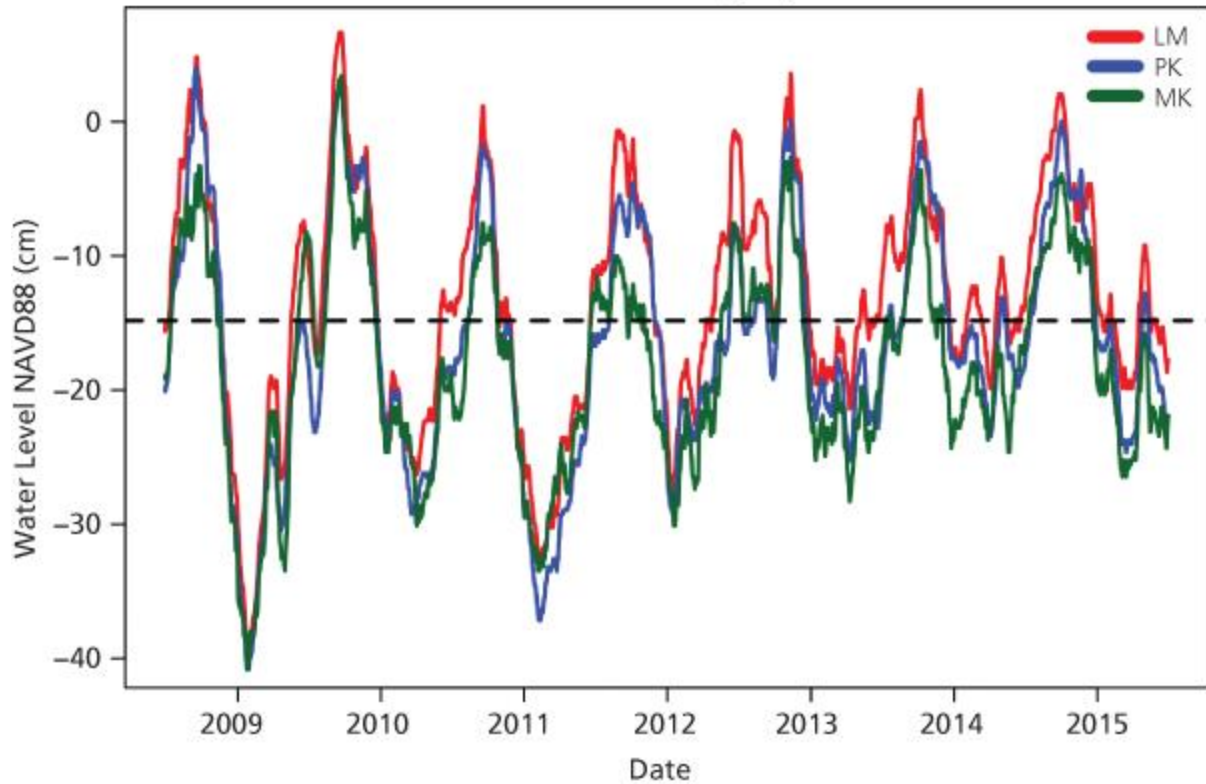


Figure 2. Thirty-day moving averages of daily mean sea level at Murray Key (MK), Peterson Key (PK), and Little Madeira Bay (LM) in Florida Bay. The dashed line is the mean of all three data sets. Data are available in the linked file.

Table 1A. Sea-level rise projection: NAVD88 (cm)											
Year	Low	High	Year	Low	High	Year	Low	High	Year	Low	High
2015	-14.8	-14.8	2045	6.8	18	2075	35.8	76.6	2105	68.3	159.9
2016	-14.2	-13.8	2046	7.7	19.6	2076	36.9	79	2106	69.5	162.7
2017	-13.6	-12.8	2047	8.6	21.1	2077	38	81.5	2107	70.8	165.4
2018	-12.9	-11.8	2048	9.6	22.8	2078	39.2	84	2108	72	168.3
2019	-12.3	-10.8	2049	10.5	24.4	2079	40.3	86.5	2109	73.2	171.2
2020	-11.6	-9.8	2050	11.4	26.2	2080	41.4	89.2	2110	74.4	174.2
2021	-10.9	-8.9	2051	12.3	27.9	2081	42.6	91.8	2111	75.6	177.2
2022	-10.2	-7.9	2052	13.2	29.7	2082	43.7	94.5	2112	76.7	180.3
2023	-9.5	-6.9	2053	14.1	31.6	2083	44.8	97.2	2113	77.9	183.5
2024	-8.8	-5.9	2054	15	33.5	2084	45.9	100	2114	79	186.8
2025	-8.1	-4.9	2055	15.9	35.4	2085	47.1	102.8	2115	80.1	190.1
2026	-7.4	-3.9	2056	16.8	37.3	2086	48.2	105.6	2116	81.2	193.4

2027	-6.7	-2.9	2057	17.7	39.3	2087	49.3	108.5	2117	82.2	196.8
2028	-6	-1.9	2058	18.6	41.2	2088	50.3	111.3	2118	83.3	200.2
2029	-5.3	-0.9	2059	19.5	43.2	2089	51.4	114.2	2119	84.4	203.7
2030	-4.6	0.2	2060	20.4	45.2	2090	52.4	117.2	2120	85.4	207.2
2031	-3.9	1.2	2061	21.4	47.1	2091	53.4	120.1			
2032	-3.2	2.2	2062	22.3	49	2092	54.4	123			
2033	-2.6	3.2	2063	23.3	51	2093	55.4	125.9			
2034	-1.9	4.3	2064	24.3	52.9	2094	56.3	128.9			
2035	-1.2	5.3	2065	25.3	54.9	2095	57.3	131.8			
2036	-0.5	6.4	2066	26.3	56.9	2096	58.3	134.7			
2037	0.2	7.6	2067	27.3	58.9	2097	59.3	137.6			
2038	0.9	8.7	2068	28.3	60.9	2098	60.3	140.5			
2039	1.6	9.9	2069	29.4	63	2099	61.3	143.3			
2040	2.4	11.2	2070	30.4	65.2	2100	62.4	146.2			
2041	3.2	12.4	2071	31.5	67.3	2101	63.5	148.9			
2042	4.1	13.8	2072	32.6	69.6	2102	64.7	151.7			
2043	5	15.1	2073	33.6	71.8	2103	65.9	154.4			
2044	5.9	16.6	2074	34.7	74.2	2104	67.1	157.1			

Notes: Sea-level rise in centimeters NAVD88 from Kopp et al. (2014) at Vaca Key, Florida. Values between decades (e.g., 2010, 2020) have been interpolated with a third-order polynomial fit. Low is the 50th percentile of the RCP 8.5 projection, high the 99th percentile. An offset of 1.4 cm (0.6 in) has been added to account for sea-level rise from 1992 to 2000 to convert the Kopp projections starting in 2000 to the NTDE MSL datum of 1992. The NAVD88 datum is 25.3 cm (10.0 in) above the NTDE MSL so that 25.3 cm has been subtracted to convert NTDE MSL to NAVD88. The projections have been offset to match observed mean sea level over the period 2008–2015 in Florida Bay of -14.8 cm (-5.8 in) NAVD88 (see [appendix 1](#)).

Table 1B. Sea level rise projection: NAVD88 (ft)

Year	Low	High	Year	Low	High	Year	Low	High	Year	Low	High
2015	-0.49	-0.49	2045	0.22	0.59	2075	1.17	2.51	2105	2.24	5.25
2016	-0.47	-0.45	2046	0.25	0.64	2076	1.21	2.59	2106	2.28	5.34
2017	-0.45	-0.42	2047	0.28	0.69	2077	1.25	2.67	2107	2.32	5.43
2018	-0.42	-0.39	2048	0.31	0.75	2078	1.29	2.76	2108	2.36	5.52
2019	-0.40	-0.35	2049	0.34	0.80	2079	1.32	2.84	2109	2.40	5.62

2020	-0.38	-0.32	2050	0.37	0.86	2080	1.36	2.93	2110	2.44	5.72
2021	-0.36	-0.29	2051	0.40	0.92	2081	1.40	3.01	2111	2.48	5.81
2022	-0.33	-0.26	2052	0.43	0.97	2082	1.43	3.10	2112	2.52	5.92
2023	-0.31	-0.23	2053	0.46	1.04	2083	1.47	3.19	2113	2.56	6.02
2024	-0.29	-0.19	2054	0.49	1.10	2084	1.51	3.28	2114	2.59	6.13
2025	-0.27	-0.16	2055	0.52	1.16	2085	1.55	3.37	2115	2.63	6.24
2026	-0.24	-0.13	2056	0.55	1.22	2086	1.58	3.46	2116	2.66	6.35
2027	-0.22	-0.10	2057	0.58	1.29	2087	1.62	3.56	2117	2.70	6.46
2028	-0.20	-0.06	2058	0.61	1.35	2088	1.65	3.65	2118	2.73	6.57
2029	-0.17	-0.03	2059	0.64	1.42	2089	1.69	3.75	2119	2.77	6.68
2030	-0.15	0.01	2060	0.67	1.48	2090	1.72	3.85	2120	2.80	6.80
2031	-0.13	0.04	2061	0.70	1.55	2091	1.75	3.94			
2032	-0.10	0.07	2062	0.73	1.61	2092	1.78	4.04			
2033	-0.09	0.10	2063	0.76	1.67	2093	1.82	4.13			
2034	-0.06	0.14	2064	0.80	1.74	2094	1.85	4.23			
2035	-0.04	0.17	2065	0.83	1.80	2095	1.88	4.32			
2036	-0.02	0.21	2066	0.86	1.87	2096	1.91	4.42			
2037	0.01	0.25	2067	0.90	1.93	2097	1.95	4.51			
2038	0.03	0.29	2068	0.93	2.00	2098	1.98	4.61			
2039	0.05	0.32	2069	0.96	2.07	2099	2.01	4.70			
2040	0.08	0.37	2070	1.00	2.14	2100	2.05	4.80			
2041	0.10	0.41	2071	1.03	2.21	2101	2.08	4.89			
2042	0.13	0.45	2072	1.07	2.28	2102	2.12	4.98			
2043	0.16	0.50	2073	1.10	2.36	2103	2.16	5.07			
2044	0.19	0.54	2074	1.14	2.43	2104	2.20	5.15			

Notes: Sea-level rise in feet NAVD88 from Kopp et al. (2014) at Vaca Key, Florida. Values between decades (e.g., 2010, 2020) have been interpolated with a third-order polynomial fit. Low is the 50th percentile of the RCP 8.5 projection, high the 99th percentile. An offset of 0.55 inch (1.40 cm) has been added to account for sea-level rise from 1992 to 2000 to convert the Kopp projections starting in 2000 to the NTDE MSL datum of 1992. The NAVD88 datum is 0.83 feet (0.25 m) above the NTDE MSL so that 0.83 feet has been subtracted to convert NTDE MSL to NAVD88. The projections have been offset to match observed mean sea level over the period 2008–2015 in Florida Bay of -0.49 feet (-0.15 m) NAVD88 (see [appendix 1](#)).

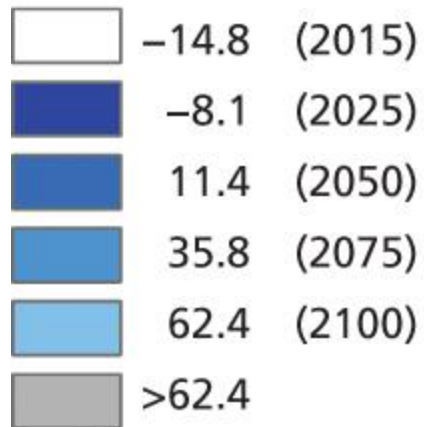
Hypsographic maps

The impact of sea-level rise on a landscape is largely controlled by topography. In southwestern Florida, Everglades National Park contains a broad, flat, freshwater slough (Shark River Slough) that connects to the coastal ocean by rivers along the west coast, and by small passes through a slightly elevated marl ridge on the southern coast. Directly south of this coastal ridge is Florida Bay, a basin formed approximately 4,000 years ago as rising sea level flooded the region. In southeastern Florida, Biscayne National Park contains a mangrove fringe bordered by canals and developed properties, and islands within the park are typically less than 2 m (6.6 ft) above sea level. Not far away are the low-lying islands of Dry Tortugas National Park, located about 113 km (70 mi) west of Key West. Each of these areas will be affected by sea-level rise in different ways as shown in figures 3 and 4, which are water-level elevation maps based on the sea-level rise projections through 2100 overlaid on a digital elevation model of the region (Fennema et al. 2013). These projections do not include tides or storm surge and are available online at <http://nps.maps.arcgis.com> (Alarcón 2016).

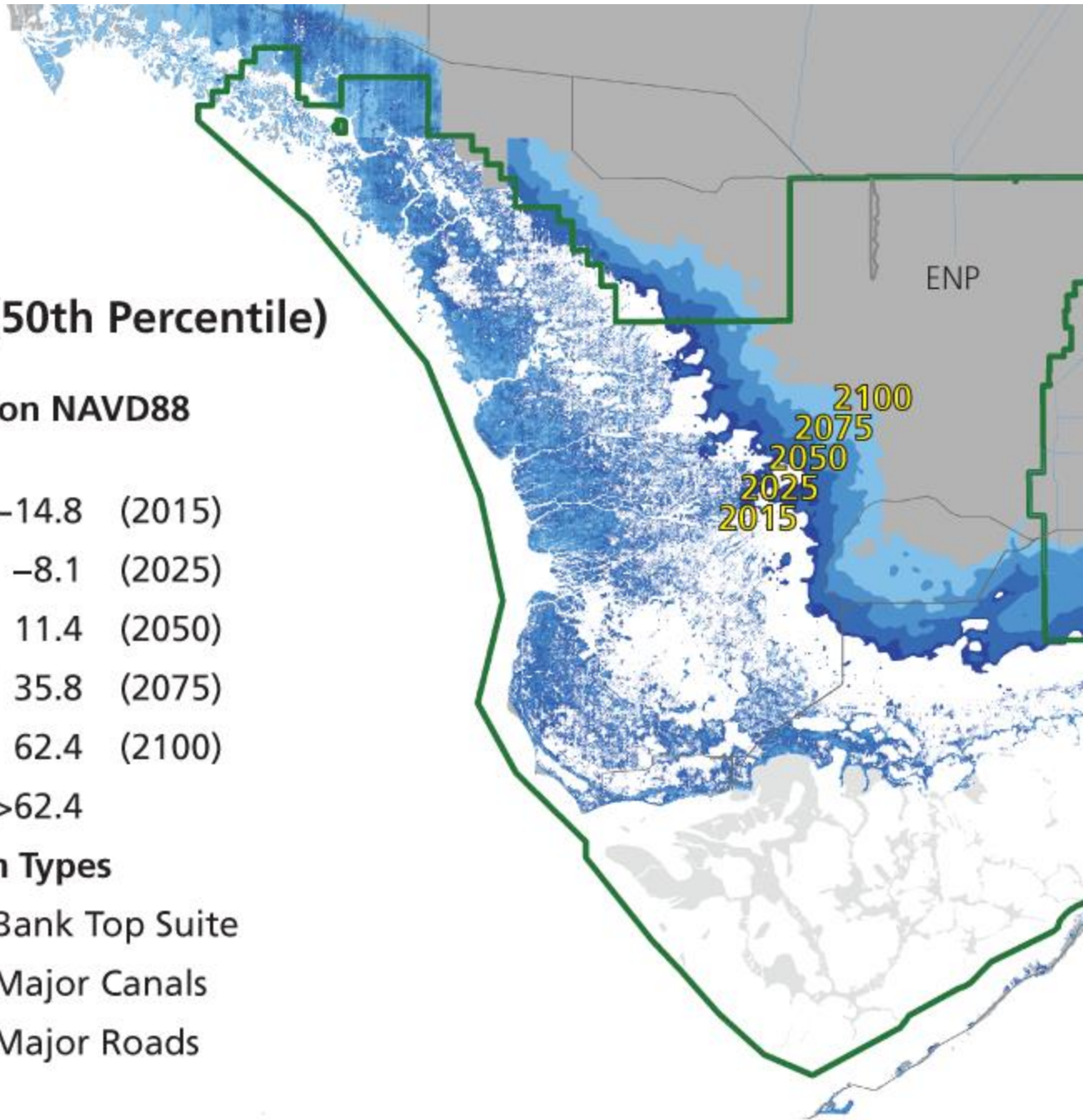
COMPARISON OF 50TH AND 99TH PERCENTILE SEA-LEVEL RISE PROJECTIONS

Low (50th Percentile)

Elevation NAVD88
cm



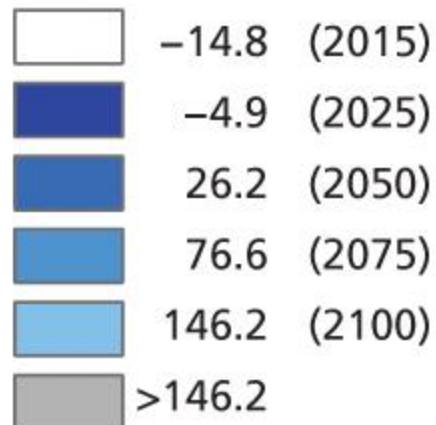
Bottom Types



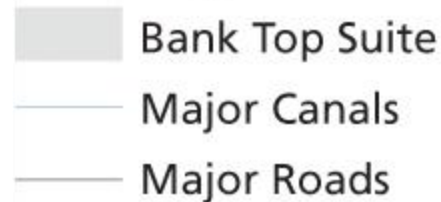
High (99th Percentile)

Elevation NAVD88

cm



Bottom Types



NPS/Everglades National Park
NPS/Everglades National Park

Figure 3. Mean sea-level elevation maps for South Florida including Everglades and Biscayne National Parks for the median (50th, left [A]) and high (99th percentile, right [B]) RCP 8.5 projections using current topography and NAVD-referenced digital elevation data. Tides and storm surges are not included in either projection.

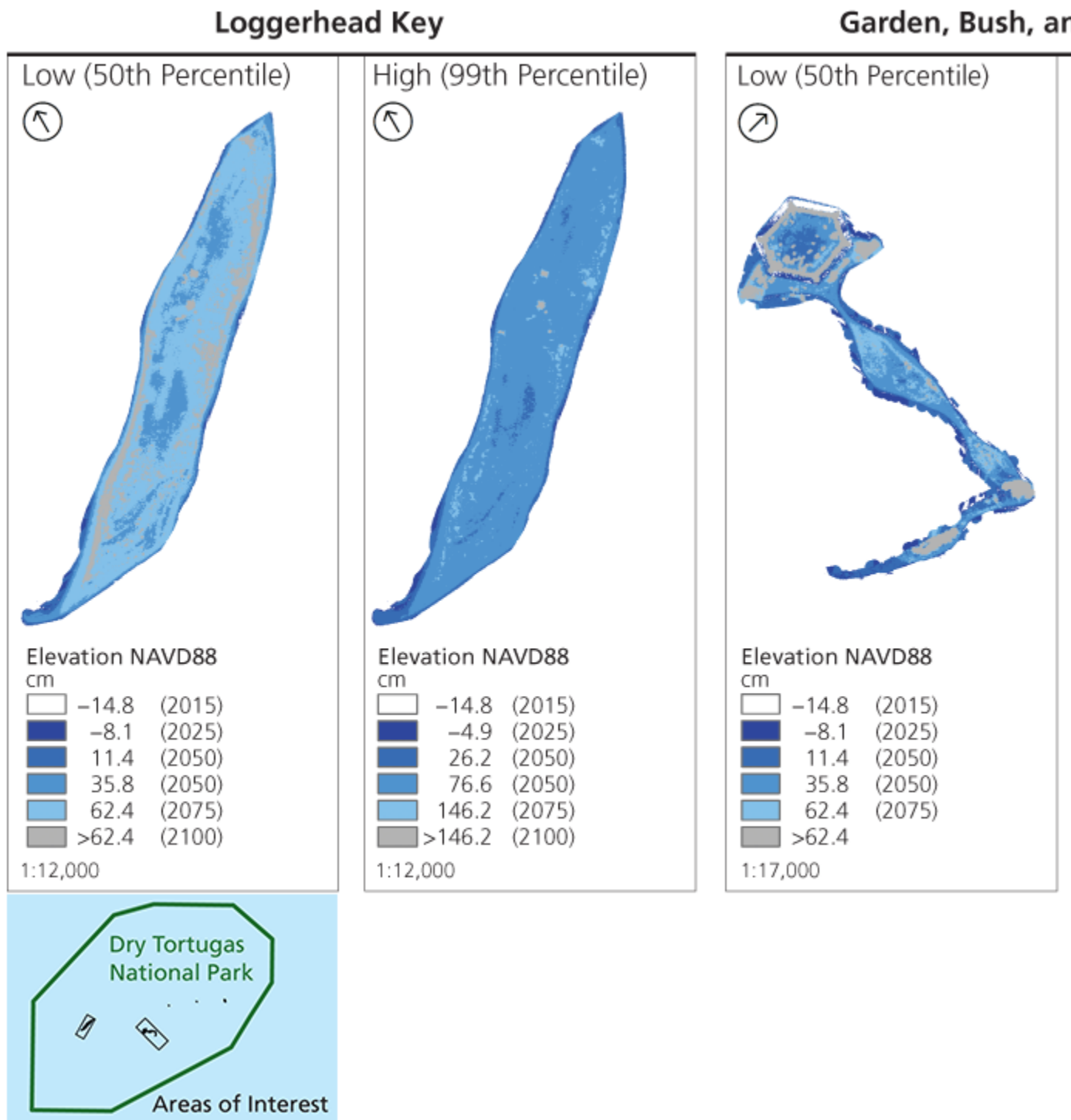
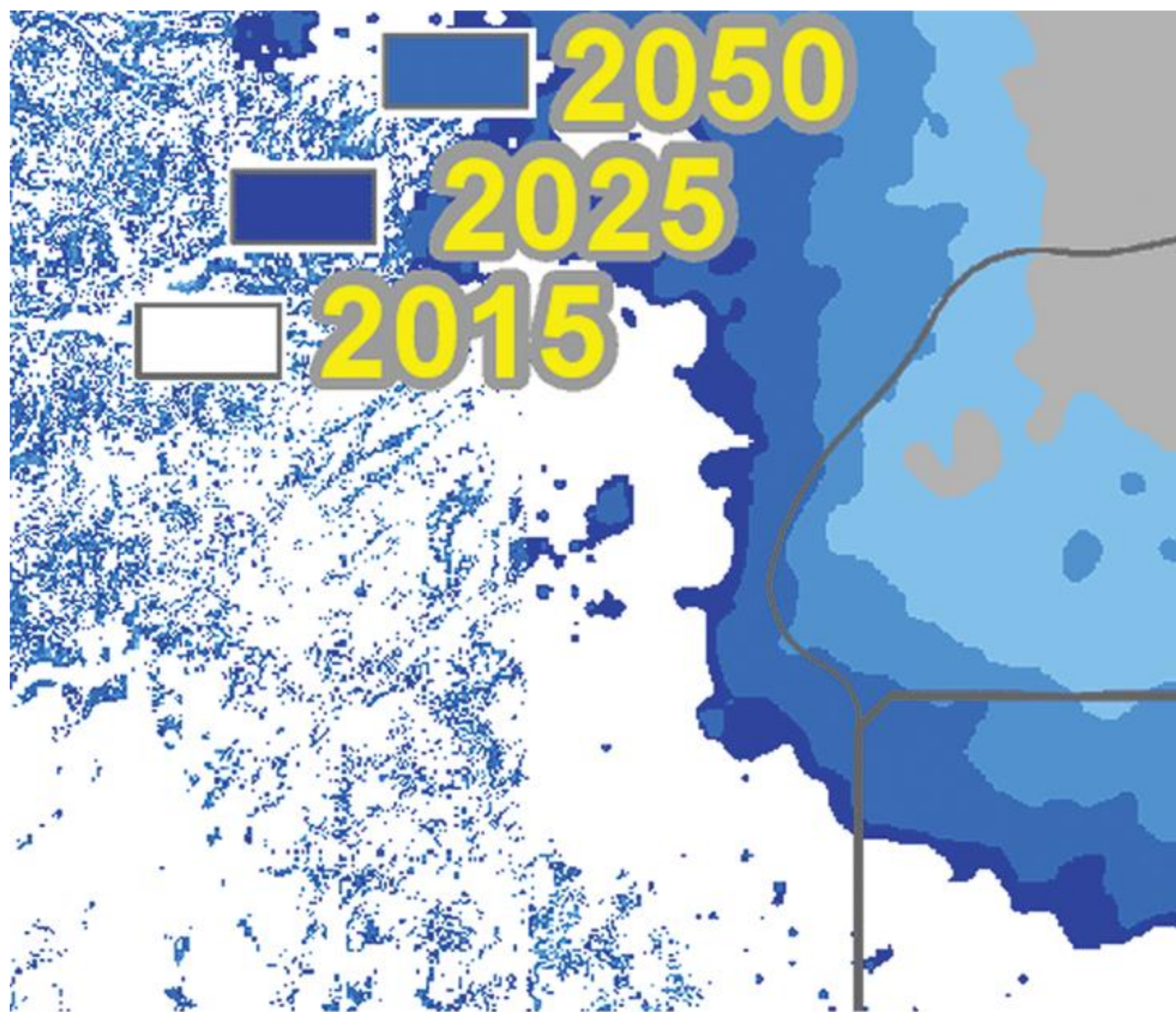


Figure 4. Mean sea-level elevation maps for Dry Tortugas National Park showing conditions at Loggerhead, Garden, Bush, and Long Keys for the median (50th) and high (99th percentile) RCP 8.5 projections using current topography and NAVD. Tides and storm surges are not included in this projection. Data are presented in the linked file.

As previously noted, the projections are adjusted to match mean sea level in Florida Bay over the period 2008–2015 (–14.8 cm NAVD88), which is represented in the maps with a white color level. This could be misleading since it indicates that southern Everglades National Park is currently at mean sea level and possibly inundated with seawater. However, these regions are freshwater marsh and freshwater to salt-tolerant transition zones. It is important to realize there is a dynamic equilibrium between freshwater flowing from the Everglades and the sea, and with sufficient freshwater elevation the seawater is effectively kept at bay. Another important factor is the buttonwood and mangrove ridge defining the boundary between Florida Bay and freshwater marsh that serves as a hydraulic barrier allowing the freshwater to maintain elevations above mean sea level, thus limiting saltwater intrusion. This ridge will eventually be permanently inundated, allowing seawater to flow freely inland, but even then as Florida Bay expands, freshwater flowing downstream will serve to mitigate the extent of saltwater intrusion. As a result, mean sea-level elevations on the maps may not correspond to a marine environment. For example, figure 5 compares the current and projected sea-level elevations at the 50th percentile with an aerial photograph of the region near the Ingraham Highway in Everglades National Park. Although the current mean sea-level elevation dominates the lower portion of the region, this is not a marine environment but a transition zone between mangroves and freshwater marsh.

COMPARISON OF SEA-LEVEL ELEVATIONS—MAP AND AERIAL PHOTO





NPS/Everglades National Park
NPS/Everglades National Park

Figure 5. Comparison of sea-level elevations applied to digital elevation data (left) with an aerial photograph of the corresponding mangrove and marsh transition zone (right).

Influences of sea-level rise

Over the next 10 years, represented by the 2025 estimates, dramatic change in sea level is not anticipated. The expected sea-level rise is 7 cm (3 in) for the low scenario and 10 cm (4 in) for the high projection. These changes will result in more frequent tidal inundation along coastal regions; however, the buttonwood ridge located along the north shore of Florida Bay will remain above sea level. This modest increase is not likely to have an impact on the terrestrial portions of Dry Tortugas or Biscayne National Parks; however, the increased sea level will likely reduce freshwater flow from the Biscayne Bay coastal wetlands into Biscayne National Park.

By 2050 sea level is expected to increase between 26 and 41 cm (10 to 16 in). The effect on Shark Slough is similar for both projections with an increase in perennially inundated areas. It is difficult to project ecological impacts here since the amount of freshwater exerts important influence over the ecological response. Taylor Slough appears to experience significant impact under both scenarios with increasing pressure from sea level advancing up the slough perhaps as far as the Old Ingraham Highway. The eastern panhandle of the park is more heavily impacted by the high estimate than the low estimate simply because the high estimate exceeds the land surface elevation in this area and begins to overtop the buttonwood ridge.

By 2075 sea-level elevations are expected to increase by 51 and 91 cm (20 and 36 in) for the low and high projections, respectively. Assuming that the buttonwood ridge does not increase in elevation from accretion or deposition, it appears that sometime between 2050 and 2075 much of the buttonwood ridge will be permanently inundated. This could signal an important tipping point in the ecological response of freshwater marshes since freshwater basins delineated by the ridge will no longer be viable. It appears likely that these impacts will extend to the Ingraham Highway.

By 2100 the projected sea-level rise is 77 cm (30 in) for the low projection and 161 cm (63 in) for the high scenario. It is likely that widespread ecological changes will be evident around the coastal Everglades as Florida Bay expands. In the case of the low-lying islands of Biscayne and Dry Tortugas National Parks, many of these can be expected to become submerged.

One important caveat is that these inundation projections do not account for land elevation changes, either positive or negative, as may be observed as water level and salinity change over time. It is well understood that increased freshwater flow, as expected with Everglades restoration efforts, will help to protect against freshwater peat collapse by maintaining soil elevation and reducing the extent of saltwater intrusion (NRC 2014).

Park infrastructure

In addition to natural system ecological changes as sea level rises, visitor facilities and park infrastructure will also accrue impacts. For example, figure 6 presents application of the two sea-level rise scenarios to the Everglades National Park main entrance and Ernest F. Coe Visitor Center. These are comparisons of projected mean sea level with the best available land elevations surrounding the infrastructure and do not represent

the actual finished floor elevations of the structures, which are likely higher than the surrounding land elevation. It is also important to note that mean sea level in Florida Bay fluctuates by approximately 30–40 cm in a yearly oceanographic cycle, as well as monthly and daily cycles from tides, so that effects of tidal inundation will be observed before the projected dates when mean sea level reaches a specific land elevation.

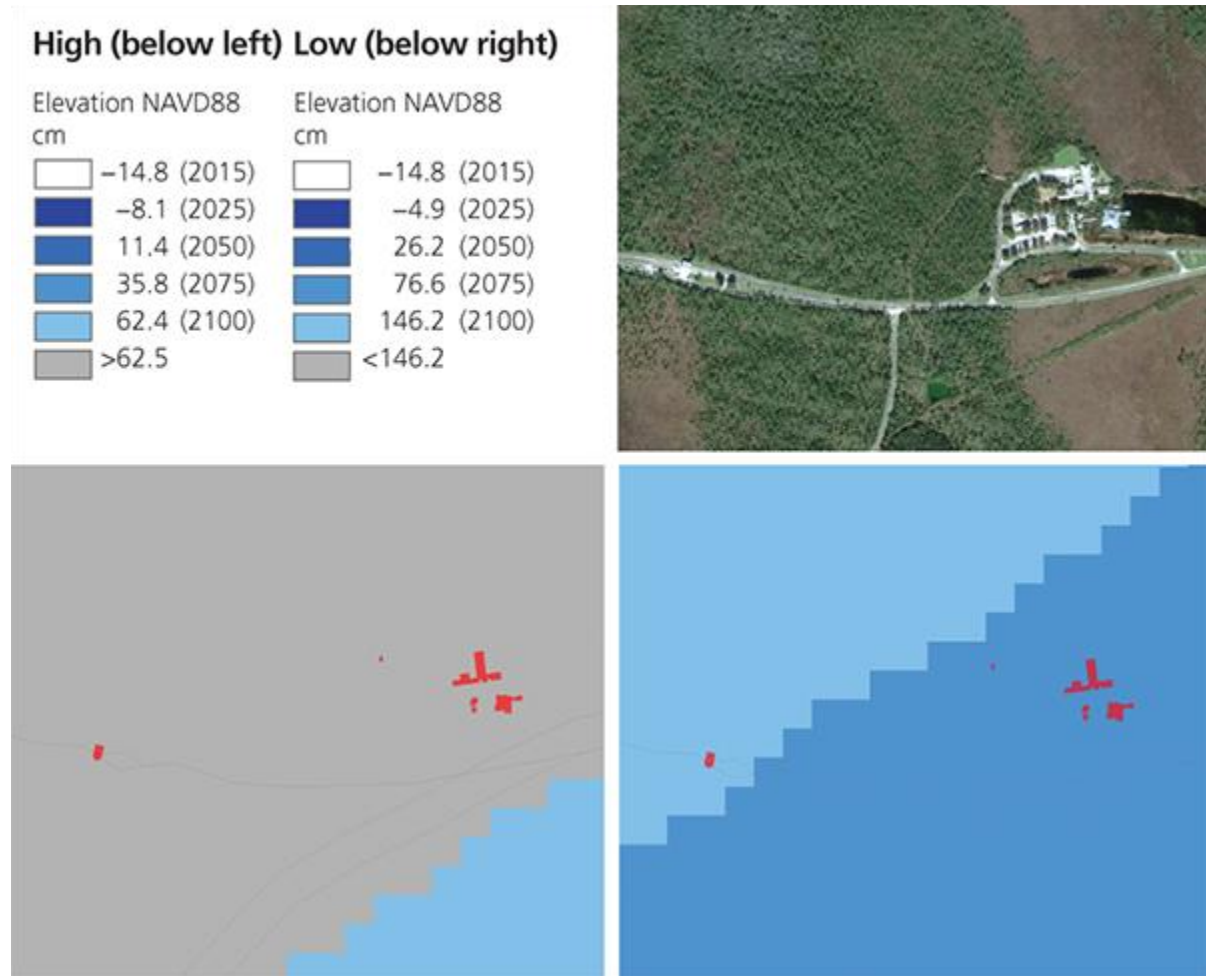


Figure 6. Projected mean sea-level elevations at Ernest F. Coe Visitor Center, Everglades National Park, and the main park entrance. Under the low sea-level rise scenario these buildings will not be perennially inundated out to 2100 (lower left). In the high projection (lower right), land surrounding the visitor center can be expected to be tidally inundated by 2075, while the park entrance will experience tidal inundation by 2100.

NPS/Everglades National Park

While some Everglades infrastructure such as the Ernest F. Coe Visitor Center, main park entrance, and Daniel Beard and Robertson Centers are projected to be unaffected by the low sea-level rise scenario out to 2100, all of these locations would be tidally inundated under the high sea-level rise projection at horizons from 2075 to 2100. Everglades central receiving, the Royal Palm Visitor Center, and the Nike missile silos are expected to be at mean sea level by 2100 under the low projection and by 2075 under the high scenario. Conditions at Flamingo are mixed, with the low projection forecasting the housing and visitor center to remain above mean sea level out to 2100,

but with the boat basin, maintenance yard, and water plant reaching mean sea level by 2100. Under the high projection the housing area is at mean sea level by 2100, the visitor center will be partially inundated by 2050, and the maintenance yard and water plant will be tidally inundated by 2075.

At Dry Tortugas National Park the projections indicate that as early as 2075 or as late as 2100 Loggerhead Key will be tidally submerged. At Fort Jefferson the north coal docks and campground remain above mean sea level to 2100 while areas around the ferry dock and the isthmus to Bush and Long Keys are expected to be at mean sea level by 2075 under the low sea-level rise projection. Under the high projection much of the north coal dock and campground will be at mean sea level by 2075, as will much of the land between the ferry dock and moat, although a portion of this will be at sea level by 2050. The isthmus to Bush Key will be at mean sea level by 2050.

Florida Current

These mean sea-level estimates represent the contemporary state of the art in local sea-level rise projection. However, knowledge of all processes and feedbacks driving sea levels is limited, and the models on which these projections are based are necessarily incomplete. The models do not have the spatial resolution required to resolve significant fine-scale oceanographic processes such as variability in the Florida Current. The Florida Current is one of the strongest and most climatically important ocean currents and forms the headwater of the Gulfstream (Gyory et al. 1992). As the Florida Current fluctuates in intensity, sea levels along the Atlantic coast of Florida respond by falling when the current increases, and rising when current decreases (Montgomery 1938).

The Gulfstream and Florida Current are components of the Atlantic meridional overturning circulation (AMOC), a component of the global ocean conveyor belt. Climate models agree that as the ocean warms and fresh meltwater is added, there will be a decline in the strength of the AMOC (Rahmstorf et al. 2015). If the Florida Current decreases in strength, then sea levels will rise along the Florida east coast and in Florida Bay, which is the southernmost extent of Everglades National Park. The extent of this change is difficult to forecast, but recent evidence suggests that a 10% decline in transport has contributed 60% of the roughly 7 cm (2.8 in) increase in sea level at Vaca Key over the last decade (Park and Sweet 2015). It is therefore plausible that a drastic slowdown of the AMOC and Florida Current could contribute an additional 10–15 cm (3.9–5.9 in) of sea-level rise to South Florida over this century. This potential is not reflected in the sea-level rise projections, but should be acknowledged by authorities and planners who use them.

Inundation and nuisance (recurrent) flooding

Sea-level rise is slow and difficult to discern when compared to the dynamic impacts of changing seasons and storms. Though a drastic change in sea level requires centuries or millennia, pronounced changes in the frequency and heights of coastal inundation

along low-lying coastlines can occur in decades, and such changes are now evident around the United States over the last few decades as sea levels rise (Sweet and Park 2014). For example, the number of daily water-level exceedances per year above the 1993–2011 mean water level in Long Sound of Florida Bay within Everglades National Park is shown in figure 7. The curves show best-fit models based on general linear and geometric growth, suggesting that in the last decade the frequency of low-level inundations has transitioned from a slow, steady increase to one of escalating occurrences. These changes are a consequence of sea-level rise transitioning high water-level exceedances from low-chance events to common events, and this change is accelerating.

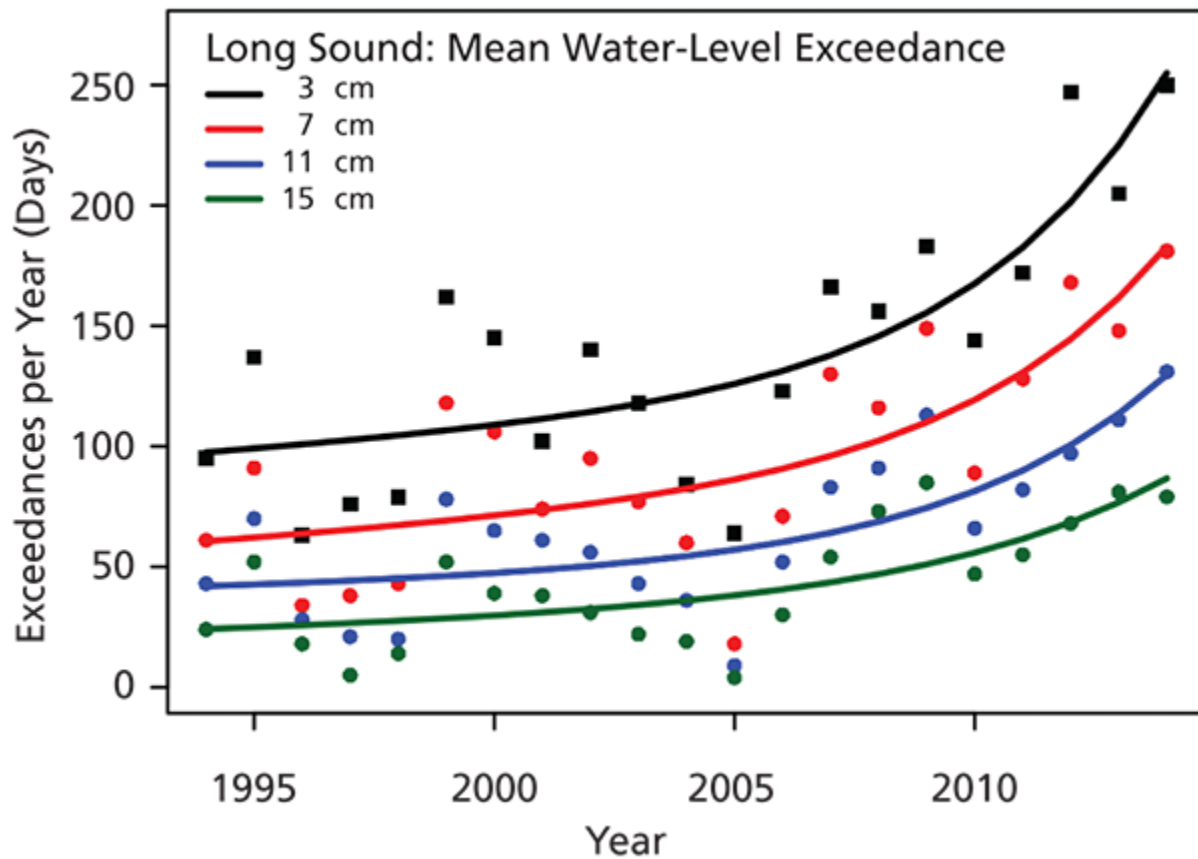


Figure 7. Daily water-level exceedances above the 1993–2011 mean water level in Long Sound of Florida Bay, Everglades National Park.

NPS/Everglades National Park

Infrequent high-impact flooding (storm surge)

Although sea-level rise and the associated increases in recurrent flooding are important physical stresses on South Florida natural areas, it is the infrequent but high-impact storm surge events that drastically change the landscape over the course of a few hours. For example, Hurricane Wilma in 2005 had a profound impact on the ecology of the Cape Sable region of Everglades National Park (Smith et al. 2009; Whelan et al.

2009), producing extensive damage at the Flamingo Visitor Center and permanently closing the Flamingo Lodge and Buttonwood Cafe.

Storm surge is highly dependent on the severity and path of the storm, as well as the local bathymetric and topographic features of the coast, and since it occurs infrequently it is difficult to develop robust predictions of these rare events. A popular approach is to fit an extreme-value probability distribution to the highest water levels observed at a water-level monitoring gauge. However, gauges have short periods of record, typically a few decades at most, and they fail or are destroyed during extreme storms such that peak water levels are not recorded. A predictive storm surge database, SurgeDat, was developed in part to address this shortcoming by providing a statistical combination of data from multiple events in an area of interest (Needham et al. 2013). SurgeDat records storm surge water levels from all available sources, often from post-event high-water marks where gauge data are not available. SurgeDat then applies a statistical regression to estimate storm surge recurrence intervals. A recurrence interval is the length of time over which one can expect a storm surge to meet or exceed a specific inundation level. A familiar example is the 100-year flood level, which is really a 100-year recurrence interval at the specified flood level. In other words, in any one year there is a 1/100 or 1% chance that the flood level will be matched or exceeded. An excellent discussion of this can be found at the following US Geological Survey webpage: <https://water.usgs.gov/edu/100yearflood.html>.

Relevant to South Florida, a subset of SurgeDat was selected within a 40 km (25 mi) radius of 25.2° N, 80.7° as listed in table 2. Based on these events, the SurgeDat projection for storm surge recurrence intervals shown in figure 8 and table 3 suggests that a 180 cm (6 ft) surge event can be expected every 20 years. This same level of sea-level rise is not expected to occur until at least 2100.

Storm	Year	Longitude	Latitude	Surge (m)	Datum	Location
Katrina	2005	-81.0369	25.1294	1.22		Extreme SW Florida
Inez	1966	-80.5297	24.9976	1.10	Above Normal	Plantation Key
Alma	1966	-80.5135	25.0110	0.30	Above Normal	Tavernier
Gordon	1994	-80.5139	25.0108	1.22	Above Sea Level	Upper Florida Keys
Betsy	1965	-80.5148	25.0096	2.35	Mean Low Water	Tavernier
Donna	1960	-80.6353	24.9133	4.11		Upper Matecumbe Key

Andrew	1992	-80.9120	25.1431	1.50		Flamingo
Rita	2005	-80.7200	24.8605	1.22	NGVD 29	Middle and Upper Keys
Unnamed	1929	-80.3885	25.1848	2.68	Mean Sea Level	Key Largo
Wilma	2005	-81.0352	25.3523	2.50		Shark River 3
Gladys	1968	-80.5135	25.0110	0.15	Above Normal	Tavernier
David	1979	-80.6263	24.9231	0.61	Above Normal	Islamorada
Labor Day	1935	-80.7375	24.8516	5.49		Lower Matecumbe, Ferry Slip, Camp 3

Notes: Storm surge heights from these events are fit to a water-level exceedance and recurrence interval model to predict expected storm surge heights near Florida Bay with results shown in figure 8 and listed in table 3.

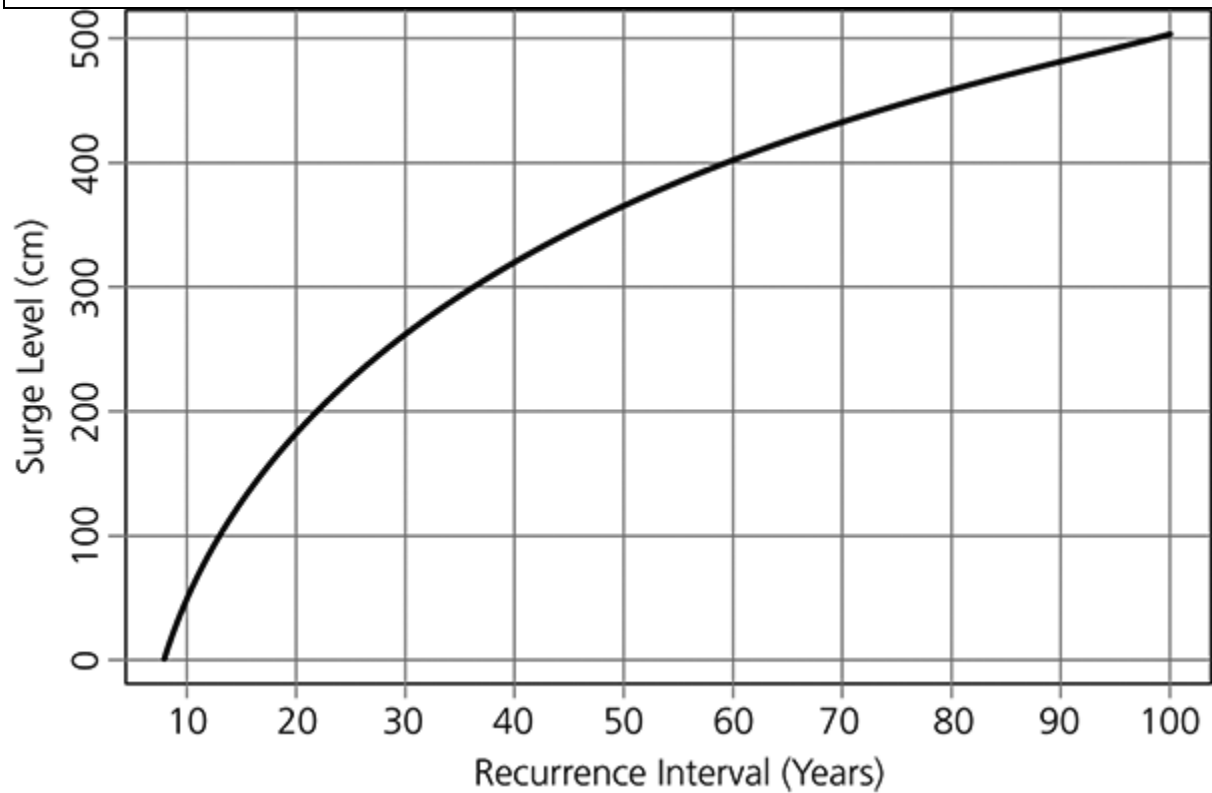


Figure 8. Storm surge recurrence intervals from the SurgeDat database and return periods predictor for a 25-mile radius centered on 25.2° N, 80.7° W.

NPS/Everglades National Park

Table 3. Storm surge height recurrence intervals			
Interval (year)	Surge (cm)	Interval (year)	Surge (cm)

10	45	56	388
12	82	58	395
14	112	60	402
16	139	62	408
18	162	64	415
20	183	66	421
22	202	68	427
24	219	70	433
26	235	72	438
28	250	74	444
30	264	76	449
32	277	78	454
34	289	80	459
36	300	82	464
38	311	84	469
40	321	86	473
42	331	88	478
44	340	90	482
46	349	92	487
48	357	94	491
50	365	96	495
52	373	98	499
54	381	100	503

Note: Recurrence interval projection in years shown in figure 8 from the hurricane data in table 2. The interval is the expected number of years one would wait for the associated hurricane storm surge to occur at least once. Note that this projection does not take into account future sea-level rise.

The recurrence interval projection is by necessity based on a sparse data set, and caution should be used in its interpretation. As projection intervals become longer, it is more likely that the observed data are inadequate to robustly represent all possibilities. Also, these projections do not incorporate changes from sea-level rise, or from a changing climate, which can alter the strength and frequency of storms. An important aspect of sea-level rise is that it significantly shortens the expected recurrence intervals of storm surge. For example, under a median sea-level rise projection at Key West,

Park et al. (2011) find that a 1-in-50-year storm surge based on historical data in 2010 can be expected to occur once every five years by 2060.

Conclusion

Sea-level rise is one of the most robust indicators of climate change and a warming planet. The national parks of South Florida are intimately tied to the ocean, and are already experiencing physical and ecological changes in response to sea-level rise. Based on a review of the available science, we have developed a projection to inform park interests on sea-level rise and inundation, trends in the frequency of nuisance flooding, and recurrence intervals of storm surge. The sea-level rise projections are based on the RCP 8.5 emissions scenario published by the ICPP AR5, as this scenario is deemed the most likely given the current inability of the global industrial complex to realistically pursue emission reductions. Two estimates are provided that bracket the expected range of sea-level rise. The low projection is the 50th percentile (median) forecast, while the high projection is intended for worst-case planning and corresponds to the 99th percentile with only a 1% chance of occurring. However, these projections do not incorporate contributions from a collapse of Antarctic ice sheets, changes in the Florida Current, or inundation due to tides or storms. Although the high projection is deemed to have only a 1% chance of occurrence under current conditions, a collapse of the Antarctic ice sheets could render it more plausible. Regardless of the specific sea-level rise projection, Everglades restoration with increased freshwater flow into the Everglades will serve to mitigate the impacts of sea-level rise over the next century.

Management actions in natural coastal systems will necessarily be location and project specific. An appropriate planning horizon is a crucial component of managerial design since benefits observed today may be offset by changing conditions within the planned lifespan of the project. Updates to the climate projections presented here are almost certain to occur and adaptive management practices should be incorporated when considering project alternatives, and, when appropriate, preference given to solutions that are flexible and can be adjusted as our understanding of current and expected impacts changes. These practices should be institutionalized as part of the ongoing monitoring and assessment process, incorporated into our education and outreach efforts, and used to best manage the influence of climate change on park resources.

Acknowledgments

The authors would like to thank Caryl Alarcón for GIS support. This work is a product of the South Florida Natural Resources Center, which is administered for the National Park Service by Everglades National Park.

References

Alarcón, C. 2016. Sea level rise projections for South Florida, 50th and 99th percentiles. 99th percentile:

<http://nps.maps.arcgis.com/home/webmap/viewer.html?layers=b61db3e154104ea486528c031390066c>; 50th percentile: <http://nps.maps.arcgis.com/home/webmap/viewer.html?layers=87e87e094680431eab085a18adb36836>.

Cazenave, A., and G. Le Cozannet. 2014. Sea level rise and its coastal impacts. *Earth's Future* 2(2):15–34. doi:[10.1002/2013EF000188](https://doi.org/10.1002/2013EF000188).

Center for Operational Oceanographic Products and Services. 2000. Tidal datums and their applications. Special Publication NOS CO-OPS 1. National Oceanic and Atmospheric Administration, National Ocean Service Center for Operational Oceanographic Products and Services, Silver Spring, Maryland, USA. http://tidesandcurrents.noaa.gov/publications/tidal_datums_and_their_applications.pdf.

———. 2013. Tidal datums. National Oceanic and Atmospheric Administration, National Ocean Service Center for Operational Oceanographic Products and Services, Silver Spring, Maryland, USA. http://tidesandcurrents.noaa.gov/datum_options.html.

DeConto, R. M., and D. Pollard. 2016. Contribution of Antarctica to past and future sea-level rise. *Nature* 531(7596):591–597. doi:[10.1038/nature17145](https://doi.org/10.1038/nature17145).

Fennema, R., L. Pearlstine, and J. Parsons. 2013. EVER Elevation (version 1): A multi-sourced digital elevation model for Everglades National Park. Report. South Florida Natural Resources Center, Everglades National Park, Homestead, Florida, USA.

Gyory, J., E. Rowe, A. Mariano, and E. Ryan. 1992. The Florida Current. Gulf of Mexico Research Initiative, Consortium for Advanced Research on Transport of Hydrocarbon in the Environment, and Rosenstiel School of Marine and Atmospheric Science; University of Miami, Florida, USA. <http://oceancurrents.rsmas.miami.edu/atlantic/florida.html>.

Holland, P. R., A. Brisbourne, H. F. J. Corr, D. McGrath, K. Purdon, J. Paden, H. A. Fricker, F. S. Paolo, and A. H. Fleming. 2015. Oceanic and atmospheric forcing of Larsen C Ice-Shelf thinning. *The Cryosphere* 9:1005–1024. doi:[10.5194/tc-9-1005-2015](https://doi.org/10.5194/tc-9-1005-2015).

Intergovernmental Panel on Climate Change (IPCC). 2013. Climate change 2013: The physical science basis. Contribution of Working Group I to the Fifth Assessment Report of the Intergovernmental Panel on Climate Change. T. F. Stocker, D. Qin, G.-K. Plattner, M. Tignor, S. K. Allen, J. Boschung, A. Nauels, Y. Xia, V. Bex, and P. M. Midgley, editors. Cambridge University Press, Cambridge, UK, and New York, USA.

Jones, G. A., and K. J. Warner. 2016. The 21st century population-energy-climate nexus. *Energy Policy* 93:206–212. doi:[10.1016/j.enpol.2016.02.044](https://doi.org/10.1016/j.enpol.2016.02.044).

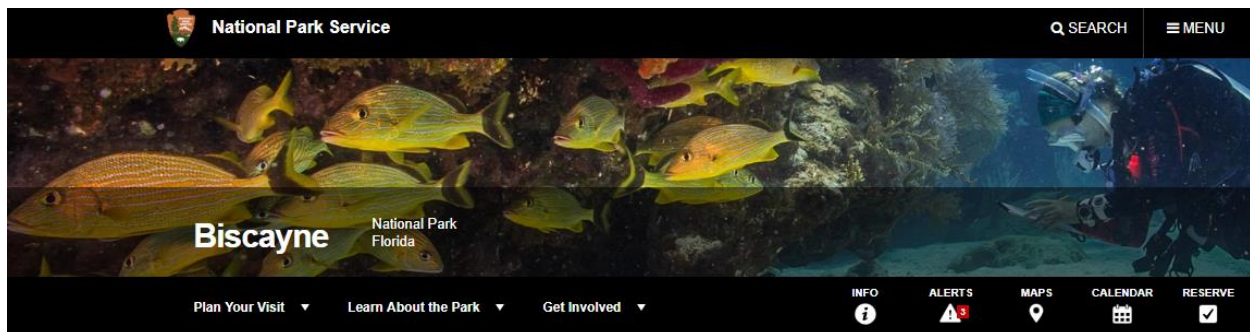
- Kopp, R. W., R. M. Horton, C. M. Little, J. X. Mitrovica, M. Oppenheimer, D. J. Rasmussen, B. H. Strauss, and C. Tebaldi. 2014. Probabilistic 21st and 22nd century sea-level projections at a global network of tide gauge sites. *Earth's Future* 2(8):383–406. doi:[10.1002/2014EF000239](https://doi.org/10.1002/2014EF000239).
- Krauss, K. W., A. S. From, T. W. Doyle, T. J. Doyle, and M. J. Barry. 2011. Sea-level rise and landscape change influence mangrove encroachment onto marsh in the Ten Thousand Island region of Florida, USA. *Journal of Coastal Conservation* 15(4):629–638. doi:[10.1007/s11852-011-0153-4](https://doi.org/10.1007/s11852-011-0153-4).
- Montgomery, R. B. 1938. Fluctuations in monthly sea level on eastern U.S. coast as related to dynamics of western north Atlantic Ocean. *Journal of Marine Research* 1:165–185.
- National Research Council (NRC). 2014. Progress toward restoring the Everglades: The fifth biennial review—2014. Committee on Independent Scientific Review of Everglades Restoration Progress, Water Science and Technology Board, Board on Environmental Studies and Toxicology; Division on Earth and Life Studies; National Research Council, Washington, DC, USA. doi:[10.17226/18809](https://doi.org/10.17226/18809).
- Needham, H. F., B. D. Keim, D. Sathiaraj, and M. Shafer. 2013. A global database of tropical storm surges. *EOS Transactions American Geophysical Union*. 94(24):213–214. doi:[10.1002/2013EO240001](https://doi.org/10.1002/2013EO240001).
- Park, J., J. Obeysekera, M. Irizarry, J. Barnes, P. Trimble, and W. Park-Said. 2011. Storm surge projections and implications for water management in South Florida. *Climatic Change* 107(1) (Special Issue: Sea level rise in Florida: An emerging ecological and social crisis):109–128. doi:[10.1007/s10584-011-0079-8](https://doi.org/10.1007/s10584-011-0079-8).
- Park, J., and W. Sweet. 2015. Accelerated sea level rise and Florida Current transport. *Ocean Science* 11:607–615. doi:10.5194/os-11-607-2015.
- Rahmstorf, S., J. E. Box, G. Feulner, M. E. Mann, A. Robinson, S. Rutherford, and E. J. Schaffernicht. 2015. Exceptional twentieth-century slowdown in Atlantic Ocean overturning circulation. *Nature Climate Change* 5:475–480. doi:[10.1038/nclimate2554](https://doi.org/10.1038/nclimate2554).
- Smith, T. J., G. H. Anderson, K. Balentine, G. Tiling, G. A. Ward, and K. R. T. Whelan. 2009. Cumulative impacts of hurricanes on Florida mangrove ecosystems: Sediment deposition, storm surges, and vegetation. *Wetlands* 29(1):24–34. doi:[10.1672/08-40.1](https://doi.org/10.1672/08-40.1).
- Steffen, W., W. Broadgate, L. Deutsch, O. Gaffney, and C. Ludwig. 2015. The trajectory of the Anthropocene: The Great Acceleration. *The Anthropocene Review* 2(1):81–98. doi:[10.1177/2053019614564785](https://doi.org/10.1177/2053019614564785).

Sweet, W. V., and J. Park. 2014. From the extreme to the mean: Acceleration and tipping points of coastal inundation from sea level rise. *Earth's Future* 2(12):579–600. doi:[10.1002/2014EF000272](https://doi.org/10.1002/2014EF000272).

US Army Corps of Engineers (USACE). 2014. Procedures to evaluate sea level change: Impacts, responses, and adaptation. U.S. Army Corps of Engineers, Washington, DC, USA. Technical Letter No. 1100-2-1, 30 June 2014. http://www.publications.usace.army.mil/Portals/76/Publications/EngineerTechnicalLetters/ETL_1100-2-1.pdf.

Whelan, K. R. T., T. J. Smith III, G. H. Anderson, and M. L. Ouellette. 2009. Hurricane Wilma's impact on overall soil elevation and zones within the soil profile in a mangrove forest. *Wetlands* 29(1):16–23. doi:[10.1672/08-125.1](https://doi.org/10.1672/08-125.1).

Wouters, B., A. Martin-Español, V. Helm, T. Flament, J. M. van Wessem, S. R. M. Ligtenberg, M. R. van den Broeke, and J. L. Bamber. 2015. Dynamic thinning of glaciers on the Southern Antarctic Peninsula. *Science* 348(6237):899–903. doi:[10.1126/science.aaa5727](https://doi.org/10.1126/science.aaa5727).



[NPS.nyu](#) / [Park Home](#) / [Learn About the Park](#) / [Nature](#) / [Animals](#) / [Threatened & Endangered Animals](#)

Protected Animals

The following park animals are listed as threatened or endangered. If you are lucky enough to observe them in the park, cherish the sighting and please give them space (interference is prohibited). Click [here](#) to report sightings. Please include as much information as possible (date, location, number, size, photographs, . .). For more information on threatened park species click [here](#). For a list of federal endangered species, click [here](#), and for state endangered species, click [here](#).

	Occurrence in Park	Federal Classification	State Classification
MARINE INVERTEBRATES			
Pillar coral	Rare	-	Endangered
Elkhorn coral	Common	Threatened	-
Staghorn coral	Common	Threatened	-
TERRESTRIAL INVERTEBRATES			
Florida tree snail	Occasional	-	Special Concern
Miami blue butterfly	Rare	Endangered	Endangered
Schaus swallowtail butterfly	Rare	Endangered	Endangered
FISH			
Smalltooth sawfish	Rare	Endangered	-
REPTILES			

American alligator	Uncommon	Similarity of appearance	Special Concern
American crocodile	Occasional	Threatened	Endangered
Eastern indigo snake	Rare	Threatened	Endangered
Sea Turtle- green	Common	Endangered	Endangered
Sea Turtle- hawksbill	Common	Endangered	Endangered
Sea Turtle- Kemp's ridley	Rare	Endangered	Endangered
Sea Turtle- leatherback	Rare	Endangered	Endangered
Sea Turtle- loggerhead	Common	Threatened	Threatened
BIRDS			
Brown Pelican	Common	Delisted- recovery	Special Concern
Least tern	Common	-	Threatened
Little blue heron	Common	-	Special Concern
Osprey	Common	Special Concern	Special Concern
Piping plover	Uncommon	Threatened	Threatened
Reddish egret	Occasional	Special Concern	Special Concern
Roseate spoonbill	Uncommon	-	Special Concern
Snowy egret	Common	-	Special Concern
Southeastern American kestrel	Uncommon	Special Concern	Threatened
Tricolored heron	Common	-	Special Concern
White ibis	Common	-	Special Concern
White-crowned pigeon	Common	Special Concern	Threatened
Wood stork	Occasional	Endangered	Endangered
MARINE MAMMALS			
Fin (finback) whale	Rare, if at all	Endangered	Endangered

Florida manatee	Common	Endangered	Endangered
Humpback whale	Rare, if at all	Endangered	Endangered
North Atlantic right whale	Rare, if at all	Endangered	Endangered
Sei whale	Rare, if at all	Endangered	Endangered
Sperm whale	Rare, if at all	Endangered	Endangered
TERRESTRIAL MAMMALS			
Key Largo woodrat	Historical, not known to occur presently	Endangered	Endangered
Key Largo cotton mouse	Historical, not known to occur presently	Endangered	Endangered

Special protection measures are in place for the following species to ensure their survival:

- All stony corals
- Fire corals
- Sea fans
- Queen conch
- Bahama starfish
- Longspine sea urchin (Diadema)
- Nassau grouper
- Goliath grouper
- Manta ray
- Spotted eagle ray
- Spearfish- longbill, Mediterranean and roundscale
- Sturgeon
- Sharks - many species are protected. Visit www.myfwc.com for a complete list.
- All marine mammals
- All ornamental tropical fish, plants & invertebrates (regulation applies to this park)
- Sponges (regulation applies to this park)
- Lobsters (within the Biscayne Bay Lobster Sanctuary- click [here](#) for more details)

Last updated: February 22, 2017

PATTERNS AND PROJECTIONS OF HIGH TIDE FLOODING ALONG THE U.S. COASTLINE USING A COMMON IMPACT THRESHOLD



Photo: New York City Harbor

**Silver Spring, Maryland
February 2018**

noaa National Oceanic and Atmospheric Administration

U.S. DEPARTMENT OF COMMERCE
National Ocean Service
Center for Operational Oceanographic Products and Services

Center for Operational Oceanographic Products and Services
National Ocean Service
National Oceanic and Atmospheric Administration
U.S. Department of Commerce

The National Ocean Service (NOS) Center for Operational Oceanographic Products and Services (CO-OPS) provides the National infrastructure, science, and technical expertise to collect and distribute observations and predictions of water levels and currents to ensure safe, efficient and environmentally sound maritime commerce. The Center provides the set of water level and tidal current products required to support NOS' Strategic Plan mission requirements, and to assist in providing operational oceanographic data/products required by NOAA's other Strategic Plan themes. For example, CO-OPS provides data and products required by the National Weather Service to meet its flood and tsunami warning responsibilities. The Center manages the National Water Level Observation Network (NWLON), a national network of Physical Oceanographic Real-Time Systems (PORTS[®]) in major U. S. harbors, and the National Current Observation Program consisting of current surveys in near shore and coastal areas utilizing bottom mounted platforms, subsurface buoys, and horizontal sensors. The Center: establishes standards for the collection and processing of water level and current data; collects and documents user requirements, which serve as the foundation for all resulting program activities; designs new and/or improved oceanographic observing systems; designs software to improve CO-OPS' data processing capabilities; maintains and operates oceanographic observing systems; performs operational data analysis/quality control; and produces/disseminates oceanographic products.

Patterns and Projections of High Tide Flooding Along the U.S. Coastline Using a Common Impact Threshold

William V. Sweet

National Oceanic and Atmospheric Administration, National Ocean Service, Center for Operational Oceanographic Products and Services, Silver Spring, MD, USA

Greg Dusek

National Oceanic and Atmospheric Administration, National Ocean Service, Center for Operational Oceanographic Products and Services, Silver Spring, MD, USA

Jayantha Obeysekera

South Florida Water Management District, West Palm Beach, FL

John J. Marra

National Oceanic and Atmospheric Administration, National Environmental Satellite, Data, and Information Services, National Centers for Environmental Information, Honolulu, HI, USA

February 2018



U.S. DEPARTMENT OF COMMERCE

Wilbur Ross, Secretary

National Oceanic and Atmospheric Administration

RDML Tim Gallaudet, Ph.D., USN Ret.

**Assistant Secretary of Commerce for Oceans and Atmosphere and
Acting Under Secretary of Commerce for Oceans and Atmosphere**

National Ocean Service

Dr. Russell Callender, Assistant Administrator

Center for Operational Oceanographic Products and Services

Richard Edwing, Director

NOTICE

Mention of a commercial company or product does not constitute an endorsement by NOAA. Use of information from this publication for publicity or advertising purposes concerning proprietary products or the tests of such products is not authorized.

TABLE OF CONTENTS

TABLE OF CONTENTS	III
LIST OF FIGURES	IV
LIST OF TABLES	VI
EXECUTIVE SUMMARY	VII
1.0 INTRODUCTION	1
2.0 DEFINING A CONSISTENT COASTAL FLOOD ELEVATION THRESHOLD	7
3.0 HISTORICAL PATTERNS OF HIGH TIDE FLOODING	13
3.1 TRENDS IN HIGH TIDE FLOODING.....	13
3.2 YEAR-TO-YEAR VARIABILITY IN HIGH TIDE FLOODING DUE TO ENSO.....	17
3.3 SEASONAL CYCLES IN HIGH TIDE FLOODING	20
4.0 FUTURE PROJECTIONS OF HIGH TIDE FLOODING	23
5.0 SUMMARY REMARKS	31
ACKNOWLEDGEMENTS	35
REFERENCES	35
APPENDIX 1	41
APPENDIX 2	44

LIST OF FIGURES

- Figure 1.** a) Long-term (>30 years record) RSL trends around the U.S. coastline measured and/or computed by NOAA (Zervas, 2009), b) multi-year empirical (smoothed) distributions for daily highest water levels in Norfolk, Virginia for the 1960s and 2010s, showing extent that local RSL rise has increased the flood probability relative to impact thresholds defined locally by the NOAA NWS for minor (~0.5 m: nuisance level), moderate (~0.8 m) and major (~1.2 m: local level of Hurricane Sandy in 2012) impacts, relative to mean higher high water (MHHW) tidal datum and in c) are annual flood frequencies (based upon 5-year averages) in Norfolk for high tide floods with minor impacts shown as accelerating by the quadratic trend fit (goodness of fit [R²]=0.84). Figure from Sweet et al. (2017a). 3
- Figure 2.** a) Long-term tide gauges with official NOAA flood thresholds for minor (high tide) flooding with exposed topography (red) mapped by the NOAA SLR Viewer and b) the annual summation of days with high tide flooding at locations shown in a) during 2016 as monitored by NOAA (Sweet et al., 2017b). 4
- Figure 3.** Scatter plot of NOAA tide gauge locations with official NOAA coastal flood thresholds (y-axis) shown relative to MLLW tidal datum for minor, moderate and major impacts and the diurnal tide range (GT). There are 66 tide gauges with minor (high tide), 48 with moderate and 46 with major flood thresholds. Locations in the continental U.S. are shown as circles, whereas those in Alaska are designated by triangles. No official NOAA coastal flood thresholds exist for island states or territories. Linear regression fits (black line and boxed equation) and the 90% confidence interval (5% and 95% as red dashed lines) are also shown. Derived thresholds are obtained by solving the regression equations for a particular location. For example, y (the minor derived flood threshold for a location) = 1.04 * x (the local GT tidal datum) + 0.50 m. All NOAA official flood thresholds were obtained in July 2017. 8
- Figure 4.** The official NOAA and derived elevation thresholds for high tide/minor (a, b), moderate (c, d) and major (e, f) flooding. Note that the legend scales increase by 0.3 m (about 1 foot) between minor, moderate and major flooding threshold elevations. Black dots denote locations without an official NOAA flood threshold. 10
- Figure 5.** Recurrence intervals for the NOAA and derived elevation thresholds for high tide/minor (a, b), moderate (c, d) and major (e, f) flooding adjusted to year 2000 sea levels. Black dots denote locations without a NOAA flood threshold. 12
- Figure 6.** Annual number of high tide floods (days per year) at NOAA tide gauge locations. A year is defined in terms of a meteorological year (May–April). Note: White squares indicate no data or that hourly data was less than 80% complete within a year. 14
- Figure 7.** Number of days per year with a high tide flood at a) Atlantic City, New Jersey, b) Norfolk, Virginia, c) San Diego, California and d) Seattle, Washington. San Diego and Seattle are fit with a linear least-squares fit, whereas Atlantic City and Norfolk are fit with a quadratic. Note: the annual series is shown here as compared to a 5-year average series in Figure 1c. 15
- Figure 8.** a) Number of days in 2015 with a high tide flood derived by trend (linear or quadratic fits above the 90% significance level) or 19-year average (1998–2016) where no significant trend exists. Black dots denote locations with no floods over the 1998–2016 period and b) is the percent change since 2000 based upon trend fits also used in a). Black dots denote locations as in a) or where no significant trend exists. 16

Figure 9. a) Variance of 1998–2016 daily highest water levels, b) the ratio between variances of daily highest predicted tidal component of water level to observed water levels and examples at c) Norfolk, Virginia and d) San Diego, California showing daily highest waters (red), contribution from daily highest predicted tide (blue); both are shown relative to their minor derived flood threshold (green), and the ratio is listed in parentheses. 17

Figure 10. Parametric probability distribution (normal) fit for 3 years characterized by stronger El Niño, stronger La Niña and ENSO-neutral conditions. In parentheses are the mean and standard deviation (or square of the variance) of the distributions shown in the figures. Water levels have been detrended to enable multi-year comparisons. Not shown are the 95% confidence intervals for the distribution parameters which suggest a significant change of conditions during El Niño along both of these (and other) West and East Coast locations. 18

Figure 11. Trends in annual frequencies of high tide flooding (black line) are fit to observed annual flood frequencies (black line-dots) over the 1950–2016 period (or beginning of record) as shown in Figure 6. Predictions of high tide flooding based on both trend and annual averaged ENSO effects (ONI) are also shown (red line-dots) for a) Atlantic City, b) Norfolk, c) San Diego and D) Seattle. 19

Figure 12. a) Characterization of regression trend estimates of increasing decadal annual high tide flood frequencies: accelerating (quadratic) or linear increasing or no trend (black dot) and b) locations whose high tide flood frequencies change on an interannual basis due to phases of ENSO as illustrated in Figure 11. Specifically, in b) are predictions for days in 2015 (May 2015–April 2016) with high tide flooding considering the predicted strength of El Niño (based upon ONI) relative to values based on the trend-derived or 19-year average value as shown in Figure 8a. Kwajalein Island (blue dot) in Figure 12b is opposite the other locations—flood frequencies drop during El Niño and rise during La Niña. 20

Figure 13. a) Percentage of high tide floods caused solely by tidal forcing over latest 19-year tidal epoch (1998–2016), with black dots designating locations with no high tide floods caused by tides alone or for locations with no high tide flooding during this period. For instance, 20% of San Diego’s high tide floods are caused by tides alone, whereas in New York City, the tide alone is insufficient to cause flooding, b) and c) high tide flooding in San Diego and New York City (NYC) since 1980 distributed by month and d) is the percentage of high tide flood days experienced over 1998–2016 by month at 99 NOAA tide gauges. 21

Figure 14. Projected annual frequencies of high tide flooding in response to scenarios of global sea level rise (Sweet et al., 2017) estimated at NOAA tide gauges in a) New York City (The Battery), b) Miami (Virginia Key), Florida and c) San Francisco, California considering observed patterns (combined tidal and nontidal water level components) and d), e) and f) at the same locations but assuming predicted tide forcing only. Derived high tide flood levels are 0.56 m, 0.53 m and 0.57 m, respectively. 24

Figure 15. Projected annual frequencies of high tide flooding by 2050 (average over the 2041–2050 period) in response to the a) Intermediate Low and c) Intermediate Scenarios of global sea level rise (Sweet et al., 2017a) estimated at 99 NOAA tide gauges based upon historical patterns and percentage of floods caused by tide forcing alone in b) and d), respectively. Black dots in b) denote locations where tide alone does not exceed the minor derived flood threshold. 25

Figure 16. As in Figure 15, but for projected annual frequencies of high tide flooding by 2100 (average over the 2091–2100 period). 26

Figure 17. a) Empirical probability densities for daily highest water levels over 1998-2016 at Miami, Florida and New York City showing differences in variance (color-coded in box and in units of m^2), b) locations with linear trends (significant above 90% level) in variance computed for daily high water levels per year and relative comparison between annual mean sea level and standard deviation (variance^{0.5}) and fitted linear trends of daily highest levels per year at c) Bergen Point, New York and d) Beaufort, North Carolina where significant trends in annual variance occur. 27

Figure 18. a) Daily exceedance probabilities (1-cumulative distribution) within a year for New York City (The Battery), Norfolk (Sewells Point), Virginia and Miami (Virginia Key), Florida based upon daily highest water levels over the 1998–2016 period with their average high tide/minor, moderate and major flood thresholds labeled. The decade when MHHW reaches the b) high tide/minor threshold, c) moderate threshold and d) major threshold levels for coastal flooding for local RSL projections under the Intermediate Scenario developed by the Federal Interagency Sea Level Rise and Coastal Flood Hazard Task Force (Sweet et al., 2017a). 29

LIST OF TABLES

Table 1. Processes affecting water levels and their temporal scales. Tide gauges, whose samples are composed of multi-minutes averages, generally do not include wave contributions or their effects. Modification of Table 1 of Sweet et al. (2017a). 2

EXECUTIVE SUMMARY

For forecasting purposes to ensure public safety, NOAA has established three coastal flood severity thresholds. The thresholds are based upon water level heights empirically calibrated to NOAA tide gauge measurements from years of impact monitoring by its Weather Forecast Offices (WFO) and emergency managers. When *minor* (more disruptive than damaging), *moderate* (damaging) or *major* (destructive) coastal flooding is anticipated (not associated with tropical storms), NOAA issues either a flood *advisory* (for minor) or *warning* (for moderate or major). Less than half of NOAA tide gauges located along the U.S. coastline have such ‘official’ NOAA flood thresholds, and where they exist, the heights can vary substantially (e.g., 0.3–0.6 meter within minor category). They differ due to the extent of infrastructure vulnerabilities, which vary by topography and relief, land-cover types or existing flood defenses.

We find that all official NOAA coastal flood thresholds share a common pattern based upon the local tide range (possibly in response to systematic development ordinances). Minor, moderate and major coastal flooding typically begin about 0.5 m, 0.8 m and 1.2 m above a height slightly higher than the multi-year average of the daily highest water levels measured by NOAA tide gauges. Based upon this statistical (regression-based) relationship, a ‘derived’ set of flood threshold proxies for minor, moderate or major impacts are permissible for almost any location along the U.S. coastline.

The intent of this report is not to supplant knowledge about local flood risk. Rather, the intention is to provide an objective and nationally consistent set of impact thresholds for minor/moderate/major coastal flooding. Such definitions are currently lacking, which limits the ability to deliver new products as well as the effectiveness of existing coastal flood products. Coastal communities along all U.S. coastlines need consistent guidance about flooding, which is 1) forecasted in the near future (e.g., severity/depth of 4-day predictions of storm surge heights ‘above ground level’), 2) likely in the coming season or year (e.g., probabilistic outlooks) or 3) possible over the longer term (e.g., decadal to end-of-century scenarios). Our primary emphasis is to use the derived threshold for minor flooding, which we refer to as ‘high tide’ flooding (also known as ‘nuisance’, ‘sunny day’ and ‘recurrent tidal’ flooding), to assess nationally how exposure—and potential vulnerability—to high tide flooding has and will continue to change with changing sea levels.

High tide flooding today mostly affects low-lying and exposed assets or infrastructure, such as roads, harbors, beaches, public storm-, waste- and fresh-water systems and private and commercial properties. Due to rising relative sea level (RSL), more and more cities are becoming increasingly exposed and evermore vulnerable to high tide flooding, which is rapidly increasing in frequency, depth and extent along many U.S. coastlines. Today, high tide flooding is likely more disruptive (a nuisance) than damaging. The cumulative effects, however, are becoming a serious problem in several locations including many with strategic importance to national security such as Norfolk, Virginia, San Diego, California and Kwajalein Island in the U.S. Marshall Islands.

Over the last several decades, annual frequencies of high tide flooding are found to be linearly increasing in 31 locations (out of 99 tide gauges examined outside Alaska) mostly along the coasts of the Northeast/Southeast Atlantic and the Eastern/Western Gulf of Mexico, and to a lesser extent, along the Northwest and Southwest Pacific coasts. Annual frequencies are accelerating (nonlinearly increasing) in 30 locations mostly along the Northeast and Southeast Atlantic Coasts. Currently, high tide flood

frequencies are increasing at the highest overall rates (and likely becoming most problematic) along the coasts of the Southeast Atlantic and to a lesser extent along the Northeast Atlantic and the Western Gulf. Between 2000 and 2015, annual frequencies increased (median values) by about 125% (from 1.3 days to 3.0 days/year) along the Southeast Atlantic, by 75% (from 3.4 days to 6.0 days/year) along the Northeast Atlantic and by 75% (from 1.4 days to 2.5 days/year) along the Western Gulf.

High tide flooding is currently less problematic along the coasts of the Northwest and Southwest Pacific and the U.S. Pacific (Kwajalein Island being an exception) and Caribbean Islands for two main reasons: 1) the local height of the high tide flood threshold is above the reach of all or most of the annual highest water levels due to a combination of generally calmer weather conditions or bathymetric constraints that limit storm surge potential and 2) regionally RSL rise rates have been relatively low over the last several decades. In these locations, however, large waves (swells) and their high-frequency dynamical effects, which are generally not inherent to NOAA tide gauge measurements, can override high tides and cause dune overwash, coastal erosion and flooding.

High tide flooding regionally occurs more often in certain seasons and during certain years, which is important for awareness and preparedness purposes. The seasonality in flood frequency occurs in response to a spatially varying mixture of rhythmic astronomical tides ('tidal forcing'), repetitive seasonal mean sea level cycles and less-predictable episodic changes in wind and ocean currents that are nontidal in origin. Frequencies are relatively high during September–April along the Northeast Atlantic Coast and generally peak in October–November. Along the Southeast Atlantic and Gulf Coasts, frequencies are highest during September–November with a secondary peak in June–July. Along both the Northwest and Southwest Pacific, frequencies are highest during November–February with a secondary peak in June–July along the Southwest Pacific.

High tide flood frequencies vary year-to-year due to large-scale changes in weather and ocean circulation patterns, such as during the El Niño Southern Oscillation (ENSO). During the El Niño phase, high tide flood frequencies are amplified at 49 (about half of examined) locations along the U.S. West and East Coasts beyond underlying RSL rise-forced trend increases. This predictable ENSO response may better inform annual budgeting in some flood-prone locations for emergency mobilizations and proactive responses. For example, during 2015, high tide flood frequencies were predicted to be 70% and 170% higher than normally would be expected (e.g., above trend values) along the East and West Coasts, respectively, based upon the predicted El Niño strength about a year in advance. Subsequent monitoring the following year verified that a strong El Niño formed, and flood frequencies occurred at or above the trend/ENSO predicted values at many locations.

With continued RSL rise, high tide flood frequencies will continue to rapidly increase and more so simply from tidal forcing, which today is very rare. We assess future changes locally projected under a subset of the global rise scenarios of the U.S. Federal Interagency Sea Level Rise and Coastal Flood Hazard Task Force, specifically the Intermediate Low (0.5 m global rise by 2100) and Intermediate (1.0 m global rise) scenarios. Under these two scenarios, by 2050, annual high tide flood frequencies along the Western Gulf (80 and 185 days/year, respectively) and Northeast Atlantic (45 and 130 days/year) are higher largely because RSL rise is projected to be higher. Along coasts of the Southeast Atlantic (25 and 85 days/year), the Eastern Gulf (25 and 80 days/year), the Southwest (15 and 35 days/year) and Northwest Pacific (15 and 30 days/year), the Pacific (5 and 45 days/year) and Caribbean Islands (0 and 5 days/year), high tide flooding occurs less often because RSL rise projections are lower or weather conditions are typically

calmer; however, the rate of increase in annual flood frequencies will eventually increase at very rapid rates. On average across all regions, high tide flooding by 2050 will occur about 35% and 60% of the times solely from tidal forcing under the Intermediate Low and Intermediate Scenarios, respectively.

By 2100, high tide flooding will occur ‘every other day’ (182 days/year) or more often under the Intermediate Low Scenario within the Northeast and Southeast Atlantic, the Eastern and Western Gulf, and the Pacific Islands with tidal forcing causing all (100%) of the floods except within the Eastern Gulf (80% caused by tides). By definition, ‘every other day’ high tide flooding would bring to fruition the saying championed by NOAA’s (late) Margaret Davidson: “*Today’s flood will become tomorrow’s high tide.*” Under the Intermediate Scenario, high tide flooding will become ‘daily’ flooding (365 days/year with high tide flooding) within nearly all regions with tide forcing alone, causing 100% of flooding.

Lastly, these results illustrate how close U.S. coastal cities are to a tipping point with respect to flood frequency, as only 0.3m to 0.7 m separates infrequent damaging-to-destructive flooding from a regime of high tide flooding—or minor floods from moderate and major floods. This suggests a particular interpretation for ‘freeboard’ and other engineering adaptive methods as the desired level of protection in terms of flood type, in both the present and future. This recognition may in turn facilitate a more systematic implementation of freeboard guidelines nationally.

1.0 INTRODUCTION

Tide gauges of the National Oceanic and Atmospheric Administration (NOAA) National Ocean Service (NOS) have been measuring water levels along U.S coastlines for more than a century¹. Their real-time data resolve a range of motion and variability associated with a variety of processes (Table 1). Their observations resolve the rhythmic nature of the astronomical tides ('tidal forcing'), seasonal changes in local mean sea level and episodic, often-damaging, storm surges (Table 1); both the tidal and seasonal cycles are included in NOAA tide predictions² and provide highly accurate (non-storm-related) forecasts about water levels at any time and place along the U.S. coastline. As such, NOAA's national tide gauge network is key to supporting maritime safety and commerce, defining the country's maritime-economic boundaries and preparing for emergencies during coastal storms. Tide gauge data also reveal that relative sea levels (RSL) have been increasing by about 2–5 mm/year (0.8–2.0 inches/decade) or more over the last several decades around much of the continental U.S., Hawai'i and island territories (Figure 1a)³ due to a variety of factors affecting regional sea surface height and land elevations (Table 1: Zervas, 2009; Church and White, 2011; Hay et al., 2015; Kopp et al., 2015; Sweet et al., 2017a, Hsu and Velicogna, 2017). As the vertical gap between coastal infrastructure and the ocean decreases, the risk of flooding increases (Figure 1b). Decades ago, powerful storms typically caused coastal flooding, but due to RSL rise, rather common wind events and seasonally high tides now more often cause the ocean to spill into communities (Sweet et al., 2014). Other impacts include infiltration and degradation of stormwater (Obeysekera et al., 2011) and wastewater (Flood and Cahoon, 2011) systems and saltwater intrusion that raises coastal groundwater tables (Sukop et al., 2018). Flood severity becomes further compounded if large swells (Serafin et al., 2017), heavy rainfall (Wahl et al., 2015) or high river flows occur (Moftakhari et al., 2017a) concurrently, the effects of which, however, are not generally measured by tide gauges (Table 1).

¹ <https://tidesandcurrents.noaa.gov>

² https://tidesandcurrents.noaa.gov/tide_predictions.html

³ <https://tidesandcurrents.noaa.gov/sltrends/sltrends.html>

Table 1. Processes affecting water levels and their temporal scales. Tide gauges, whose samples are composed of multi-minutes averages, generally do not include wave contributions or their effects. Modification of Table 1 of Sweet et al. (2017a).

Physical Process	Temporal Scale	Potential Magnitude (yearly)
Wind Waves (e.g., dynamical effects, runup)	seconds to minutes	< 10 meters
Tsunami	minutes to hours	< 10s of meters
Storm Surge (e.g., tropical storms or nor'easters)	minutes to days	< 15 meters
Tides	hours	< 15 meters
Seasonal Cycles	months	< 0.5 meters
Ocean/Atmospheric Variability (e.g., ENSO)	months to years	< 0.5 meters
Ocean Eddies and Planetary Waves	months to years	< 0.5 meters
Ocean Gyre and Over-turning Variability	years to decades	< 0.5 meters
Land Ice Melt/Discharge	years to centuries	millimeters to centimeters
Thermal Expansion	years to centuries	millimeters to centimeters
Vertical Land Motion	minutes to centuries	millimeters to meters

Over the last several decades, a rapid—accelerating in many locations—change in the annual frequencies of tidal flooding has been documented at NOAA tide gauges along the U.S. coastline (Figure 1c). The cause for the increase is RSL rise (Ezer and Atkinson, 2014; Sweet et al., 2014; Sweet et al., 2017a, c), with annual flood frequencies in several U.S. East and West Coast cities further influenced on a year-to-year basis by the El Niño Southern Oscillation (ENSO) (Sweet and Park, 2014). In many coastal cities, ‘minor’ tidal flooding now occurs several times a year and is often referred to as ‘recurrent’, ‘sunny-day’, ‘shallow coastal’ or ‘nuisance’ flooding. More-severe (deeper, more widespread and typically storm-driven) ‘moderate’ and ‘major’ flooding has become and will continue to become more probable (e.g., Tebaldi et al., 2012; Salas and Obeysekera, 2014; Sweet et al., 2013, 2017a; Kopp et al., 2014; Buchanan et al., 2016, 2017; Vitousek et al., 2017). Flood heights are operationally forecasted by NOAA’s National Weather Service (NWS) Weather Forecast Offices (WFO). If flooding above the minor, moderate or major impact categories (not associated with tropical cyclones) is likely or imminent, NOAA issues guidance to inform the public of potential risks and assist local emergency managers (NOAA, 2017)⁴.

⁴ See <http://water.weather.gov/ahps>

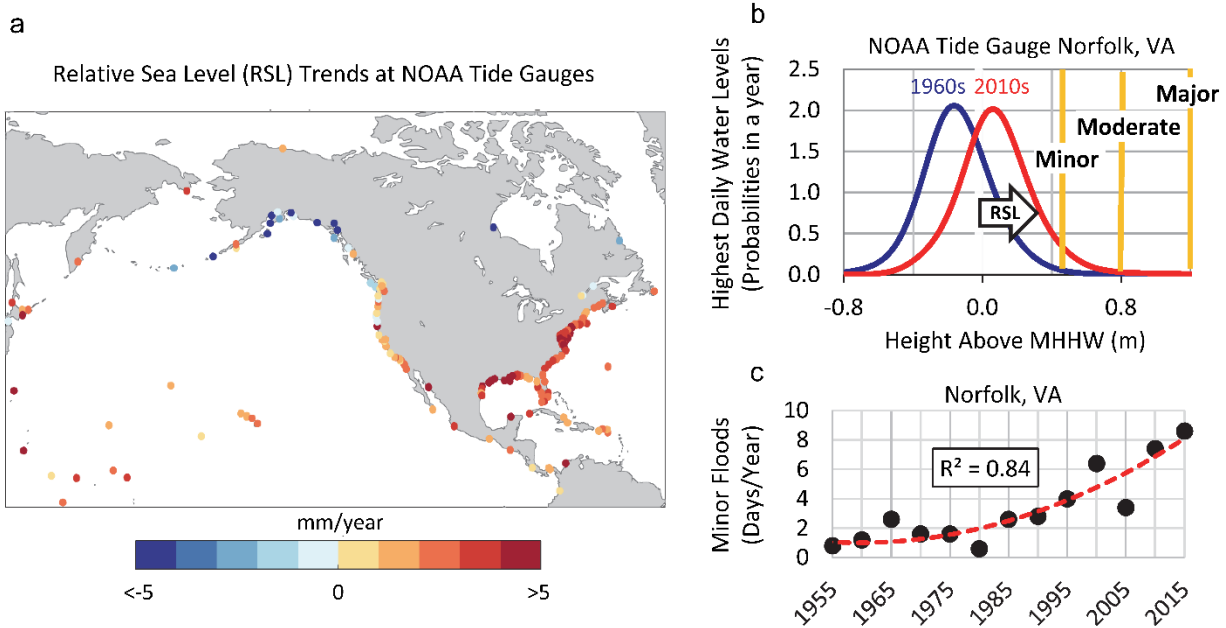


Figure 1. a) Long-term (>30 years record) RSL trends around the U.S. coastline measured and/or computed by NOAA (Zervas, 2009), b) multi-year empirical (smoothed) distributions for daily highest water levels in Norfolk, Virginia for the 1960s and 2010s, showing extent that local RSL rise has increased the flood probability relative to impact thresholds defined locally by the NOAA NWS for minor (~0.5 m: nuisance level), moderate (~0.8 m) and major (~1.2 m: local level of Hurricane Sandy in 2012) impacts, relative to mean higher high water (MHHW) tidal datum and in c) are annual flood frequencies (based upon 5-year averages) in Norfolk for high tide floods with minor impacts shown as accelerating by the quadratic trend fit (goodness of fit $[R^2]=0.84$). Figure from Sweet et al. (2017a).

The extent and severity of impacts under the three flood categories have been empirically calibrated to some—but not all—NOAA tide gauge levels through years of impact monitoring by NOAA NWS WFOs and local city emergency managers. Periodically, the thresholds are adjusted to reflect a change in infrastructure vulnerabilities or for communication purposes (e.g., minimize ‘warning fatigue’). NOAA coastal flood elevation thresholds (henceforth referred to as ‘official NOAA’ thresholds) vary by location as shown for a subset of tide gauges recently analyzed by Sweet et al. (2017b) (Figure 2). According to WFOs around the U.S., differences reflect the location and extent of exposed infrastructure in a given region of emphasis (e.g., a particular roadway or an entire city section), which are a function of topography, land use and existing flood mitigation strategies (e.g., hurricane floodwalls). For instance, in Wilmington, North Carolina, the official NOAA minor flood threshold is 0.25 m above the mean higher high water (MHHW) tidal datum, whereas it is about 0.5 m and 0.75 m above MHHW in Norfolk, Virginia and Galveston, Texas, respectively. When minor (henceforth referred to as ‘high tide’) flooding is likely, NOAA typically issues a coastal flood ‘advisory’, whereas when more-severe moderate and major flooding is imminent—usually due to localized storm effects—a coastal flood ‘warning’ of serious risks to life and property is issued (NOAA, 2017).

As sea levels continue to rise, not only will the frequency, depth, and extent of coastal flooding continue to rapidly increase, but they will do so largely in response to repetitive astronomical and seasonal forcing alone (Ray and Foster, 2016). The U.S. military recognizes that changes in RSL rise-related flooding pose a serious risk to their efforts and have developed tools for their engineers to estimate future sea levels and

flood risk (Moritz et al., 2015; Hall et al., 2016)⁵. It is important for planning purposes that U.S. coastal cities become better informed about the extent that high tide flooding is increasing and will likely increase in the coming decades. Of concern is that the cumulative flood toll and response costs of many lesser floods will overtake that of major, but much rarer, events (Moftakhari et al., 2017b). This concern arises because annual flood frequencies of lesser extremes are projected to (or continue to) accelerate at a faster pace (Sweet and Park, 2014; Dahl et al., 2017; Moftakhari et al., 2015; Sweet et al., 2017a) as has been observed over the last several decades at a set of actively monitored U.S. tide gauge locations (Figure 2b).

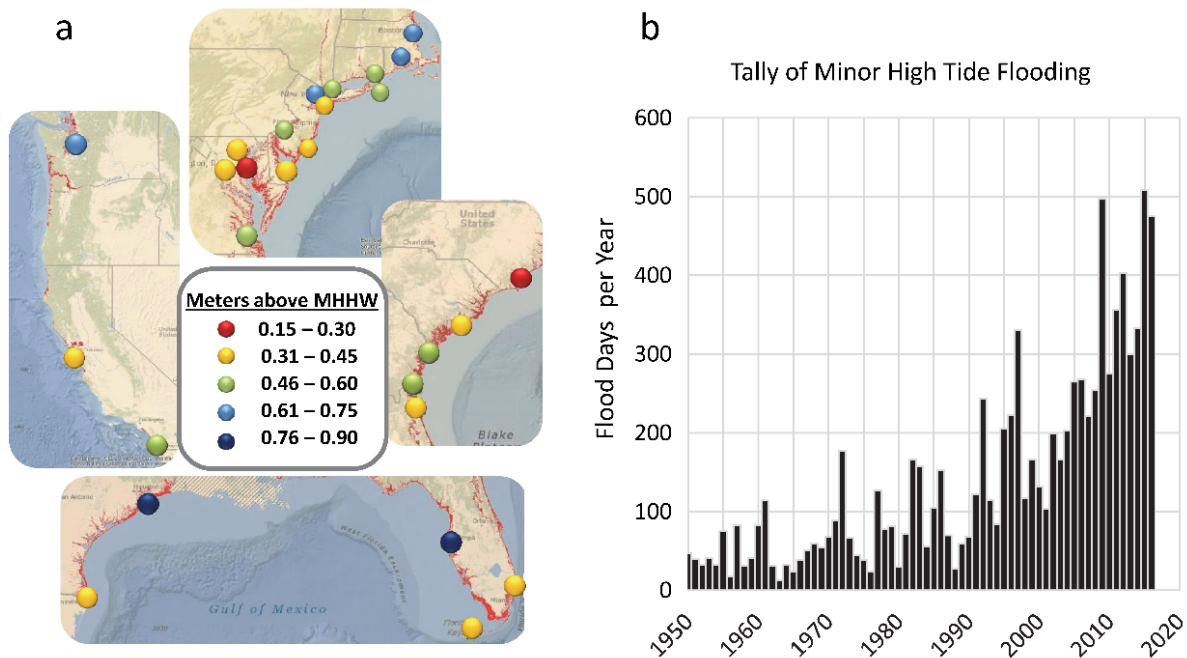


Figure 2. a) Long-term tide gauges with official NOAA flood thresholds for minor (high tide) flooding with exposed topography (red) mapped by the NOAA SLR Viewer⁶ and b) the annual summation of days with high tide flooding at locations shown in a) during 2016 as monitored by NOAA (Sweet et al., 2017b).

The intent of this report is not to supplant knowledge about local flood risk. Rather, the goal is to use the set of NOAA flood heights—where they exist—to derive a nationally consistent definition of coastal flooding and impacts used in quantifying and communicating risk⁷. Such a set of spatially consistent coastal flood thresholds (henceforth referred to as ‘derived’ flood thresholds) is currently lacking, which limits the ability to develop new products or the effectiveness of existing products that provide national coverage. A few examples include describing flood severity associated with an anticipated storm surge or coastal flood (e.g., relative to ‘ground level’), seasonal/annual monitoring and predictions of flood frequency changes (Sweet and Marra, 2015, 2016; Sweet et al., 2017b; Widlansky et al., 2017) and multi-decadal vulnerability assessments considering current and future possible sea level rise (Hall et al., 2016; Sweet et al., 2017a, c).

After presenting the derived set of flood elevation thresholds, the remainder of the report utilizes these derived thresholds for high-tide flooding (unless otherwise noted) to examine flood-frequency changes

⁵ See also <http://www.corpsclimate.us/ccaceslcurves.cfm>

⁶ See <https://coast.noaa.gov/slr/>

⁷ See http://www.weather.gov/images/akq/hydro/Coastal_Flooding/CoastalFloodingThresholds.png

and patterns at 99 NOAA tide gauge locations with >20 years of hourly data. In many instances the results are presented by geographic region (listed in Appendix 1), which are defined as tide gauge locations within the 1) Northeast Atlantic (Maine to Virginia), Southeast Atlantic (North Carolina to Florida), Caribbean Islands (Virgin Islands and Puerto Rico), Eastern Gulf of Mexico (Florida to Mississippi), Western Gulf (Louisiana to Texas), Southwest Pacific (San Diego to Arena Cove, California), Northwest Pacific (Humboldt Bay, California to Washington State) and the Pacific Islands (Hawai'i, Guam, American Samoa, Kwajalein, Midway and Wake Islands).

Flood frequency changes are documented in terms of past patterns, current conditions and future projections, specifically detailing:

- **current trends** to raise awareness of where and to what depth and possible topographic extent flood risks are rising and threatening coasts now due to RSL rise (Ezer and Atkinson, 2014; Sweet et al., 2014; Sweet and Park, 2014; Karegar et al., 2017);
- **seasonal cycles** to support preparedness efforts by identifying when during the year flooding is most typical;
- **year-to-year changes from ENSO** to support experimental 'next-year' predictions in response to forecasted ENSO phases and historical trend continuation (Sweet and Marra, 2015, 2016; Sweet et al., 2017b), which will become increasingly important for municipal budgeting purposes (mobilization costs for closing streets, installing pumps, sandbags, in-flow stormwater preventers, etc.);
- **projections in response to future sea level rise scenarios** (Sweet et al., 2017a) in terms of both historical water level observations (tides + nontidal 'weather') and predictions based upon tidal forcing alone to assist long-term planning concerned with flood risk reduction and freshwater management (Sweet and Park, 2014; Moftakhari et al., 2015; Hughes and White, 2016; Ray and Foster, 2016; Dahl et al., 2017; Habel et al., 2017; Sweet et al., 2017a).

2.0 DEFINING A CONSISTENT COASTAL FLOOD ELEVATION THRESHOLD

Most, but not all, of the official NOAA coastal flood thresholds established locally by emergency managers and NOAA WFOs are shown in the Advanced Hydrologic Prediction System⁸. This system warns of possible, predicted or ongoing hydrologic threats across the U.S., though it is primarily focused on inland flooding and tracks a vast array of national river gauges. It also tracks conditions along the coast and currently includes (subject to change) about 75 flood-hazard definitions for minor (i.e., high tide) and 50 for moderate and major coastal flooding that reference levels on NOAA tide gauges.

Previous efforts have attempted to broadly describe the official NOAA coastal flood thresholds based upon statistical analysis of flood frequencies (e.g., Kriebel and Geiman, 2014; Sweet et al., 2017a). However, such an approach assumes that all regions at some point in their (tide gauge) recorded history likely experienced a water level consistent with such an empirically based flood definition (i.e., minor, moderate or major), which is not necessarily a valid assumption. Here, we assess official NOAA coastal flood thresholds based upon heights above the local tide range or more specifically, the great diurnal (GT) tidal datum as defined by NOAA (Gill and Schultz, 2001), which is the height difference between the MHHW tidal datum and the mean lower low water (MLLW) tidal datum. The GT datum can be closely approximated as the average difference between daily highest and lowest water levels over a 19-year tidal epoch (1983–2001 is the current NOAA epoch). The GT datum, which is based upon observed water levels that form in response to tidal forcing, seasonal cycles in mean sea level and to a lesser degree storm surge climatologies, is closely related to the variance/standard deviation in daily highest water levels relative to mean sea level.

When discussing flooding, the preferred and more intuitive datum of reference should be MHHW (exceeded about 182 days per year on average) since locally this height typically delineates perennial inundation⁹. However, based upon holdover of historical precedents focused on maritime navigational services, official NOAA coastal flood thresholds are typically established and reported using the local low-water nautical-chart datum (i.e., MLLW). Following suit, when comparing the official NOAA coastal flood thresholds (relative to MLLW) with diurnal tide range (GT, which is the height difference between MHHW and MLLW tidal datums), we find a consistent pattern becomes evident through statistical regression: minor, moderate and major flooding thresholds scale linearly and can be approximated as being 0.50 m (± 0.19 m: root mean square error of linear regression), 0.80 m (± 0.25 m) and 1.17 m (± 0.39 m) above the local diurnal tide range with a small (3–4%) amplification factor (Figure 3). The tide gauges included in Figure 3 (66 with minor, 48 with moderate and 46 with major NOAA flood thresholds) represent most NOAA tide gauges with >20 years of verified data.

The Alaskan tide gauges in Figure 3 (designated by triangles) are not included in the linear regression for several reasons (personal communication with the Juneau, Alaska WFO; November, 2017): 1) Many locations have extreme tide ranges that usually buffer any storm surge that might occur (i.e., probability of joint concurrence of peak seasonal high tide and storm surge is quite low), and thus, storm surge flooding mostly affects elevations below the seasonally high tide range; 2) topography is generally steep

⁸ <http://water.weather.gov/ahps/>

⁹ <https://coast.noaa.gov/slr/>

with limited areas exposed to coastal flooding; 3) very few locations have tidal-to-geodetic elevation connections used to empirically associate and map inland flood extent and severity; 4) due to remoteness of Alaskan towns historically, infrastructure is not placed in exposed areas; and 5) the rapid drop in RSL is making coastal flooding less likely in time. It is also important to note that currently there do not exist any official NOAA coastal flood thresholds for U.S. islands, though coastal ('King Tide') flooding is becoming increasingly problematic. Sweet et al. (2014) provide a flood threshold for Honolulu (0.22 m above MHHW), but this value was not obtained via NOAA NWS; rather, it was a value obtained from the Pacific Island Ocean Observing System (PacIOOS¹⁰) and therefore is not included in the regression (Figure 3). Thus, the derived thresholds presented in this report, which are based upon regression fits to official NOAA flood threshold values, are not necessarily reflective (and no subsequent analysis using derived thresholds are provided) for locations 1) within Alaska, 2) where the tidal ranges are above about 4 m (e.g., Northern Maine) or 3) where RSL trends are decreasing (Figure 1a). Though no official NOAA thresholds exist for any U.S. island states or territories, the derived thresholds are still considered valid (and subsequent analysis is presented), since coastal flooding is an issue and island topographic characteristics and tide ranges are represented by locations with official NOAA thresholds (e.g., South Florida stations).

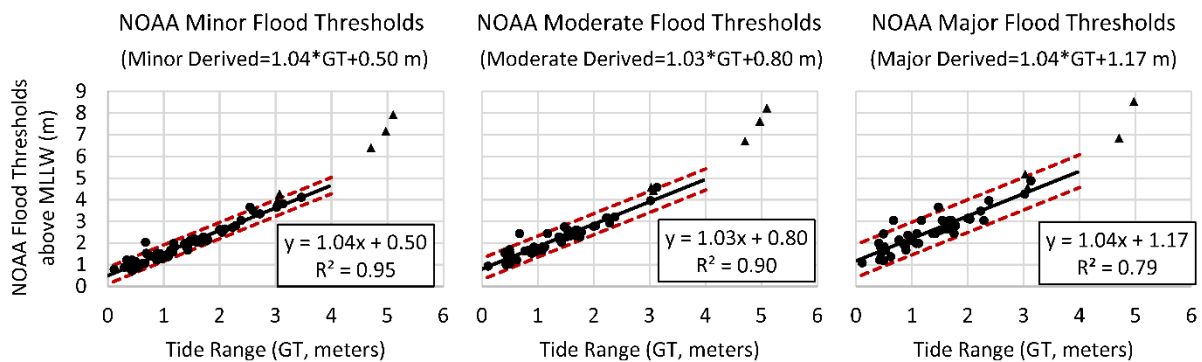


Figure 3. Scatter plot of NOAA tide gauge locations with official NOAA coastal flood thresholds (y-axis) shown relative to MLLW tidal datum for minor, moderate and major impacts and the diurnal tide range (GT). There are 66 tide gauges with minor (high tide), 48 with moderate and 46 with major flood thresholds. Locations in the continental U.S. are shown as circles, whereas those in Alaska are designated by triangles. No official NOAA coastal flood thresholds exist for island states or territories. Linear regression fits (black line and boxed equation) and the 90% confidence interval (5% and 95% as red dashed lines) are also shown. Derived thresholds are obtained by solving the regression equations for a particular location. For example, y (the minor derived flood threshold for a location) = $1.04 * x$ (the local GT tidal datum) + 0.50 m. All NOAA official flood thresholds were obtained in July 2017.

Comparison between the official NOAA and derived high tide flood thresholds (computed via the statistical regression equations in Figure 3) reveal some similarities and discrepancies (Figure 4). For instance, the derived thresholds (Figure 4b) are lower than some of the official NOAA thresholds (Figure 4a: Galveston, Texas, St. Petersburg, Florida, Alaskan locations), about the same (Norfolk, Virginia; Seattle, Washington) or higher in other locations (Wilmington, North Carolina; Miami, Florida). Woods Hole, Massachusetts is an outlier in Figure 3, whose official NOAA minor and moderate threshold is statistically above the trend's 95% confidence interval. Partial reasoning for the discrepancies reflects the intended geographic extent of the flood elevation threshold (personal communication with WFOs

¹⁰ www.pacioos.hawaii.edu

October–November 2017 and published location-specific information¹¹). For instance, high tide flooding in St. Petersburg, Florida, which has one of the highest official NOAA thresholds in the U.S. (0.84 m above MHHW), and Wilmington, North Carolina, which has one of the lowest (0.25 m MHHW), have very different consequences: high tide flooding impacts a major elevated thoroughfare along Tampa Bay and in the other location, only a minor and relatively undeveloped highway along the low-lying Cape Fear River floodplain is impacted, respectively. Accordingly, there have been no instances of high tide flooding (above the official NOAA threshold) in the St. Petersburg region over the last several decades, whereas Wilmington had 84 days of high tide flooding in 2016 (Sweet and Marra, 2015, 2016; Sweet et al., 2017b). However, due to the lack of news reports or citizen science documentation in either location, it is unclear which set of flood thresholds (official NOAA or the derived set) better align with impacts *noticeable* to coastal residents. In both locations, though impacts might be spatially limited or not necessarily observable, stormwater systems are reported to be degraded, which increases the risk of compound flooding during heavy rains (Wahl et al., 2015).

¹¹ <http://water.weather.gov/ahps/>

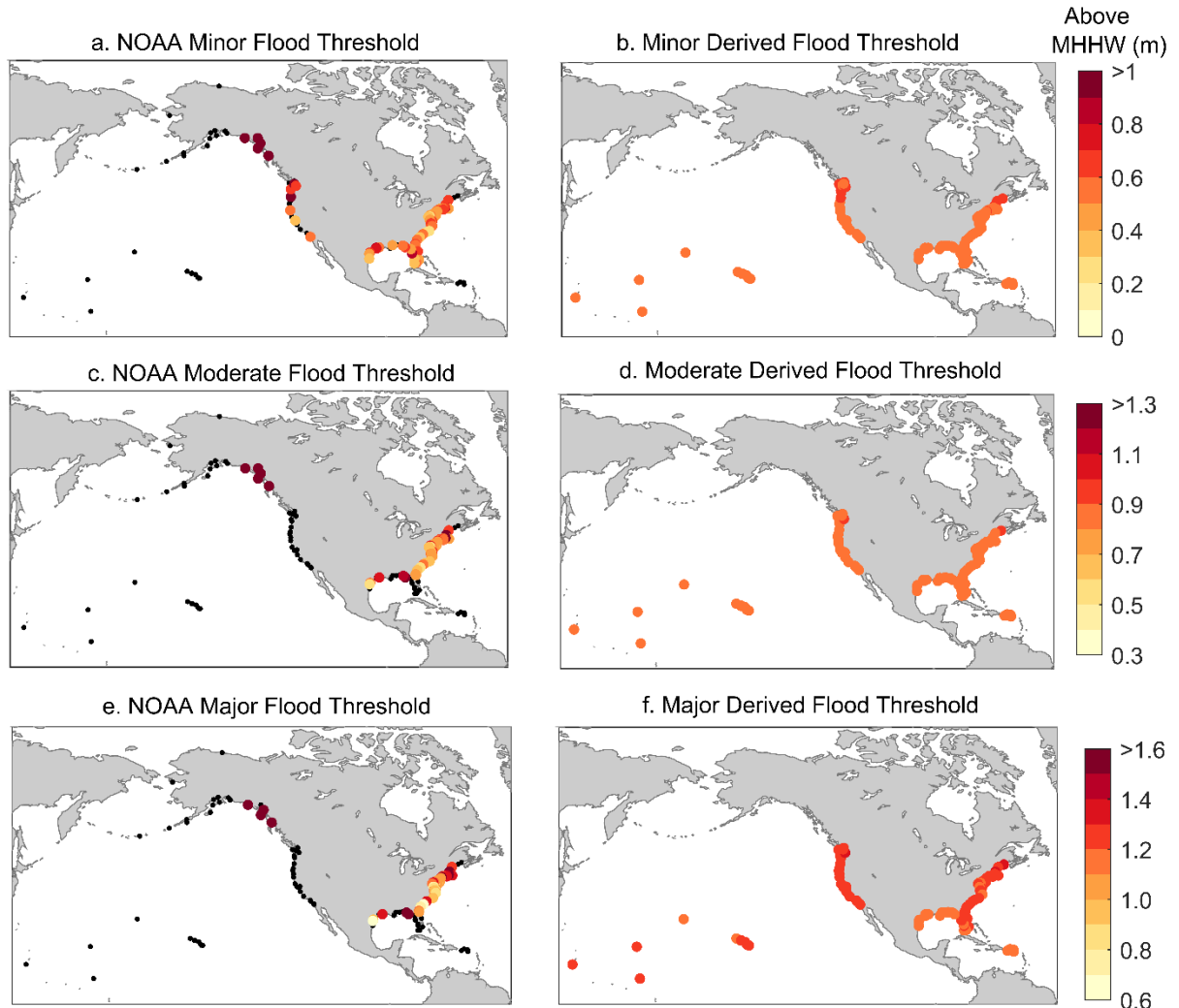


Figure 4. The official NOAA and derived elevation thresholds for high tide/minor (a, b), moderate (c, d) and major (e, f) flooding. Note that the legend scales increase by 0.3 m (about 1 foot) between minor, moderate and major flooding threshold elevations. Black dots denote locations without an official NOAA flood threshold.

Extreme value analysis is used to estimate recurrence intervals (inverse of the probability of exceeding a particular elevation) associated with the official NOAA and derived high tide/minor, moderate and major flood thresholds in order to assess the frequency patterns by region and identify spatial outliers (Figure 5). Intervals are estimated following methods of Sweet et al. (2014), who use a Peak Over Threshold (POT)/Point Process approach with a Generalized Pareto Distribution (GPD) (Coles, 2001) fit of events (peak water level over a 3-day window) above the 97th percentile of daily maximum water levels to characterize extreme exceedance properties. The recurrence intervals are ‘snapshots’ valid for a particular time period, since their underlying probabilities continue to change as sea levels change. The recurrence intervals in Figure 5 are shown relative to year 2000 local sea levels (instead of the middle [1992] of the 1983–2001 NOAA tidal epoch) as to align with the start date of the sea level rise scenarios (Sweet et al., 2017a), which are discussed below in the ‘Projections’ section. For consistency, intervals are not computed beyond a 20-year period since some of the tide gauge records are only 20 years long, and

NOAA typically does not compute extreme value statistics for tide gauges with <30 years of records (Zervas, 2013)¹².

Water levels exceeding the high tide/minor flood threshold for official NOAA thresholds (Figure 5a) generally occur at a sub-annual frequency at most locations (median value of about 0.5 years), whereas moderate and major flooding occur at about (median) 5- and 15-year intervals, respectively (Figure 5c, e). Focusing solely on minor flooding (Figure 5a), we find several locations with official NOAA thresholds with relatively long intervals (from 10 to >20 years), including Woods Hole, Massachusetts.; Vaca Key, Florida; St. Petersburg, Florida; Rockport, Texas; South Beach, Oregon; and Port Townsend, Washington. Also of note are the greater-than-20-year recurrence intervals for the official NOAA minor flood thresholds at several Alaskan locations (Figure 5a) that exceed the 100-year recurrence interval (e.g., Skagway and Ketchikan, Alaska) as estimated here (not shown) and by NOAA¹³. As noted earlier, several Alaskan locations are experiencing very rapid rates of RSL fall (Zervas, 2009), which further complicates efforts to define a contemporary definition for coastal flooding.

The recurrence intervals for the flood thresholds highlight the regional propensity of an extreme nontidal water level component (i.e., as measured by tide gauges with frequencies from minutes to days like storm surge) (Table 1) to contribute to observed high waters; patterns are clearer using the derived thresholds (Figure 5b, d, f). For instance, relatively long recurrence intervals for the derived minor and/or moderate levels (Figure 5b, d) are found along the coasts of the Southeast Atlantic, the Southwest Pacific, the Caribbean and some of the Pacific Islands. In these regions, calmer weather conditions tend to prevail and/or storm surge magnitudes are constrained due to narrow continental shelves (Tebaldi et al., 2012; Zervas, 2013; Hall et al., 2016; Sweet et al., 2017a). For instance, a water level exceeding the derived threshold for minor flooding in Honolulu, Hawai'i (0.52 m above MHHW) has never been measured in its 100+ year record; however, there were 45 days during 2015 that did exceed the 0.22 m MHHW (PacIOOS-derived) flood threshold as discussed earlier and which generated local media reports of inland flooding (Sweet et al., 2017b).

Along regions with narrow continental shelves (e.g., the Southwest Pacific and the Pacific and Caribbean Islands), dynamical wave effects like wave setup, runup/swash or harbor seiche are often a major component of the observed 'total water level' that can cause flooding, erosion and dune overtopping (Stockdon et al., 2006; Ruggiero, 2013; Moritz et al., 2015; Serafin et al., 2017; Rueda et al., 2017). Wave effects, for the most part, do not affect 'still' water levels measured and reported by NOAA tide gauges due to their sampling regime, protective wells and location mostly within protected harbors (Table 1). But their effects are significant when discussing impacts, as their vertical excursion can exceed the other nontidal water level components (e.g., storm surge) at tide gauges several times per year within high wave/low surge environments like those occurring along the California and U.S. island coasts (Sweet et al., 2015). On the other hand, in regions with wide and shallow continental shelves whose coasts are regularly exposed to extreme weather (e.g., Alaska, the Northwest Pacific and the Northeast Atlantic) or tropical storms (e.g., Western Gulf), even the derived thresholds for major flooding are exceeded every several years on average.

¹² See also <https://tidesandcurrents.noaa.gov/est/>

¹³ <https://tidesandcurrents.noaa.gov/est/>

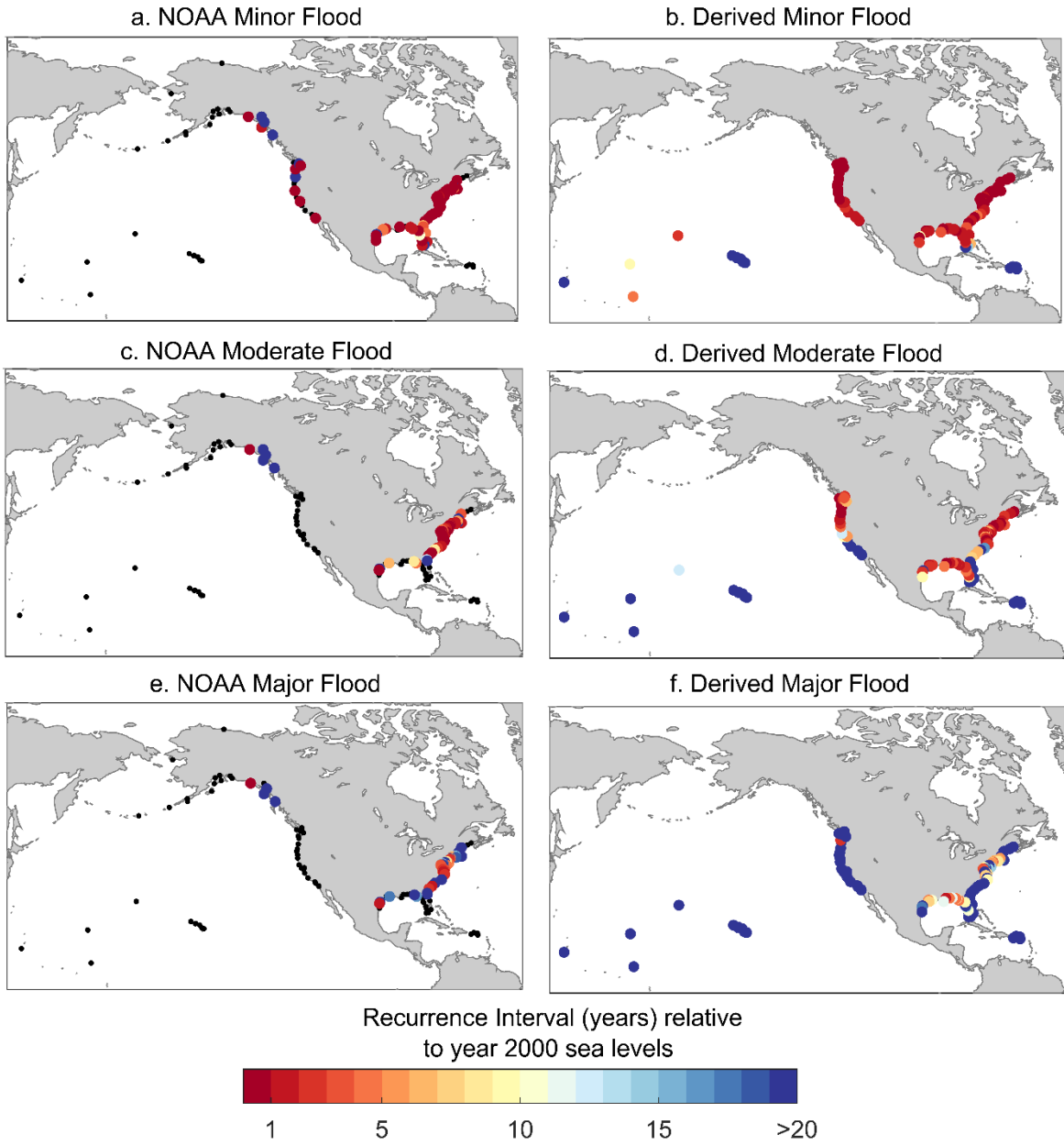


Figure 5. Recurrence intervals for the NOAA and derived elevation thresholds for high tide/minor (a, b), moderate (c, d) and major (e, f) flooding adjusted to year 2000 sea levels. Black dots denote locations without a NOAA flood threshold.

3.0 HISTORICAL PATTERNS OF HIGH TIDE FLOODING

Coastal tide gauge records reveal regionally pronounced increases in minor (high tide) flood frequencies over the last several decades (Ezer and Atkinson, 2014; Sweet et al., 2014; Sweet and Park, 2014). This increase is mostly a response to increases in local RSL as changes in storm characteristics have remained more consistent through time (Zhang et al., 2000; Sweet et al., 2017c). If RSL was not rising along most of the U.S. coastline (outside of Alaska), significant trends in high tide flood frequencies would be rare, as would changes in probabilities of more-severe moderate and major ocean-related flooding. But RSL is rising, and it is important to know how a change in mean sea level affects the frequency of high tide and storm surge-related flooding. This section documents how high tide flood frequencies have varied at 99 NOAA tide gauge locations scattered along most U.S. coastlines. Daily highest water levels are used to estimate flood frequency changes per the derived high tide/minor flood threshold shown in Figure 4b 1) over the course of decades, 2) on an interannual basis in response to ENSO forcing and 3) by season.

3.1 Trends in High Tide Flooding

Annual changes in high tide flood frequencies (henceforth referring to exceedances above the derived threshold for minor flooding) are shown in Figure 6 for 99 NOAA tide gauges. All tide gauge locations have greater than 20 years of hourly data, are outside Alaska, have tide ranges greater than 4 m and do not have a decreasing RSL trend. A 'year' in this report is based on a meteorological year (May–April) as to not divide the winter season (important to account for ENSO variability). Along coasts of the Pacific and Caribbean Islands, high tide flooding has been generally nonexistent as the derived high tide/minor flood thresholds are relatively high as compared to even annual highest water levels (not considering wave-related impacts). Along the coasts of the Northeast and Southeast Atlantic and the Western Gulf Coast, high tide flood frequencies are becoming increasingly more frequent (orange-to-red colors in Figure 6). Along the coasts of the Southwest and Northwest Pacific, high tide flood frequencies are growing more slowly, but frequencies in both regions stand out during El Niño years (also seen along part of the East Coast; examined in Section 3.2). Overall, frequencies are higher within the Northwest Pacific than along the Southwest likely due to the increased frequency of winter storms and associated storm surges and time-averaged wave effects (e.g., wave setup) during these events. Elevated water levels from dynamical wave effects that persist for several minutes or longer during sampling at NOAA tide gauges is not common (Aucan et al., 2012; Sweet et al., 2015). Typically, tide gauges are located within protected harbors, and their protective wells attenuate wind wave effects as well (Park et al., 2014). One particular outlier in this regard is the tide gauge at Toke Point, Washington, whose location on the northern end of a semi-enclosed embayment leaves the gauge exposed to conditions that include setup from both breaking waves and strong southerly wind forcing during winter storms (personal communications with Heidi Moritz of the U.S. Army Corps of Engineers and Peter Ruggiero of Oregon State University; November, 2017).

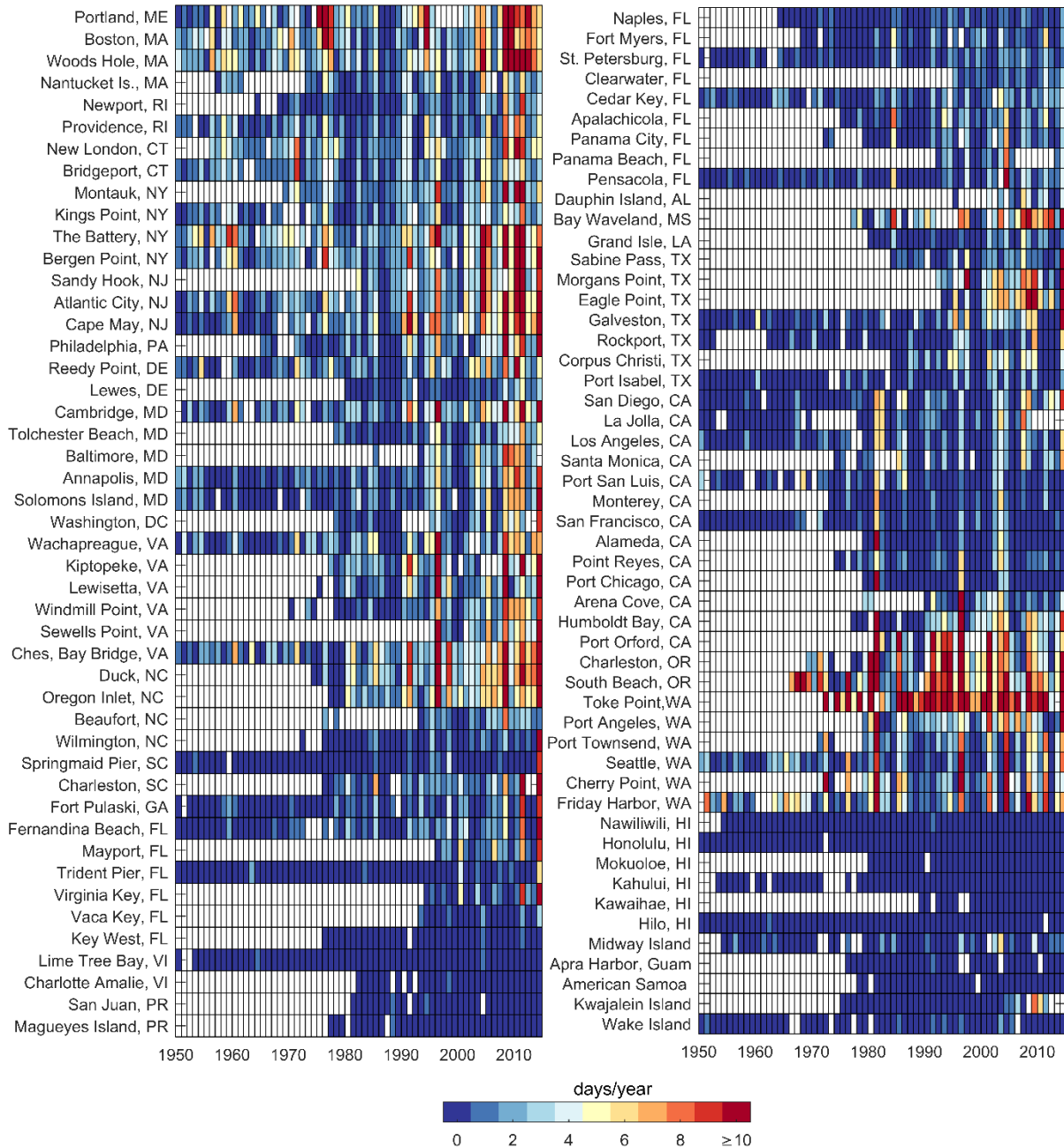


Figure 6. Annual number of high tide floods (days per year) at NOAA tide gauge locations. A year is defined in terms of a meteorological year (May–April). Note: White squares indicate no data or that hourly data was less than 80% complete within a year.

A few locations are shown in Figure 7 to illustrate the nature of change as assessed by linear or quadratic fits (here and elsewhere, fits are always significant above 90% level [p value <0.1]) in annual flood frequencies along different U.S. coastlines. In Atlantic City, New Jersey (Figure 7a), flood frequencies are rapidly changing and are accelerating with a very similar response to Norfolk, Virginia (Figure 7b). At San Diego, California (Figure 7c) and Seattle, Washington (Figure 7d), annual flood frequencies are linearly increasing over time, largely due to punctuated increases in RSL during El Niño scattered throughout the record (increasing RSL is less monotonic). The nonlinear (accelerating) response in annual high tide flood frequencies occurs in response to a consistent rise of the annual distribution of daily

highest water levels, which are approximately Gaussian relative to the flood threshold (Sweet and Park, 2014) as illustrated in Figure 1b.

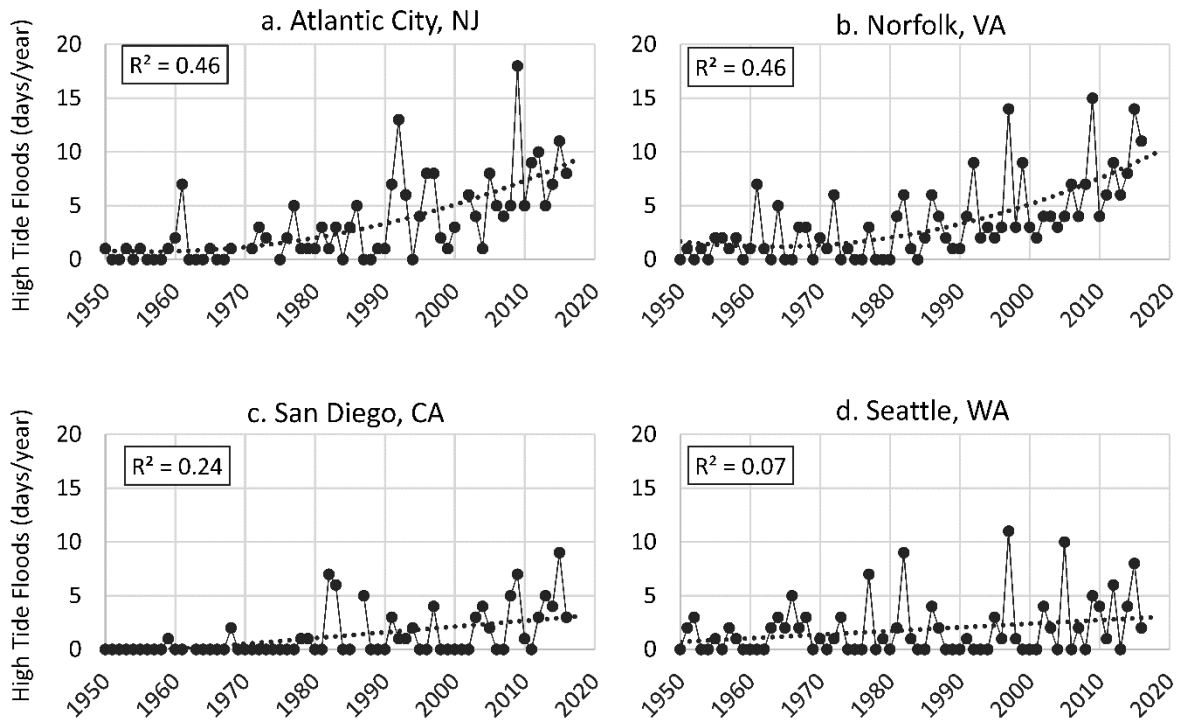


Figure 7. Number of days per year with a high tide flood at a) Atlantic City, New Jersey, b) Norfolk, Virginia, c) San Diego, California and d) Seattle, Washington. San Diego and Seattle are fit with a linear least-squares fit, whereas Atlantic City and Norfolk are fit with a quadratic. Note: the annual series is shown here as compared to a 5-year average series in Figure 1c.

Contemporary annual frequencies (days per year) are estimated for high tide flooding based upon either regression (linear or quadratic depending upon significance of fit) or a 19-year average (1998–2016) where no statistically significant trend is present (Figure 8a). High tide flooding today occurs on average 6.0 ± 2.4 (1 sigma) days/year along the Northeast Atlantic, 3.0 ± 2.4 days/year along the Southeast Atlantic, 2.4 ± 1.7 days/year along the Eastern Gulf, 4.8 ± 6.4 days/year along the Western Gulf, 1.4 ± 0.8 days/year along the Southwest Pacific, 5.4 ± 3.0 days/year along the Northwest Pacific and 1.1 ± 2.0 days/year along the Pacific Islands (Figure 8b). No high tide flooding (severity defined by tide gauge water levels) occurs along the Caribbean Islands.

The extent that high tide flood frequencies have changed in the last decade or so is likely to be informative as to which regions are becoming increasingly exposed and evermore vulnerable to impacts (Figure 8b). From 2000 to 2015, frequencies have increased the most along the Atlantic Coast. Flood frequencies rose on average by about 75% (from 3.4 days to 6.0 days/year) along the Northeast Atlantic and 125% (from 1.3 days to 3.0 days/year) along the Southeast Atlantic where numerous news reports of problematic high tide flooding anecdotally support this statistical metric (see Sweet et al., 2017b for several news links). The Southeast Atlantic has been experiencing a sharp increase in RSL over the last several years (Valle-Levinson et al., 2017), contributing to a rapid increase in the probability of high tide and rainfall-related coastal flooding (Wdowinski et al., 2016). Along the Eastern and Western Gulf,

frequencies rose on average by about 45% and 155%, respectively, with the Western Gulf heavily skewed by sharp increases measured at Eagle Point, Texas (median rise of 75% in the Western Gulf). Along the entire West Coast, the frequency of high tide flooding has remained nearly constant (no trend) with only a few locations, namely San Diego, La Jolla, Los Angeles, Humboldt Bay and Seattle, experiencing a 25% to 50% increase. The relatively stagnant growth in high tide flood frequencies is partially related to the less-than-global RSL rise along the U.S. West Coast between about 1980 and 2010 (Sweet et al., 2017c). This is in contrast to the changes along Kwajalein Island, where frequencies have grown to more than 5 days/year on average from less than 1 day/year in 2000 because of extremely high rates of RSL rise over the last several decades within the Western Equatorial Pacific; no other frequency increases occurred within the Pacific Island region (see Appendix 1) except for a small frequency increase at Midway Island. This cross-Pacific RSL rise rate differential stems largely from changes in wind forcing associated with the Pacific Decadal Oscillation (PDO; Bromirski et al., 2011; Merrifield, 2011) that appears to have undergone a phase shift since about 2012 (Hamlington et al., 2016).

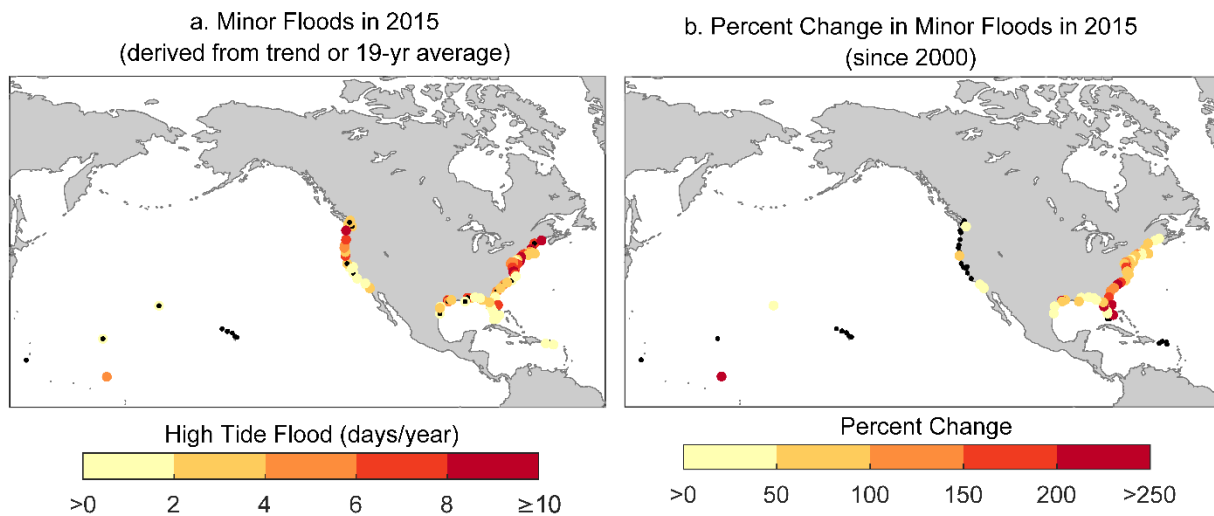


Figure 8. a) Number of days in 2015 with a high tide flood derived by trend (linear or quadratic fits above the 90% significance level) or 19-year average (1998–2016) where no significant trend exists. Black dots denote locations with no floods over the 1998–2016 period and b) is the percent change since 2000 based upon trend fits also used in a). Black dots denote locations as in a) or where no significant trend exists.

In all cases, the local rates of RSL change (Figure 1a) primarily explain ($R^2=0.61$ for quadratic fit, p value <0.01) the changes in local high tide flood frequencies (Figure 8b and Sweet et al., 2014). However, the average variance of daily highest water levels (1998–2016 average shown in Figure 9a) is a secondary factor that when combined with RSL rise rates largely explains changes in high tide flood frequencies ($R^2=0.80$ in a bivariate quadratic fit), similar to findings of Sweet and Park (2014). Or simply—where local RSL rates are higher, high tide flooding is increasing more so than where RSL rates are lower; where RSL rates are similar, locations with higher water level variance generally have experienced more high tide flooding. Variance is typically higher where tide ranges are higher or where storm surges are larger and occur more often (e.g., along coasts of the Northwest Pacific and the Northeast Atlantic). A simple ratio (Merrifield et al., 2013; Sweet et al., 2014) between the 19-year variances of the tidal-forced and observed water level (tide + nontidal) contributions (Figure 9b) helps distinguish the underlying mechanisms causing high water to form (though not necessarily causing high tide flooding). Where the ratio is closer to zero, daily highest water levels are driven more by nontidal factors (e.g., storm surge and

sea level anomalies); where they are closer to one, storm surges typically are quite small and high waters are more tidally dominated. The daily highest water levels (observations in red) and the contribution from daily highest predicted tide level (blue) at Norfolk, Virginia and San Diego, California illustrate a nontidally and a tidally dominated regime, respectively (Figures 9c and d).

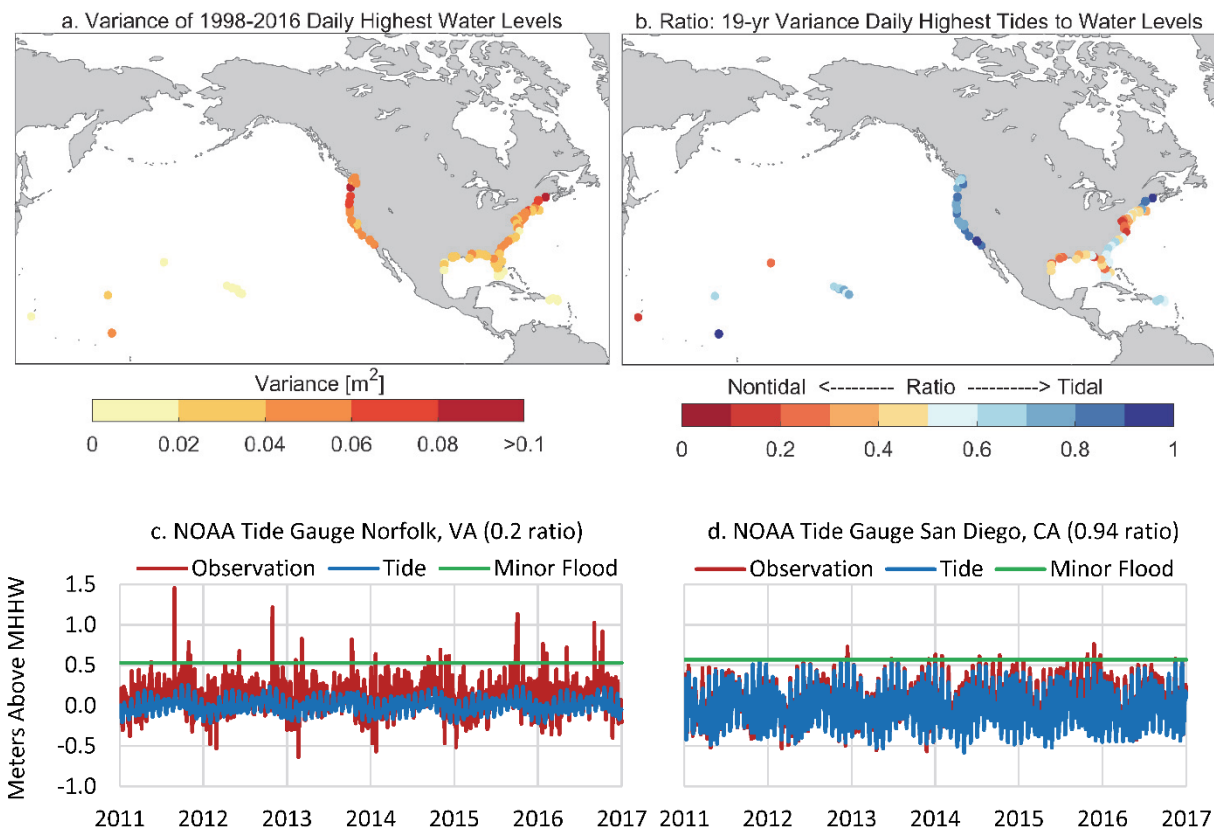


Figure 9. a) Variance of 1998–2016 daily highest water levels, b) the ratio between variances of daily highest predicted tidal component of water level to observed water levels and examples at c) Norfolk, Virginia and d) San Diego, California showing daily highest waters (red), contribution from daily highest predicted tide (blue); both are shown relative to their minor derived flood threshold (green), and the ratio is listed in parentheses.

3.2 Year-to-Year Variability in High Tide Flooding due to ENSO

Not only are annual frequencies of high tide flooding rapidly increasing in many regions due to trends in RSL (Figure 8b), they can vary substantially on a year-to-year basis (Figures 6, 7) due to climatic modes of variability affecting weather and ocean circulation patterns¹⁴. A major driver of interannual global climate is ENSO, and both probabilities of high tide and more major coastal flooding have been previously found to be especially sensitive to the El Niño phase along the U.S. West and East Coasts (Menendez and Woodworth, 2010; Sweet and Park, 2014; Sweet and Marra, 2015, 2016). Other climatic patterns besides ENSO also affect high tide frequencies as well as the probabilities of major, rarer flooding (e.g., Menendez and Woodworth, 2010; Wahl and Chambers, 2016). We focus on ENSO, since NOAA operationally tracks and predicts ENSO conditions (in terms of the Oceanic Niño Index [ONI]¹⁵),

¹⁴ See <https://www.esrl.noaa.gov/psd/data/climateindices/list/> for a list of regional indices.

¹⁵ http://origin.cpc.ncep.noaa.gov/products/analysis_monitoring/ensostuff/ONI_v5.php

which allows for future predictions based upon historical response relationships. The increased high tide flood frequencies during El Niño stem from a combination of higher sea level (from higher ocean temperatures and deeper thermoclines) along the West Coast (Enfield and Allen, 1980; Chelton and Davis, 1982). Along the East Coast, atmospheric patterns during El Niño typically favor a more coastally oriented winter-storm track (Hirsch et al., 2001; Eichler and Higgins, 2006) and prevailing winds that drive a combination of higher sea levels and a higher frequency of storm surges (Sweet and Zervas, 2011; Thompson et al., 2013).

Two probability distributions (using parametric-normal distributions for illustrative purposes only) are fit to daily highest water levels during the three years characterized by strong El Niño (1982/83, 1997/98 and 2009/10), by strong La Niña (1988/89, 1999/2000 and 2010/11) and by neutral conditions (1993/94, 2001/02 and 2012/13) at Norfolk, Virginia and San Francisco, California (Figure 10). The distributions quantify and illustrate changes in both the mean and variance (storminess) associated with ENSO.

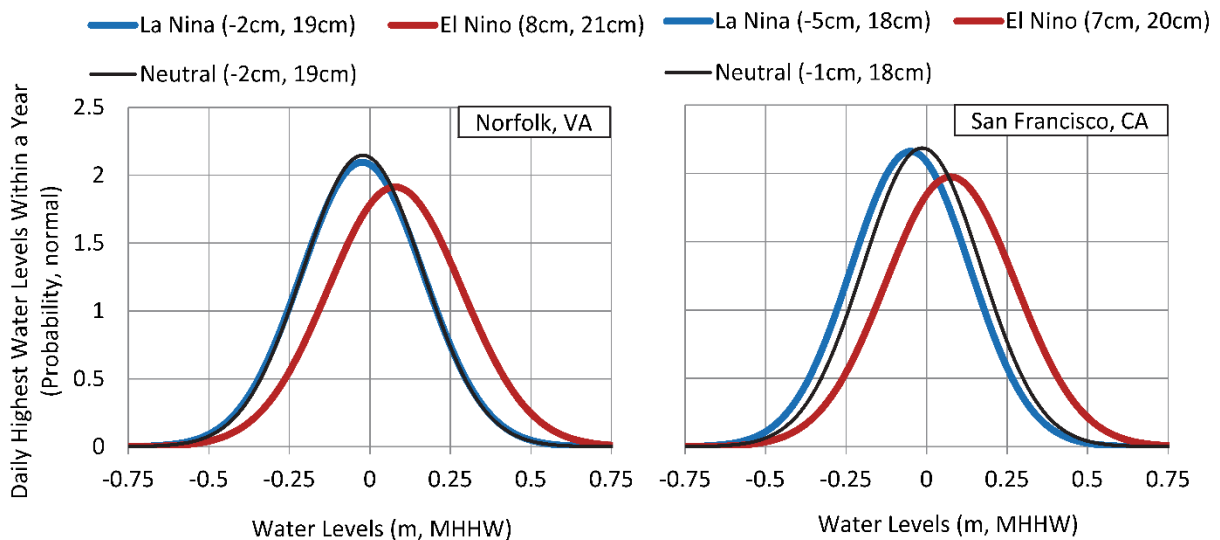


Figure 10. Parametric probability distribution (normal) fit for 3 years characterized by stronger El Niño, stronger La Niña and ENSO-neutral conditions. In parentheses are the mean and standard deviation (or square of the variance) of the distributions shown in the figures. Water levels have been detrended to enable multi-year comparisons. Not shown are the 95% confidence intervals for the distribution parameters which suggest a significant change of conditions during El Niño along both of these (and other) West and East Coast locations.

Considering this ENSO response, a substantial amount of year-to-year variability in high tide flooding along the West and East Coasts is driven by ENSO-related conditions (Figure 11). For many locations already experiencing an upward trend in high tide flooding due to changing RSL (as in Figure 7), including annual-average ONI values in a bivariate regression significantly improves the historical characterization of year-to-year flood frequencies (as in Sweet and Park, 2014). At Atlantic City, NJ and Norfolk, VA, about one-half to two-thirds ($R^2=0.54, 0.63$) of the year-to-year variability is explained through the bivariate fit (quadratic and ENSO); at San Diego, CA and Seattle, WA about one-quarter to one-half of the variability is explained ($R^2=0.45, 0.23$). The probability of flooding is more likely during El Niño even where no significant temporal trends exist in high tide flood frequencies such as along the West Coast (e.g., San Francisco); moderate and major flooding become more probable as well in these regions (Menendez and Woodworth, 2010).

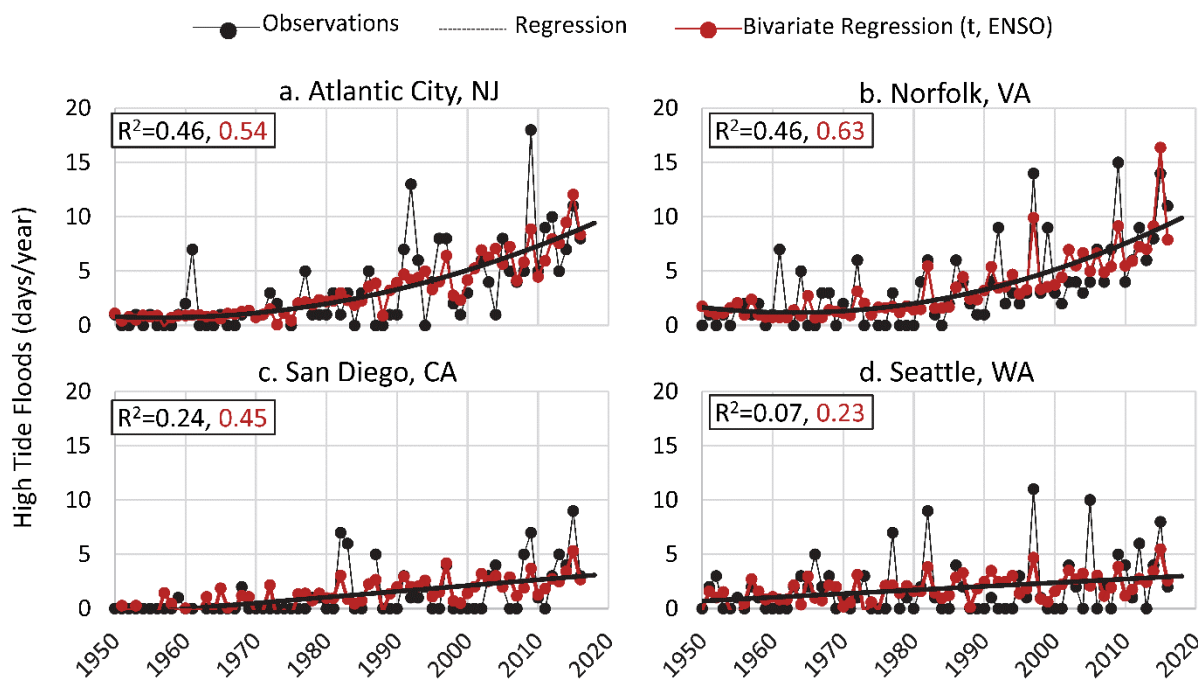


Figure 11. Trends in annual frequencies of high tide flooding (black line) are fit to observed annual flood frequencies (black line-dots) over the 1950–2016 period (or beginning of record) as shown in Figure 6. Predictions of high tide flooding based on both trend and annual averaged ENSO effects (ONI¹⁶) are also shown (red line-dots) for a) Atlantic City, b) Norfolk, c) San Diego and D) Seattle.

Locations whose annual frequencies of high tide flooding are increasing (Figure 12a) and/or reveal past sensitivity to ENSO phases (Figure 12b) will be used to support NOAA’s experimental annual high tide flood ‘outlooks’ (e.g., Sweet and Marra, 2015, 2016; Sweet et al., 2017b), which utilize ENSO phase predictions for the coming year produced by an international modeling ensemble¹⁷. Specifically, Figure 12a shows how annual high tide flood frequencies are changing on a decadal basis, and Figure 12b shows where they also change on a year-to-year basis with ENSO phase. Specifically, Figure 12b illustrates the percent change relative to (above) the trend-based or 19-year average values (Figure 8a) expected a year in advance in response to a strong El Niño that was predicted to occur. Along the East Coast, the average percentage frequency increase above the trend-derived (or 19-year average where no trend exists) value during 2015 was estimated to be about 70%; along the West Coast, it was about 170%. Subsequent monitoring verified that higher frequencies of high tide flooding did occur in many of these locations (Sweet and Marra, 2016).

In summary, of the 99 NOAA tide gauges examined, multi-decadal trends in high tide flood frequencies are accelerating (nonlinearly increasing) at 30 locations mostly along the East Coast and linearly increasing at 31 locations along the East and Gulf Coasts. On an interannual basis, flood frequencies are higher than the trend values (e.g., linear or accelerating) during El Niño at 49 locations; at one location (Kwajalein Island), frequencies are higher during La Niña.

¹⁶ http://origin.cpc.ncep.noaa.gov/products/analysis_monitoring/ensostuff/ONI_v5.php

¹⁷ <https://iri.columbia.edu>

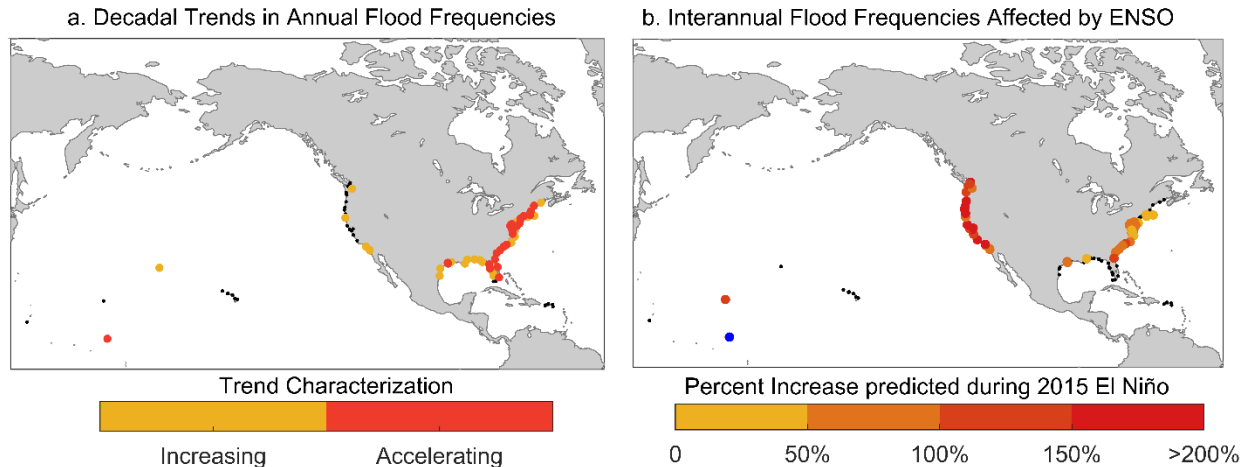


Figure 12. a) Characterization of regression trend estimates of increasing decadal annual high tide flood frequencies: accelerating (quadratic) or linear increasing or no trend (black dot) and b) locations whose high tide flood frequencies change on an interannual basis due to phases of ENSO as illustrated in Figure 11. Specifically, in b) are predictions for days in 2015 (May 2015–April 2016) with high tide flooding considering the predicted strength of El Niño (based upon ONI) relative to values based on the trend-derived or 19-year average value as shown in Figure 8a. Kwajalein Island (blue dot) in Figure 12b is opposite the other locations—flood frequencies drop during El Niño and rise during La Niña.

3.3 Seasonal Cycles in High Tide Flooding

For preparedness purposes (e.g., mobilization and budgeting reasons) it is advantageous to know when during the year high tide flooding most often occurs. In some locations, high water formation (not necessarily causing flooding) is largely driven by tidal forcing (Figure 9b). In these locations, high tide flooding most likely occurs during times of highest full/new-moon spring (or perigean spring) tides in months adjacent to the summer and winter solstices, when there is maximum declination in the earth–sun system (Merrifield et al., 2007). Such an example is shown for San Diego (Figure 9d), where the seasonal cycles in spring tides, which are highest June/July and December/January, are evident in the tide predictions and largely dictate when higher waters happen. There are actually few locations along the Southwest and Northwest Pacific and the Northeast Atlantic where high tide floods can occur *solely* from tidal forcing (Figure 13a). It should be noted that NOAA tide predictions do not incorporate long-term RSL change (Figure 1a); the effects of RSL change (more so rise than fall) are reconciled during subsequent 19-year datum updates.

Some locations are nontidally driven (tide range is small) or dependent upon both types of forcing (Figure 9b). In nontidally-driven locations, such as the Chesapeake Bay and Gulf of Mexico, high tide flooding occurs in response to short-period events regardless of predicted tide level. An example is Norfolk, Virginia (Figure 9c) where northeasterly winds—either locally or regionally prevailing—during fall through spring typically cause high tide flooding. In mixed locations (ratios about 0.3–0.7 in Figure 9b), high tide flooding is more likely to occur during periods of highest spring (full/new moon) tides during the year, which along the Southeast Atlantic, for instance, occurs in fall when the mean sea level cycle is at its seasonal maximum. Seasonal mean sea level cycles form in response to regular changes in seasonal ocean water temperature or density, prevailing winds and ocean currents (e.g., Figure 9d and further discussed in Zervas, 2009 and Sweet et al., 2014). Since the periods of the seasonal mean sea level response override an annual and semi-annual astronomical tidal constituent, they are incorporated into NOAA tide predictions. But in mixed locations, a somewhat sizable (e.g., 20–30 cm) nontidal water level

contribution is necessary for high tide flooding to occur. Nontidal contributions form in response to local wind storms or high sea level ‘anomalies,’ which can persist for days to weeks in response to more-distant wind forcing or transport slow-downs in ocean boundary currents like the Gulf Stream (Sweet et al., 2009; Ezer and Atkinson, 2014; Sweet et al., 2016).

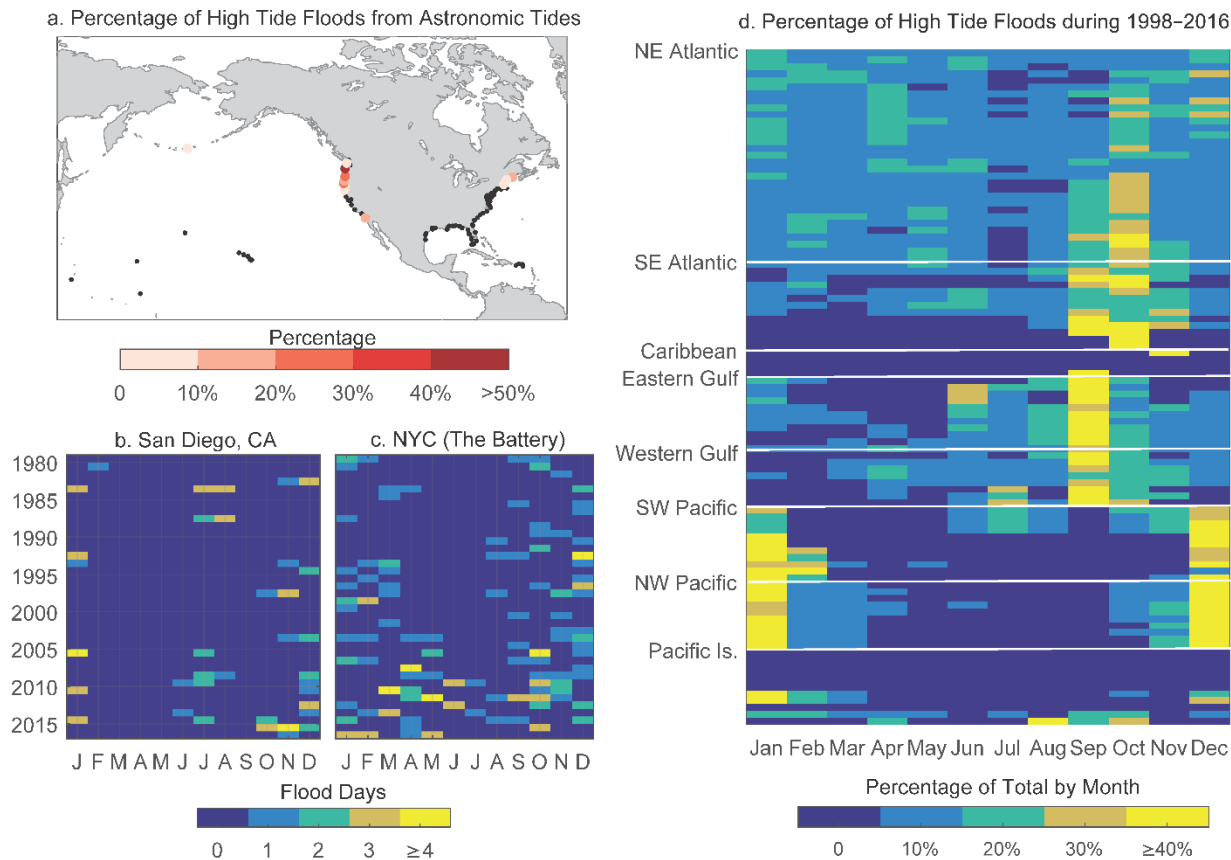


Figure 13. a) Percentage of high tide floods caused solely by tidal forcing over latest 19-year tidal epoch (1998–2016), with black dots designating locations with no high tide floods caused by tides alone or for locations with no high tide flooding during this period. For instance, 20% of San Diego’s high tide floods are caused by tides alone, whereas in New York City, the tide alone is insufficient to cause flooding, b) and c) high tide flooding in San Diego and New York City (NYC) since 1980 distributed by month and d) is the percentage of high tide flood days experienced over 1998–2016 by month at 99 NOAA tide gauges.

Within the Northeast Atlantic, daily highest water levels occur in response to a range of forcing types: nontidally dominated, tidally forced or a mixed response (Figure 9b). There are three seasonal patterns that emerge in terms of high tide flood frequencies; they are 1) generally highest from September to October at the height of the mean sea level cycle (Figure 13 c and d), 2) higher near the winter solstice (December–January) in the northern tidally dominated sub-region and 3) relatively high across the whole region throughout the cool season (September–April) due to higher incidence of storm surges from northeasterly winds events (Sweet and Zervas, 2011). Along the Southeast Atlantic and the Eastern/Western Gulf Coasts, where high water formation is tidally and nontidally mixed (ratio in Figure 9b between about 0.3 and 0.7), high tide flood frequencies are highest September–November when seasonal mean sea level cycles are at their maximum. They are higher (secondary peak) June–July as well due to a combination of tide range increases near the summer solstice and the semi-annual peak in the mean sea level cycle. Tropical cyclones are also a factor and can cause minor to major flooding

depending upon the storm track. Along the tidally forced West Coast (Figure 9b and d), high tide flooding occurs more often during spring (or perigean spring) tides in months adjacent to the winter/summer solstices (June–July and December–January) in the Southwest Pacific (Figure 13b and d); along the coast of the Northwest Pacific, the concurrence of fall/winter extratropical coastal storms reinforces highest frequencies more broadly over the November–February period (Figure 13d). Within the Caribbean and Pacific Islands, daily high-water variability is very low (Figure 9a), is mostly tidally forced (Figure 9b) and where high tide flooding has occurred, the seasonality tends to follow patterns of the Southeast Atlantic and West Coast, respectively.

The seasonality described above for each region assumes that on an interannual basis, high tide flood frequency is relatively consistent. Inspection of monthly high tide flood distributions for the last 35 years at San Diego (Figures 13b) and New York City (Figure 13c) mostly support this assumption. However, it is recognized that annual frequencies are influenced by ENSO (Figure 12a) and long-period lunar cycles affecting tide ranges as well (e.g., 4.4-year and 18.6-year cycles; Haigh et al., 2011; Sweet et al., 2016).

4.0 FUTURE PROJECTIONS OF HIGH TIDE FLOODING

Due to increasing RSL along most of the U.S. coastline (Figure 1a), high tide flood frequencies will continue to rapidly increase (Sweet and Park, 2014; Dahl et al., 2017; Mofstakhari et al., 2015; Sweet et al., 2017a, c). Here, we use the new federal interagency global sea level rise scenarios for the U.S. (Sweet et al., 2017a), which are projected onto a 1-degree grid for the entire U.S. shoreline and include additional RSL changes that result from changes in land elevation, Earth's gravitational field and rotation, and ocean circulation to project changes in high tide flood frequencies. Following methods of Sweet and Park (2014), flood frequencies are estimated through the year 2100 by projecting forward in time two separate empirical (kernel) probability estimates for the most recent 19-year period (1998–2016). The first distribution is fit to the daily highest water levels, and the second is fit to only the tidally forced component composed of official NOAA tide predictions. Separating the predicted tide component provides an approximation of the ratio of future high tide flooding likely to be forced solely by tides.

The flood frequency projections originate in the year 2000 (water level data inherent to the distribution have been detrended to year 2000) as to align with the start of the RSL projections of the global scenarios of Sweet et al. (2017a). An empirical distribution is utilized (instead of an extreme value distribution or GPD) to enable the estimation of recurrence intervals ≤ 1 year. Though the probability of floods with a recurrence interval ≤ 1 year are very well resolved with >20 years of observations (the median of the upper 95% confidence intervals is about 2.5 cm or less; not shown), year-to-year fluctuations in flood frequencies do occur due to changes in ENSO (Figure 12; Menendez and Woodworth, 2010; Sweet and Park, 2014), long-period tide cycles (Menendez et al., 2009; Haigh et al., 2011) and Gulf Stream transport (Sweet et al., 2009; Ezer and Atkinson, 2014; Sweet et al., 2016). To compensate for interannual variability (e.g., Figure 11), future frequency changes estimated only on a decadal basis are provided as to also align with the resolution of the RSL projections (Sweet et al., 2017a).

With future RSL rise, high tide flood frequencies will—or continue to—undergo an accelerated increase as illustrated for New York City, Miami, Florida and San Francisco, California (Figure 14). The annual number of high tide flood days is projected to increase fastest at New York City, with a slower rate increase in Miami (Virginia Key) and slower still in San Francisco due to a combination of higher RSL projected under the scenarios (see Figure 14 in Sweet et al., 2017a), exposure to more frequent storms and/or higher propensity for larger storm surges (Figure 9). In all three locations, daily flooding (365 days per year) occurs by the end of the century under the Intermediate (1 m global mean sea level rise by 2100), the Intermediate High (1.5 m), the High (2.0 m) and the Extreme Scenario (2.5 m) due strictly from tide forcing alone, which implies that when considering nontidal effects, high tide flooding will become deeper and more severe—causing more than minor impacts (as would be expected). If global mean sea level rise continues to follow the current trend of about 3 mm/year¹⁸ or the Low Scenario (0.3-m rise between 2000 and 2100), New York City, Miami and San Francisco will experience about 130, 60 and 30 days of high tide flooding by 2100, respectively, with about 80% from tidal forcing.

¹⁸ <https://sealevel.nasa.gov/>

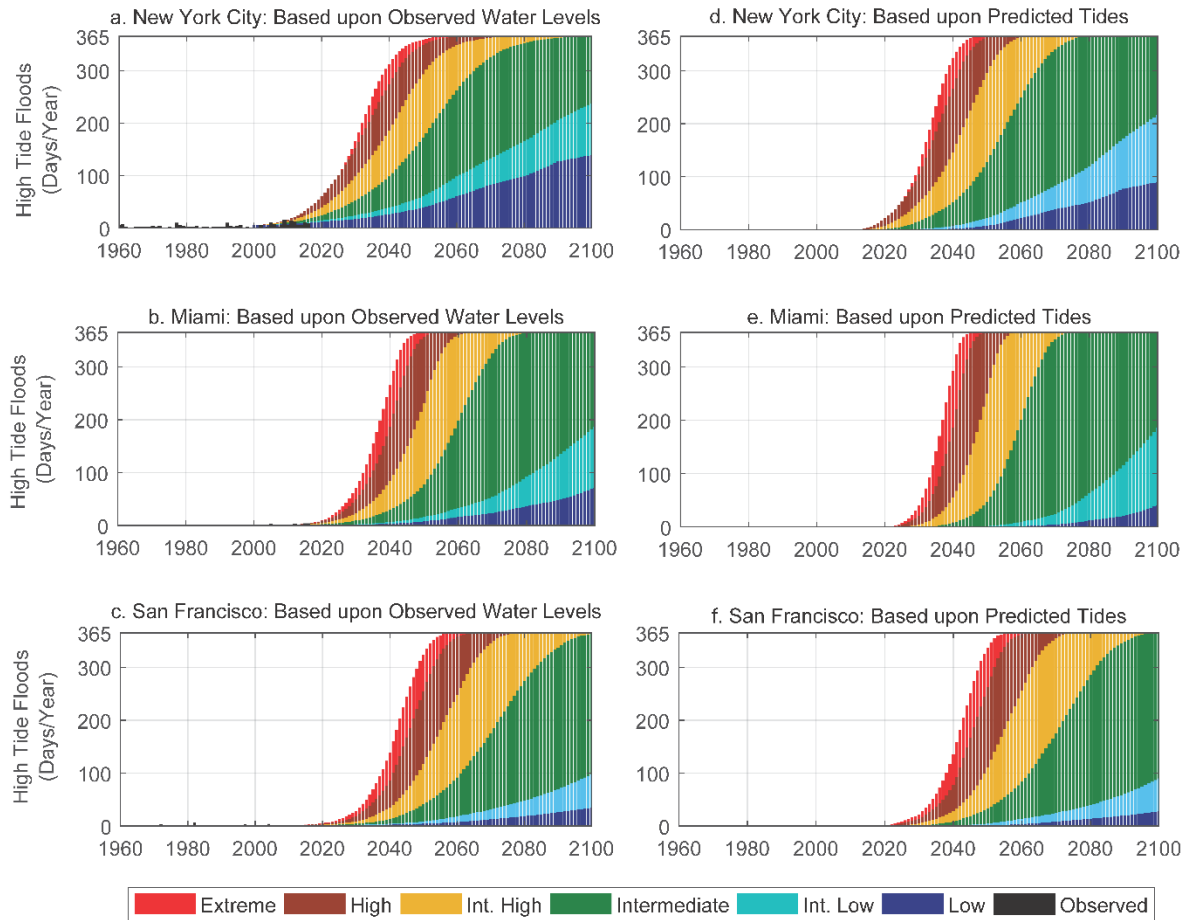


Figure 14. Projected annual frequencies of high tide flooding in response to scenarios of global sea level rise (Sweet et al., 2017) estimated at NOAA tide gauges in a) New York City (The Battery), b) Miami (Virginia Key), Florida and c) San Francisco, California considering observed patterns (combined tidal and nontidal water level components) and d), e) and f) at the same locations but assuming predicted tide forcing only. Derived high tide flood levels are 0.56 m, 0.53 m and 0.57 m, respectively.

Estimates of high tide flood frequencies by 2050 (average of 2041–2050) and the percentage caused solely by tidal forcing projected for local RSL rise under the Intermediate Low and Intermediate Scenarios for global mean sea level rise (Sweet et al., 2017a, c) are shown in Figure 15. These scenarios bound rise associated with the low-end and high-end ‘likely’ (about a 66% chance of occurrence) ranges for the representative concentration pathway (RCP) 4.5 and RCP 8.5 emissions scenarios for future global temperatures, respectively. By 2050, flood frequencies on average (spatial average) will reach about (rounded to a multiple of 5) 45 and 130 days/year (with 30 and 45% from tidal forcing) along the Northeast Atlantic and 25 and 85 days/year (35 and 65% from tides) along the Southeast Atlantic, respectively (regional values listed in Appendix 2). Along the Eastern Gulf, frequencies will reach about 25 and 80 days/year (0 and 55% from tides) and 80 and 185 days/year (45 and 80% from tides) along the Western Gulf, respectively. Along the Northwest Pacific, frequencies will reach about 15 and 30 days/year (25 and 65% from tides) and 15 and 35 days/year (75 and 85% from tides) along the Southwest Pacific coasts, respectively. Along the Caribbean, frequencies will reach about 0 and 5 days/year (0 and 10% from tides) and 5 and 45 days/year (40 and 65% from tides) along the Pacific Islands, respectively.

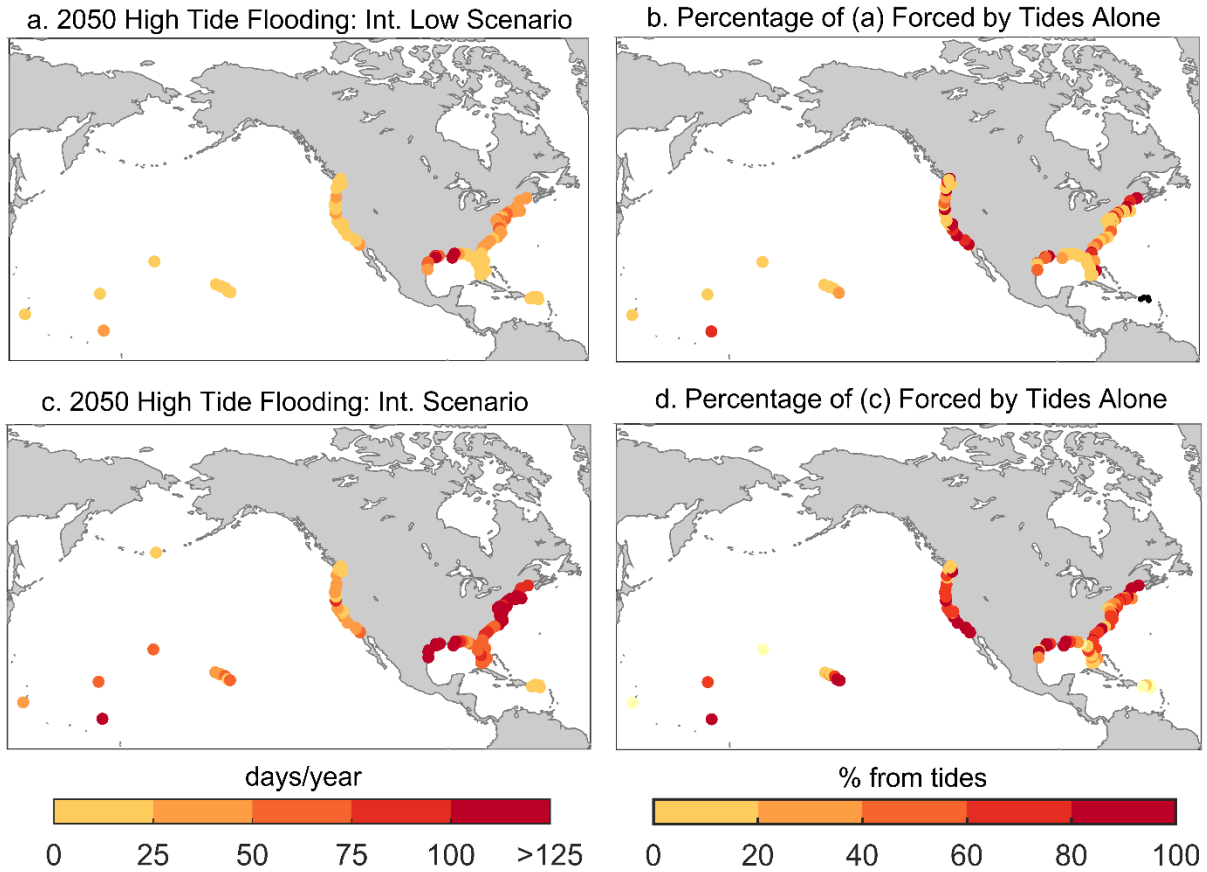


Figure 15. Projected annual frequencies of high tide flooding by 2050 (average over the 2041–2050 period) in response to the a) Intermediate Low and c) Intermediate Scenarios of global sea level rise (Sweet et al., 2017a) estimated at 99 NOAA tide gauges based upon historical patterns and percentage of floods caused by tide forcing alone in b) and d), respectively. Black dots in b) denote locations where tide alone does not exceed the minor derived flood threshold.

By 2100, along the Northeast Atlantic flood frequencies will reach on average about 235 and 365 days/year (with 95 and 100% from tides) and 195 and 365 days/year (100% under both scenarios from tides) along the Southeast Atlantic, respectively. Along the Eastern Gulf, frequencies will reach about 200 and 365 days/year (80 and 100% from tides) and 350 and 365 days/year (100% from tides) along the Western Gulf, respectively. Along the Northwest Pacific, frequencies will reach about 65 and 280 days/year (45 and 100% from tides) and 85 and 345 days/year (100% from tides) along the Southwest Pacific coasts, respectively. Along the Caribbean, frequencies will reach about 140 and 365 days/year (65 and 100% from tides) and 185 and 365 days/year (100% from tides) along the Pacific Islands, respectively.

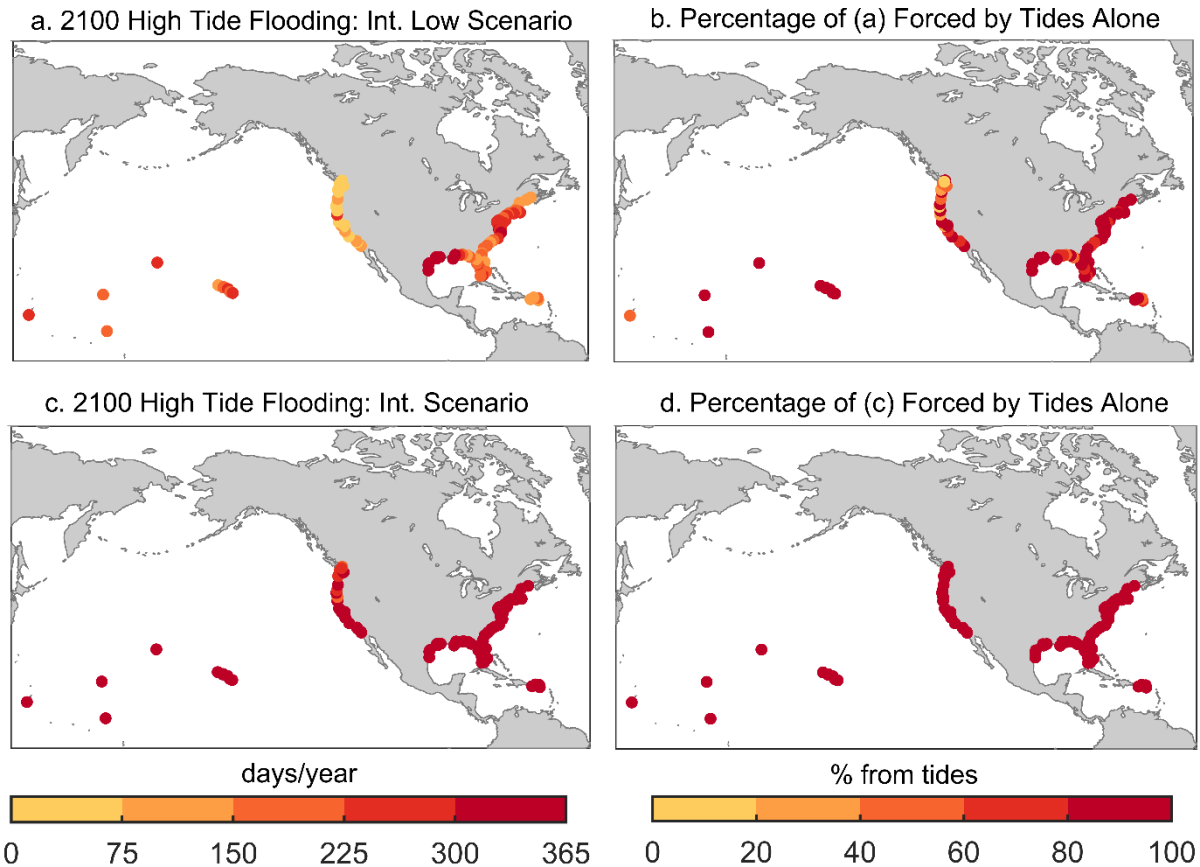


Figure 16. As in Figure 15, but for projected annual frequencies of high tide flooding by 2100 (average over the 2091–2100 period).

There is a general pattern inherent to changes in both future (Figures 14 a–c, 15a and c, 16 a and c) and historical high tide flood frequencies (Figure 8b). Namely, the rate of increase in high tide flood frequencies is primarily a function of the rate/amount of future RSL rise, which is prescribed by scenarios of Sweet et al. (2017a). Another factor is the variance in daily highest water levels (Figures 9a, 17a), which is assumed to be stationary over relatively long periods. For instance, under the Intermediate Low and Intermediate Scenarios (Figure 15a, c), spatial differences in high tide flood days in 2050 are largely explained ($R^2=0.94$ and 0.91 , respectively, by a bivariate quadratic fit significant above the 95% level) considering both the RSL amount through 2050 and a location’s high-water variance as defined over the most recent 19-year period (1998–2016) shown in Figure 9a. Or simply, high tide flood frequencies will increase in the future sooner where RSL rise rates and high-water variances are higher (Figure 14). Where variance is less (Figures 9a) and RSL rates are similar, a lagged but more-rapid rate of increase in high tide flooding will occur. On the other hand, in terms of how the percentage of high tide flooding explained by tides alone (Figure 13a) will change in the future (Figures 15b, d and 16b, d), the variance ratio between the tidal component and the daily highest observed water levels (Figure 9b) is the more informative factor.

These projections of future high tide flood frequencies are entirely dependent upon the amount of RSL rise under a particular scenario and assume that variance in local daily highest water levels (as defined over 1998–2016) will not undergo any substantial changes this century. Such an assumption may not necessarily be valid by the end of this century. As discussed above, there is year-to-year variability;

conditions typical during ENSO phases (Figure 10) affect the mean and variance of highest daily water levels and long-period tidal cycles (e.g., 18.6-year nodal cycle) alter annual tide ranges. However, there is some evidence that annual high-water variances have experienced long-term changes (albeit small) with trends evident at several U.S. locations (Figure 17b). Past variance changes are associated with both increased tidal range and storm surge magnitudes, which have been shown to be related to harbor-channel dredging activities (e.g., Talke et al., 2014; Familkhalili and Talke, 2016). Comparison between trends in annual RSL and daily high-water variance for two locations (Bergen Point, New York and Beaufort, North Carolina) whose channels have been deepened over the last century (Figure 17 c and d), nevertheless, confirm that changing RSL is the primary factor in flood frequency changes (as quantified by Sweet and Park, 2014). We note that 1) future channel deepening or other morphological changes, and possibly RSL itself, may alter high-water variance characteristics in some locations, and 2) in some regions, storm intensities (e.g., more intense hurricanes) are projected to increase, though such changes would likely be more of a factor to lower probability events with recurrence intervals >1 year (USGCRP, 2017) and are not particularly relevant to this analysis. Since this is still an active research question, the assumption of long-term stationarity of high-water variances is considered reasonable in this assessment of future exposure to high tide flooding this century.

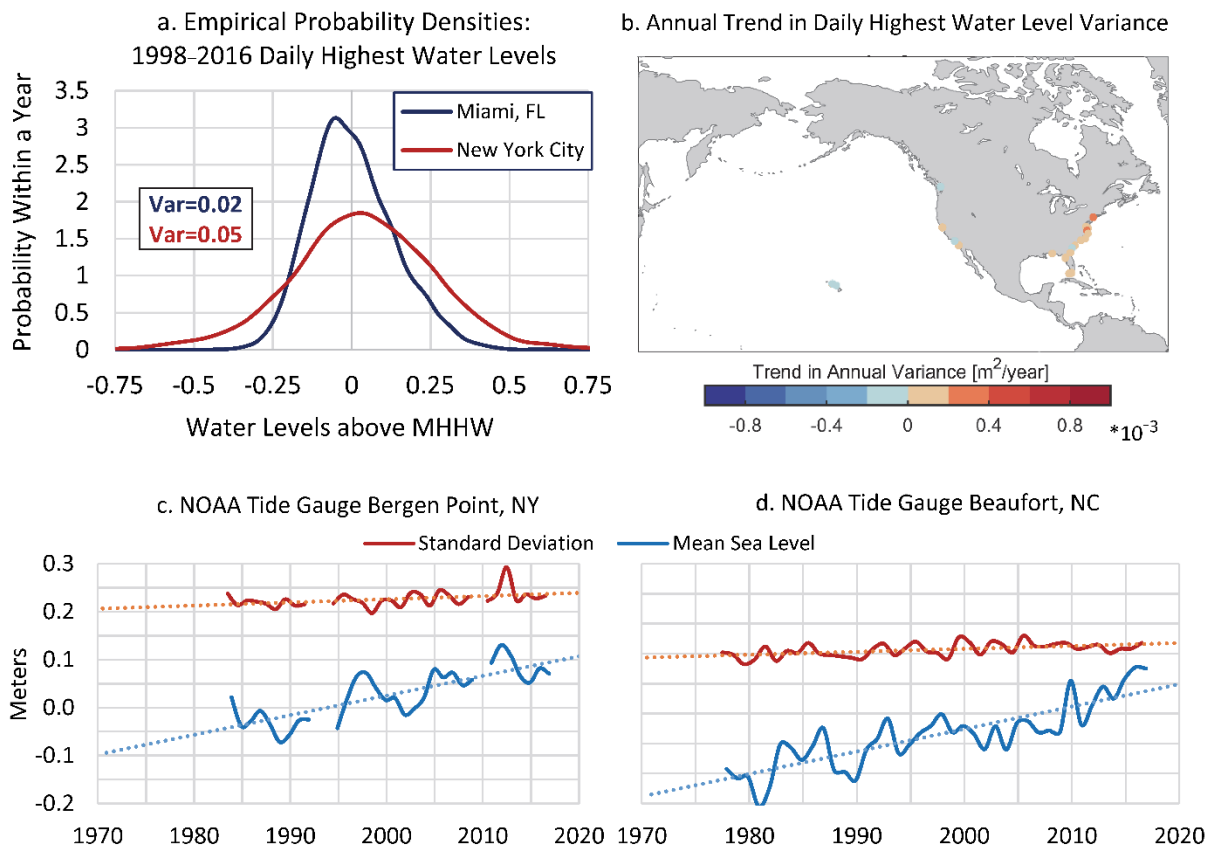


Figure 17. a) Empirical probability densities for daily highest water levels over 1998-2016 at Miami, Florida and New York City showing differences in variance (color-coded in box and in units of m^2), b) locations with linear trends (significant above 90% level) in variance computed for daily high water levels per year and relative comparison between annual mean sea level and standard deviation (variance^{0.5}) and fitted linear trends of daily highest levels per year at c) Bergen Point, New York and d) Beaufort, North Carolina where significant trends in annual variance occur.

Lastly, though flood frequencies are presented through the year 2100, which causes many locations to reach saturation or ‘daily’ high tide flooding (365 days a year with a flood, e.g., Figures 14 and 16), in reality, current flood defenses will likely be updated in many locations as to prevent daily or even every-other-day impacts. Recognizing that the MHHW tidal datum represents a height that is exceeded by water levels approximately $50 \pm 5\%$ of the days per year at a location (Figure 18a;), flood-frequency ‘tipping points’ could be considered to exist sometime prior to when a particular (minor, moderate or major) flood threshold (e.g., Figure 4b, d, e) becomes the new MHHW. Or put another way, using the phrase championed by NOAA’s (late) Margaret Davidson, there will be a time in the coming future when *“Today’s flood will become tomorrow’s high tide.”* Using the Intermediate Scenario of the U.S. Federal Interagency Sea Level Rise and Coastal Flood Hazard Task Force (Sweet et al., 2017a) as an example, the decade when the current NOAA MHHW tidal datum reaches the high tide/minor (Figure 18b), moderate (Figure 18c) and major (Figure 18d) flood elevations would be considered a likely upper bound to a frequency-based tipping point for these flood regimes. Using this scenario and approach (MHHW tidal datum instead of 50% days per year with flood), today’s daily highest tide on average reaches the high tide/minor, moderate and major flood threshold on average by or before 2060, 2080 and 2100 within the Northeast and Southeast Atlantic, the Eastern and Western Gulf and the Pacific Islands with the other regions following behind by a few decades or so.

While the rate and overall amount of RSL rise over this century (and beyond) is uncertain, as it is linked to future amounts of emissions and global temperature rise (USGCRP, 2017), it is nearly certain that high tide flooding will become increasingly chronic within coastal communities over the next several decades simply under current rates of local RSL rise. In some locations, the derived flood thresholds presented in this report may or may not necessarily reflect current vulnerabilities (Figure 4); in some locations, they may be higher or lower than the official NOAA thresholds, which are set for emergency response purposes. In addition, future enhancements to a location’s flood defenses may change its exposure/vulnerability to high tide flooding. Incremental changes in flood height thresholds can substantially change associated annual flood frequencies and their trend characterizations (Sweet and Park, 2014; Sweet et al., 2017b). For instance, there is a 10-fold increase in annual flood frequencies associated with arbitrary flood thresholds of 0.6 m and 0.3 m MHHW in Norfolk, Virginia (Figure 18a). As such, it would be advantageous if sea levels and a range of informative coastal flood metrics (e.g., various flood heights) for locations to be operationally tracked and monitored relative to historical climatologies and scenarios that bound future possible conditions to keep community planners informed of the changing nature of coastal flood risks.

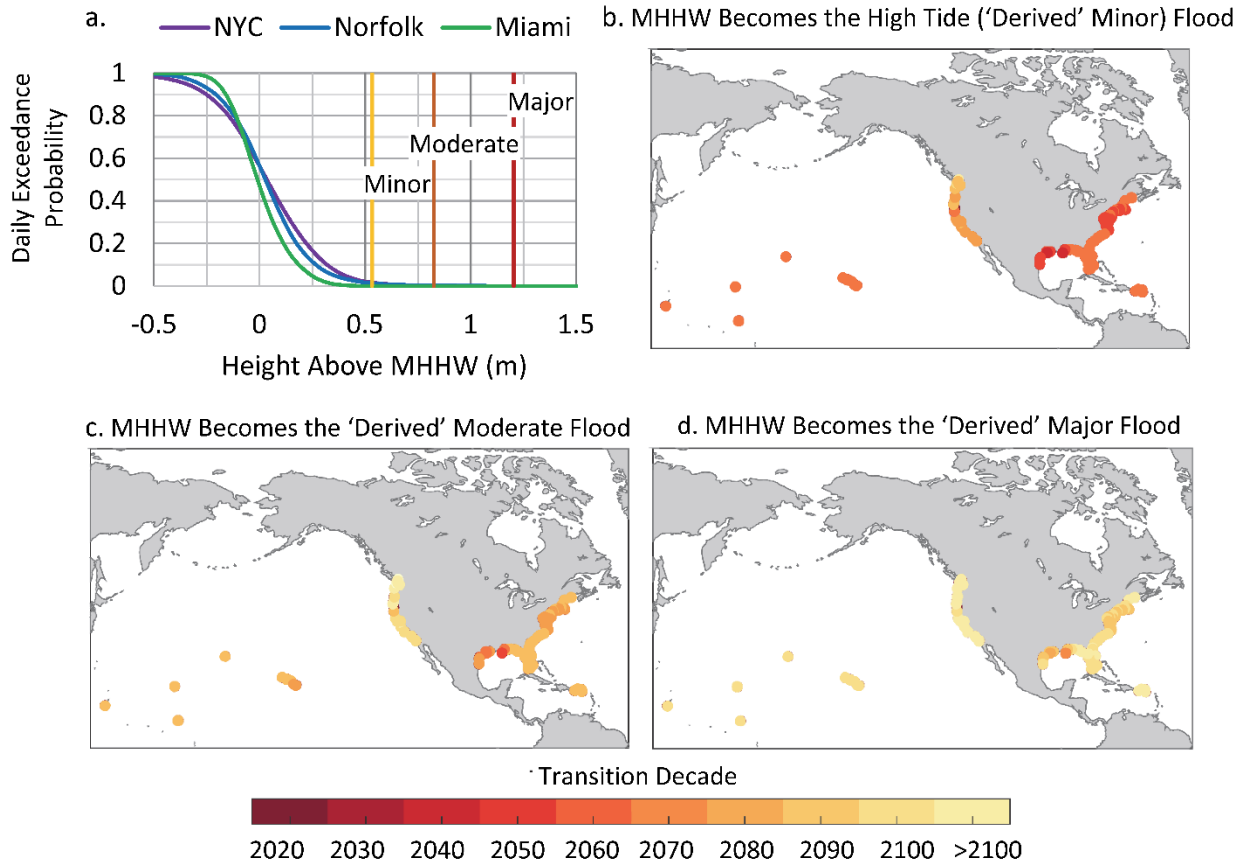


Figure 18. a) Daily exceedance probabilities (1-cumulative distribution) within a year for New York City (The Battery), Norfolk (Sewells Point), Virginia and Miami (Virginia Key), Florida based upon daily highest water levels over the 1998–2016 period with their average high tide/minor, moderate and major flood thresholds labeled. The decade when MHHW reaches the b) high tide/minor threshold, c) moderate threshold and d) major threshold levels for coastal flooding for local RSL projections under the Intermediate Scenario developed by the Federal Interagency Sea Level Rise and Coastal Flood Hazard Task Force (Sweet et al., 2017a).

5.0 SUMMARY REMARKS

There exists a remarkable consistency along the U.S. coastline in terms of the elevations that define impact severities (ranging from disruptive to destructive) to coastal flooding. Using the existing ‘official NOAA’ flood elevation impact thresholds (they exist only at several dozen U.S. coastal locations), which have been empirically calibrated to NOAA tide gauges by the NWS WFOs and local emergency managers, we find that when water levels exceed about 0.5 m, 0.8 m and 1.17 m above a height slightly higher (3–4%) than the local tide range, minor, moderate and major flooding will occur (Figure 3). With such a tide-range-based flood definition, a spatially continuous set of thresholds can be estimated for most U.S. coastlines. NOAA coastal flood thresholds—like inland river flood thresholds—are used to alert the general public of forecasted impacts (NOAA, 2017); coastal flood ‘advisories’ and ‘warnings’ are issued when minor flooding is likely (referred to as ‘high tide’ flooding that is mostly disruptive or a nuisance) and when more severe moderate or major flooding (not associated with tropical cyclones) is imminent or occurring (which pose a significant risk to life and property), respectively.

The derived flood thresholds are not intended to supplant local knowledge or existing products concerning flood risk but rather provide spatial insights about national infrastructure vulnerabilities along the coast where such information is lacking. In some instances, locations may be less susceptible to impacts at the derived levels, the extent of which is likely due to differences in topography, land use and existing flood defenses. Unfortunately, due to continued RSL rise (Figure 1a), the remaining ‘freeboard’ or difference between average highest tide (MHHW) and flood thresholds (i.e., derived or official NOAA minor, moderate or major) is decreasing along most U.S. coastlines outside Alaska. In response, the risk of coastal flooding is rapidly increasing; in fact, annual high tide flood frequencies are already linearly increasing or accelerating at most locations examined (Figure 12a). In this report, we provide a method to derive three coastal flood height impact thresholds. What is lacking is an analogous frequency–duration impact threshold for coastal flooding. Such a flood-frequency ‘tipping point’ is becoming more apparent as several coastal cities with infrastructure increasingly vulnerable to high tide flooding undertake large-scale and costly upgrades to combat effects of high tide flooding. For instance, within Norfolk, Virginia, Charleston, South Carolina and Miami Beach, Florida (among others), large-scale engineering solutions are being planned or implemented when only about 5–10 days of flooding per year are being experienced (per 2015 trend values).

For community planning and preparedness purposes, the lesser-extreme/more-probable flood instances (high tide flooding) appear to be a telling indicator of RSL rise-related impacts that should be tracked and monitored. Using the derived thresholds for minor (high tide) flooding, we find that several flood frequency characteristics are important to explaining regional differences and temporal patterns.

- Currently, high tide flood frequencies are increasing at faster rates (and therefore likely most problematic) along the coasts of the Southeast Atlantic and to a lesser extent along the Northeast Atlantic and Western Gulf of Mexico. Between 2000 and 2015, annual frequencies have increased on average by about 125% (1.3 to 3.0 days/year) along the Southeast Atlantic, by 75% (3.4 to 6.0 days/year) along the Northeast Atlantic and by (median values) 75% (1.4 to 2.5 days/year) along the Western Gulf (Figure 8b).
- Decadal trends in annual flood frequencies are accelerating (nonlinearly increasing) at 30 locations mostly along the East Coast and linearly increasing at 31 locations along the East, Gulf

and Pacific Coasts. This implies that once flooding becomes problematic locally, frequencies/impacts are likely to become chronic rather quickly (e.g., Figure 14).

- At 50 East and West Coast locations, high tide flood frequencies change with ENSO phase. At 49 locations, they are higher on a year-to-year basis during El Niño and one location is higher during La Niña (Figure 12b), which is especially problematic since the underlying trends are already increasing or accelerating in many locations (Figure 11). The coastal-flood frequency response to El Niño can be significant. For example, during 2015, high tide flood frequencies were predicted to increase on average by about 70% at dozens of East Coast locations and 170% along West Coast locations. Subsequent monitoring the following year verified that indeed several of these cities experienced high tide flood frequencies in-line with predictions produced the year prior.
- Along the Northeast Atlantic, high tide flooding occurs in response to both tidal forcing (i.e., during spring tides) and episodic nontidal effects (e.g., storm surges). It is most frequent in the fall when the mean sea level cycle is at its highest, but it is relatively frequent throughout the cool season (September–April) when northeasterly winds and nor'easters prevail (Figure 13d). Along the coasts of the Southeast Atlantic (tidally driven) and the Gulf of Mexico (nontidally driven), high tide flooding is most frequent in the fall but with a secondary emphasis in early summer. Along the West Coast (tidally driven), high tide flooding occurs most during the winter extratropical storm season (November–February) with emphasis in the months adjacent to the winter (Northwest Pacific) as well as the summer (Southwest Pacific) solstices when tide ranges are highest in response to maximum earth–sun declination.
- High tide flood frequencies are expected to rapidly increase along the U.S. coastline and increasingly due to tidal forcing alone (Figures 15 and 16), which currently is very rare (Figure 13a). We highlight changes associated with RSL rise projected under the Intermediate Low and Intermediate scenarios for global sea level rise (Sweet et al., 2017a). These scenarios are chosen because they bound the ‘likely’ range (66% contingent probability) of global sea level rise for a range of (steadily rising) global temperature futures—the RCP 4.5 and RCP 8.5 emissions scenarios. By 2050, high tide flooding will occur on average about
 - 45 and 130 days/year (30 and 45% from tidal forcing alone) along the Northeast Atlantic and 25 and 85 days/year (35 and 65% from tides) along the Southeast Atlantic, respectively;
 - 25 and 80 days/year (0 and 55% from tides) along the Eastern Gulf and 80 and 185 days/year (45 and 80% from tides) along the Western Gulf, respectively;
 - 15 and 30 days/year (25 and 65% from tides) along the Northwest Pacific and 15 and 35 days/year (75 and 85% from tides) along the Southwest Pacific, respectively;
 - 0 and 5 days/year (0 and 40% from tides) along the Caribbean and 5 and 45 days/year (40 and 65% from tides) along the Pacific Islands, respectively.
- By 2100, high tide flooding will become or exceed on average ‘every other day’ flooding under the Intermediate Low scenario within the Northeast and Southeast Atlantic, the Eastern and Western Gulf, and the Pacific Islands with tidal forcing causing all (100%) of the floods except within the Eastern Gulf (80% by tides).
- By 2100, high tide flooding will become ‘daily’ flooding under the Intermediate scenarios within all regions (Figure 18b) except for Southwest (345 days/year) and Northwest (280 days/year) Pacific coasts; tides will cause all (100%) flooding in all regions.
- In general, high tide flood frequencies will continue to increase sooner—but more gradually—where RSL rise rates are higher and within high-energy environments with frequent storm surges

and other nontidal-related high waters (Figure 9b) such as along the Western Gulf and Northeast Atlantic Coasts (Figures 14, 15 and 16). On the other hand, where RSL rise rates are lower, weather conditions are typically calmer and water levels are more tidally dominated (e.g., the Southeast Atlantic, Southwest Pacific and Caribbean and Pacific Island Coasts), high tide flood frequencies will experience (eventually) the fastest rate of increase, which may be especially problematic as impacts will transition from mild to chronic very rapidly.

In closing, the derived thresholds for high tide flooding provide a more consistent national coastal flood metric that likely reflects current development patterns/regulations. Such consistency in flood definition could help inform NOAA and other agency/commercial products and services such as those 1) estimating the depth of an anticipated storm surge recognizable by a local population, 2) providing seasonal-to-annual outlooks of flood frequencies (Sweet and Marra, 2015, 2016; Sweet et al., 2017b; Widlansky et al., 2017) for preparedness and resource budgeting or 3) assessing coastal-flood vulnerabilities due to increasing sea levels this century (Hall et al., 2016; Sweet et al., 2017a, c). It is important to note that coastal flooding in this report strictly refers to the phenomenon as measured by the tide gauge (still water level; Moritz et al., 2015; Hall et al., 2016); in reality, coastal flooding occurs for a variety of reasons, which varies by location. Often coastal flooding is influenced by other dynamical processes, such as from waves and their effects (Stockdon et al., 2006; Sweet et al., 2015; Serafin et al., 2017), local rainfall (Wahl et al., 2015), elevated groundwater tables (Sukop et al., 2018) or river runoff (Moftakhari et al., 2017a). Ultimately, joint investigations of water level/wave/rainfall/groundwater/discharge-driven total water levels together with local-to-regional elevation distributions are needed to quantify exposure of local infrastructure/elevations and assess contemporary and future vulnerabilities. As with all types of assessments (e.g., U.S. National Climate Assessments), a review is suggested every five years or as warranted to best reflect improvements or changes in measures taken to adapt to or mitigate against the impacts of flooding, such as changes in impervious surfaces and upgrades in tidal-flood defenses and stormwater systems.

ACKNOWLEDGEMENTS

We thank Heidi Moritz of the U.S. Army Corps of Engineers, Richard Ray of the U.S. National Aeronautics and Space Administration and Doug Marcy of NOAA's Office of Coastal Management for their reviews* of this manuscript and constructive comments (*a review does not necessarily indicate agreement on all points of the final version). We also thank Brooke Stewart of NOAA's National Centers for Environmental Information for manuscript editing assistance.

REFERENCES

- Aucan, J., R. Hoeke and M. A. Merrifield (2012). Wave-driven sea level anomalies at the Midway tide gauge as an index of North Pacific storminess over the past 60 years, *Geophys. Res. Lett.*, 39, L17603, doi:10.1029/2012GL052993.
- Bromirski, P. D., A. J. Miller, R. E., Flick and G. Auad (2011). Dynamical suppression of sea level rise along the Pacific coast of North America: Indications for imminent acceleration. *Journal of Geophysical Research: Oceans*, 116(C7).
- Buchanan, M. K., R. E. Kopp, M. Oppenheimer and C. Tebaldi (2016). Allowances for evolving coastal flood risk under uncertain local sea-level rise. *Climatic Change*, 137(3-4), 347-362.
- Buchanan, M. K., M. Oppenheimer and R. E. Kopp (2017). Amplification of flood frequencies with local sea level rise and emerging flood regimes. *Environmental Research Letters*, 12(6), p.064009.
- Chelton, D. B. and R. E. Davis (1982). Monthly mean sea level variability along the west coast of North America, *J. Phys. Oceanogr.*, 12(8), 757–784.
- Coles, S.G. (2001). An introduction to statistical modeling of extreme values. London, Springer. 208pp.
- Church, J. A. and N. J. White (2011). Sea-level rise from the late 19th to the early 21st century. *Surveys in Geophysics*, 32(4-5), 585-602.
- Dahl, K.A., M. F. Fitzpatrick and E. Spanger-Siegfried (2017). Sea level rise drives increased tidal flooding frequency at tide gauges along the U.S. East and Gulf Coasts: Projections for 2030 and 2045. *PLOS ONE*, 12, e0170949. <http://dx.doi.org/10.1371/journal.pone.0170949>
- Eichler, T. and W. Higgins (2006). Climatology and ENSO-related variability of North American extratropical cyclone activity. *J. Climate*, 19, 2076–2093.
- Enfield, D. B. and J. S. Allen (1980). On the structure and dynamics of monthly mean sea level anomalies along the Pacific coast of North and South America, *J. Phys. Oceanogr.*, 10, 557–578, doi:10.1175/1520-0485(1980)010<0557:OTSADO>2.0.CO;2.
- Ezer, T. and L.P. Atkinson (2014). Accelerated flooding along the U.S. East Coast: on the impact of sea-level rise, tides, storms, the Gulf Stream, and the North Atlantic Oscillations. *Earth's Future*, 2, 362-382. doi:10.1002/2014EF000252.

Familkhalili, R. and S. A. Talke (2016). The effect of channel deepening on tides and storm surge: A case study of Wilmington, NC, *Geophys. Res. Lett.*, 43, 9138–9147, doi:10.1002/2016GL069494.

Flood, J.F. and L. B. Cahoon (2011). Risks to coastal wastewater collection systems from sea-level rise and climate change. *Journal of Coastal Research*, 27(4), 652–660. West Palm Beach (Florida), ISSN 0749-0208.

Gill, S. and J. Schultz (2001). Tidal datums and their applications, Special Publication NO. CO-OPS1, NOAA, National Ocean Service Center for Operational Oceanographic Products and Services, 111p, appendix.

Habel, S., C. H. Fletcher, K. Rotzoll and A. I. El-Kadi (2017). Development of a model to simulate groundwater inundation induced by sea-level rise and high tides in Honolulu, Hawai'i. *Water Research*, 114, pp.122-134.

Haigh, I. D., M. Eliot and C. Pattiaratchi (2011). Global influences of the 18.61 year nodal cycle and 8.85 year cycle of lunar perigee on high tidal levels, *J. Geophys. Res.*, 116, C06025, doi:10.1029/2010JC006645.

Hall, J.A., S. Gill, J. Obeysekera, W. Sweet, K. Knuuti, and J. Marburger (2016). Regional Sea Level Scenarios for Coastal Risk Management: Managing the Uncertainty of Future Sea Level Change and Extreme Water Levels for Department of Defense Coastal Sites Worldwide. U.S. Dept of Defense, Strategic Envir. Research and Development Program. 224 pp.

Hamlington, B.D., S.H. Cheon, P.R. Thompson, M.A. Merrifield, R.S. Nerem, R.R. Leben and K.Y. Kim (2016). An ongoing shift in Pacific Ocean sea level. *Journal of Geophysical Research Oceans*, 121, 5084-5097. <http://dx.doi.org/10.1002/2016JC011815>

Hay, C. C., E. Morrow, R. E. Kopp, and J. X. Mitrovica (2015). Probabilistic reanalysis of twentieth-century sea-level rise. *Nature*, 517(7535), 481-484.

Hirsch, M. E., A. T. DeGaetano and S. J. Colucci (2001). An East Coast winter storm climatology. *J. Climate*, 14, 882–899.

Hsu, C.-W. and I. Velicogna (2017). Detection of sea level fingerprints derived from GRACE gravity data., *Geophys. Res. Lett.*, 44, doi:10.1002/2017GL074070.

Hughes, J.D. and J. T. White (2016). Hydrologic conditions in urban Miami-Dade County, Florida, and the effect of groundwater pumpage and increased sea level on canal leakage and regional groundwater flow (ver. 1.2, July 2016): U.S. Geological Survey Scientific Investigations Report 2014–5162, 175 p., <http://dx.doi.org/10.3133/sir20145162>.

Karegar, M. A., T. H. Dixon, R. Malservisi, J. Kusche, and S. E. Engelhart (2017). Nuisance Flooding and Relative Sea-Level Rise: the Importance of Present-Day Land Motion. *Scientific Reports*, 7.

Kopp, R. E., R. M. Horton, C. M. Little, J. X. Mitrovica, M. Oppenheimer, D. J. Rasmussen, B. Strauss and C. Tebaldi (2014). Probabilistic 21st and 22nd century sea-level projections at a global network of tide-gauge sites. *Earth's Future*, 2(8), 383-406.

- Kopp, R. E., C. C Hay, C. M Little and J.X. Mitrovica (2015). Geographic variability of sea-level change. *Current Climate Change Reports*, 1(3), 192-204.
- Kriebel, D. L. and J. D. Geiman (2014). A Coastal Flood Stage to Define Existing and Future Sea-Level Hazards. *Journal of Coastal Research*: Volume 30, Issue 5: pp. 1017 – 1024.
- Menéndez, M., F. J. Méndez and I. J. Losada (2009). Forecasting seasonal to interannual variability in extreme sea levels, *ICES J. Mar. Sci.*, 66(7), 1490–1496, doi:10.1093/icesjms/fsp095.
- Menéndez, M. and P.L. Woodworth (2010). Changes in extreme high water levels based on a quasi-global tide-gauge data set. *Journal of Geophysical Research*, **115**, C10011. <http://dx.doi.org/10.1029/2009JC005997>
- Merrifield, M. A., Y. L. Firing, and J. J. Marra (2007). Annual Climatologies of Extreme Water Levels, paper presented at Extreme Events: Proceedings 15th ‘Aha Huliko’ a Hawaiian Winter Workshop, University of Hawai’i at Manoa, Honolulu, HI.
- Merrifield, M.A. (2011). A shift in western tropical Pacific sea level trends during the 1990s. *Journal of Climate*, 24, 4126-4138. <https://doi.org/10.1175/2011JCLI3932.1>
- Merrifield, M. A., A. S. Genz, C. P. Kontoes and J. J. Marra (2013). Annual maximum water levels from tide gauges: Contributing factors and geographic patterns, *J. Geophys. Res. Oceans*, 118, 2535–2546, doi:10.1002/jgrc.20173.
- Moftakhari, H.R., A. AghaKouchak, B.F. Sanders, D.L. Feldman, W. Sweet, R.A. Matthew and A. Luke (2015). Increased nuisance flooding along the coasts of the United States due to sea level rise: Past and future. *Geophysical Research Letters*, **42**, 9846-9852. <http://dx.doi.org/10.1002/2015GL066072>
- Moftakhari, H.R., G. Salvadori, A. AghaKouchak, B. F. Sanders and R. A. Matthew (2017a). Compounding effects of sea level rise and fluvial flooding. *Proceedings of the National Academy of Sciences*, 114(37), pp.9785-9790.
- Moftakhari, H. R., A. AghaKouchak, B. F. Sanders and R. A. Matthew (2017b). Cumulative hazard: The case of nuisance flooding. *Earth's Future*, 5: 214–223. doi:10.1002/2016EF000494
- Moritz, H., K. White, B. Gouldby, W. Sweet, P. Ruggiero, M. Gravens, P. O'Brien, H. Moritz, T. Wahl, N.C. Nadal-Caraballo and W. Veatch (2015). USACE adaptation approach for future coastal climate conditions. *Proceedings of the Institution of Civil Engineers - Maritime Engineering*, **168**, 111-117. <http://dx.doi.org/10.1680/jmaen.15.00015>
- NOAA (2017). National Weather Service Instruction 10-320. Surf Zone Forecast and Coastal/Lakeshore Hazard Services. <http://www.nws.noaa.gov/directives/sym/pd01003020curr.pdf>
- Obeysekera, J., M. Irizarry, J. Park, J. Barnes and T. Dessalegne (2011). Climate Change and Its Implication for Water Resources Management in South Florida. *Journal of Stochastic Environmental Research and Risk Assessment*, 25(4), 495.

- Park, J., R. Heitsenrether and W. Sweet (2014). Water Level and Wave Height Estimates at NOAA Tide Stations from Acoustic and Microwave Sensors. *J. Atmos. Oceanic Technol.* doi:10.1175/JTECH-D-14-00021.1
- Ray, R. D. and G. Foster (2016). Future nuisance flooding at Boston caused by astronomical tides alone. *Earth's Future*, 4: 578–587. doi:10.1002/2016EF000423
- Rueda, A., S. Vitousek, P. Camus, A. Tomás, A. Espejo, I. J. Losada, P. L. Barnard, L. H. Erikson, P. Ruggiero, B. G. Reguero and F. J. Mendez (2017). A global classification of coastal flood hazard climates associated with large-scale oceanographic forcing. *Scientific Reports*, 7, p.5038.
- Ruggiero, P. (2013). Is the intensifying wave climate of the US Pacific northwest increasing flooding and erosion risk faster than sea-level rise? *J. Waterway Port Coastal Ocean Eng.*, 139(2), 88–97.
- Salas, J.D. and J. Obeysekera (2014). Revisiting the Concepts of Return Period and Risk for Nonstationary Hydrologic Extreme Events. *ASCE J. Hydrol. Engr.*, 19(3), 554-568.
- Serafin, K., P. Ruggiero and H. Stockdon (2017). The relative contribution of waves, tides, and non-tidal residuals to extreme total water levels on US West Coast sandy beaches: REL CONT EXTREME TWL. *Geophysical Research Letters*. 10.1002/2016GL071020.
- Stockdon, H.F., R.A. Holman, P.A. Howd, and A.H. Sallenger, Jr. (2006). Empirical parameterization of setup, swash, and runup. *Coastal Engineering*, **53**, 573-588.
<http://dx.doi.org/10.1016/j.coastaleng.2005.12.005>
- Sukop, M.C., M. Rogers, G. Guannel, J. M. Infanti and K. Hagemann (2018). High temporal resolution modeling of the impact of rain, tides, and sea level rise on water table flooding in the Arch Creek basin, Miami-Dade County Florida USA. *Science of The Total Environment*, 616, pp.1668-1688.
- Sweet, W., C. Zervas and S. Gill (2009). Elevated East Coast Sea Levels Anomaly: June–July 2009. NOAA Technical Report NOS CO-OPS 051, 28p.
https://tidesandcurrents.noaa.gov/publications/EastCoastSeaLevelAnomaly_2009.pdf
- Sweet, W. V. and C. Zervas (2011). Cool-season sea level anomalies and storm surges along the U.S. East Coast: Climatology and comparison with the 2009/10 El Niño. *Mon. Wea. Rev.*, 139, 2290–2299.
- Sweet, W.V., C. Zervas, S. Gill, J. Park (2013). Hurricane Sandy Inundation Probabilities Today and Tomorrow [In “Explaining Extreme Events of 2012 from a Climatic Perspective”], *Bull Amer. Meteor. Soc.* 94 (9), S17–S20.
- Sweet, W. V., J. Park, J. J. Marra, C. Zervas and S. Gill (2014). Sea level rise and nuisance flood frequency changes around the U.S. NOAA Technical Report NOS CO-OPS 73, 53p.
http://tidesandcurrents.noaa.gov/publications/NOAA_Technical_Report_NOS_COOPS_073.pdf
- Sweet, W.V. and J. Park (2014). From the extreme and the mean: Acceleration and tipping point of coastal inundation from sea level rise. *Earth Futures*, 2 579-600. doi: 10.1002/2014EF000272

- Sweet, W.V. and J. J. Marra (2015). 2014 State of Nuisance Tidal Flooding [supplement in NOAA NCEI, *State of the Climate: National Overview for August 2015*]. <http://www.ncdc.noaa.gov/sotc/national/201508>.
- Sweet, W. V., J. Park, S. Gill, and J. J. Marra (2015). New ways to measure waves and their effects at NOAA tide gauges: A Hawaiian-network perspective, *Geophys. Res. Lett.*, 42, doi:10.1002/2015GL066030.
- Sweet, W. V. and J. J. Marra (2016). 2015 State of U.S. Nuisance Tidal Flooding [supplement to *State of the Climate: National Overview* for May 2016]. <http://www.ncdc.noaa.gov/monitoring-content/sotc/national/2016/may/sweet-marra-nuisance-flooding-2015.pdf>
- Sweet, W., M. Menendez, A. Genz, J. Obeysekera, J. Park and J. J. Marra (2016). In Tide's Way: Southeast Florida's September 2015 Sunny-day Flood [in "Explaining Extremes of 2015 from a Climate Perspective"]. *Bull. Amer. Meteor. Soc.*, 97 (12), S25–S30, <https://doi.org/10.1175/BAMS-D-16-0117.1>
- Sweet, W.V., R.E. Kopp, C. Weaver, J. Obeysekera, R. Horton, E.R. Thieler and C. Zervas (2017a). Global and Regional Sea Level Rise Scenarios for the United States. NOAA Technical Report NOS CO-OPS 83. tidesandcurrents.noaa.gov/publications/techrpt83_Global_and_Regional_SLR_Scenarios_for_the_US_final.pdf
- Sweet, W.V., J. J. Marra and G. Dusek (2017b). 2016 State of U.S. High Tide Flooding and a 2017 Outlook [supplement to *State of the Climate: National Overview for May 2017*]. https://www.ncdc.noaa.gov/monitoring-content/sotc/national/2017/may/2016_StateofHighTideFlooding.pdf
- Sweet, W.V., R. Horton, R.E. Kopp and A. Romanou (2017c). Sea level rise. In: Climate Science Special Report: Sustained Assessment Activity of the U.S. Global Change Research Program [Wuebbles, D.J., D.W. Fahey, K.A. Hibbard, D.J. Dokken, B.C. Stewart, and T.K. Maycock (eds.)]. U.S. Global Change Research Program, Washington, DC, USA.
- Talke, S. A., P. Orton and D. A. Jay (2014). Increasing storm tides in New York Harbor, 1844–2013, *Geophys. Res. Lett.*, 41, 3149–3155, doi:10.1002/2014GL059574.
- Tebaldi, C., B. H. Strauss and C. E. Zervas (2012). Modelling sea level rise impacts on storm surges along US coasts. *Environmental Research Letters*, 7(1, Jan-March 2012), 014032. doi: 10.1088/1748-9326/7/1/014032
- Thompson, P. R., G. T. Mitchum, C. Vonesch, and J. Li (2013). Variability of winter storminess in the eastern United States during the twentieth century from tide gauges, *J. Clim.*, 26, 9713–9726, doi:10.1175/JCLI-D-12-00561.1.
- USGCRP (2017). Climate Science Special Report: Fourth National Climate Assessment, Volume I [Wuebbles, D.J., D.W. Fahey, K.A. Hibbard, D.J. Dokken, B.C. Stewart, and T.K. Maycock (eds.)]. U.S. Global Change Research Program, Washington, DC, USA, 628 pp.

- Valle-Levinson, A., A. Dutton and J. B. Martin (2017). Spatial and temporal variability of sea level rise hot spots over the eastern United States, *Geophys. Res. Lett.*, 44, 7876–7882, doi:10.1002/2017GL073926.
- Wahl, T., S. Jain, J. Bender, S. D. Meyers and M. E. Luther (2015). Increasing risk of compound flooding from storm surge and rainfall for major US cities. *Nature Climate Change*, 5(12), 1093-1097. doi:10.1038/nclimate2736
- Wahl, T. and D. P. Chambers (2016). Climate controls multidecadal variability in U. S. extreme sea level records, *J. Geophys. Res. Oceans*, 121, 1274–1290, doi:10.1002/2015JC011057.
- Wdowinski, S., B. Ronald, B. P. Kirtman and Z. Wu (2016). Increasing flooding hazard in coastal communities due to rising sea level: Case study of Miami Beach, Florida. *Ocean Coastal Manage.*, 126, 1–8, doi:10.1016/j.ocecoaman.2016.03.002.
- Widlansky, M. J., J. J. Marra, M. R. Chowdhury, S. A. Stephens, E. R. Miles, N. Fauchereau, C. M. Spillman, G. Smith, G. Beard and J. Wells (2017). Multimodel Ensemble Sea Level Forecasts for Tropical Pacific Islands. *Journal of Applied Meteorology and Climatology*, 56(4), pp.849-862.
- Vitousek, S., P. L. Barnard, C. H. Fletcher, N. Frazer, L. Erikson and C. D. Storlazzi (2017). Doubling of coastal flooding frequency within decades due to sea-level rise. *Scientific Reports*, 7(1), 1399.
- Zervas, C. (2009). Sea Level Variations of the United States 1854–2006. NOAA Technical Report NOS CO-OPS 053, 75p, Appendices A–E. https://tidesandcurrents.noaa.gov/publications/Tech_rpt_53.pdf
- Zervas, C. (2013). Extreme Water Levels of the United States 1893-2010. NOAA Technical Report NOS CO-OPS 67 56p, Appendices I-VIII. https://tidesandcurrents.noaa.gov/publications/NOAA_Technical_Report_NOS_COOPS_067a.pdf
- Zhang, K., B. C. Douglas and S. P. Leatherman (2000) Twentieth century storm activity along the U.S. East coast. *J. Climate*, 13, 1748–1760.

APPENDIX 1

Geographic regions, NOAA tide gauge information and ‘official’ NOAA and derived (in this study) coastal flood severity thresholds

Region	Station Name	Lat	Long	NOAA ID	Data Start*	NOAA Flood Threshold (m, MHHW)			Derived Threshold (m, MHHW)		
						Minor	Moderate	Major	Minor	Moderate	Major
Northeast Atlantic	Bar Harbor, ME	44.4	-68.2	8413320	1947	----	----	----	0.64	0.90	1.31
	Portland, ME	43.7	-70.2	8418150	1920	0.64	0.94	1.25	0.62	0.89	1.29
	Boston, MA	42.4	-71.1	8443970	1921	0.68	1.44	1.75	0.63	0.89	1.30
	Woods Hole, MA	41.5	-70.7	8447930	1958	1.37	1.77	2.38	0.53	0.82	1.20
	Nantucket Island, MA	41.3	-70.1	8449130	1965	0.43	0.74	1.35	0.54	0.83	1.21
	Newport, RI	41.5	-71.3	8452660	1930	0.81	1.27	1.87	0.55	0.84	1.22
	Providence, RI	41.8	-71.4	8454000	1938	0.66	1.27	2.18	0.56	0.84	1.23
	New London, CT	41.4	-72.1	8461490	1938	0.58	0.88	1.43	0.54	0.83	1.21
	Bridgeport, CT	41.2	-73.2	8467150	1970	0.49	0.95	1.25	0.59	0.87	1.26
	Montauk, NY	41.0	-72.0	8510560	1947	0.61	0.86	1.37	0.53	0.82	1.20
	Kings Point, NY	40.8	-73.8	8516945	1931	0.67	0.82	1.58	0.60	0.87	1.27
	The Battery, NY	40.7	-74.0	8518750	1920	0.65	1.05	1.51	0.56	0.85	1.23
	Bergen Point, NY	40.6	-74.1	8519483	1981	0.52	0.91	1.37	0.57	0.85	1.24
	Sandy Hook, NJ	40.5	-74.0	8531680	1922	0.45	0.76	1.06	0.56	0.85	1.23
	Atlantic City, NJ	39.4	-74.4	8534720	1920	0.43	0.73	1.04	0.56	0.84	1.23
	Cape May, NJ	39.0	-75.0	8536110	1965	0.38	0.69	0.99	0.57	0.85	1.24
	Philadelphia, PA	39.9	-75.1	8545240	1920	0.46	0.77	1.07	0.58	0.86	1.25
	Reedy Point, DE	39.6	-75.6	8551910	1973	0.42	0.72	1.02	0.57	0.85	1.24
	Lewes, DE	38.8	-75.1	8557380	1920	0.41	0.72	1.02	0.56	0.84	1.23
	Cambridge, MD	38.6	-76.1	8571892	1979	0.45	0.60	0.75	0.52	0.82	1.19
	Tolchester Beach, MD	39.2	-76.2	8573364	1971	0.54	0.84	1.15	0.52	0.82	1.19
	Baltimore, MD	39.3	-76.6	8574680	1920	0.41	1.02	1.32	0.52	0.82	1.19
	Annapolis, MD	39.0	-76.5	8575512	1928	0.29	0.57	1.39	0.52	0.81	1.19
	Solomons Island, MD	38.3	-76.5	8577330	1979	0.39	0.77	1.07	0.52	0.81	1.19
	Washington, DC	38.9	-77.0	8594900	1924	0.32	0.65	1.17	0.54	0.83	1.21
	Wachapreague, VA	37.6	-75.7	8631044	1978	0.61	0.91	1.06	0.56	0.84	1.23
	Kiptopeke, VA	37.2	-76.0	8632200	1976	0.48	0.63	0.78	0.54	0.83	1.21
	Lewisetta, VA	38.0	-76.5	8635750	1970	0.46	0.61	0.76	0.52	0.81	1.19
	Windmill Point, VA	37.6	-76.3	8636580	1996	0.49	0.64	0.80	0.52	0.81	1.19
	Sewells Point, VA	36.9	-76.3	8638610	1927	0.53	0.84	1.14	0.53	0.83	1.20
	Chesapeake Bay Br., VA	37.0	-76.1	8638863	1975	0.64	0.79	0.94	0.54	0.83	1.21

Region	Station Name	Lat	Long	NOAA ID	Data Start*	NOAA Flood Threshold (m, MHHW)			Derived Threshold (m, MHHW)		
						Minor	Moderate	Major	Minor	Moderate	Major
Southeast Atlantic	Duck, NC	36.2	-75.7	8651370	1978	0.55	0.71	0.86	0.54	0.83	1.21
	Oregon Inlet, NC	35.8	-75.5	8652587	1974	----	----	----	0.51	0.81	1.18
	Beaufort, NC	34.7	-76.7	8656483	1967	0.29	0.60	0.90	0.54	0.83	1.21
	Wilmington, NC	34.2	-78.0	8658120	1935	0.25	0.62	----	0.56	0.84	1.23
	Springmaid Pier, SC	33.7	-78.9	8661070	1976	0.58	0.88	1.34	0.57	0.85	1.24
	Charleston, SC	32.8	-79.9	8665530	1921	0.38	0.53	0.68	0.57	0.85	1.24
	Fort Pulaski, GA	32.0	-80.9	8670870	1935	0.52	0.64	0.76	0.59	0.87	1.26
	Fernandina Beach, FL	30.7	-81.5	8720030	1920	0.63	0.78	1.15	0.58	0.86	1.25
	Mayport, FL	30.4	-81.4	8720218	1928	0.56	0.78	1.08	0.56	0.85	1.23
	Trident Pier, FL	28.4	-80.6	8721604	1994	0.64	----	----	0.55	0.84	1.22
	Virginia Key, FL	25.7	-80.2	8723214	1994	0.40	----	----	0.53	0.82	1.20
	Vaca Key, FL	24.7	-81.1	8723970	1975	0.59	----	----	0.51	0.81	1.18
Key West, FL	24.6	-81.8	8724580	1920	0.33	----	----	0.52	0.82	1.19	
Caribbean	Lime Tree Bay, VI	17.7	-64.8	9751401	1982	----	----	----	0.51	0.81	1.18
	Charlotte Amalie, VI	18.3	-64.9	9751639	1975	----	----	----	0.51	0.81	1.18
	San Juan, PR	18.5	-66.1	9755371	1977	----	----	----	0.52	0.81	1.19
	Magueyes Island, PR	18.0	-67.0	9759110	1954	----	----	----	0.51	0.81	1.18
Eastern Gulf	Naples, FL	26.1	-81.8	8725110	1965	0.35	----	----	0.53	0.83	1.20
	Fort Myers, FL	26.6	-81.9	8725520	1969	----	----	----	0.52	0.81	1.19
	St. Petersburg, FL	27.8	-82.6	8726520	1946	0.84	----	----	0.53	0.82	1.20
	Clearwater, FL	28.0	-82.8	8726724	1996	----	----	----	0.53	0.83	1.20
	Cedar Key, FL	29.1	-83.0	8727520	1920	0.43	----	----	0.55	0.83	1.22
	Apalachicola, FL	29.7	-85.0	8728690	1976	0.65	1.20	1.93	0.52	0.81	1.19
	Panama City, FL	30.2	-85.7	8729108	1973	0.52	1.13	1.59	0.52	0.81	1.19
	Panama City Beach, FL	30.2	-85.9	8729210	1993	----	----	----	0.52	0.81	1.19
	Pensacola, FL	30.4	-87.2	8729840	1923	----	----	----	0.52	0.81	1.19
	Dauphin Island, AL	30.3	-88.1	8735180	1996	----	----	----	0.51	0.81	1.18
Bay Waveland, MS	30.3	-89.3	8747437	1978	0.45	----	----	0.52	0.82	1.19	
Western Gulf	Grand Isle, LA	29.3	-90.0	8761724	1980	----	----	----	0.51	0.81	1.18
	Sabine Pass, TX	29.7	-93.9	8770570	1985	0.58	1.04	1.34	0.52	0.81	1.19
	Morgans Point, TX	29.7	-95.0	8770613	1993	----	----	----	0.52	0.81	1.19
	Eagle Point, TX	29.5	-94.9	8771013	1993	0.88	----	----	0.51	0.81	1.18
	Galveston Pier 21, TX	29.3	-94.8	8771450	1920	0.79	----	----	0.52	0.81	1.19
	Rockport, TX	28.0	-97.0	8774770	1937	0.67	0.82	0.98	0.50	0.80	1.17
	Corpus Christi, TX	27.6	-97.2	8775870	1983	0.40	0.55	0.70	0.52	0.81	1.19
	Port Isabel, TX	26.1	-97.2	8779770	1944	0.34	----	----	0.52	0.81	1.19

Region	Station Name	Lat	Long	NOAA ID	Data Start*	NOAA Flood Threshold (m, MHHW)			Derived Threshold (m, MHHW)		
						Minor	Moderate	Major	Minor	Moderate	Major
Southwest Pacific	San Diego, CA	32.7	-117.2	9410170	1920	----	----	----	0.57	0.85	1.24
	La Jolla, CA	32.9	-117.3	9410230	1924	0.51	----	----	0.56	0.85	1.23
	Los Angeles, CA	33.7	-118.3	9410660	1923	----	----	----	0.57	0.85	1.24
	Santa Monica, CA	34.0	-118.5	9410840	1973	----	----	----	0.57	0.85	1.24
	Port San Luis, CA	35.2	-120.8	9412110	1948	----	----	----	0.56	0.85	1.23
	Monterey, CA	36.6	-121.9	9413450	1973	----	----	----	0.57	0.85	1.24
	San Francisco, CA	37.8	-122.5	9414290	1920	0.35	----	----	0.57	0.85	1.24
	Alameda, CA	37.8	-122.3	9414750	1976	----	----	----	0.58	0.86	1.25
	Point Reyes, CA	38.0	-123.0	9415020	1973	----	----	----	0.57	0.85	1.24
	Port Chicago, CA	38.1	-122.0	9415144	1979	----	----	----	0.56	0.84	1.23
Arena Cove, CA	38.9	-123.7	9416841	1979	----	----	----	0.57	0.85	1.24	
Northwest Pacific	Humboldt Bay, CA	40.8	-124.2	9418767	1977	0.56	----	----	0.58	0.86	1.25
	Port Orford, CA	42.7	-124.5	9431647	1978	----	----	----	0.59	0.87	1.26
	Charleston, OR	43.3	-124.3	9432780	1970	----	----	----	0.59	0.87	1.26
	South Beach, OR	44.6	-124.0	9435380	1967	1.12	----	----	0.60	0.88	1.27
	Toke Point, WA	46.7	-124.0	9440910	1972	0.63	----	----	0.61	0.88	1.28
	Port Angeles, WA	48.1	-123.4	9444090	1975	----	----	----	0.59	0.86	1.26
	Port Townsend, WA	48.1	-122.8	9444900	1972	0.91	----	----	0.60	0.88	1.27
	Seattle, WA	47.6	-122.3	9447130	1920	0.65	----	----	0.64	0.90	1.31
	Cherry Point, WA	48.9	-122.8	9449424	1971	----	----	----	0.61	0.88	1.28
	Friday Harbor, WA	48.5	-123.0	9449880	1934	----	----	----	0.59	0.87	1.26
Pacific Islands	Nawiliwili, HI	22.0	-159.4	1611400	1954	----	----	----	0.52	0.82	1.19
	Honolulu, HI	21.3	-157.9	1612340	1920	----	----	----	0.52	0.82	1.19
	Mokuoloe, HI	21.4	-157.8	1612480	1981	----	----	----	0.53	0.82	1.20
	Kahului, HI	20.9	-156.5	1615680	1954	----	----	----	0.53	0.82	1.20
	Kawaihae, HI	20.0	-155.8	1617433	1990	----	----	----	0.53	0.82	1.20
	Hilo, HI	19.7	-155.1	1617760	1927	----	----	----	0.53	0.82	1.20
	Midway Island	28.2	-177.4	1619910	1955	----	----	----	0.52	0.81	1.19
	Apra Harbor, Guam	13.4	144.7	1630000	1976	----	----	----	0.53	0.82	1.20
	Pago Pago, Am. Samoa	-14.3	-170.7	1770000	1977	----	----	----	0.53	0.83	1.20
	Kwajalein Island	8.7	167.7	1820000	1976	----	----	----	0.55	0.84	1.22
Wake Island	19.3	166.6	1890000	1950	----	----	----	0.53	0.82	1.20	

APPENDIX 2

Average (± 1 standard deviation) high tide flood frequencies over 2041–2050 and 2091–2100 within U.S. regions projected to occur for relative sea level (RSL) rise under the Intermediate Low and Intermediate scenarios for global sea level rise (Sweet et al., 2017a).

U.S. Region	2041-2050 Average				2091-2100 Average			
	Int. Low Scenario	% tides	Int. Scenario	% tides	Int. Low Scenario	% tides	Int. Scenario	% tides
Northeast Atlantic	44 \pm 11	31%	132 \pm 26	46%	234 \pm 56	95%	363 \pm 2	100%
Southeast Atlantic	26 \pm 14	35%	85 \pm 33	65%	193 \pm 59	100%	364 \pm 2	100%
Caribbean	0 \pm 0	NA	6 \pm 3	11%	142 \pm 15	67%	365 \pm 0	100%
Eastern Gulf	23 \pm 29	2%	81 \pm 44	53%	199 \pm 66	79%	364 \pm 2	100%
Western Gulf	80 \pm 35	46%	184 \pm 45	79%	350 \pm 11	100%	365 \pm 0	100%
Southwest Pacific	13 \pm 9	75%	36 \pm 15	85%	84 \pm 29	100%	345 \pm 11	100%
Northwest Pacific	17 \pm 12	25%	32 \pm 21	66%	67 \pm 62	43%	281 \pm 58	100%
Pacific Islands	7 \pm 12	42%	44 \pm 27	66%	187 \pm 52	100%	365 \pm 0	100%



IN REPLY REFER TO:

1.A.2

United States Department of the Interior

National Park Service
Biscayne National Park
9700 S. W. 328th Street
Homestead, Florida 33033-5634



May 13, 2016

Mr. James D. Giattina, Director
Water Protection Division
US EPA Region 4
61 Forsyth Street
Atlanta, GA 30303

Mr. Jonathan P. Steverson, Secretary
Florida Department of Environmental Protection
3900 Commonwealth Blvd
Tallahassee, FL 32339

Mr. Jack Osterholdt, Director
Department of Regulatory and Economic Resources
Stephen P. Clark Center
111 NW 1st Street, 11th Floor
Miami, FL 33128

Dear Sirs:

Biscayne National Park (BNP) has ongoing concerns with the operation of Units 3 & 4 of Florida Power and Light's (FPL) Turkey Point facility. A primary concern is the potential for salt, nutrients and other pollutants in the facility's Cooling Canal System (CCS) to flow and disperse via ground or surface water connections into Biscayne Bay and BNP. Recent monitoring data has confirmed that water from the CCS is hydrologically connected to the Bay, with CCS water moving through or under CCS berms. These data have also confirmed that nutrients (phosphorus and nitrogen) have been added to the Bay system in concentrations that exceed the Numeric Nutrient Criteria (NNC) (62-302.532 F.A.C.) adopted by the State of Florida Department of Environmental Protection (FDEP) and approved by the U.S. Environmental Protection Agency (EPA) for Biscayne Bay. These nutrients can stimulate algal growth and increase chlorophyll *a* concentrations above the NNC criterion. We are aware that discussions are occurring among the regulatory agencies regarding how to best address this situation. BNP respectfully requests that you include the National Park Service (NPS) in your deliberations. The NPS is required by law to "conserve the scenery, natural and historic objects, and wild life... in such manner and by such means as will leave them unimpaired for the enjoyment of future generations." (54 USC 100101(1)) Because of our special expertise regarding BNP and Biscayne Bay, we are well suited to provide assistance.

The original scope and extent of sampling identified in the Units 3 and 4 Uprate Monitoring Plan, approved in the Fifth Supplemental Agreement with the South Florida Water Management District (SFWMD), FDEP, and Miami-Dade County Regulatory and Economic Resources Division of Environmental Resources Management (RER-DERM), needs to be reestablished as a requirement in order to assess the impacts of the CCS. In addition, we request the following new requirements be added.



First, we call for establishing a more extensive nearshore water quality monitoring network that is maintained by FPL and provides data on potential loading of nutrients and other contaminants to the Bay, as well as identifying the ecological impacts that FPL operations have on the Bay. BNP would like to participate in developing this monitoring plan and would like the data to be made available to BNP and regulatory agencies on the same schedule and under the same Quality Assurance Plan that initially was adopted for implementation of the Uprate Monitoring Plan. This monitoring effort would serve as an early warning system to alert all affected parties of any increases in nutrients and other contaminants to the Bay from CCS operations. Moreover, this monitoring could be linked to other monitoring efforts so that managers and decision makers have a broader view of water quality and any potential impacts in the Bay.

Second, we call for FPL to be required to develop a strategy for managing CCS salinity, nutrients, and other potential pollutants to prevent impacts to the Bay. This strategy should be developed in concert with BNP and the regulatory agencies. Every feasible aspect of controlling nutrient and salinity loadings to the Bay should be considered, while not affecting freshwater flows to BNP or the Comprehensive Everglades Restoration Plan (CERP). Performance criteria for the CCS should be established for nutrients (particularly phosphorous, ammonia, total nitrogen and total suspended solids) and salinity. We suggest having this strategy as a requirement of FPL's NPDES (National Pollutant Discharge Elimination System) permit for the CCS.

Third, BNP is concerned with the relatively shallow (45') injection well used for wastewater discharge at the plant. We suggest there is the potential for nutrient-laden wastewater to migrate via the groundwater connection to the Bay, and also contribute to cooling system biofouling which requires chemicals to control. We suggest that the regulatory agencies work with FPL to facilitate wastewater transfer to the regional sewage treatment system or implement another treatment and disposal route that is protective of adjacent waters.

Finally, we suggest the establishment of an interagency adaptive management working group that would biannually review monitoring data and performance criteria, and recommend any adjustments necessary to ensure the water resources of the Bay are protected. The performance criteria established would provide the basis for management actions, should the data indicate the potential for water quality issues and impacts associated with algal blooms, changes in biotic communities, seagrass die-offs, or other ecological concerns. This group would also be valuable in monitoring the effects of construction activities for the proposed Units 6 & 7, should those reactors be built. We recommend that this group be comprised of members of the regulatory community (DERM, FDEP, SFWMD, EPA), as well as the NPS and FPL.

We appreciate your consideration of these matters, irrespective of any enforcement actions the regulatory agencies may take. We believe this level of vigilance is warranted to protect BNP now and in the future. Questions can be addressed to BISC_Superintendent@nps.gov, or you can contact me at 786-335-3646.

Sincerely,

Elsa M. Alvear

for
William L. Cox
Interim Superintendent



Carlos A. Gimenez, Mayor

Department of Regulatory and Economic Resources

Environmental Resources Management

701 NW 1st Court, 6th Floor

Miami, Florida 33136-3912

T 305-372-6902 F 305-372-6630

miamidade.gov

October 2, 2015

Randall R. LaBauve, Vice President
Environmental Services
NextEra Energy, Inc.
700 Universe Blvd.
Juno Beach, Florida 33408

Certified Mail No. 7009 0080 0000 1050 7878
Return Receipt Requested

Eric E. Silagy, President
Florida Power & Light Company
700 Universe Blvd.
Juno Beach, Florida 33408

Certified Mail No. 7009 0080 0000 1050 7861
Return Receipt Requested

Re: FPL Turkey Point power plant facility located at, near or in the vicinity of 9700 SW 344 Street, Unincorporated, Miami-Dade County, Florida.

**NOTICE OF VIOLATION AND
ORDERS FOR CORRECTIVE ACTION**

Dear Messrs. LaBauve and Silagy:

Miami-Dade County Department of Regulatory and Economic Resources, Division of Environmental Resources Management (DERM) has reviewed data submitted in monitoring reports related to the Florida Power & Light (FPL) power plant at Turkey Point. This review revealed levels of chloride in samples collected from groundwater monitoring wells, including but not limited to TPGW-L3, TPGW-L5, TPGW-1 and TPGW-12. These wells are located outside of the FPL Cooling Canal System (CCS) and beyond the boundaries of the property. The chloride levels constitute violations of the water quality standards in Section 24-42(4) of the Code of Miami-Dade County.

In addition, these elevated chloride levels exceed the applicable groundwater clean-up target level set forth in Section 24-44 and therefore constitute water pollution as defined in Section 24-5. On September 26, 2012, the South Florida Water Management District identified tritium as the tracer for determining the presence of CCS water. A review of tritium data shows that the groundwater originating from the CCS has expanded beyond FPL property boundaries. Based on the foregoing information, DERM maintains that hypersaline water attributable to FPL exists in the groundwater outside the CCS and outside the property boundaries.

Be advised that the above constitutes violations of Chapter 24 of the Code of Miami-Dade County, specifically:

Section 24-42(3), of said Ordinance, inasmuch as it shall be unlawful for any person to dewater or to discharge sewage, industrial wastes, cooling water and solid wastes, or any other wastes into the waters of this County, including but not limited to surface water, tidal salt water estuaries, or ground water in such quantities, and of such characteristics as may cause the receiving waters, after mixing with the waste streams, to be of poorer quality than the water quality standards set forth in Section 24-42(4), or cause water pollution as defined in Section 24-5 or cause a nuisance or sanitary nuisance as herein defined and

Delivering Excellence Every Day

October 2, 2015

Section 24-42(4), of said Ordinance, inasmuch as it shall be unlawful for any person to breach the values set forth within this section.

This Notice is to advise FPL of violations of the Code of Miami-Dade County attributable to the Turkey Point power plant and, as discussed, to seek an agreement which will provide a vehicle to correct said violations.

Based on the above and pursuant to the authority granted to me under Chapter 24, of the Code of Miami-Dade County, I am hereby ordering you to:

1. Upon receipt of this NOTICE, **take immediate action to address** water quality violations or water pollution which is in violation of Chapter 24 of the Code of Miami-Dade County.
2. In order to resolve the violations outlined above, the Department will at this time, provide you with the opportunity to enter into an *Administrative Consent Agreement* within **thirty (30) days** of receipt of this correspondence. If you choose to enter into an agreement you must notify the undersigned within **ten (10) days** of receipt of this Notice.

Any person aggrieved by any action or decision of the DERM Director, may appeal said action or decision to the Environmental Quality Control Board (EQCB) by filing a written notice of appeal along with submittal of the applicable fee, to the Code Coordination and Public Hearings Section of DERM within fifteen (15) days of the date of the action or decision by DERM.

If you have any questions concerning the above, please contact me at 305-372-6514 or email brownb@miamidade.gov.

Sincerely,



Barbara Brown
Code Enforcement Officer
Regulatory Service

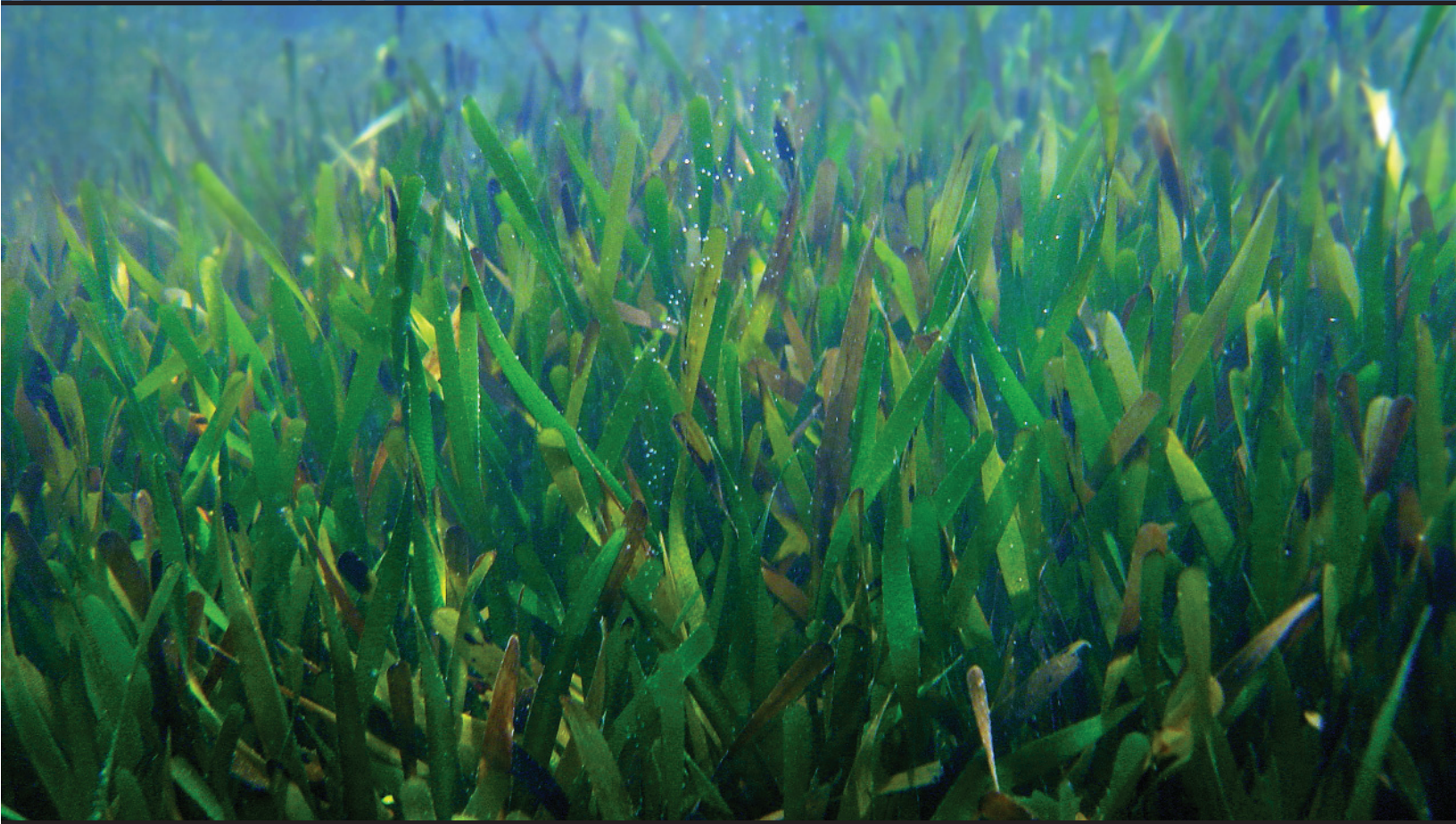
cc: Mike Kiley, Site Vice President
Florida Power & Light Company
Turkey Point Nuclear Power Plant
9760 SW 344 Street
Homestead, Florida 33035

Certified Mail No. 7009 0080 0000 1050 7854
Return Receipt Requested



RESOURCE
EVALUATION
REPORT

SFNR Technical Series
2008:2



ESTIMATES OF FLOWS TO MEET SALINITY TARGETS

for Western Biscayne National Park

Estimates of Flows to meet Salinity Targets for Western Biscayne National Park

EXECUTIVE SUMMARY

This paper uses several methods to estimate the flow volume of freshwater needed to reach salinity targets in Biscayne National Park. The salinity targets were developed previously, based on a determination of desired ecological conditions in a seagrass-dominated area of 10,000 acres in the western Bay zone of Biscayne National Park (DOI Discussion Paper April 2006). The seasonally-based salinity targets are: less than 30 ppt from November through March, from 15 to 25 ppt from March through August, and less than 20 ppt from September through October.

Analytical and empirical methods were applied to arrive at estimates of the flows necessary to reach these target salinities. It was determined that approximately 960,000 acre-feet/year of freshwater flows would be required to meet the salinity targets described above in the 10,000 acre area of seagrass habitat. In the absence of adequate circulation models to provide greater detail, an analysis of seasonal targets was done at a basic level: about 37 K acre-ft per month is needed during the dry season, and 149 K acre-ft per month in the wet season.

Recent time series of flows into Biscayne Bay were analyzed. A time-series comparison of the target with the existing flows showed that some transient peak-flow freshwater deliveries met or exceeded the targets. It is, however, apparent that the stable estuarine conditions desired in Biscayne Bay are not achieved by current freshwater inflows, both because the total volume is too little and because the timing and distribution are too unnatural. The restoration of natural timing of flows could produce stable estuarine conditions, but without an increase in the volume of water available, the salinity targets cannot be achieved throughout the year. Increasing the total volume of flows, and in particular providing adequate flows throughout the dry season, would provide significant benefits to the ecological system in Biscayne National Park.

INTRODUCTION

In the discussion paper, entitled “Ecological Targets for Western Biscayne National Park” (April 2006), the Department of the Interior presented descriptive and quantitative ecological targets in the estuarine zone based on biological communities in Biscayne National Park. Two key elements of the ecological targets paper are pertinent to the development of hydrologic targets for Biscayne National Park.

Element 1: Target Area

There are many possibilities for a target area for restoration within Biscayne Bay and Biscayne National Park. The Southern Estuaries team from the Comprehensive Everglades Restoration Plan’s (CERP) Restoration Coordination and Verification (RECOVER) committee developed salinity performance measures for Biscayne Bay (see www.evergladesplan.org) that proposed and defined such an area. These performance measures suggested a nearshore target area that reached 250m from the coastline during the dry season, and 500m from the shoreline during the wet season (Figure 1.) This target area is appropriate for some important ecological functions in the estuarine zone. However, the 250/500m nearshore bands do not take into consideration all available information about the current and historical geomorphology of the Bay which help define the extent of the estuarine zone in Biscayne National Park.

For the current analysis, maps of substrate type in the Bay were examined, as were maps of the current distribution of seagrasses within the Park. Substrate type is a good indicator of the both the historical and the future bottom community: areas that are currently hardbottom are more likely to have supported hardbottom communities such as soft corals and sponges, whereas areas that are covered with soft sediment are an indication of the presence of seagrasses in the past.

Examination of this information revealed an area of 10,000 acres in the Western Bay which shows evidence of the influence of significant freshwater flow, and which has supported productive estuarine seagrass communities in the past. Anecdotal and paleoecological evidence indicates that this 10,000 Western Bay Zone is probably significantly smaller than the estuarine area that was affected by freshwater flows in the historical past (Wingard et al., 2004). However, the re-establishment of stable estuarine conditions in the 10,000 acre Western Bay Zone would provide significant restoration of the natural values of Biscayne National Park.

Additional information and maps of the geographic areas of the Bay referenced in this document can be found in the April 2006 document.

Element 2: Desired Ecological Conditions for the Western Bay Zone of Biscayne National Park

The desired condition for the Western Bay Zone of Biscayne National Park is defined as a range of salinities that is consistently estuarine for support of a productive, diverse benthic community based on seagrass. These environmental conditions also support Federally-listed endangered species, such as the American crocodile (*Crocodylus acutus*) and West Indian manatee (*Trichechus manatus*), and create productive nursery habitat that sustains local and regional (e.g. Florida Keys) fishery resources. Species which would be supported under these conditions include gamefish such as the spotted seatrout (*Cynoscion nebulosus*), forage fish such as mojarras (*Eucinostomus spp.*), and mollusks like the Eastern oyster (*Crassostrea virginica*). The

decline during the last several decades of the abundance of these species, as well as the increased presence of marine species such as bonefish (*Albula vulpes*) and permit (*Trachinotus falcatus*), in the Western Bay Zone is thought to be due to the loss of sufficient extent and stability of estuarine conditions.

A more detailed description of desired ecological conditions can be found in the April 2006 Discussion paper cited above, or in SFNRC Technical Report 2006 (1). It should be emphasized that the desired ecological and salinity conditions described for the western Bay zone of Biscayne National Park are not equivalent to pre-drainage conditions. Rather, the pre-drainage estuarine area is likely to have extended farther east, where submerged aquatic vegetation and soft bottom substrate can still be found as far out as Featherbed Bank (Figure 1).

The current discussion paper utilizes several methods to estimate the freshwater flows needed to achieve the desired salinity targets and produce stable estuarine conditions over the 10,000 acre Western Bay Zone of Biscayne National Park.

HYDROLOGIC TARGETS FOR BISCAYNE NATIONAL PARK

Two pragmatic metrics exist for the physical conditions needed to reach the target ecological conditions for Biscayne National Park: 1) measurement of salinities in the estuarine zone and 2) quantification of the flows themselves through the coastal structures.

Though quantification of flows is easily attained, how these flows influence the salinity distributions throughout the Western Bay Zone (WBZ) is a complex physical question that depends on currents, winds, vertical and horizontal shear, insolation, tidal exchange, and mixing rates, among other variables. The coastal freshwater flows to Biscayne Bay are almost entirely managed and are a calculated parameter in current water management planning tools. We explored the link between these managed freshwater flows and the salinity in the WBZ using a variety of estimations.

Salinity

In several ways, salinity is the best metric to use as a base for the calculation of flows needed to produce the target ecological conditions. Evidence of the requirements of a number of species presented demonstrates that salinity is a key habitat factor for the bay ecosystem.

Figure 2 summarizes the optimal salinity ranges for Biscayne National Park ecosystem indicators, including primary producers, primary consumers, and predators. While these estuarine species can survive at least for short periods in a wide range of salinities, the majority of these indicator species prefer salinities between 5 and 20 ppt for growth and reproduction. Based on this observation and taking into account that other species (such as seatrout and oysters) may require periods of time with slightly higher or lower salinities, we propose the following salinity targets to achieve the ecological goals for the WBZ of Biscayne National Park:

- From November through March (early dry season to late dry season), average daily salinities should not exceed 30 ppt. It is particularly critical to measure and track salinities during this time period in order to determine the spatial pattern of estuarine and marine conditions within the Western Bay Zone. Current salinities in the Park frequently exceed 30 ppt in much of the Western Bay Zone during this time period (Biscayne National Park, 2006). Re-establishment of salinities under 30 ppt would create conditions important to the recovery of important fishery species with life-cycles that require estuarine conditions:
 - recreational and commercial fish species that rely on the forage fish for prey, such as adult sea trout, as well as snapper and grouper species
 - forage species (mojarras, pinfish), post-larval juvenile shrimp, and oysters, which rely on brackish water as a refuge from marine predators.
- From March through August (late dry season - early wet season), average daily salinities should range between 15-25 ppt. This would allow recovery of:
 - key spawning habitat for sea trout, adult habitat for forage species (mojarras, silver perch)
 - a healthy, productive, and diverse seagrass community that can be sustained in a zone that is subject to freshwater runoff
 - an extensive brackish water refuge from marine predators. Seagrass cover is a required feature of nursery habitat for important juvenile fish species.

- From September through October (late wet season), daily salinities should average less than 20 ppt. Creation of these conditions would provide:
 - a benefit to juvenile crocodiles that have a stringent physiological requirement for low salinity conditions.
 - conditions that promote the recovery of important forage fish species in coastal mangroves that do best at oligohaline to mesohaline conditions (such as sheepshead minnow, gold-spotted killifish).
 - indirect benefits to all upper trophic level species that consume these forage fish in the mangrove zone, including wading birds, mammals, and crocodiles.

There are considerations other than the average daily salinities which are important ecologically. The salinity changes should be gradual and reflect changes in hydroperiod that approximate a natural system. All vegetation, fish, and invertebrate species benefit from gradual changes in salinity that avoid physiological stress. The salinity gradient should extend away from the coastline, from lowest salinities nearest the coast to higher salinities towards the sea. And perhaps most importantly in an estuary:

- at no time should daily average salinities exceed 30 ppt.

This threshold defines estuarine conditions, as compared to marine conditions, and so is a bare minimum requirement. Exceeding the threshold of 30 ppt in the Western Bay Zone results in environmental conditions that negatively affect all of the Park's estuarine resources at some point in their lifecycle.

From Salinity Metrics to Estimates of Freshwater Target Flows

Salinity provides a dynamic link between the biological and physical coastal environments because it is an accurate and integral measure of the net results of the total freshwater inputs, mixing rate of marine and freshwater flows, wind mixing, net evaporative losses, and amount of tidal exchange. The freshwater inflows needed for maintenance of ecologically-required target salinities can be calculated in a number of ways. Ideally, a computer-based simulation that provides estimates of the spatial and temporal salinity distributions under various conditions would be used to arrive at estimates of freshwater flows to meet spatially-dependent salinity targets. A verified hydrodynamic model of Biscayne Bay that is forced by observed atmospheric and marine inputs and that is coupled with a hydrologic model to provide surface water and groundwater inputs would be such a tool. Though tools like this are currently under development, at this date an operational tool is not yet available. Therefore, we used several alternative approaches, including statistical models, dynamic box models, other modeling studies, and static volumetric estimation based on analytic estimates of water budgets and the balance of advective/diffusive processes. These different methods provide a range of freshwater flow quantities within the WBZ given the salinity targets described above. The limitations and advantages of each are discussed and reasonable approximations of freshwater flow quantity are provided.

Spatial Distribution and Timing: Much of the available information on flow is based on current canal discharges, which do not mimic natural conditions either in spatial distribution or in

timing. The analyses of required volumes of water included here assume the current distribution system, where the freshwater reaching Biscayne Bay is delivered via canals (through structures S-22, S-123, S-21, S-21A, S-20G, S-20F, S-20, and S-197). The current distribution system is less than optimal for achieving estuarine salinities in the nearshore area of the Bay, because much of the freshwater is transported from these point-source discharges via plumes that bypass the WBZ and are transported offshore to the marine environment. The optimal distribution system to target the WBZ would be that which existed in the pre-drainage past: a large volume of surface water elevated inland behind the coastal ridge which induces a large, broad groundwater seep into the marsh all along the coastline, with surface waters entering into the bay via many dozens of small creeks. This type of distribution system is ideal since it delivers fresh water to the WBZ in a highly efficient manner, resulting in a larger impact on nearshore salinities for the same volume of water than would be provided by a series of large point-source discharges.

The desired persistent salinity gradient oriented parallel to the coastline can be most economically maintained by the steady flow of waters away from the coast and all along the coastline, as would be provided by a coastal freshwater/brackish marsh such as the historic coastal wetlands of BISC (this phenomenon is explained more fully in Appendix A). An approximately constant freshwater flux is likewise desired at the historic river and creek mouths in order to maintain the estuarine salinity targets and avoid ecological damage that is similarly caused by cessation of flows or large pulses of freshwaters. Under current conditions, pulsed discharges of large volumes of freshwater are typical following large rain events and often result in locally low salinities near canal discharge points. The desired spatial and temporal distributions apply to all of the target flows derived in this section.

Flow Volume:

Until sufficient results are compiled from the desired hydrological models, which are coupled to a range of inflow conditions, some alternate performance measures and targets can be developed to estimate flow volumes that produce target salinity values. We examine five different methods to estimate flow volumes: 1) RECOVER Southern Estuaries sub-team performance measures, 2) Advection-Diffusion estimates, 3) Hypersalinity prevention estimate, 4) TABS-MDW hydrodynamic model estimate, and 5) Volumetric estimate. The RECOVER performance measures are currently accepted for use in the design of CERP projects: the additional estimates examined here provide information to test the utility of and/or potentially modify the RECOVER targets. Estimates 2) and 3) are rough estimates of target flows across wet and dry seasons, gleaned from simple calculations of the flows required to maintain a persistent salinity gradient parallel to the coastline, and no periods of hypersaline conditions. These two estimates are minimal targets, but they must be achieved first in order to reach other, more voluminous, desired restoration target flows. The flows needed to achieve the restoration targets are calculated in 4) an analytical estimate, and 5) a more refined, seasonally-varying volumetric estimate driven by ecosystem requirements that parameterizes the mixing and flow in the bay in order to arrive at more robust target flows.

1) RECOVER Target Estimates. There are a number of RECOVER performance measures that apply to specific areas of Biscayne Bay for which flow or salinity targets have been developed by the Southern Estuaries sub-team, and are currently in use as targets for CERP projects. For the purpose of estimating target flows for Central to Southern Biscayne Bay, the current Southern Estuaries Salinity Performance Measure (PM) is applicable. This PM specifies a persistent salinity gradient parallel to the southern coast of Biscayne Bay at 250 m (dry season) and 500 m

(wet) from shore by meeting oligohaline to mesohaline nearshore targets, and it was estimated by Meeder et al. (2002) that about 65 K acre-ft/month in the wet season and 21 K acre-ft/month in the dry season (470 K acre-ft/yr) are required to meet these salinity requirements. Alleman (2003) arrived at a similar figure of 40 K acre-ft/month in the wet season and 23 K acre-ft/month in the dry season (325 K acre-ft/yr) for the RECOVER PM targets from a historical data analysis, which lends support to the range of this estimate. In addition, the Southern Estuaries Salinity PM stipulates persistent flows of 1.25 K acre-ft/month (15 K acre-ft/yr) out of Snapper Creek and into Central Bay to maintain the ecosystem found at the creek mouth. Thus the RECOVER total for these target flows for South Bay and nearby waters is 66 K acre-ft/month for the wet season and 22 K acre-ft/month in the dry season, for a total volume of 485 K acre-ft/yr. Note that estimates of flows needed to reach estuarine salinity targets for the 10,000 acre WBZ will be much greater because it is 5,800 acres larger than the area used in the RECOVER performance measure for southern Biscayne Bay.

2) *Advection Diffusion Estimate.* Due to urban coastal development, the only area in which CERP projects could restore coastal marsh conditions and natural spatial distribution of flow to the park is from Deering Estate to Mangrove Point. If water could be distributed all along the 26 km of park coastline at a steady rate under the aforementioned optimal distribution system, a one-dimensional advection versus diffusion approach would be applicable. As developed in Appendix A, a persistent salinity gradient can be maintained by balancing the advection of freshwater flows away from the coast with the diffusion of salt from the marine waters offshore towards the fresher waters inshore. Given these assumptions, it is found that a sufficient net seaward flow to overcome shoreward diffusive effects all along the park shoreline is over 60 K acre-ft/month, regardless of season, or 800 K acre-ft/yr.

Other estimates of required volumes to reach target conditions have been developed independently as well. To just meet the 250 m- and 500 m-from-shoreline salinity requirements put forth by RECOVER, another advection versus diffusion estimate was developed by Downer, Klochak and Mullins (2005), and Nuttle and Downer (personal comm.). They used long-term averages of modern salinities measured at several points at different distances from the coast in Biscayne National Park and an assumed logarithmic shape of the seaward salinity gradient to arrive at an effective diffusivity of 12 m²/s. In light of this relatively high rate of mixing, to maintain just the 250 m/500 m salinity targets they estimated between 60-117 K acre-ft/month (700 – 1,400 K acre-ft/yr) of freshwater needed to be provided along the coastline through the marshes between Shoal and Turkey Points. Since the area considered for this exercise was confined to the nearshore zone, the estimate for the full 10,000 acres would likely be much higher still.

3) *Hypersalinity Prevention Estimate.* Another type of rough estimate may be developed by considering the volumes required to prevent hypersalinity in the bay. The estimated flow needed to avoid reaching the hypersalinity threshold gives a lower bound on the amount of freshwater needed to maintain living natural resources characteristic of any current areas of the Bay, and provides a context for the estimates of the flows required to reach restoration goals.

The net water budget is,

$$dV/dt = P - E - FW_{in} + GW_{in} - GW_{out} + SW_{in} + SW_{out}$$

where V is the total volume of the coastal basin, P is precipitation, E is evaporation, FW is fresh surface water, and GW is the groundwater volume. The net seawater volume, $SW_{in} - SW_{out}$, over several tidal periods will be small except when there are significant freshwater inputs or outputs,

since any excess of freshwater will be moved to sea, and any evaporation-induced deficit of estuarine water within the bay will be replaced by seawater if no surface or groundwater is available. A deficit of water induced by any excess of evaporation over precipitation ($P-E < 0$) can be replaced by seawater which will drive the salinities even higher by adding more salt to the bay, or by freshwater flows which will maintain or lower the salinity.

The outcome of this dynamic process depends largely upon the efficiency with which the tides move seawater into the bay, mix with the bay waters, and export this mixed water back to sea. Biscayne Bay is a semi-enclosed shallow basin with an average depth of about 10 ft and an area of 141,000 acres. All exchange with ocean water is limited to certain areas (Safety Valve, Government Cut, Baker's Haulover Cut, Norris Cut, Bear Cut, and the ABC Creeks), with the 9 km opening at Safety Valve by far the largest source of ocean waters (Wang et al. 2003). The tidal mixing in Biscayne Bay is generally efficient, with a tidal prism (inter-tidal volume) of about 250 K acre-ft – this means that, in theory, the entire volume of the bay could be exchanged with only six tidal cycles (three days). In practice the less-voluminous North Bay is even more easily flushed by virtue of the many cuts opened to the Atlantic, while South Bay is not flushed as easily, with exchange restricted by the three narrow ABC Creeks to the east and at the northern end by the shallow Featherbed Banks that stretch into mid-bay perpendicular to the long axis to the bay. Consequently, South Bay frequently has been frequently been observed to be hypersaline in recent years while North Bay has not experienced hypersalinity periods.

Even with a large annual rainfall, there is a net annual loss of water to evaporation for Biscayne Bay. Considering the entire Bay as a whole, the estimated mean evaporation rate of 1.66 m/yr (Royal Palm measurements) contrasts with 1.27 m/yr (Mowry Canal, chosen for its proximity to the bay) of precipitation, giving a net evaporative loss estimate of about 180 K acre-ft per year over the 141,000 acres, or about 1.25 ft per acre. Though these E and P estimates are highly variable and not equally applicable to all areas of the bay, it clearly illustrates the importance of the distribution of flows, and the different exchange rates at work in Biscayne Bay. With an evaporative loss of only 16% of the bay's total volume, a total average freshwater input of 92 K acre-ft/month (1,100 K acre-ft/yr) from canals would at first glance seem more than sufficient to protect against hypersalinity. However, parts of South Bay now routinely become hypersaline, which indicates that the 1,100 K acre-feet/yr is not distributed adequately in time and space. To compound matters, groundwater levels in the Biscayne Coastal Wetlands are maintained at artificially low stages to provide flood protection in the urban area, and are even further reduced entering into the dry season to benefit agricultural interests – such practices ensure that freshwater flows to the bay via groundwater are minimized.

For South Bay alone on an annual basis, at least 125 K acre-ft/yr would, therefore, be required to offset the evaporative net loss of freshwaters and prevent hypersalinity. Most of this water, at a rate of about 16 K acre-ft/month, is required during the dry season when precipitation is scarce. During these periods, with no rainfall or canal discharges available, net salinity increases in coastal waters have been observed in excess of 0.15 ppt per day. These estimates of freshwater flows would prevent hypersaline conditions, but would not reach target restoration salinities.

4) *TABS-MDS Hydrodynamic Model Estimate.* The use of a hydrodynamic model for Biscayne Bay to estimate the necessary freshwater flows is advantageous since it can incorporate explicitly the impact of tidal exchange, mixing, bathymetry, and coastal currents as well as freshwater flows on the nearshore salinities at different points in the Bay. A 3-D version of the TABS-MDS (RMA10; see Brown, et al., 2003) hydrodynamic model for central and southern Biscayne Bay was recently used by Alleman and Parrish (2005) to calculate the volume of water necessary to reach the paleo-salinities estimated by Wingard, et al., (2004) from cores taken at three sites between Shoal Point and Turkey Point, two of which are within the proposed 10,000 acre target

zone. The freshwater input distribution from the Natural System Model (NSM462) was increased until the modeled freshwater volumes for the years 1965-2000 produced salinities at these sites that were largely within the range of their circa-1900 salinities (Black Point, 5-18ppt; Featherbed, 25-35ppt; No Name Bank 18-30ppt). Parrish and Alleman concluded that the total (surface and ground) freshwater flow rate under such a 'natural' distribution necessary to maintain these salinities at these sites in South Bay was approximately 1,500 cfs. This instantaneous rate equates to about 91 K acre-ft per month to South Bay, or 1,100 K acre-ft/yr.

5) *Volumetric Estimate*. These estimates can be contrasted with a simple volumetric estimate of the freshwater flux needed to maintain a constant salinity (in the absence of wind mixing), which could be estimated by:

$$F = (\text{Area} * \text{Depth}) * (S_m - S_t) / S_m * X$$

where the product of Area and Depth is the volume of the target location, S_m is the marine salinity, S_t is the target salinity, and X is the tidal exchange factor. Geometries and the desired conditions determine all parameters except for the tidal exchange factor. Though the tidal exchange factor will be variable with space (both on/offshore as a function of distance from tidal inlets, and along the bay axis due to bathymetric variations) and even time (spring/neap tides, seasonal sea level fluctuations), a conservative estimate of 15% daily water exchange for nearshore conditions may be sufficiently representative of mean conditions in Biscayne National Park. Lee and Rooth (1976) estimated the residence time in southern Biscayne Bay during the summer months to be on the order of a week; if it would take seven days for a parcel of water to be exchanged, that would mean about 1/7 of the volume there (15%) is exchanged daily, neglecting mixing efficiency. In reality, the tidal mixing factor will be a function of the distance to the openings to the ocean, the rate of wind-induced mixing, and the distance from local embayments and shoals which restrict exchange. In contrast to the weekly residence time scale in Biscayne National Park, residence times in Northern Biscayne Bay are typically a few days (about 33% exchange daily), and may be as long as many months in Card and Barnes Sound at the extreme south end of the bay (<1% of waters exchanged daily by the tides).

A first volumetric estimate is based on RECOVER's wet/dry seasonally-variable salinity targets within Biscayne National Park, with 1600 acres within the 250 m zone at 5ppt/15ppt and 1600 acres within its 250-to-500 m zone at 10ppt/20ppt, and an average depth of 1.5 ft and 3.0 ft, respectively. When applied seasonally in the equation above these figures produce dry season estimates of a 16 K acre-ft/month, and a wet season estimate of 25 K acre-ft/month, for a total annual target flow of 244 K acre-ft/yr, given the daily mixing rate for the area of 15%. Since the volume estimate is directly proportional to the mixing rate, it is very sensitive to its value. To demonstrate the sensitivity of this estimate to the size of the mixing rate; if the estimate was increased to 20% the resulting flows would be approximately 20 K acre-ft and 33 K acre-ft per month for dry and wet seasons, with an annual total of 325 K acre-ft/yr for the limited 3200 acre area.

The second volumetric estimate presented here is based on the larger area of 10,000 acres of SAV habitat that are found in the WBZ, which we believe is a preferable target to the 250m/500 m salinity targets since it is representative of the geomorphic underpinnings and the ecological potential of the Bay, not just the distance from the shoreline. A similar application of the volumetric estimate to the aforementioned wet season/dry season salinity targets of 20 ppt/30 ppt (using 20 ppt as the mean of the 15-25 ppt range for the late wet season) over the 10,000 acres of grass beds included with the same 15% net tidal exchange provides a dry season estimate of 37 K acre-ft/month and a wet season estimate of 110 K acre-ft/month. Integrated over a year, the

10,000 acre are therefore requires a net total of about 960 K acre-ft/yr to meet the salinity targets outlined previously.

This second volumetric measurement also provides a means of estimating the amount of freshwater flow necessary to just maintain estuarine conditions, <30 ppt, throughout the year. Assuming at least an adequate dry season flow volume for 12 months, the volume to prevent marine conditions from dominating in the WBZ is estimated to be 440 K acre-ft per year.

Summary of Freshwater Flow Targets

These rough estimates of target flows have produced a range of values (Table 1) that encompass either the smaller RECOVER target area or the larger 10,000 acre target. The diffusive-process-based estimates span the range from 60 to 120 K acre-ft/month, but are sensitive to the magnitude of the effective diffusivities used. As a lower bound on the problem, it was shown that approximately 16 K acre-ft/month are required just to offset evaporation and avoid hypersaline conditions in the bay, so the actual target flows should be well in excess of that. The volumetric estimates arrived at an estimate of 37 K acre-ft/month in the dry season and 110 K acre-ft/month in the wet season for the full 10,000 acre target area. This is consistent with other estimates and is supported by estimates of the flows in the much smaller 3,200 acre target area (22 K acre-ft / 66 K acre-ft per month in the dry/wet season) required to meet a similar salinity requirement. The dry season monthly estimate of 37 K acre-ft/month also represents the flow required to simply maintain estuarine conditions. The fourth column of Table 1 provides the annual quantity of water per acre calculated to meet salinity targets, further demonstrating the consistency of the estimates. Thus the 37 K acre-ft / 110 K acre-ft per month flow targets represent a reasonable estimate of the required dry/wet season freshwater flows to meet ecological targets in the 10,000 acres area and will be adopted as the standard estimate, at least until such time that subsequent analyses are available that more properly take into account the dynamic nature of the flows within Biscayne Bay.

	Estimates Average annual flow volumes (K ac-ft per year)	Target Area (acres)	Estimated flow volume per unit area (ac-ft per acre of habitat)	Notes
RECOVER	325	3200	102	The estimate provides flows for RECOVER 250/500m region and utilizes the limited salinity observations available in the WBZ; Alleman (2003)
RECOVER	475	3200	148	Provides flows for 250/500m targets area; Meeder et al. (2002)
Hypersalinity prevention	125	NA	NA	Prevents hypersalinity in the Bay but does not attempt to satisfy salinity targets
Advection-Diffusion	800-1,400	3200	250-438	Based on a range of diffusivities (A=1 m ² /s to A=12 m ² /s) applied using an advection-dispersion relation and applied to the RECOVER 250/500m target area
Hydrodynamic Model	1090	~10,000	109	Uses TABS-MDS model to calculate flows need to achieve ca. 1900 paleosalinity targets from Wingard et al. (2004); Alleman (2005)
Volumetric	960	10,000	96	Provides flows for 10,000 ac WBZ using an effective tidal mixing of 15%

Table 1. Estimates of the average annual flow volumes required to enter Biscayne Bay between the S-22 and S-197 structures in order to reach the salinity ranges that support the biological targets.

Estimation of Current Flows

The hydrologic pattern in Biscayne National Park has been altered by regional drainage, canal construction and operation, and urban development, as well as construction of roads, levees, and other hydrologic barriers to surface flow. The bay currently receives freshwater inflow almost entirely as surface water in the form of canal flows, with only minor overland flow and very little groundwater flow.

Groundwater. When there are no surface flows or rainfall available, groundwater is the only possible source of freshwaters and is vital to counteract the onset of hypersaline conditions. Although the contribution of groundwater to total flows may have been quite large during pre-drainage conditions as anecdotal evidence suggests (Kohout and Kolipinski 1967), studies show that the modern fresh groundwater inputs into Biscayne Bay are very small (<10% of the surface flows; Langevin 2001). In addition, the saltwater intrusion line in south Florida has been stable or has encroached further inland over the past two decades (Sonenshein 1995) despite efforts to protect the water supply from saltwater intrusion, and hypersaline conditions are commonplace during droughts. Both of these observations support the understanding that groundwater flow to

Biscayne Bay is limited under current conditions. Because of the relatively small contribution groundwater makes to the total water budget and the limited availability of observed data, groundwater flows were not accounted for in this analysis. However, because of the importance of groundwater flow during the dry season and in drought conditions, these flows could be included in the estimates of mean annual water volume if a reliable means for quantifying the groundwater flows to the bay existed. Work underway to estimate groundwater flows may provide additional information for estimating comprehensive flow volumes in future analyses.

Surface Water. Canal flow estimates are derived from the head and tail water elevations across the coastal flow control structures maintained by the SFWMD and are stored in its DBHYDRO database. The observed flow data from the coastal control structures S197, S20, S20F, S20G, S21, S21A, S123, S22, S25B, G93, S26, S27, S28, S29, and S29Z for the time period 1985-2005 were examined. On average, 1,210 K acre-ft/yr (accurate to about +/- 5%, (Alleman, pers comm.)) of total surface freshwater flows enter any part of Biscayne Bay. For just the waters entering the boundaries of Biscayne National Park (direct flows through S20F, S20G, S21A, S21, and S123 at the northern coastal boundary are included, as are indirect flows from S22 Central Bay, S20 into Card Sound, and S197 into Barnes Sound all of which eventually pass through park waters), the average freshwater flux is much less, about 534 K acre-ft/yr or 44% of the total. These flows either directly or indirectly into Biscayne National Park in South Bay will be the focus of this discussion.

Figures 3 and 4 show the volume of flow contributed by each of the structures relative to each other. Of the annual average of 534 K acre-ft of canal flows that are discharged to southern Biscayne Bay from 1985-2005, 138 K acre-ft (26% of all annual flows) entered directly into Biscayne National Park through C-103 (S-20F), 113 K acre-ft (21%) through C-1 (S-21), 73 K acre-ft (14%) through C-102 (S-21A), and a minor amount through Military Canal. In addition, there were indirect flows to the park waters through C-100 (S-123) (46 K acre-ft, or 9%), and C-2 (S-22) (100 K acre-ft, 19%). Additional freshwater eventually enters the park through its southern boundary at the entrance to Card Sound. The freshwater in Card Sound and Barnes Sound section comes primarily from discharges from the Sea Dade Canal (S-20, 18 K acre-ft/yr, 3%) and the C-111 Canal (S-197, 28 K acre-ft/yr, 5%) into Manatee Bay in western Barnes Sound, with some additional unquantified contributions from overland runoff from extensive freshwater and coastal wetlands contiguous with the mainland shoreline of these two basins. Because no other significant or quantifiable source of surface or groundwater exists, these coastal structure flows into southern Biscayne Bay are considered in this analysis to be the only freshwater inflows along the coast.

The temporal variability of these flows and how they relate to the flow targets outlined above is of the utmost importance for the discussion of ecosystem restoration goals. The time series (1985-2005) of the South Bay flows (from S-22 in the north to S-197 in the south) and targets is shown in Figure 5. The average monthly flows from these input sources are depicted in yellow in Figure 6, as are the target flows (red) of 37 K acre-ft / 110 K acre-ft for the dry/wet season in the 10,000 acre WBZ region. The flows necessary to maintain estuarine conditions are shown as a dashed line. The 1st quartile (lowest 25%) of monthly flows, representing typical dry conditions during the 20 year time period, is depicted in green. Figure 7 shows the monthly deficit (target minus actual) of flows to Biscayne National Park in blue, with the dry conditions' deficit depicted in green. Though the wet season flow deficit is larger, when the same relationship is shown in Figure 8 and expressed as a percentage of the total mean monthly flow available to South Bay (blue), it is seen that the relative magnitude of the deficit increases throughout the dry season, peaking in April at over 250%, and is proportionally higher than the wet season deficit. During dry periods (green) these trends remain consistent. During a mean year, the fresh water

deficit is a total of 20 K acre-ft (average of 5 K acre-ft/month) during the early dry season and 485 K acre-ft (60 K acre-ft/month) during the late dry and early wet season. An inspection of the time series and the targets reveals that during the 20-year time period, monthly wet season flows met or exceeded the target less than 10% of the time; meeting late dry season targets was even more infrequent. Paradoxically, early dry season statistics come closer to the targets due to seasonal water management practices that unnaturally reduce groundwater stages in southern Miami-Dade by inducing large outflows to Biscayne Bay during November and December (the southern “agricultural drawdown”; Kearns et al., 2008).

Southern Biscayne Bay therefore is thus currently in a state of almost constant water deficit. Ongoing deleterious effects on the estuarine organisms within the western reaches of the Bay are to be expected, since the estuarine ecological functions in the Bay are inhibited both by the shortfall in freshwater volumes as well as the unnatural timing of those limited flows that are available. Though it appears that an adequate volume of fresh water is currently available to the bay on an *annual* basis to at least maintain the bare minimum estuarine conditions, the timing of this flow is inadequate to do so.

Salinity. The salinities present in Biscayne Bay are directly dependent upon these freshwater fluxes. Under the current water management scheme, large plumes of relatively freshwaters (<25ppt) extend away from the canal mouths towards the bay axis during periods of high rainfall. These fresher waters are then mixed into the other bay waters and are subject to partial exchange with marine waters (35 ppt) through tidal processes. The result in a typical year is an average bay salinity less than marine (<35ppt) during the wet season and approaching or exceeding marine during the dry season, though during years with less-than-average canal run discharges it is common to observe hypersaline (>37ppt) conditions through large portions of southern Biscayne Bay, including the western shoreline.

Time series of salinity data have been collected by Miami-Dade Department of Environmental Resources Management (DERM), Florida International University (FIU), and NPS at scattered points at different intervals within Biscayne Bay for more than 10 years. The salinity at a given station is largely a function of the efficiency of tidal exchange at that location (usually related to the distance from the ocean with its typical salinity of 35-37 ppt), the freshwater surface flow to the bay (mostly local but some remote influences dependent on location), the time history of evaporation and precipitation in the bay, the volume of intra-bay transports, and any wind events within the past few weeks that greatly influence mixing rates and on/offshore transports. These individual time series offer little help in assessing the synoptic distribution of spatial gradients within the bay, and very few are in the WBZ that is the region of greatest interest for salinity targets due to their ecological importance there. Taken as a whole, however, these salinity data can help elucidate the net result of all the influences on salinities in the bay.

If these observed data are integrated over 30 days, and grouped by their general location within the bay and their distance from the coastline (approximating the effect of both distance from the freshwater flows and the ocean influences), some interesting general trends emerge when correlated against the integrated observed flows from the coastal structures (Figure 9). Nearshore (<2 km from shore, but more than 0.7 km from any canal mouth to avoid aliasing from any freshwater plume emanating from it) there is a dramatic decrease in the monthly salinity with increasing flow. However, with increasing flows there is a proportionally decreasing influence on the salinity, with a fairly well-defined $1/x^n$ shape but with a significant random error about the mean. Beyond a flow rate of about 25-35 K acre-ft/month there is substantially less salinity reduction effect, so while it takes a flow rate of 25 K acre-ft/month to lower mean salinities by greater than 20 ppt over 30 days time in the very nearshore region, to reduce them a further 5 ppt appears to take about 60 K acre-ft/month more. This is consistent

with the increased volumes required to meet wet season salinity targets, and is mostly a reflection of conservation of volume – the increased volumes of freshwaters displace the mixed and marine waters to sea as the bay’s volume stays the same – coupled with the efficiency of tidal exchange and turbulent diffusion.

An important conclusion drawn from these results relative to the WBZ is that it would be expected that the northeastern corner of the WBZ would be most difficult to affect with additional flow volumes. Since this area is the farthest from the shoreline as well as from any existing source of fresh water output, this area would be an ideal location for monitoring efforts for future restoration programs that seek to redistribute large volumes of fresh water.

DISCUSSION

Prior to the significant changes in the freshwater flow patterns in south Florida caused by the creation of a water control system in the early 20th century, Biscayne Bay was a true estuarine system. Large amounts of freshwater in the form of both surface and groundwater were present throughout most of the year and supported a wide range of flora and fauna. When these freshwater sources were diminished and their distribution altered by water management practices, the vegetation in the bay, as well as the juveniles of many fish and invertebrate species, were adversely affected and the ecosystem in the bay changed drastically. The ecosystem that exists today in Biscayne Bay is largely marine in nature, as the volume, timing, and distribution of freshwater flows are insufficient to maintain an estuarine environment over ecologically-significant temporal and spatial scales. In keeping both with the Everglades restoration efforts and the NPS mandate to preserve unimpaired the nation’s natural resources within the parks, this document provides targets for desired salinity conditions in Biscayne National Park in terms of salinity, and provides a range of estimates for the restoration target flows required to reach the desired salinity conditions that are necessary for the ecological targets within the park.

The spatial focus of the discussion of ecologic targets includes the Western Bay Zone (WBZ) of Biscayne National Park – the 10,000 acre area along the western shoreline which contains the portion of the ecosystem that most benefits from freshwater flows. The shallow waters of the WBZ contain thousands of acres of seagrasses as well as a fringing mangrove forest. The desired condition, or overarching goal, for the western zone of Biscayne National Park is the existence of stable estuarine conditions that persist through the dry season, to be achieved through more natural timing and distribution of freshwater flows. These stable estuarine conditions support a productive, diverse benthic community based on seagrass. These conditions will also support endangered species and sustain productive nursery habitat for local and regional fishery resources.

The appropriate restoration area to consider was discussed in this document. The existing RECOVER wet season performance measures for Southern Biscayne Bay focus on a narrow (500 m) strip of coastline that encompasses 3200 acres of park waters. The more-inclusive approach used here is to focus on existing geomorphological information to define an area of soft bottom suitable for seagrasses: this approach seeks to extend the area already identified by RECOVER to the wider WBZ. This target habitat in the WBZ includes roughly 10,000 acres of park area. This larger region was chosen as the target area for stable estuarine conditions because it is based on bay geomorphology, a factor that is fundamental to bay ecology.

The ecological targets for the WBZ were based upon an approach that includes the benthic community, endangered species, and important fishery resources in the western bay. Because seagrass is important nursery and growth habitat for indicator species, a fundamental resource

management and restoration goal is to maximize coverage by SAV beds at sustainable levels. Under appropriate salinity and water quality conditions, it is expected that this area will support excellent SAV growth where sediment and water depth are appropriate for such growth. One explicit restoration target is an increase in the vitality and diversity of the WBZ seagrass community, with widgeon grass as the dominant SAV species at the mangrove edge within the nearshore ecotone and shoal grass becoming co-dominant with turtle grass through much of the rest of the WBZ. Another explicit target is the restoration of the community of seagrass-associated fauna that have been largely extirpated from South Bay, and the enhancement of habitat for others, such as crocodiles and pink shrimp that will likewise benefit substantially from the target salinity conditions.

These ecological targets require freshwater flows that produce mesohaline conditions throughout most of the year at the bottom of the bay, with salinities ranging from 5 to 20 ppt over the soft bottom areas of the WBZ that have the substrate necessary to sustain SAV. In particular, in order to preserve the estuarine character of the WBZ, the measured salinity should not exceed 30 ppt anywhere in the zone. The ecological and salinity targets that link mesohaline conditions and associated seagrass and faunal communities for this area are not currently being met because current freshwater deliveries are insufficient in terms of quantity, timing, and distribution.

Simple volumetric estimates of the restoration target flows to reach these salinity goals in the 10,000 acres of the tidally-driven system result in monthly flows of 37 K acre-ft/month in the dry season and 110 K acre-ft/month in the wet season. This results in a target annual flow of 960 K acre-ft/yr. Other types of flow target estimates – diffusive, empirical, semi-empirical – discussed in this document fall close to this range as well. In the absence of more complete hydrological modeling results which could reduce the range of estimates, the volumetric estimate will suffice as a flow target for comparison against the existing flows. Future work should focus on hydrological modeling results that will not only help refine the volumetric estimates, but also provide information concerning the expected spatial and temporal distribution of the freshwater flows, including work to improve the distribution, timing and quantity of flow through the coastal wetland and mangrove shoreline areas of the Park.

The existing flows analyzed here are comprised of the managed water flows through the control structures at the end of the canals that empty directly in or adjacent to the WBZ. Groundwater flows were omitted from hydrologic analysis in this assessment because the built system has vastly reduced them and the likelihood of generalized groundwater increases to Biscayne is very small. Groundwater flows could potentially be beneficial in the dry season; however, for the last several decades early dry season groundwater flows have been actively eliminated from the study area by water management operations.

A comparison of the canal discharges from S-22 south to S-197 indicated that the waters reaching Biscayne National Park are well below the volumes determined by the salinity requirements for ecological targets. The mean deficit of fresh water flows to meet those restoration salinity targets is 5 K acre-ft/month (20 K acre-ft total) during the early dry season and 60 K acre-ft/month (485 K acre-ft total) during the late dry and early wet seasons. The percentage of the deficit as a function of the mean monthly volume of water available to BISC rises throughout the dry season and peaks in April at over 250%. During dry conditions (when canal discharges are within the lowest 25% of flows) these deficits are exacerbated, with the April deficit exceeding 350%. The frequency with which the flow targets have been met over the period of record is extremely low, less than 10% of the time.

The historical record of salinity in Biscayne National Park indicates that the current timing and distribution of canal discharge waters is largely ineffective at maintaining estuarine conditions or even preventing hypersalinity during the dry season. Volumetric estimates of the

required flow to maintain minimal estuarine conditions of <30ppt are 440 K acre-ft per year, which is currently available on an annual basis from the water management system but has such an unnatural timing and distribution that these flows fall far short of maintaining the estuary. Without the pre-drainage groundwater flows and historic creeks that used to provide waters to South Bay during the dry season, there is not enough flow to South Bay to prevent evaporation-driven hypersalinity. The situation is even more pronounced in Barnes and Card Sounds, located immediately to the south of Biscayne National Park. With tidal inflows restricted to those spilling from South Bay over the shallow Cutter Bank at the mouth of Card Sound, characteristic long residence times (months), and with few freshwater surface inputs (C-111), Barnes and Card Sounds quickly become hypersaline during the dry season and periods of mild drought.

This paper has discussed the ecological targets for Biscayne National Park and provided annual estimates of freshwater flows needed to reach them. A gross estimate of how the annual flow is distributed between the wet and dry seasons was also provided. As restoration projects develop to provide additional flows to Biscayne National Park, further analysis will be needed to develop metrics for the seasonal and interannual variability associated with hydrologic restoration targets for the park, as well as to address spatial variability within Biscayne Bay. These ecological and hydrologic targets are critical for evaluation of potential benefits of restoration projects for Biscayne National Park and to assess progress toward ecosystem restoration.

Key Technical Conclusions and Management Implications for Biscayne National Park

1. To promote restoration of estuarine habitats (seagrasses) and estuarine species, salinities in the Western Bay Zone should range between 15-25 ppt from March through August (late dry season-early wet season), and should be consistently under 20 ppt during the end of the wet season (September-October). This report uses a variety of estimates to conclude that, given the current drainage canal-based distribution system along the coast, the volumes of water required to reach these targets are approximately 37 K acre-ft per month from December through April, and 110 K acre-ft per month from May through November, for a total annual volume of 960 K acre-ft.
2. To maintain minimal estuarine conditions, the fresh water reaching the southern Bay must have sufficient volume, adequate timing, and effective distribution to maintain salinities of less than 30 ppt (daily average) all year round in the Western Bay Zone. Salinities in the Western Bay Zone currently surpass this threshold, and cause a loss of estuarine ecological function. This loss of estuarine function may be reversed given adequate changes in fresh water deliveries to the Bay.
3. Analyses of existing flows indicate that essentially all the water currently reaching Biscayne National Park via the current distribution system is needed by the ecosystem to reach desired restoration conditions, including a healthy benthic community, endangered wildlife (American Crocodile) and important fishery resources in the Western Bay Zone.
4. Modifications to the distribution system that will produce a steady flow of waters away from the coast all along the shoreline, are needed to most efficiently create estuarine conditions with a given volume of water. These modifications will also serve to avoid the ecological damage that is caused by rapid cessation of flows due to management practice or large point-source pulses of freshwaters following storm events.

FIGURES

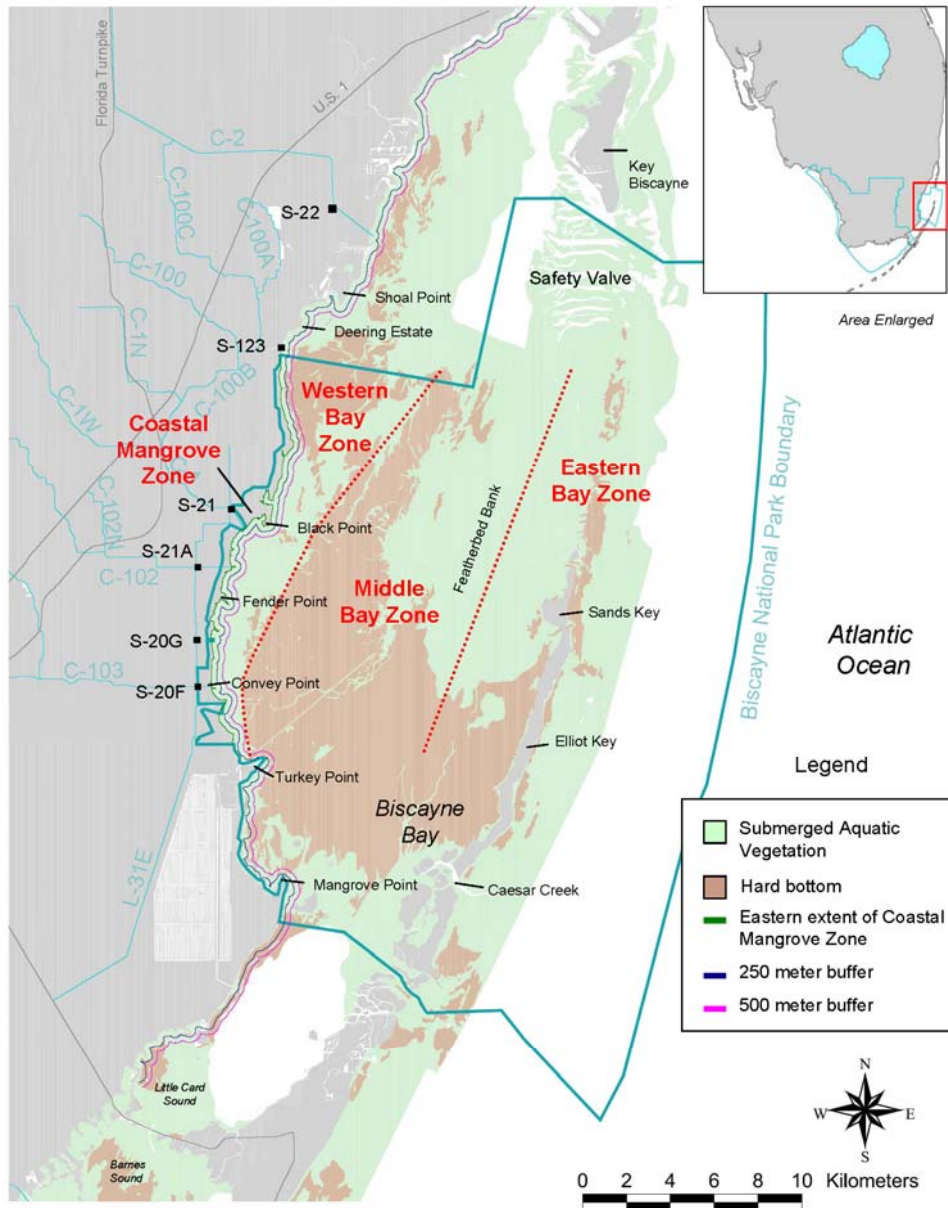


Figure 1. Biscayne National Park, showing the Western Bay Zone that was described based on the current and potential distribution of submerged aquatic vegetation on the bay bottom.

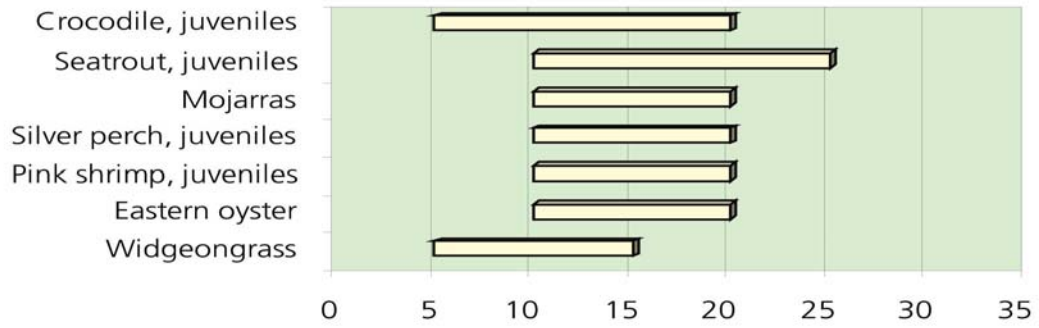


Figure 2. Optimal salinity ranges (units in ppt) for Biscayne National Park ecosystem indicators.

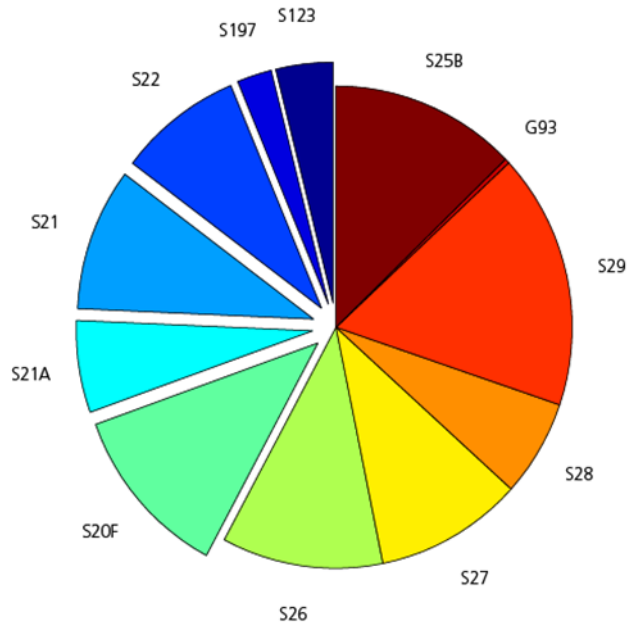


Figure 3. Average distribution of total annual canal flow (1,210 K ac-ft) to all of Biscayne Bay by SFWMD structure for 1985-2005. The highlighted portions represent those structures which discharge a total of 534 K ac-ft into Southern Biscayne Bay.

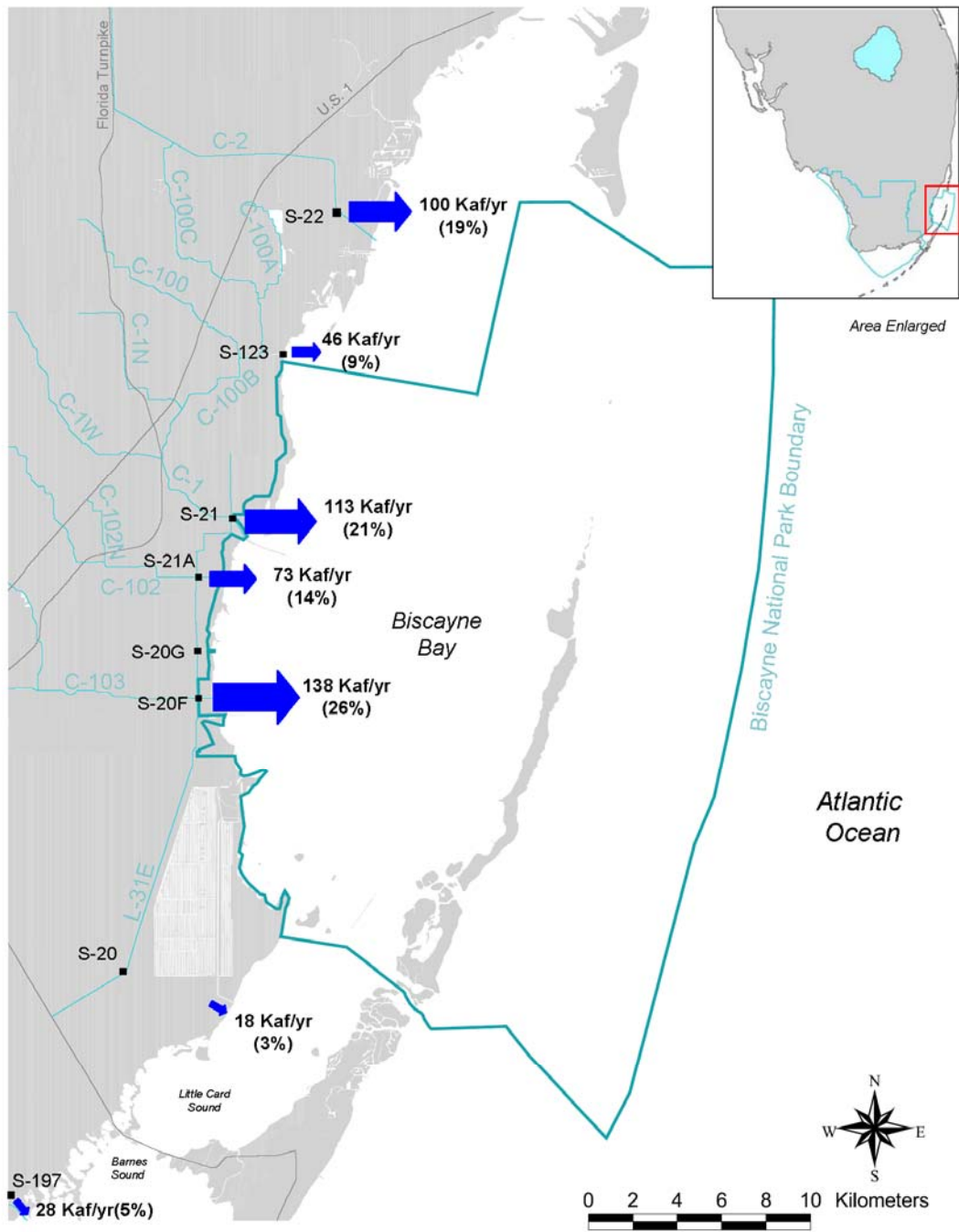


Figure 4. Location and the annual average (percent of total) of canal discharges to southern Biscayne Bay.

Monthly Time Series of Flows to Biscayne Bay

Observed_{South} = green, Target_{10k} = red

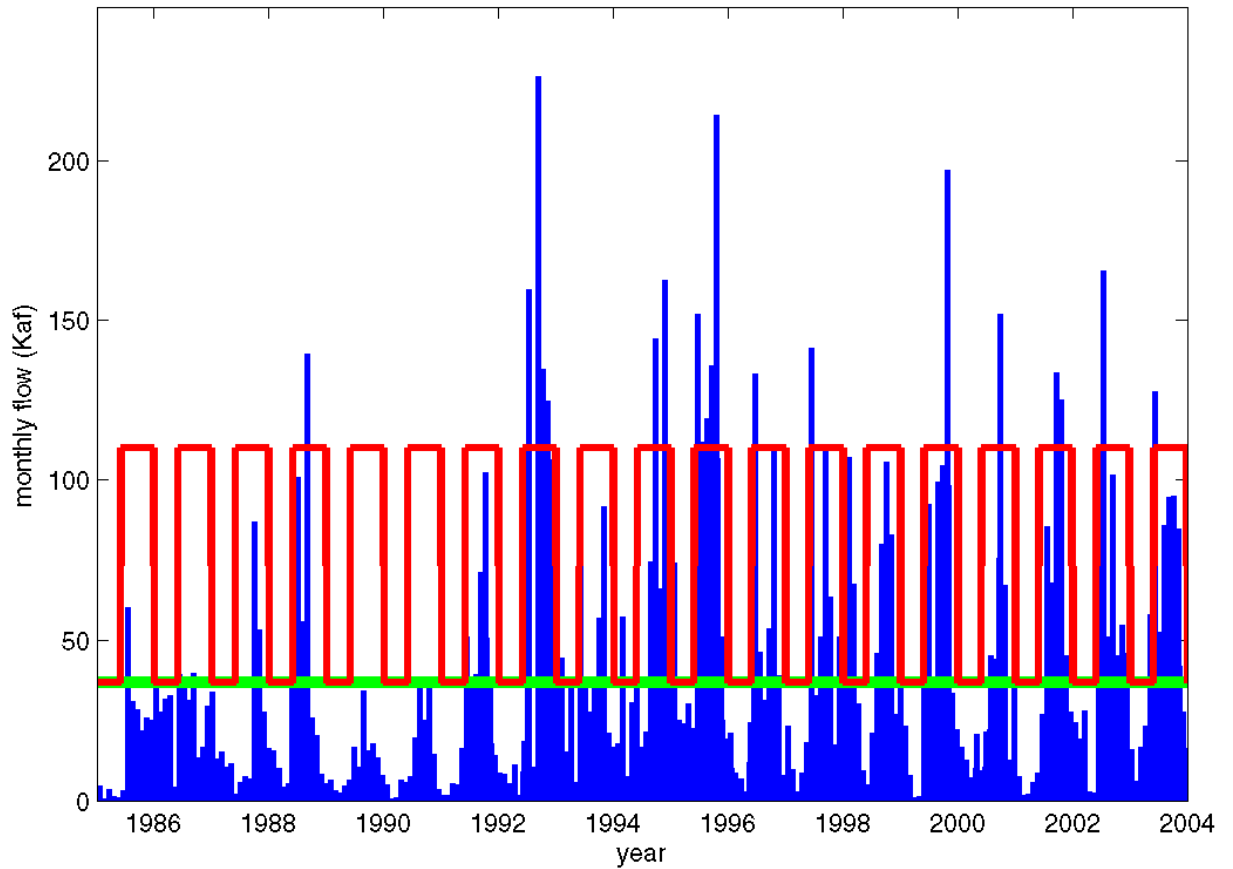


Figure 5: The monthly flows to Biscayne National Park from 1985-2004. The blue are observed flows in K acre-ft/month, while the red are the flows required to meet salinity and ecological targets. The time series shows that target flows are met only 8% of the time in the wet season, and 4% of the time in the dry season. **The green line represents a minimum flow that would be required to just barely maintain estuarine conditions throughout the year.**

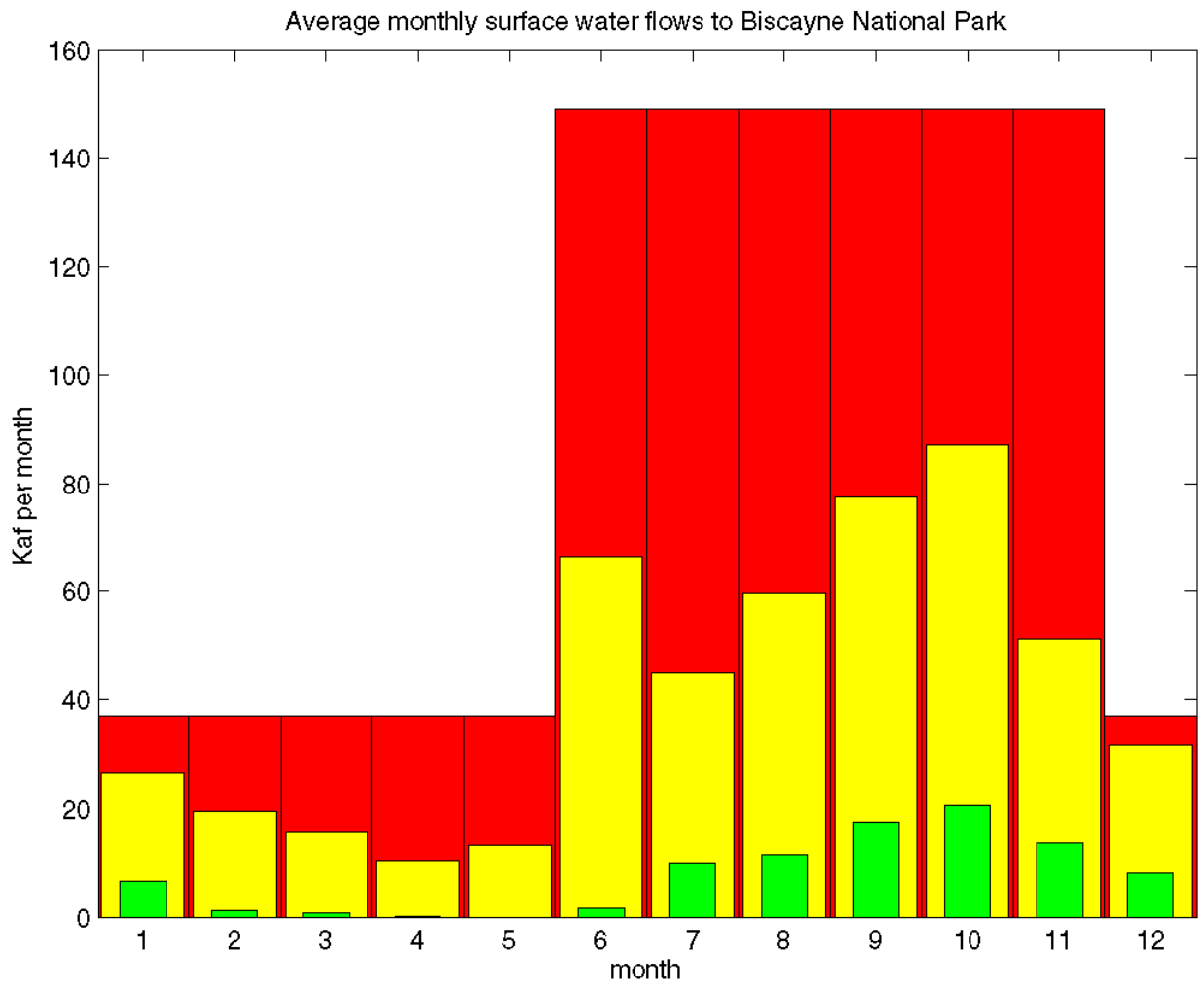


Figure 6: The average monthly flows into Biscayne National Park waters (yellow), the target flows required to meet ecosystem goals (red), the average monthly flows during dry periods (green; for the lower quartile of flows).

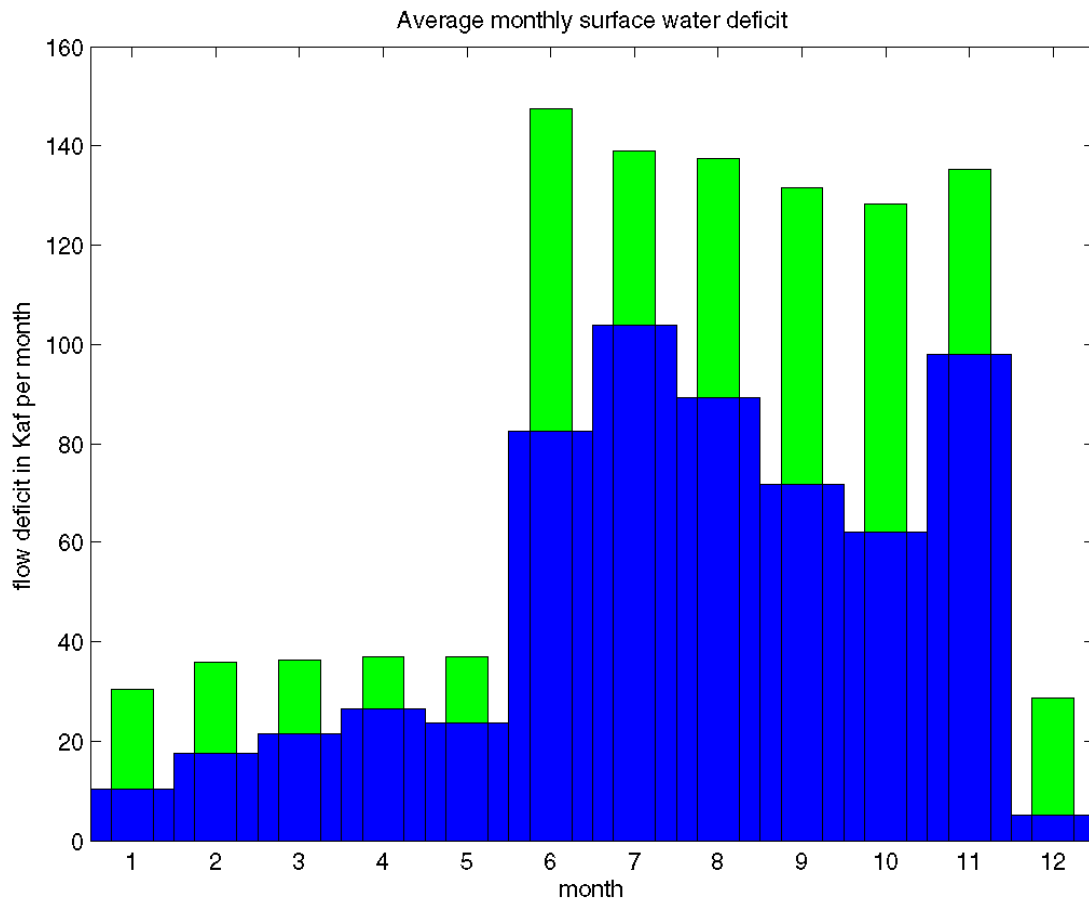


Figure 7. The average monthly flow deficit (target minus actual) for Biscayne National Park is depicted in blue; the deficit for the driest 25% of the record is shown in green.

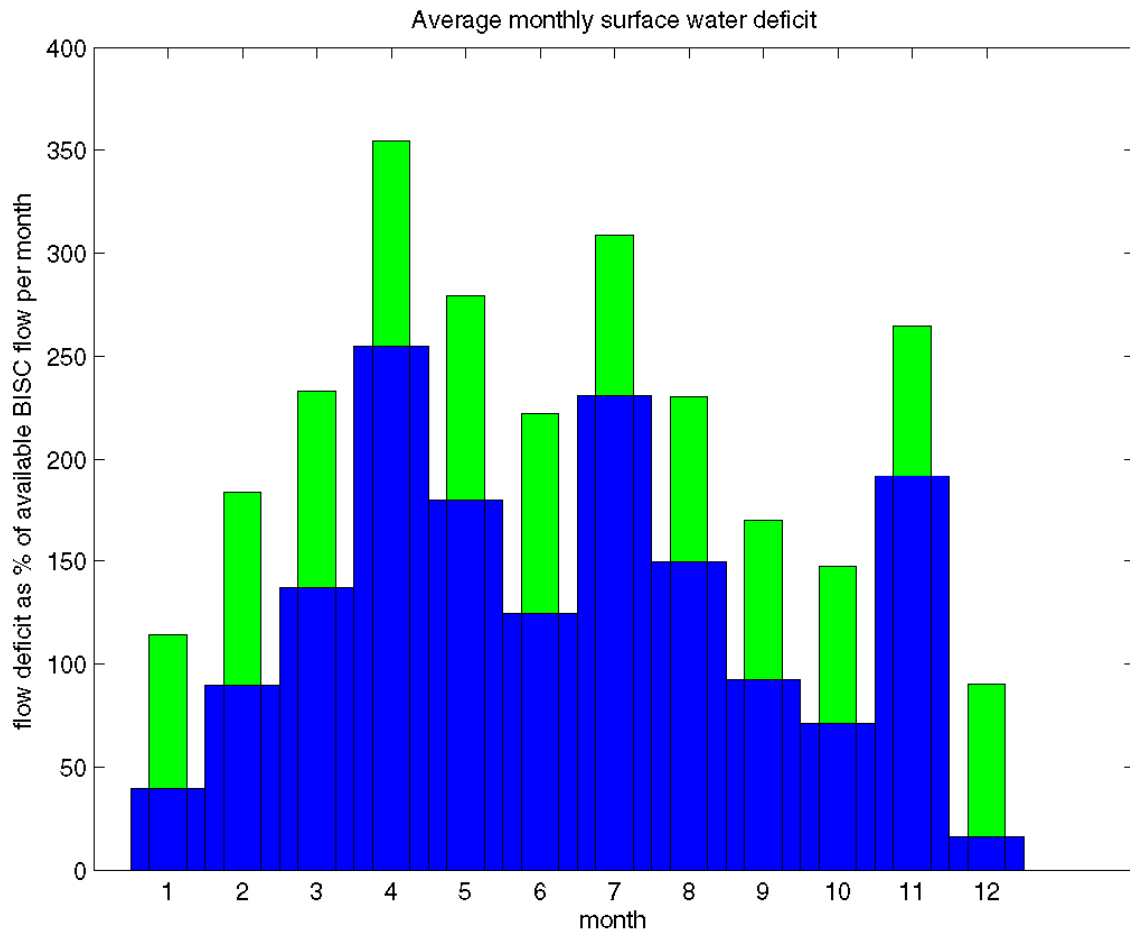


Figure 8. The average monthly flow deficit (target minus actual) for Biscayne National Park expressed as a percentage of the average flows available for each month for all conditions (blue) and the driest 25% of the period of record (green).

Net Effect of Surface Flow on Salinity in South Bisc Bay

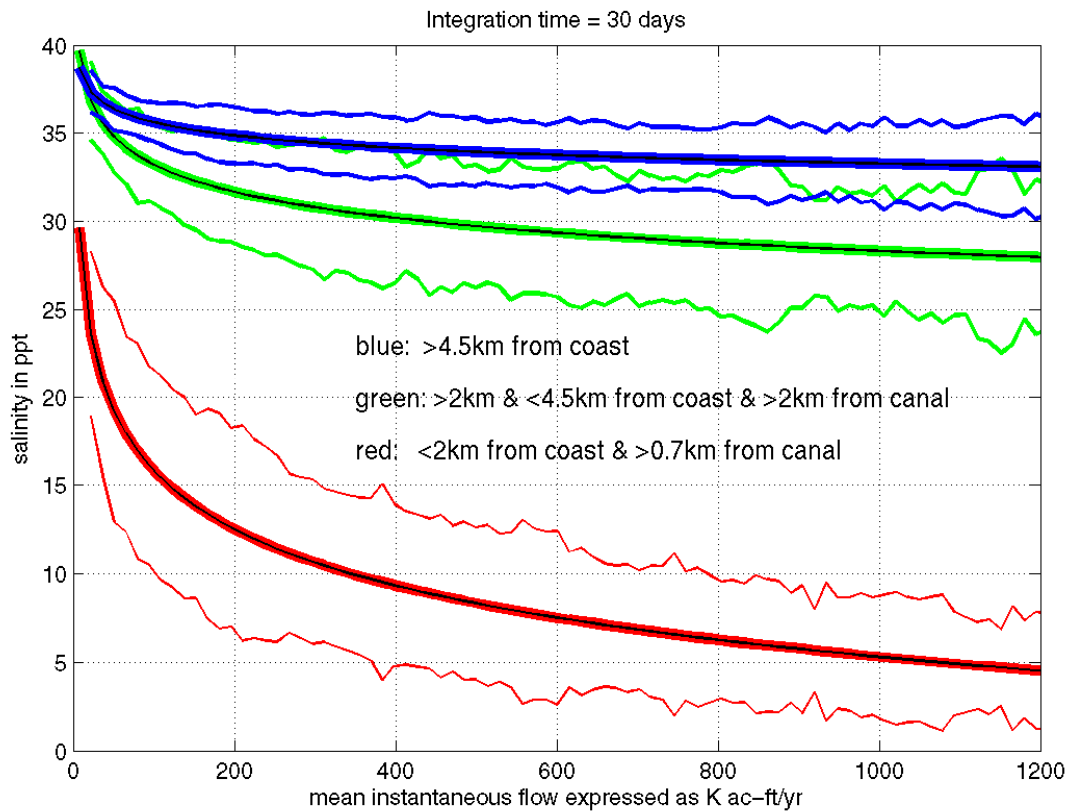


Figure 9. Observed south Biscayne Bay salinity data integrated over 30 days and grouped according to their distance from the coastline vs. flow rates expressed as K acre-ft/yr. the thick red curve denotes the area away from canal mouths but within 2 km from the western shoreline (encompassing approximately 6400 acres), the green line denotes the area from 2 km to 5 km from shore, and the blue line denotes >5km from shore. The thin lines denote an envelope of +/-1 standard deviation of the residuals from the fitted curve.

LITERATURE CITED

- Alleman, R. 2003. Historic salinity contours. PowerPoint presentation to Regional Evaluation Team Southern Estuarine Team on May 21 2003. South Florida Water Management District, West Palm Beach, Florida.
- Alleman, R. and D. M. Parrish. 2005. Hindcasting salinity in Biscayne Bay. Pp. 201-202. In: Proceedings of the Florida Bay and Adjacent Marine Systems Science Conference. University of Florida, IFAS. December 11-14, 2005. Duck Key, FL.
- Biscayne National Park. 2006. Salinity sampling in Biscayne Bay. Annual Report. A report to the U.S. Army Corps of Engineers for the Monitoring and Assessment Plan of the Comprehensive Everglades Restoration Plan for RECOVER Assessment Team, Southeast Estuary Subteam. Homestead, FL.
- Brown, G.L., R. McAdory, G.H. Nail, M. S. Sarruff, C. Berger, and M.A. Granat, 2003. Development of Two-Dimensional Numerical Model of Hydrodynamics and Salinity for Biscayne Bay, Florida. US Army Corps of Engineers Coastal and Hydraulic Laboratory Report ERDC/CHL TR-3-10. 173 pp.
- Downer, C., J. Klochak, and T. Mullins. 2005. Biscayne Bay Coastal Wetlands Alternative P Specifications. Prepared for Comprehensive Everglades Restoration Program, Biscayne Bay Coastal Wetlands Project Delivery team.
- Department of the Interior 2006. Ecological Performance Measures for Western Biscayne National Park. Discussion paper prepared by the office of the Director of Everglades Restoration Initiatives, Office of the Secretary, Florida International University, Miami FL.
- Kearns, E.J., A. Renshaw, and S. Bellmund, 2008. Environmental Impacts of the Annual Agricultural Drawdown in Southern Miami Dade County. Joint Assembly of the American Geophysical Union, Ft. Lauderdale, FL.
- Kohout, F. A. and Kolipinski, M. C. 1967, Biological zonation related to groundwater discharge along the shore of Biscayne Bay, Miami, Florida; In: G. H. Lauff (Ed.). Estuaries: American Association for the Advancement of Science, Publication no. 83: 488-499.
- Langevin, C. D. 2001. Simulation of Ground-Water Discharge to Biscayne Bay, Southeastern Florida. U.S.G.S. Water-Resources Report 00-425, 127pp.
- Lee, T. and C. G. H. Rooth. 1976. Circulation and Exchange Processes in Southeast Florida's Coastal Lagoons. Biscayne Bay Symposium, University of Miami Sea Grant Report No. 5. Rosenstiel School of Marine and Atmospheric Science, Miami, FL.
- Meeder, J. F., P. W. Harlem, and A. Renshaw. 2002. Restoration of the Black Creek Coastal Wetlands and adjacent nearshore estuarine zone of Biscayne Bay. Report to the South Florida Water Management District, West Palm Beach, Florida. Southeast Environmental Research Program, Florida International University.
- SFNRC Technical Report 2006 (1). Ecological and Hydrologic Targets for Western Biscayne National Park. South Florida Natural Resources Center, Everglades National Park, Homestead, FL. SFNRC Technical Series 2006:1: 25 pp.
- Sonenshein, R. S. 1995. Delineation of Saltwater Intrusion in the Biscayne Aquifer, Eastern Dade County, Florida. USGS Water-Resources Investigations Report, 96-4285.

- Wang, J.D., E. Daddio, M.D. Horwitz, 1978. Canal Discharges into South Biscayne Bay. Report to the Department of Environmental Resources Management, Metropolitan Dade County. 57 pp.
- Wang, J. D., J. Luo, and J. S. Ault. 2003. Flows, salinity, and some implications for larval transport in south Biscayne Bay, Florida, *Bulletin of Marine Science* 72: 311-329.
- Wingard, G. L., T. M. Cronin, C. W. Holmes, D. A. Willard, G. Dwyer, S. E. Ishman, W. Orem, C.P. Williams, J. Albietz, C. E. Bernhardt, C. A. Budet, B. Landacre, T. Lerch, M. Marot, and R. E. Ortiz. 2004. Ecosystem history of southern and central Biscayne Bay: Summary report on sediment core analyses – Year Two. Open File Report 2004-1312. U.S. Geological Survey.

APPENDIX A: ADVECTION VERSUS DIFFUSION

A one-dimensional flow of water and salt in the x direction can be expressed in a steady-state, vertically-mixed form as:

$$D(US)/dz = d/dx (A dS/dx)$$

where S is the salt content, U is the horizontal velocity, and A is the horizontal turbulent diffusion coefficient. If one assumes that U is independent of the distance x from the coast (which is a very reasonable assumption for a flow distributed all along a coastline, and an unreasonable assumption for a point source flow), and that A is likewise independent of x (a poor but pragmatic choice) then:

$$U dS/dx = A d^2S/dx^2$$

Given the assumptions, the analytical solution is exponential. The importance of this solution is that, in the absence of other transient forcing, a steady flow offshore gives a persistent exponential gradient located near the coast. As the speed of the flow increases, this gradient will move farther offshore and will become sharper (larger magnitude). As the mixing becomes more intense or efficient (i.e., the magnitude of A increases) the gradient will move closer to shore and the gradient's magnitude will decrease. The ratio of A/U is the length, or e-folding scale, and, as such, is a good estimate of the width of the offshore gradient region. While the velocity U along a coastline can be determined by metering out a known volume of water at a known rate along a length of shoreline, the horizontal turbulent diffusion coefficient A is not as simple and is often several orders of magnitude greater than equivalent molecular diffusivities. It is a function of the flow and resulting friction in the area and, as such, will be dependent on the tides, winds, and topography, and can vary by several orders of magnitude.

The advection dispersion estimate provided on page 21 is derived from a horizontal diffusivity of $A = 1 \text{ m}^2/\text{s}$ and steady offshore velocity $U = 0.001 \text{ m/s}$ for 26 km of coastline with an average depth of 1 m. The value of the diffusivity A has been shown by Wang et al. (1978) to vary from $0.5 \text{ m}^2/\text{s}$ to $5 \text{ m}^2/\text{s}$ along the western shoreline, producing a theoretical range of net offshore velocities from 0.0005 m/s to 0.005 m/s . These velocities translate to freshwater fluxes of 400 K acre-ft/yr to 4 Maf/yr, respectively – a considerable span of values. However, the diffusivity is highly variable with time and space, including dependencies on wind speed, current speed, water depth, and the distance to the shoreline. Since the shallow areas adjacent to the coastline are not subject to the largest tidal velocities and wind/wave effects, they will likely have effective diffusivities on the lower end of the range in all but the most extreme (storm) events. The 800 K acre-ft/yr target flow estimate was arrived at by a conservative evaluation of these factors and assuming an average diffusivity in the Western Bay Zone of $1 \text{ m}^2/\text{s}$.



United States Department of the Interior
National Park Service

Biscayne National Park
9700 SW 328 Street
Homestead, FL 33033

Everglades National Park
40001 State Road 9336
Homestead, FL 33034



In reply refer to: L54

July 2, 2008

Ms. Carol Ann Wehle

Executive Director
South Florida Water Management District
3301 Gun Club Road
West Palm Beach, FL 33406

Dear Ms. Wehle:

The National Park Service received a letter from your agency in April of 2005, requesting technical information relevant to the establishment of reservations for Biscayne Bay. In response to this letter and to more recent ongoing conversations with your agency, the National Park Service has developed the attached document, entitled “Estimates of Flows to meet Salinity Targets for Western Biscayne National Park”. The present document represents technical work that follows on a previous document, titled “Ecological Targets for Western Biscayne National Park”, transmitted to your agency on June 16, 2006. We hope that these technical analyses will be helpful as your agency addresses projects that affect Biscayne National Park resources, including water management operations, Florida State water law processes such as reservations and Minimum Flows and Levels, and the design of the Biscayne Bay Coastal Wetlands project.

The technical analysis in the attached document supports the National Park Service’s broad responsibility for the preservation of our nation’s natural and cultural resources. In the context of the ecosystem restoration efforts in South Florida, this translates into the responsibility for determining the ecological and underlying physical conditions that represent the restored natural resources of the South Florida Parks.

The attached document represents a joint effort by Biscayne National Park resource management staff and staff at the South Florida Natural Resources Center at Everglades National Park. During the early evolution of this document, valuable comments and input were received from staff at the U.S. Fish and Wildlife Service Office of Ecological Services in Vero Beach.

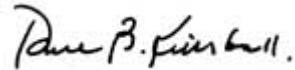


We anticipate that continuing collaboration with your staff will be beneficial in developing further metrics associated with the hydrologic restoration targets for Biscayne National Park. We are looking forward to continued cooperation in the establishment of restoration targets for our South Florida National Parks, and to working with your agency to provide the needed water for restoration of these nationally important natural areas.

Sincerely,



Mark Lewis, Superintendent
Biscayne National Park



Dan B. Kimball, Superintendent
Everglades National Park

Cc: Kameran Onley, U.S. Department of the Interior
Michael Collins, SFWMD Governing Board Member
Chip Merriam, SFWMD Deputy Executive Director, Water Resources Management
John Mulliken, SFWMD Director, Water Supply
Cecelia Weaver, SFWMD, Director of the Florida Keys Service Center
Beth Carlson Lewis, SFWMD Office of Counsel
Joan Lawrence, U.S. Department of the Interior
Terrence "Rock" Salt, U.S. Department of the Interior
Robert Johnson, U.S. National Park Service
Paul Souza, U.S. Fish and Wildlife Service
Pamela Repp, U.S. Fish and Wildlife Service



Florida Department of Environmental Protection

Bob Martinez Center
2600 Blair Stone Road
Tallahassee, Florida 32399-2400

Rick Scott
Governor

Carlos Lopez-Cantera
Lt. Governor

Jonathan P. Steverson
Secretary

April 25, 2016

Florida Power & Light Company, Inc.
c/o J.E. Leon, Registered Agent
4200 West Flagler Street
Suite 2113
Miami, Florida 33134

Certified US Mail Return Receipt
#7013 2630 0001 2651 6081

Re: Warning Letter #WL16-00015IW13SED
Turkey Point Power Plant
Facility ID No.: FL0001562
Miami-Dade County

Dear Sir:

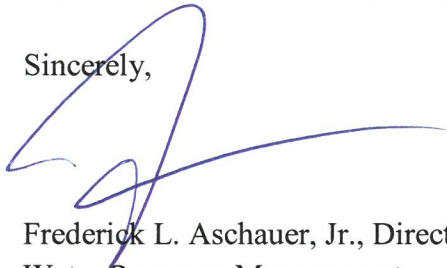
The Department is in receipt of a March 2016 "Report on Recent Biscayne Bay Water Quality Observations associated with Florida Power and Light Turkey Point Cooling Canal System Operations" (Report). The Report indicates recent sampling events "provide compelling evidence that water originating from the Cooling Canal System is reaching these tidal surface waters connected to Biscayne Bay." Information in the Report indicates possible violations of chapter 403, Florida Statutes, and chapters 62-302 and 62-520, Florida Administrative Code.

Violations of Florida Statutes or administrative rules may result in liability for damages and restoration, and the judicial imposition of civil penalties, pursuant to section 403.161, Florida Statutes.

Please contact Elsa Potts, at (850) 245-8665, within **15 days** of receipt of this Warning Letter to arrange a meeting to discuss this matter. The Department is interested in receiving any facts you may have that will assist in determining whether any violations have occurred. You may bring anyone with you to the meeting that you feel could help resolve this matter.

Please be advised that this Warning Letter is part of an agency investigation, preliminary to agency action in accordance with section 120.57(5), Florida Statutes. We look forward to your cooperation in completing the investigation and resolving this matter.

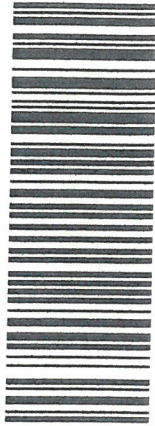
Sincerely,

A handwritten signature in blue ink, appearing to read 'F. Aschauer, Jr.', with a long horizontal flourish extending to the right.

Frederick L. Aschauer, Jr., Director
Water Resource Management
Florida Department of Environmental Protection

cc: Elsa Potts, DEP

PLACE STICKER AT TOP OF ENVELOPE TO THE RIGHT OF THE RETURN ADDRESS. FOLD AT DOTTED LINE
CERTIFIED MAIL™



7013 2630 0001 2651 6081
 7013 2630 0001 2651 6081

U.S. Postal Service™
CERTIFIED MAIL™ RECEIPT
 (Domestic Mail Only; No Insurance Coverage Provided)

For delivery information visit our website at www.usps.com
OFFICIAL USE

Postage	\$
Certified Fee	
Return Receipt Fee (Endorsement Required)	
Restricted Delivery Fee (Endorsement Required)	
Total Postage & Fees	\$

Postmark
Here

Sent To
 Florida Power & Light Company, Inc.
 c/o J.E. Leon, Registered Agent
 Street, Apt. No.; or PO Box No. 4200 West Flagler Street, Suite 2113
 City, State, ZIP+4 Miami, FL 33134

PS Form 3800, August 2006 See Reverse for Instructions

SENDER: COMPLETE THIS SECTION	COMPLETE THIS SECTION ON DELIVERY
<ul style="list-style-type: none"> Complete items 1, 2, and 3. Also complete item 4 if Restricted Delivery is desired. Print your name and address on the reverse so that we can return the card to you. Attach this card to the back of the mailpiece, or on the front if space permits. 	<p>A. Signature <input checked="" type="checkbox"/> X <input type="checkbox"/> Agent <input type="checkbox"/> Addressee</p> <p>B. Received by (Printed Name) _____ C. Date of Delivery _____</p> <p>D. Is delivery address different from item 1? <input type="checkbox"/> Yes <input type="checkbox"/> No If YES, enter delivery address below: _____</p>
<p>1. Article Addressed to:</p> <p>Florida Power & Light Company, Inc. c/o J.E. Leon, Registered Agent 4200 West Flagler Street, Suite 2113 Miami, FL 33134</p>	<p>3. Service Type</p> <p><input checked="" type="checkbox"/> Certified Mail <input type="checkbox"/> Express Mail <input type="checkbox"/> Registered <input checked="" type="checkbox"/> Return Receipt for Merchandise <input type="checkbox"/> Insured Mail <input type="checkbox"/> C.O.D.</p>
<p>2. Article Number (Transfer from service label)</p> <p>7013 2630 0001 2651 6081</p>	<p>4. Restricted Delivery? (Extra Fee) <input type="checkbox"/> Yes</p>
<p>PS Form 3811, February 2004 Domestic Return Receipt 4/25/10 Ltr.-FPL ABM 10095-02-M-1540</p>	

-COE-FL-090243-Fv.3 -

uu

RECEIVED
JUL 10 2009
20090243

**CENTRAL AND SOUTHERN FLORIDA PROJECT
COMPREHENSIVE EVERGLADES RESTORATION PLAN
C-111 SPREADER CANAL WESTERN PROJECT**

FINAL ENVIRONMENTAL IMPACT STATEMENT



July 2009



**US Army Corps
of Engineers**
U.S. ARMY CORPS OF ENGINEERS
JACKSONVILLE DISTRICT

NORTHWESTERN UNIVERSITY
LIBRARY
JUL 21 2009
TRANSPORTATION



SOUTH FLORIDA WATER
MANAGEMENT DISTRICT

operators remain vigilant to ensure that this risk continues to be considered when applying any necessary adaptive management measures.

D.6 STANDING INSTRUCTIONS TO PROJECT OPERATORS

The standing instructions which follow are to be used for the normal day-to-day operations for all proposed and existing structures. Unless otherwise noted, existing structures will continue to be operated under the current IOP for the protection of the CSSS, until such time that these operations are superseded by the Combined Operating Plan for the MWD and South Dade C-111 Projects.

The proposed C-111 SCWF Project will result in two new operable pump stations upstream of S-177 (S-200 and S-199), and a new gated spillway between S-18C and S-197 (S-198). Pump Station S-200, to be constructed downstream of S-176, is intended to initiate pumping prior to reaching the open trigger for flood control operations at S-177 (currently when the headwater stage at S-177 reaches elevation 4.2 feet NGVD). It consists of three individual 75 cfs electric pumps which will trigger according to the schedule depicted in *TABLE D-1* below.

TABLE D-1: PUMP STATION S-200 ON/OFF TRIGGERS
(*w/ S-177 Open/Close Shown for Comparison)

Pump	Rating	Pump On Elevation	Pump Off Elevation
S-200A	75 CFS	3.8 ft (NGVD)	3.6 ft (NGVD)
S-200B	75 CFS	3.9 ft (NGVD)	3.6 ft (NGVD)
S-200C	75 CFS	4.0 ft (NGVD)	3.6 ft (NGVD)
*S-177	1400 CFS	Open 4.3 ft (NGVD)	Close @ 3.6 ft NGVD

As described in the Existing Features section of this document, open trigger at S-177 will be conditionally increased by 0.1 foot in order to accommodate the addition of three new pump trigger elevations. The 0.1 foot increase will be specifically conditioned on the ability of the two new electric pump stations to be fully operational. If something (e.g. loss of electric power) should render either station temporarily inoperable, S-177's open trigger will revert to its current elevation of 4.2 feet NGVD.

During current operations of the S-332D Pump Station, a significant amount of the pumped water returns to the C-111 Canal as seepage from one or more of the S-332D cells. In order to reduce S-177 openings, the S-200 pumps may also be used on a "one-to-one" basis with the 125 cfs pumps at Pump Station S-332D, at any time that the S-176 headwater is at or above elevation 3.8 feet NGVD. For example if two of the 125 cfs diesel pumps are on at S-332D, and S-177's

headwater is at least 3.8 feet NGVD, then up to two of the S-200 pumps can be turned on independent of the stages in **TABLE D-1** and **TABLE D-2**.

To avoid overtopping, and to ensure the stability of the FPDA, pumping will cease if stages in northernmost detention cell (Cell 1) reach a stage of 7.5 feet NGVD. Operations at S-200 will also cease for protection of the CSSS, if ponding at a pre-determined representative site (see Hydrologic Monitoring Annex) within designated CSSS Critical Habitat Unit 2 exceeds ten centimeters during the critical portion of the nesting season, as identified by the FWS (February 1st thru July 15th) and the Hydrologic Monitoring Annex.

Operations at Pump Station S-199, which is to be constructed immediately upstream of S-177 (downstream of Ingraham Highway (SR 9336)) will mirror those at S-200, as depicted in **TABLE D-2** below.

TABLE D-2: PUMP STATION S-199 ON/OFF TRIGGERS

(*w/ S-177 Open/Close Shown for Comparison)

Pump	Rating	Pump Elevation	On	Pump Off Elevation
S-199A	75 cfs	3.8 ft (NGVD)		3.6 ft (NGVD)
S-199B	75 cfs	3.9 ft (NGVD)		3.6 ft (NGVD)
S-199C	75 cfs	4.0 ft (NGVD)		3.6 ft (NGVD)
*S-177	1400 cfs	Open (NGVD)	4.3 ft	Close @ 3.6 ft NGVD

Similar to the Frog Pond Detention Area, in order to avoid overtopping, and to ensure the stability of, the Aerojet Canal perimeter berms, pumping will cease if stages downstream of S-199 reach a stage of 5.5 feet NGVD. Operations at S-200 will also cease for protection of the CSSS, if ponding at a pre-determined representative site (see Hydrologic Monitoring Annex) within designated CSSS Critical Habitat Unit 3 (south of the FPDA and Aerojet Canal) exceeds 0.328 feet (ten centimeters) during the critical portion of the nesting season, as identified by FWS (February 1st thru July 15th) and the Hydrologic Monitoring Annex.

The proposed structure S-198, which is to be constructed between S-18C and the existing S-197, structure is intended to reduce current levels of seepage from the lower C-111 Canal, while preserving existing levels of flood damage reduction. As such, its operations will mimic those of S-197.

As described in **Section D.3**, as part of this project, S-20 open and close trigger stages will be increased one half foot. Under the revised operational criteria, the operational triggers will be as depicted in **TABLE D-3** below.

TABLE D-3: REVISED OPERATIONAL CRITERIA FOR S-20

Trigger	Action
Normal Operations	
Headwater Rises to El. 2.9 ft NGVD	Gate Open at 6 inches/minute
Headwater Rises or Falls to El. 2.6 ft NGVD	Gates Become Stationary
Headwater Falls to El. 2.3 ft NGVD	Gate Close at 6 inches/minute
Emergency Flood Fighting Mode	
Headwater Rises to El. 1.4 ft NGVD	Gate Open at 6 inches/minute
Headwater Rises or Falls to El. 1.2 ft NGVD	Gates Become Stationary
Headwater Falls to El. 1.0 ft NGVD	Gate Close at 6 inches/minute

In addition to the changes described above, the project will also experiment with incremental increases in the open and/or close stage triggers at S-18C. Because of the experimental, incremental, and adaptive nature of the changes at S-18C, these changes are not considered part of the standing instructions to project operators, and are discussed in *Section D.7.1, Achieving Natural System Goals, Objectives, and Benefits*.

It is important to note that the spillways in the C-111 Basin are designed to pass 40 percent of the SPF without exceeding damaging levels. The spillway discharge rating curves that are being used must be applicable to the particular flow regime encountered, and spillway gates should be opened and closed gradually to provide an even transition to the new flow regime and to minimize hydraulic effects downstream. The tailwater stage should be allowed to build up before the next gate opening operation takes place. Spillway gate openings should be checked against the Maximum Allowable Gate Opening (MAGO) Curve to insure that the gate openings do not exceed the allowable gate opening for non-damaging operations. Those MAGO curves are based on retaining the hydraulic jump within the stilling basin and providing safe velocities over the riprap and to insure the safety of the structure. For large floods, the MAGO curves may be exceeded in the "Riprap Control" range, however some damage to the riprap will likely occur. The stilling basin reduces kinetic energy of the flow entering the downstream channel. The stilling basin and downstream riprap are intended to prevent scour downstream of the spillway from undermining or otherwise threatening the integrity of the structure.

D.7 OPERATIONAL STRATEGY TO MEET PROJECT OBJECTIVES

The operational strategies described in this plan are intended to meet the goals, objectives, and benefits in the PIR, and include restoration, preservation, and protection of the south Florida ecosystem, while providing for the other

https://books.google.com/books?id=LiM0AQAAAJ&pg=SL4-PA8&lpg=SL4-PA8&dq=L-31+E+S-20+structure&source=bl&ots=Ztep1DY7ME&sig=YAwqJfE1nCm8o5y5rZCCwQrf1pM&hl=en&sa=X&ved=0ahUKEwritte7c_JzcAhVkhq0KHeUIBcsQ6AEIKTAA#v=onepage&q&f=false

**UNITED STATES DISTRICT COURT
SOUTHERN DISTRICT COURT OF FLORIDA
Miami Division**

Case No.: 1:16-cv-23017-DPG

SOUTHERN ALLIANCE FOR CLEAN ENERGY
TROPICAL AUDUBON SOCIETY INCORPORATED,
and FRIENDS OF THE EVERGLADES, INC.,

Plaintiffs,

v.

FLORIDA POWER & LIGHT COMPANY,

Defendant.

EXPERT REPORT OF WILLIAM NUTTLE, PH.D, PEng (Ontario)

I have been retained by the Plaintiffs in this matter to offer expert testimony. Pursuant to Fed. R. Civ. P. 26(a)(2)(B), the following is my written report.

My opinions are based on data on hydrogeology, hydrology, hydraulics, and water quality of both surface water and groundwater available to me as of May 14, 2018, and on my prior investigation described in the attached technical report.¹ I will continue to search for new data to inform my opinions as set forth below.

OPINIONS

1. The CCS is an industrial waste facility that is not a closed-loop system.

The Cooling Canal System (CCS) at the Turkey Point Power Station provides cooling for two nuclear-powered thermo-electric generating units, Units 3 and 4. The Turkey Point plant is located on the shore of Biscayne Bay, immediately adjacent to Biscayne National Park and about 25 miles southwest of Miami. The CCS consists of a system of shallow canals that cover an area of approximately 6,100 acres, two miles wide by five miles long, Figure 1. The surrounding landscape is flat and low-lying. Wetlands occupy the area immediately adjacent to the CCS, to

¹ Nuttle, W.K., 2017. Review of the Water Budget for the FPL Turkey Point Cooling Canal System: Regional Impacts and Discharge to Groundwater. Prepared for the Southern Alliance for Clean Energy, 7 June 2017.

the west and south, and the Biscayne National Park visitor center and Homestead Bayfront Park are north, along Biscayne Bay. Florida City and Homestead, Florida are located 4.5 miles northwest of the site.

The CCS functions as a “closed-loop” system for the purposes of providing cooling for the power plants at Turkey Point, its primary function. For this reason, the CCS is classified as an industrial waste water facility by the State of Florida.² Water is recycled continuously within the system of canals and through the power plants to cool steam condensers. Heated water discharged from the power plants enters the CCS through a canal running east-west along its north boundary. From this canal, the water enters and flows south through a series of shallow, parallel canals. At the south boundary of the CCS, the circulating water is collected in a single, large canal that carries it east and into a smaller set of parallel canals, which then carry the cooled water north, back to the intake bay of the circulating water pumps at the power plants.

However, the CCS functions as an open system from the point of view of water supply. Water in the canals actively exchanges with the atmosphere and with groundwater in the underlying Biscayne aquifer and the surface water of Biscayne Bay, Figure 2. The Biscayne aquifer is a surficial, i.e. water-table, aquifer comprised of very porous limestone that has a thickness of about 100 feet at the location of the CCS. The Biscayne aquifer is the major source of drinking water for Monroe County and communities in south Miami-Dade County.

Active exchange with groundwater plays an important role in maintaining the water balance in the cooling canals. Water loss by evaporation is the largest component of the water balance. Rainfall and the addition of water from other sources balance losses from evaporation over the long term, but rainfall is highly variable. South Florida can go long periods of time with little or no rainfall. Over the long term, the net contribution of groundwater to the water budget is small, but exchange with the aquifer plays an important role offsetting day-to-day fluctuation in the shifting balance between rainfall and evaporation.

Evaporation - 40 MGD

Evaporation from the CCS removes waste heat produced by the power plants, and due to this evaporation from the CCS is 10 mgd greater than would occur under natural conditions. The cooling provided by the elevated rate of evaporation is essential both for generating electricity and for safe operation of the nuclear power plants.

Rainfall - 20 MGD

Rainfall is the major source of freshwater currently available to the CCS to replace evaporation. On average, rainfall provides enough water to replace only about half of the water removed by

² Permit number FL0001562

evaporation. But, on days with heavy rainfall can add over half a billion gallons of water to the CCS, causing water levels to rise rapidly.

Net Seepage Input from Biscayne Bay – 8 MGD

Saline water from Biscayne Bay seeps into the CCS to replace some of the water removed by evaporation. Water moves freely through the porous limestone that separates the CCS from Biscayne Bay. On a daily timescale seepage occurs both into and out of the CCS in response to fluctuations in water levels in the CCS and in Biscayne Bay.

Other Inputs of Water - 20 MGD

Other inputs of water for the CCS includes blowdown, i.e. water discharged by the power plants in addition to cooling water, water pumped from the Interceptor Ditch, and new inputs of water added beginning in 2014. New inputs of water include fresh water pumped from the L-31E canal, water from shallow saline wells, and brackish water pumped from the deep Floridan aquifer.

Groundwater Discharge from the Cooling Canals

FPL has measured and reported on the water and salt budgets for the cooling canals every month since September 2010. These data show that under current operations the cooling canals discharge more than 10 million gallons per day through the bottom of the canals into the Biscayne aquifer. These data also show that periods of groundwater flow out of the canals toward Biscayne Bay have occurred regularly throughout the period for which data are available.

Impact to Regional Water Resources

Continued operation of the CCS impacts regional fresh water resources in two ways. First, operation of the ID withdraws fresh water from the Biscayne aquifer at rates comparable to pumping from nearby public water supply wells. Second, active exchange between the CCS and the underlying aquifer feeds the growth of a plume of hypersaline water that accelerates the intrusion of saltwater toward well fields used for public water supply.

Current plans to remediate the pollution of the Biscayne aquifer and protect Biscayne Bay are inadequate. The volume of contaminated water that can be extracted using the recovery well system is barely adequate to offset the rate at which continued operation of the cooling canals adds water to the plume.

2. The functioning of the CCS depends on active exchange of water between the CCS, the underlying aquifer, and adjacent surface water.

The amount of water contained in the CCS varies constantly as a consequence of its exposure to the effects of weather and, through its connection to the aquifer, to fluctuations in water levels in Biscayne Bay and the adjacent wetlands. Water is added daily by rainfall and from other sources, including groundwater flow, and water is lost by evaporation and groundwater flow. Beginning in 2010, FPL has conducted extensive monitoring³ of water levels and water quality in the CCS, the Biscayne aquifer, Biscayne Bay and adjacent wetlands. During this period the volume of the CCS has fluctuated between 4 billion and 8 billion gallons,⁴ Figure 3. Data collected by FPL's monitoring program provide the raw information needed to evaluate the magnitude of water exchange in and out of the CCS via groundwater flow.

The active exchange of water between the CCS and the underlying aquifer plays three roles that are essential to maintaining the functionality of the CCS:

- a) Groundwater flow into the CCS canals serves as an ultimate source of water that prevents the CCS from drying out during periods of little or no rainfall. Evaporation is the main mechanism for water loss from the CCS. Evaporation is also one of the principle mechanisms that cool the heated water from the power plants. The addition of heat from the power plants causes evaporation to be about 50 percent greater than would occur from the same area of natural wetlands.⁵ Without a reliable source of water to replace the loss from evaporation the CCS would dry up and cease to function.

Rainfall replaces about half of the water lost from evaporation, over the long term. But, rainfall in South Florida is highly variable, and there can be long periods with little or no rainfall. Water added to the CCS from other sources, such as the Interceptor Ditch (ID) and water sources used for freshening, also account for about half the water loss from evaporation, but these are variable as well. Groundwater is always available to make up the difference when needed.

- b) Active exchange of water between the CCS and the aquifer regulates water levels and changes in the volume of the CCS. During periods of little or no rainfall, evaporation reduces the amount of water in the CCS, and water levels drop. Groundwater begins to flow into the CCS as water levels drop below the water-table in the surrounding wetlands and the level of water in Biscayne Bay. Groundwater flow into the CCS increases as

³ SFWMD, 2009. FPL Turkey Point Power Plant Groundwater, Surface Water, and Ecological Monitoring Plan. October 14, 2009.

⁴ FPL calculates the volume of the CCS daily, based on measured water levels, as part of their compilation of the water and salt budgets in the post-uprate monitoring program.

⁵ "The estimate of potential evapotranspiration (ETp) from open water and wetlands in the LEC Planning Area is 53 inches" (page 187; 2011–2014 Water Supply Plan Support Document September 2014), which is equivalent to a flux of 28 mgd over the total CCS area of 6100 acres when the potential evapotranspiration rate is applied to the water surface area within the CCS.

water levels continue to drop until groundwater flow has increased sufficiently so that evaporative losses are balanced. At that point water levels stabilize.

Likewise, water accumulates in the CCS during periods in which water inputs exceed losses from evaporation. This increases the volume of water in the CCS, and water levels rise. As the water levels rise above the water-table in the surrounding wetlands and the level of water in Biscayne Bay, wastewater flow out of the CCS and into the aquifer begins. Water levels and flow into groundwater and adjacent surface waters increase until outflow and evaporation are sufficient to balance the water inputs, and water levels stabilize or begin to decline.

The discharge of wastewater from the CCS into the aquifer is an important influence on water quality in the CCS. Dissolved substances, such as salt, accumulate in the CCS as the result of the evaporative loss of water. Biscayne Bay has been the major source of groundwater inflow to the CCS. Typical values of salinity in the CCS, at least since 2010, are between 2 and 3 times the salinity of Biscayne Bay. Groundwater flow out of the CCS removes this higher-concentration water, effectively flushing salt and other dissolved substances into the aquifer and into Biscayne Bay. This flushing is the only mechanism that limits the accumulation of salt and other dissolved substances in the CCS.

3. Evidence for the presence of water from the CCS in the Biscayne aquifer and nearby surface water relies on 1) the distinctive chemical characteristics of water in the CCS and 2) the occurrence of physical conditions required for flow out of the CCS through the aquifer.

Tritium is a reliable indicator of water discharged from the CCS.⁶ Water in the CCS contains tritium in concentrations⁷ hundreds of times greater than the background concentration of tritium in the aquifer and surrounding surface waters. No other source of tritium at such high concentrations exists in the region. Therefore, measured concentrations of tritium above background levels indicates the presence of water from the CCS. For this reason, the agencies cooperating in the design of FPL's monitoring program for the CCS agreed to include tritium as a water quality constituent that is routinely measured.

⁶ Janzen, J., and S. Krupa, 2011. Water Quality Characterization of Southern Miami-Dade Nearby FPL Turkey Point Power Plant. Technical Publication WS-31, South Florida Water Management District, July 2011.

⁷ Typical values for tritium concentration in the CCS are between 2000 to 18000 pCi/l.

Water in the CCS also contains salt in high concentrations, due to the evaporation concentration of groundwater inflow from Biscayne Bay.⁸ Conductance, total dissolved solids, chlorinity, and sodium measure other characteristics of CCS water directly related to salinity. The CCS is located in an area in which freshwater, from the Biscayne aquifer and surface water runoff, mixes with salt water from Biscayne Bay. Background concentrations vary from zero salinity, in groundwater fed by rainfall, to 40 psu in shallow, near-shore areas of Biscayne Bay. Therefore, using high salinity values as evidence to indicate the presence of CCS water requires additional information to establish the appropriate background levels and to rule out possible contribution from other sources of high-salinity water.

The strength of elevated salinity as evidence for the presence of CCS water is increased by other information that establishes that physical conditions also occur for water to flow from the CCS to the point of interest. Water flow requires a pathway and the appropriate arrangement of forces to drive the movement of water along the pathway. The porous limestone of the Biscayne aquifer provides pathways for water flow in all directions around the CCS. The force to drive the movement of water through the aquifer is provided by a gradient in hydraulic head, as measured by a difference in the level of standing water. Generally, water moves in the direction from an area in which water level is higher toward an area where the water level is lower.⁹

4. The discharge of water from the cooling canal system (CCS) into Biscayne Bay occurs intermittently through multiple hydrological connections provided by the Biscayne aquifer.

The Miami-Dade Department of Environment Regulation and Management (DERM) deployed a sonde device to monitor salinity in a small cave in the shallow water of Biscayne Bay near the CCS for the period 14 October 2016 to 1 February 2017. On this occasion, measurements of water depth (for tides), salinity in the cave and salinity in the overlying water column at a reference site nearby were recorded hourly over a period of several days. Changes in salinity measured in the cave with the tides and with changes in the hydraulic gradient driving flow between the CCS and Biscayne Bay, Figure 4, illustrate the episodic nature of discharge from the CCS into Biscayne Bay.

The Biscayne aquifer provides a direct connection for the flow of water between the CCS and Biscayne Bay through multiple pathways. Geologists identify three types of voids occurring in the Biscayne aquifer: matrix porosity, touching-vug porosity, and conduit porosity. Water flow

⁸ Typical values for salinity in the CCS are 60 psu (practical salinity units) and above, about twice the concentration in Biscayne Bay. Daily salinity values range from 38 psu to 97 psu.

⁹ Strictly speaking, this rule applies only where water is the same density. The rule can be applied where waters of different densities are present, as is the case around the CCS, as long as care is taken to convert measured water levels to a common density datum, i.e. equivalent freshwater head. For shallow groundwater flow, density differences require a relatively small adjustment in water levels, and these are neglected.

occurs primarily through the touching-vug porosity and the larger conduits.¹⁰ Touching-vug porosity consists of centimeter-scale voids formed from animal burrows. Conduits are formed from extensive horizontal layers of touching-vug porous material, cracks in the limestone matrix, and solution cavities. Solution cavities found in the Biscayne aquifer include vertical pipes, which are 10s of centimeters (~ 1 foot) in diameter, and larger caves.¹¹

The lower panel of Figure 4 tells a story of mixing and exchange of Biscayne Bay water and groundwater. The daily tides in Biscayne Bay are the mechanism driving mixing and exchange along a shallow groundwater pathway that connects the CCS with Biscayne Bay. Karst features similar to the cave are found throughout Biscayne Bay, where they are known to be points for groundwater discharge into the bay from the Biscayne aquifer. At the end of the 19th century, people relied on groundwater-fed springs beneath Biscayne Bay as a source for freshwater, Figure 5. Tritium in excess of background concentrations¹² has been found in this cave, indicating that a pathway exists for flow between the CCS and the cave through the Biscayne aquifer.

Salinity values measured in the cave (red trace in the lower panel of Fig.3) fluctuate with the tides. These fluctuations occur as the result of the reversing flow of water in and out of the cave.¹³ At peak high tide, salinity in the cave is comparable to the salinity in the overlying bay water (green trace), indicating that water is flowing into the cave from the bay. During falling tides salinity in the cave increases above the salinity of bay water, and the increase continues until about the mid-point of the rising tide. This indicates that water is flowing out of the aquifer through the cave and into the bay. At around the mid-point of the rising tide, salinity in the cave drops rapidly to the salinity of bay water, indicating a reversal in the flow of water.

Also shown are salinity values measured in groundwater between Biscayne Bay and the CCS (TPGW-16S), Figure 1, and in the CCS. The peak salinities measured in the cave during outflow are what would be expected for a mixture of about equal parts groundwater, similar to the groundwater at TPGW-16S, and bay water. The groundwater measurements represent conditions along a shallow flow path, in roughly the upper 30 feet of the aquifer, connecting the CCS with Biscayne Bay. Tritium was measured in a sample of groundwater from this well with a concentration of 726 pCi/l on December 12/13, 2016, confirming the presence of CCS water. For both tritium and salinity the concentrations in the shallow groundwater are what would be expected for a mixture of about equal parts water from the CCS and water from Biscayne Bay.

¹⁰ Wacker, M.A., Cunningham, K.J., and Williams, J.H., 2014, Geologic and hydrogeologic frameworks of the Biscayne aquifer in central Miami-Dade County, Florida: U.S. Geological Survey Scientific Investigations Report 2014-5138, 66 p., <http://dx.doi.org/10.3133/sir20145138>.

¹¹ Cunningham, Kevin J. and Florea, Lee J... (2009). The Biscayne Aquifer of Southeastern Florida. Caves and Karst of America, 2009, 196-199. Available at: http://digitalcommons.wku.edu/geog_fac_pub/20

¹² 10.73 pCi/l tritium on Sep 20, 2016

¹³ AOML (n.d.), Detection, Mapping, and Characterization of Groundwater Discharges to Biscayne Bay: Expanded Final Report. SFWMD Contract C-5870, Atlantic Oceanographic and Meteorological Laboratory.

Comparison between the upper and lower panels of Figure 4 illustrates the intermittent nature of groundwater discharge to Biscayne bay in response to changes in the hydraulic gradient between the CCS and Biscayne Bay. The hydraulic gradient is measured as the difference in daily average water level¹⁴ (e.g. hydraulic head) in the CCS and in Biscayne Bay. Periods with a negative hydraulic gradient, indicating flow through the aquifer from Biscayne Bay toward the CCS, alternate with periods in which the hydraulic gradient is positive, indicating flow from the CCS toward Biscayne Bay. The direction of the hydraulic gradient correlates with changes in salinity in the groundwater at TPGW-16. Groundwater salinity decreases when flow is from Biscayne Bay, and it increases when flow is from the CCS.

The direction of the hydraulic gradient, evaluated as a daily average, affects the discharge of groundwater into Biscayne Bay through the cave. In effect, the direction of the hydraulic gradient between the CCS and Biscayne Bay regulates the amount of groundwater that discharges into the bay from the cave. When the daily-averaged direction of flow along the pathway through the aquifer is from Biscayne Bay, the peak salinity in the tidally-driven discharge from the cave is reduced. Because water discharging from the cave is a mixture of water from Biscayne Bay and groundwater, a decrease in salinity indicates that the higher-salinity groundwater makes up a smaller proportion of the mixture. Likewise, when the daily-averaged direction of flow through the aquifer is from the CCS, the peak salinity in the cave discharge is increased, indicating that groundwater from the CCS makes up a larger proportion of the flow discharging from the cave.

5. The discharge of water from the CCS into Biscayne Bay is large enough to impact water quality in Biscayne Bay.

In 2014, a proposal by FPL to pump water into the CCS from the L-31E canal prompted concerns that this would increase groundwater flow out of the CCS and impact water quality in Biscayne Bay. Responding to these concerns, Miami-Dade County required an expansion of water quality monitoring.¹⁵ Results from the expanded monitoring program confirm that discharge from the CCS into Biscayne Bay occurs, and it is large enough to have an impact on water quality in the bay.

In January 2016, high concentrations of ammonia were detected in Biscayne Bay immediately adjacent to the CCS, Figure 6. This occurred during a period of sustained high water levels and following a time when the volume of water in the CCS was at or near its maximum, Figure 3. As in the previous example (Figure 4), the blue bar graph plots values of the hydraulic gradient

¹⁴ “Water level” refers to daily-average level, so the effect of diurnal tidal fluctuation in Biscayne Bay water level has been removed.

¹⁵ Conditions included in Modification to Class I Permit CLI-2014-0312, May 2015.

between the CCS and Biscayne Bay, measured as the difference in daily-average water level (i.e. hydraulic head) in the CCS and in Biscayne Bay. In contrast with the previous example, the magnitude of the positive values of hydraulic head, driving flow through the aquifer from the CCS toward Biscayne Bay, is about twice as large, and the duration of flow toward the bay is measured in months, not days. The pattern of variation in ammonia concentrations measured at TPBBSW-7, beginning at a constant low value and rising to a higher, sustained value, follows the classic breakthrough curve for discharge of a plume of contaminant traveling in groundwater.

6. Water quality in the L-31E canal is impacted by the flow of CCS wastewater toward the west.

The L-31E canal runs parallel to the western boundary of the CCS. The canal extends from Palm Drive, near the northern boundary of the CCS, south beyond the southern extent of the CCS to connect with the Card Sound canal and Card Sound. Near the southern end of the CCS, the L-31E canal connects with the S20 canal through the S20 control structure. The S20 canal connects directly to Biscayne Bay. Flow between the L-31E and S20 canals is controlled by the S20 control structure. Around 2014, FPL installed flow barriers in the L-31E canal, near Card Sound, and in the S20 canal to prevent the intrusion of salt water in the canals. These canals are surface waters of the State.

FPL reports daily-averaged salinity at three locations along the L-31E canal as part of the regular reporting from its monitoring of the CCS. These data reveal numerous occurrences of the intrusion of salt water into the normally fresh water of the canal, Figure 7. In an initial survey in 2011,¹⁶ tritium was found in the L-31E canal at a concentration above background levels, confirming the existence of a direct hydrological connection for flow between the CCS and the canal. It is also reasonable to assume that groundwater flow of Biscayne Bay water of saline water occurs from the S20 canal into the L-31E canal, by-passing the S20 control structure when water level in the S20 canal is higher than water level in the L-31E canal.

In almost every case, the appearance of salt water in the L-31E canal coincides with the occurrence of hydraulic gradients conducive of flow from the CCS toward the L-31E canal, Figure 7. Data for two hydraulic gradients are plotted: the hydraulic gradient for flow from the CCS into the L-31E canal (e.g. the difference in water level measured at CCS-1 and water level measured in the canal at SWC-1) and the hydraulic gradient between Biscayne Bay and the canal (e.g. the difference in tail water and head water levels measured at the S20 structure). Generally, conditions for flow from the CCS into the L-31E canal and from Biscayne Bay into the L-31E canal coincide, and these occur during the dry season, when the absence of recharge from rainfall and runoff lowers water levels in the L-31E canal.

In a few instances, a rise in salinity values in the L-31E canal occurs apparently in the absence of hydraulic gradients conducive of flow into the canal. However, a closer look at the data¹⁷ shows that in these instances extreme high tides in Biscayne Bay created short-lived gradients for flow into the L-31E canal that are not reflected in the hydraulic gradients calculated from daily-averaged water level data.

¹⁶ Janzen, J., and S. Krupa, 2011. Water Quality Characterization of Southern Miami-Dade Nearby FPL Turkey Point Power Plant. Technical Publication WS-31, South Florida Water Management District, July 2011.

¹⁷ Continuous data on water level in the L-31E canal and the S20 canal are recorded at the S20 structure by the South Florida Water Management District.

7. Under current operations, groundwater flow from the CCS into the aquifer amounts to 16 million gallons per day.

Groundwater flow and evaporation are the only two mechanisms that remove water from the CCS. When the volume of the CCS decreases by a known amount (c.f. Figure 3) the water lost leaves the canals either as groundwater flow into the aquifer or as evaporation. And, if the amount of evaporation is also known, then the amount of groundwater flow can be estimated by calculating the difference. A more accurate estimate of groundwater flow can be made by taking into account any water added by rainfall and other sources of water over the same period. This is the basis for using the water budget to calculate net groundwater flow.

The CCS water budget is an accounting of the amounts of water entering and leaving the CCS. Its components include water added by rainfall and from other sources, water removed by evaporation, and the net groundwater flow between the CCS and the aquifer. Other sources of water include “blowdown” water from the power plants, water pumped from the ID, and water added, beginning in 2014, from the L-31E canal and various wells for the purpose of reducing salinity in the CCS.

If the water budget accounting is complete, then the sum of all inflows minus all outflows must equal the change in the amount of water contained in the CCS, Equation 1.

$$\boxed{\text{Rainfall}} + \boxed{\text{Other inputs}} - \boxed{\text{Evap}} - \boxed{\text{Net Flow}} = \boxed{\text{Change in volume}} \quad \text{Equation 1}$$

By rearranging Equation 1, net (groundwater) flow can be calculated from the change in volume of water contained in the CCS and estimates of other components of the water budget, Equation 2. Net flow is the net of all groundwater exchange between the CCS across the bottom and sides of the canals that occurs within a given period of time, summing all outflows and subtracting all inflows.¹⁸

$$\boxed{\text{Net Flow}} = \boxed{\text{Rainfall}} + \boxed{\text{Other inputs}} - \boxed{\text{Evap}} - \boxed{\text{Change in volume}} \quad \text{Equation 2}$$

¹⁸ This approach to estimating the net groundwater flow does not rely on the calculated groundwater flow fluxes reported by FPL.

FPL compiles data and performs calculations to estimate components of the water budget with a daily time step as part of its ongoing monitoring. The data collected include pumping rates, water levels, salinity, rainfall, water temperature, and meteorological parameters related to evaporation. The calculated components of the water budget include rainfall (including runoff), evaporation, and the exchange of water by groundwater flow between the CCS and the Biscayne aquifer. The calculated rainfall input into the canals also accounts for runoff from the land surface around the canals. These calculations involve a number of adjustable parameters. The parameter values are determined by calibration, i.e. by selecting values of the adjustable parameters so that calculated values of CCS volume and salinity match observations.

I obtained FPL's reports on the water and salt budget for the CCS covering the period September 2010 through November 2017, Figure 8. Daily values for components of the water were compiled from four spreadsheet files that cover separate but overlapping periods of time: September 2010 through November 2015,¹⁹ June 2015 through November 2016,²⁰ Jun 2015 through May 2017,²¹ and May 2017 through November 2017.²²

Example 1: net groundwater flow following the 2015/2016 high water event

Water levels in the CCS peaked in December 2015 following a period of six months of relatively high inflows from rainfall and the addition of water from other sources in an effort to lower salinity in the CCS. During the first three months of 2016, water levels returned to more normal values. Over this period, the volume of water contained in the CCS decreased by 2.2 billion gallons. Evaporation removed 2.9 billion gallons; rainfall added 1.5 billion gallons; and a negligible amount of water was added from other sources. The calculated net groundwater flow from the CCS into the aquifer is 1 billion gallons, for an average daily rate of 11 mgd (million gallons per day).

Example 2: net groundwater flow caused by Hurricane Irma storm surge

¹⁹ File contents are identified by this title on the "README" tab, "Water and Salt Balance Model of the Florida Power & light Cooling Canal System (CCS)," and this statement on the "Key" tab: "This model is based on the previously calibrated balance model (September 2010 through May2015) saved with filename Water&Salt_Balance_Thru_May2015_report.xlsx." The author of the file is identified as James Ross.

²⁰ File contents are identified by this title on the "README" tab, "Water and Salt Balance Model of the Florida Power & light Cooling Canal System (CCS)," and this statement on the "Key" tab: "This model is based on the previously calibrated balance model (September 2010 through May 2016) saved with filename Balance_Model_May2016_draftfinal_v2.xlsx." The author of the file is identified as James Ross.

²¹ File contents are identified by this title on the "README" tab, "Water and Salt Balance Model of the Florida Power & light Cooling Canal System (CCS)," and this statement on the "Key" tab: "This model is based on the previously calibrated balance model (September 2010 through May 2016) saved with filename Balance_Model_May2016_draftfinal_v2.xlsx." The author of the file is identified as James Ross.

²² File contents are identified by this title on the "README" tab, "Water and Salt Balance Model of the Florida Power & light Cooling Canal System (CCS)," and this statement on the "Key" tab: "This model is based on the previously calibrated balance model (June 2015 through May 2017) saved with filename Balance_Model_May2017_v3_draftfinal.xlsx." The author of the file is identified as James Ross.

The passage of Hurricane Irma across Key West and up the southwest coast of Florida in September 2017 caused a storm surge of 4.5 feet at Turkey Point, Figure 9. Over the period September 8 to 11 the volume of water in the CCS increased by about 3 billion gallons. Rainfall accounted for 2 billion gallons of this increase, and flooding by storm surge, which can be inferred from response of water levels in the CCS, accounted for the remaining 1 billion gallons.²³

Following the storm surge, as the water drained from the adjacent wetlands and water levels receded outside the CCS, water added by the surge remained trapped within the CCS' levees until it could either evaporate or discharge into the underlying aquifer. Over a two-month period following the hurricane the volume of water in the CCS decreased by 2.1 billion gallons. Evaporation removed 2.1 billion gallons; rainfall added 1.3 billion gallons; and 1.4 billion gallons were added from other sources. The calculated net groundwater flow from the CCS into the aquifer is 2.7 billion gallons, for an average daily rate of 44 mgd.

Example 3: average net groundwater flow into the aquifer under current operations

January 2015 marks the beginning of the period of “current operations” for the CCS, Figure 3. Plant operations are a factor that influence the exchange of water between the CCS and the aquifer. The period of record from September 2010 through November 2017 spans a period in which plant operations changed in connection with work to increase the amount of power produced by the nuclear units 3 and 4. When this work was completed, in 2014, the cooling canals experienced a build-up in salinity and other water quality problems, prompting FPL to further modify operations by securing additional sources of water to replace losses from evaporation. These changes came online by the end of 2014.

Net groundwater flow can be a source of water inflow into the CCS as well, Figure 10. Equation 2 can be applied to calculate daily values of net groundwater flow from the data FPL reports from its monitoring program. Periods in which net groundwater flow is a source of inflow to the CCS alternate with periods in which net groundwater flow removes water from the CCS. These changes occur as constantly changing water levels both within the CCS and outside it, in Biscayne Bay and in the adjacent wetlands, alter the hydraulic gradients that drive flow through the aquifer.

For the period of current operations (January 2015 through November 2017), components of the water budget have the following average values: evaporation 39 mgd, rainfall 23 mgd, water input from other sources 23 mgd. The change in the volume of water in the CCS, averaged over the entire period January 2015 through November 2017, is small, 0.6 mgd. The net groundwater

²³ FPL's report on the CCS water budget for this period does not account for the amount of water and salt added to the CCS by storm surge from Hurricane Irma. I have corrected this omission in my analysis of the water budget.

flow, averaging flows into the aquifer and flows into the CCS over all the days in this period, is 8 mgd into the aquifer.

The average rate of flow into the aquifer out of the CCS is of particular interest because of its importance in regulating water quality in the CCS. Groundwater flow into the aquifer is the only mechanism for removing dissolved substances and avoiding the build-up of excessive concentrations by evaporation. Also, groundwater flow into the aquifer is the mechanism by which the CCS impacts water quality by discharging hypersaline water and other pollutants into the aquifer and, via direct hydrologic connections provided by the aquifer, into Biscayne Bay and the adjacent wetlands.

The average value for net groundwater flow into the aquifer from the CCS is 16 mgd, computed as the sum over days in which the direction of groundwater flow is into the aquifer divided by the total number of days in the period. At this rate, the entire contents of the CCS empty into the aquifer every 11 months,²⁴ and at least 8 million pounds of salt, along with other pollutants, are flushed into the aquifer each day.²⁵

8. Actions being taken by FPL with the objectives to cease harmful discharges from the CSS that threaten groundwater resources to the west, retract the hypersaline groundwater plume, and prevent releases of groundwater to surface waters connected to Biscayne Bay cannot achieve these objectives.

The 2016 Consent Order²⁶ with the Florida Department of Environmental Protection prescribes actions by FPL intended to remediate the damages by the hypersaline plume and protect Biscayne Bay. The order prescribes three main actions: installation of a recovery well system, freshening to reduce salinity in the CCS, and restoration projects along the Biscayne Bay shoreline. These actions are either demonstrably inadequate to the task or they work at cross purposes to each other and the stated objectives.

The actions being taken by FPL cannot achieve the objectives of the Consent Order because of (1) the failure of the interceptor ditch; (2) the inadequacy of the recovery well system; and (3) the increase in discharges from the CCS as a result of addition of fresher water. The actions being taken by FPL ignore the basic reality of the way the CCS interacts with groundwater and surface water.

²⁴ This calculation is based on an average volume of the CCS of 5.0 billion gallons (range from 3.8 billion gallons to 7.8 billion gallons) and 16 mgd (range from 0 mgd to 225 mgd) average daily net groundwater flow out of the CCS; both of these figures are the average for the current operations period January 2015 through November 2017.

²⁵ In this calculation I assume an average salinity in the CCS of 67 psu (range from 38 psu to 97 psu).

²⁶ Consent Order 2016. State of Florida Department of Environmental Protection v. Florida Power & Light Company, OGC File No. 16-0241.

Failure of the interceptor ditch

Since 1974, a series of agreements with the South Florida Water Management District have prescribed the operation and monitoring of the Interceptor Ditch (ID). The ID was constructed to “restrict movement of saline water from the cooling water system westward of Levee 31E adjacent to the cooling canal system to those amounts which would occur without the existence of the cooling canal system”²⁷ This was in response to concerns that water discharged to the aquifer from the CCS could harm freshwater supplies. Failure of the ID to intercept water from the CCS is evident in by the development of the hypersaline plume extending west beyond the L-31E canal. Today, freshwater resources of the Biscayne aquifer are threatened both as a result of the failure of the ID to intercept water from the CCS as well as from adverse effects resulting from the continued operation of the ID.

Operation of the ID is supposed to prevent CCS water flowing west through the aquifer from reaching the L-31E canal. Water is pumped out of the ID as needed to maintain water levels in the ID lower than water levels in the L-31E canal. This is supposed to assure that the direction of groundwater flow is always from the west into the ID. In practice, the ID has failed to prevent the westward movement of the dense hypersaline plume along the bottom of the aquifer, ~ 100 feet below the land surface. The ID is too shallow, ~20 feet deep, to retard the horizontal movement of water deep in the aquifer, especially under the conditions where flow in the aquifer is stratified.

Density stratification in the aquifer means that it imperative to maintain conditions against vertical flow as well as horizontal flow. Water in the Biscayne aquifer west of the CCS is stratified. A layer of freshwater, fed by rainfall and groundwater flow from the west, overlies the plume of hypersaline water fed by flow out of the CCS and extending west beneath the ID and the L-31E.

The stability of the interface between the freshwater and salt water layers, in a coastal aquifer, depends on maintaining the level of the fresh water-table above sea level. Applying the Gyben-Herzberg principle, the depth to the interface between freshwater and salt water beneath the L-

²⁷ Fifth Supplemental Agreement Between the South Florida Water Management District and Florida Power & Light Company, 16 October 2009

31E canal is calculated to be between 7 and 12 feet,²⁸ which coincides exactly with the bottom of the L-31E canal.²⁹

Water is pumped out of the ID for the purpose of maintaining a hydraulic barrier to westward movement of CCS water in the shallow groundwater. Pumping lowers the water level in the ID and in the wetlands immediately adjacent to it. This decreases the height of the water-table in the freshwater lens, which also decreases the depth to the freshwater/salt water interface. Therefore, by lowering the watertable, ID operations also promote the vertical flow of the CCS water in the hypersaline plume upward into the upper area of the Biscayne aquifer.³⁰

Beyond the threat arising from its failure to retard the westward movement of CCS water, operation of the ID represents a large, undocumented demand on the regional freshwater resource provided by the Biscayne aquifer. Water pumped out of the ID is a mixture of saline water discharged from the CCS and fresh groundwater flow from the west. The amount of freshwater withdrawn by ID operations can be estimated from the ID pumping rate and salinity data collected for the ID and the L-31E canal. The impact of pumping on the water table in the wetlands west of the CCS is exacerbated by the fact that pumping from the ID occurs predominantly during the dry season, January through May. This is when the amount of freshwater in the aquifer is at its seasonal low, and hydraulic gradients conducive for flow from the CCS into the L-31E canal exist.

On any day, the amount of water pumped from the ID, Q_{ID} , is the sum of an amount of water that has entered the ID from the west, from Q_{L31} , and an amount of water recycled from the CCS, Q_{RW} ;

$$Q_{ID} = Q_{L31} + Q_{RW}. \quad \text{Equation 3}$$

²⁸ The Gyben Herzberg relationship calculates the depth to the interface between freshwater and salt water in a coastal aquifer, z , as the height of the freshwater water-table above sea level, h , multiplied by a factor computed

from the densities of freshwater (nominally 1000 kg/m^3) and seawater (1025 kg/m^3); $z = \frac{\rho_f}{(\rho_s - \rho_f)} h$. For freshwater and sea water the multiplier is 40. In the situation of the L-31E canal and the hypersaline plume from the CCS, water level in the CCS plays the role of sea level. The water level in the L-31E canal is, on average, 0.3 feet above the level of the CCS; therefore the depth to the interface below the canal is computed to be 12 feet. However, the density of hypersaline water in the CSS and its plume can be higher than that of sea water; density of water with a salinity of 60 psu, roughly the long-term average for the CCS, is 1042 kg/m^3 . Using this higher density, the multiplier is 24, and the estimated depth to the interface below the L-31E canal is 7 feet.

²⁹ "The depth of the L-31E canal is around 9 feet." Janzen, J., and S. Krupa, 2011. Water Quality Characterization of Southern Miami-Dade Nearby FPL Turkey Point Power Plant. Technical Publication WS-31, South Florida Water Management District, July 2011.

³⁰ Evidence for vertical migration of the plume was discussed at a meeting at the South Florida Water Management District in February 2017; PowerPoint presentation by Jonathon Shaw, Turkey Point Power Plant Interceptor Ditch Operations, Joint Agency Meeting – SFWMD/DEP/DERM, February 9, 2017.

Similarly, the amount of salt in the water pumped from the ID is the sum of an amount carried into the ID in groundwater flow from the west and in the flow of recycled water from the CCS;

$$Q_{ID}S_{ID} = Q_{RW} S_{CCS} + Q_{L31} S_{L31}. \quad \text{Equation 4}$$

From these two equations, one can derive the following formula to calculate the portion of the total daily ID pumping that is fed by groundwater flow from the west:

$$Q_{L31} = Q_{ID} [(S_{CCS} - S_{ID}) / (S_{CCS} - S_{L31})] \quad \text{Equation 5}$$

The daily rate of pumping from the ID, Q_{ID} , and the salinity of water in the ID, S_{ID} , are measured, Table 6. The salinity measured in the L-31E canal can be taken as representative of the salinity of water flowing into the ID from the west. Shallow groundwater west of the CCS is not totally fresh, as a consequence of infrequent flooding of the wetlands there by water from Biscayne Bay. The salinity of water below the CCS is taken to be 60 gm/l, which reflects the long-term, stable average of salinity measured in a shallow well in the center of the CCS³¹.

Based on these data, calculations reveal that ID pumping removes about 3.5 mgd of mostly fresh groundwater from the Biscayne aquifer west of the CCS. This is the average of the amount of freshwater extracted calculated using Equation 5 applied with daily values of pumping rate and salinity, Table 1. The pumping rate varies from day to day, and salinity in the ID tends to be higher on days with higher rates of pumping.

This rate of extraction is large relative to other withdrawals from the aquifer. Nearby well fields operated by public water utilities³² withdraw 2 mgd (Florida City), 11 mgd (Homestead), and 17 mgd (FKAA). The withdrawal of freshwater as a consequence of ID operations is not documented in current regional water supply plans.

Regional water supply plans include data on water use by power plants. The Lower East Coast water supply plan notes the water withdrawn from the Floridan aquifer for cooling for the gas-fired Unit 5 at Turkey Point, but it does not account for the extraction of water from the Biscayne aquifer to supply water for the CCS.³³ Since the latest update to the Lower East Coast plan, FPL has obtained permits to withdraw additional water for the CCS from the L-31E and from the Floridan aquifer.

³¹ TPGW-13

³² Water use figures from Table A-8, 2013 LEC Water Supply Plan Update: Appendices, October 10, 2013.

³³ "FPL increased its power generation capacity at the existing Turkey Point plant by adding combined cycle generating technology to respond to significant population growth in South Florida. Unit 5 is a natural gas-fired combined-cycle unit that uses groundwater drawn from the Floridan aquifer while the other four units, Units 1–4, use water from the closed cycle recirculation canal system."

Table 1: Calculated rate of freshwater extraction from the Biscayne aquifer by pumping the Interceptor Ditch. Data are for the period January 2015 through November 2017.

	Calculated fresh water flow (mgd)	Measured ID Pump Rate (mgd)	ID salinity	L-31E salinity
Average	3.45	4.01	6.11	1.51
Standard deviation	8.53	9.63	3.85	1.44
Maximum	161.19	168.60	20.13	6.76
Minimum	0.00	0.00	1.92	0.27

Inadequacy of the recovery well system

The Consent Order prescribes that the recovery well system is supposed to “halt the westward migration of hypersaline water from the CCS within 3 years,” and “retract the hypersaline plume to the L-31E canal within 10 years.” To accomplish this, a series of 10 recovery wells will be sited along the western boundary of the CCS. These wells will remove water from the plume, which is to be disposed by deep well injection. Operation of the recovery well system is subject to the constraint that there be no “adverse environmental impacts.” This is assured by establishing an upper limit on the aggregate rate that the wells can withdraw water from the plume – 5.4 billion gallons per year, or 15 mgd.³⁴

At the maximum rate pumping rate, it is highly unlikely that the recovery well system can succeed in retracting the plume within 10 years. In 2013, it was estimated that the western extent of the plume contained 123 billion gallons³⁵ of water originally discharged from the CCS. This is more than twice the volume of water that can be recovered if the recovery wells are pumped at their maximum rate for 10 years. And, it is certain that, through mixing with ambient water in the aquifer and the accumulated discharge from the CCS over the past 5 years, the volume of hypersaline water that now must be removed to retract the plume is much larger. CCS water added to the aquifer with a salinity of 60 psu can be diluted with nearly an equal volume of freshwater and still be considered hypersaline.

³⁴ Water Use Individual Permit No. 13-0651-W, issued on February 27, 2017, by South Florida Water Management District

³⁵ This figure is based on calculations by SFWMD staff in 2013 of the total volume of CCS water in the mapped portion of the hypersaline groundwater plume, reported in Nuttle, W.K., 2013. Review of CCS Water and Salt Budgets Reported in the 2012 FPL Turkey Point Pre-Uprate Report and Supporting Data. Report to the South Florida Water Management District, 5 April 2013. The extent of the plume was mapped based on the presence of CCS water, even in diluted amounts, identified by its ionic and tritium chemical fingerprint. The mapped portion of the plume included only the western portion and the portion beneath the CCS. Including the unmapped portion that extends under Biscayne Bay could increase this number by a factor 1.5 to 2.

Freshening increases flow out of the CCS into the aquifer

To accomplish the objective of “cease discharges from the CCS that impair the reasonable and beneficial use of adjacent G-II ground waters to the west of the CCS,” the Consent Order directs FPL to reduce the average annual salinity to 34 psu or below within 4 years. FPL is to conduct “freshening activities” to achieve this goal. FPL describes freshening activities as “using fresher water sources to replace freshwater evaporated from the CCS and thereby reduce the average annual CCS salinity.”

Freshening activities, i.e. supplementing other inputs in the water budget to lower salinity in the CCS, distinguish the period of current operations (January 2015 through November 2017) from the preceding period in the record of data from the monitoring program (September 2010 through December 2014). Freshening activities have altered the water budget, Table 2. Water inputs from ID operation, and wells tapping the Upper Floridan aquifer and saline water beneath Biscayne Bay, have increased flows in the other inputs category by 17 mgd. Flows between the CCS and the aquifer have changed by a similar amount, from an average net inflow of 10 mgd in the earlier period to an average net outflow of 8 mgd under current operations. FPL recently reached a partnership agreement with Miami-Dade County³⁶ to secure up to 60 mgd additional water for freshening activities. Any further increase in water inputs to the CCS will result in the same increase in average net groundwater flow from the CCS into the aquifer.

Table 2: Average daily values for components of the water budget (mgd)

	Sep 2010 to Dec 2014	Jan 2015 to Nov 2017
Evaporation	36.6	38.8
Rainfall	20.2	23.4
Other inputs	6.3	23.0
Volume change	-0.3	0.6
Net groundwater flow	-9.7	7.8

The effect of “freshening activities” is exactly opposite the usual meaning of the term “cease discharges from the CCS.” In the context of the CCS water budget (Eq.’s 1 and 2), freshening activities increase the daily quantities of “other inputs.” This has two effects. First, the volume of

³⁶ Resolution approving joint participation agreements with Florida Power & Light Company providing for development of (1) an advanced reclaimed water project and (2) next generation energy projects; and authorizing the Mayor or his designee to execute the agreements and exercise the provisions contained therein, Resolution No. R-292-18, approved on April 10, 2018.

water in the CCS increases. Second, as the volume and water levels increase, the flow of water into the aquifer from the CCS increases until it balances the inflow provided by new sources of water. Likewise, the long-term reduction in salinity to 35 psu requires reducing the mass of salt in the CCS. The only mechanism that removes salt from the CCS is by flushing it into the aquifer.

To gage the impact of freshening activities on the flow of CCS water feeding the hypersaline plume, I reviewed the monthly average groundwater flows that FPL compiles in its reporting on the CCS water and salt budgets, Figure 10.^{37 38 39 40} FPL computes groundwater fluxes separately across the bottom of the CCS and each of its sides based on hydraulic gradients derived from water level data. I examined only the groundwater flow computed out through the bottom of the CCS because this is directed downward, deep into the aquifer. Therefore, bottom flow is a better indicator of the flow from the CCS that feeds the hypersaline groundwater plume. By contrast, the net flow computed from the water budget (above), includes horizontal flow at shallow depths that more likely discharges into Biscayne Bay or a canal.

FPL's computed groundwater flow into the aquifer through the bottom of the CCS was much larger during this period, 11 mgd, compared with the average groundwater flow for the preceding period since 2010, 1 mgd. Other differences are apparent in the water budget between the two periods. In particular, water inputs from pumping the ID are much larger in the recent period; ID pumping accounts for a large portion of "other inputs." "Freshening activities' may or may not have had an effect on the increased ID pumping. Therefore, it is difficult to say what portion the increased from 1 mgd to 11 mgd is attributable to freshening.

Freshening activities work at cross purposes with the recovery well system. Any increase in groundwater flow from the CCS feeding the hypersaline plume degrades the performance of the recovery well system. At a rate of inflow of 11 mgd, over two thirds of the pumping capacity of the water recovery wells is required just to intercept and remove the water that groundwater flow

³⁷ File contents are identified by this title on the "README" tab, "Water and Salt Balance Model of the Florida Power & light Cooling Canal System (CCS)," and this statement on the "Key" tab: "This model is based on the previously calibrated balance model (September 2010 through May2015) saved with filename Water&Salt_Balance_Thru_May2015_report.xlsx." The author of the file is identified as James Ross.

³⁸ File contents are identified by this title on the "README" tab, "Water and Salt Balance Model of the Florida Power & light Cooling Canal System (CCS)," and this statement on the "Key" tab: "This model is based on the previously calibrated balance model (September 2010 through May 2016) saved with filename Balance_Model_May2016_draftfinal_v2.xlsx." The author of the file is identified as James Ross.

³⁹ File contents are identified by this title on the "README" tab, "Water and Salt Balance Model of the Florida Power & light Cooling Canal System (CCS)," and this statement on the "Key" tab: "This model is based on the previously calibrated balance model (September 2010 through May 2016) saved with filename Balance_Model_May2016_draftfinal_v2.xlsx." The author of the file is identified as James Ross.

⁴⁰ File contents are identified by this title on the "README" tab, "Water and Salt Balance Model of the Florida Power & light Cooling Canal System (CCS)," and this statement on the "Key" tab: "This model is based on the previously calibrated balance model (June 2015 through May 2017) saved with filename Balance_Model_May2017_v3_draftfinal.xlsx." The author of the file is identified as James Ross.

out of the CCS continually adds to the volume of the plume. That leaves only 4 mgd of pumping capacity applied to reducing the existing volume and retracting the hypersaline plume. That's only 15 billion gallons that can be removed from the existing plume over 10 years. The current volume of the plume could easily be 10 times this amount.

Coastal restoration projects are inadequate to protect Biscayne Bay from discharges from the CCS.

The action prescribed in Consent Order in response to the objective “to prevent releases of groundwater from the CCS to surface waters connected to Biscayne Bay...” is clearly incommensurate with the scale of the challenge. The action that FPL will undertake is limited to restoring coastal habitat by partially filling two relic canals in the vicinity of the power plant. These two canals are far from the only direct hydrologic connections between the CCS and Biscayne Bay. The cave site, described above, is an example of what are likely numerous connections. In 1973, faced with a similar goal to “restrict movement of saline water from the cooling water system westward of Levee 31E”⁴¹ FPL undertook the construction and operation of the ID to create a hydraulic barrier to shallow groundwater flow along the entire western boundary of the CCS. Given the track record of the ID, it is unlikely that something on the same scale as the ID, 5 miles in extent, would be an adequate hydraulic barrier to protect Biscayne Bay from discharges from the CCS.

⁴¹ Fifth Supplemental Agreement Between the South Florida Water Management District and Florida Power & Light Company, 16 October 2009

QUALIFICATIONS

My resume is attached hereto as Exhibit B and contains my qualifications and a list of all publications that I have authored in the past 10 years.

PRIOR TESTIMONY

During the past 4 years, I have testified in deposition and at trial in the following cases:

Altantic Civil, Inc. v. Florida Power and Light Company, et al. Case No. 15-1746 (Florida Division of Administrative Hearings, Nov. 2-4, 2015).

In re Florida Power and Light Company Turkey Point Power Plant Unites 3-5 Modification to Conditions of Certification. Case No. 15-1559EPP (Florida Division of Administrative Hearings, December 1-4, 2015).

COMPENSATION

I am being compensated as follows for my work in this matter: \$175.00 per hour.

SIGNATURE

A handwritten signature in black ink, appearing to read 'W.K. Nuttle', written in a cursive style.

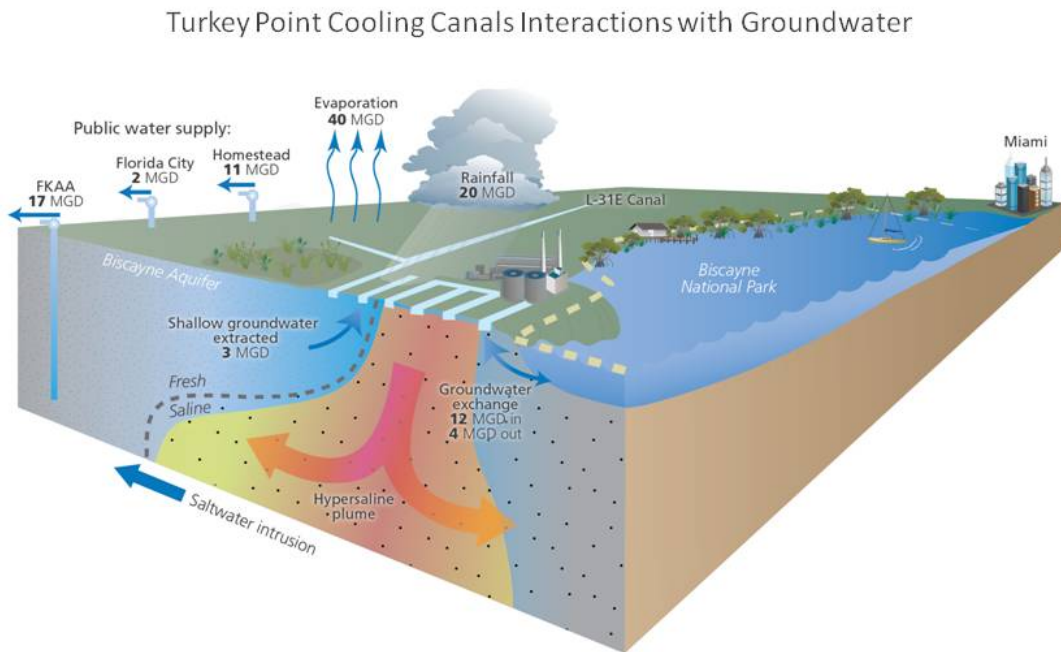
William K. Nuttle

Exhibit A: Figures

Figure 1: Turkey Point Cooling Canal System showing the main features and monitoring locations mentioned in the text.



Figure 2: The cooling canals at Turkey Point exchange water freely with the atmosphere, through rainfall and evaporation, and with the underlying Biscayne aquifer, which is the main source of freshwater for communities in south Miami-Dade County and the Florida Keys.



© 2018 Southern Alliance for Clean Energy

Figure 3: The volume of water contained in the CCS changes constantly in response to rainfall, water inputs from other sources, and the loss of water through evaporation. Water exchange between the CCS canals and the underlying aquifer sometimes adds water and sometimes removes water from the CCS. Measured changes in CCS volume combined with measurements and estimates of rainfall, other water inputs, and evaporation make it possible to calculate the volume of water exchanged with the aquifer on a daily basis.

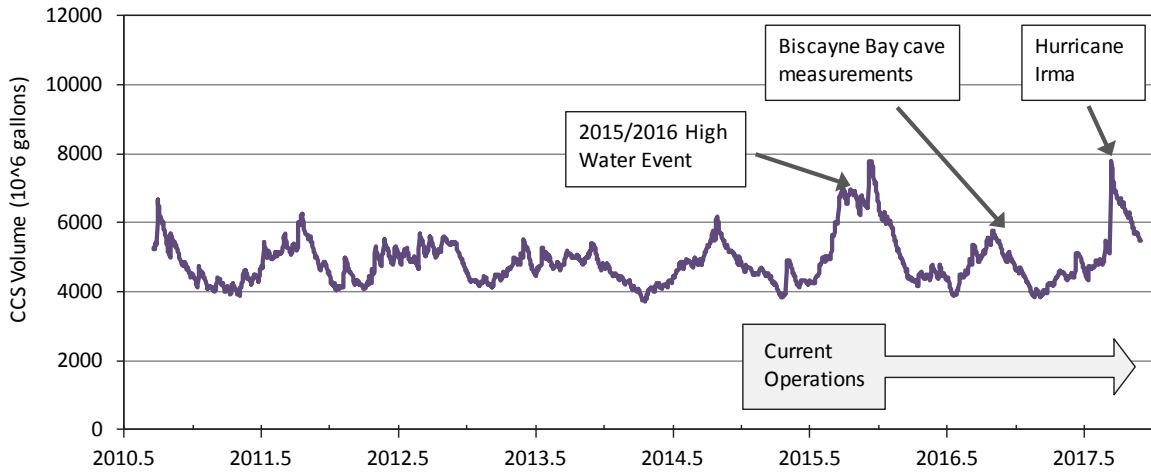


Figure 4: Changes in that direction of the hydraulic gradient between the CCS and Biscayne Bay (top panel) controls groundwater discharge into the bay through a submarine cave. The hydraulic gradient is calculated as the difference between daily average water levels in the CCS (TPSWCCS-5) and Biscayne Bay (TPBBSW-3); positive values indicate the direction of flow from the CCS toward the bay. Salinity (bottom panel) is reduced as high-salinity water from the CCS is diluted by mixing with ambient water in the aquifer as it flows from the CCS into the bay. Salinity of water inside the cave (red) fluctuates as tidal fluctuations drive water flow first into and then out of the aquifer through the cave. Inflowing water has the (lower) salinity of Biscayne Bay surface water, and outflowing water is elevated by mixing with higher-salinity water from the aquifer. Increased outflow from the aquifer, during periods in which the hydraulic gradient is positive, is reflected in higher salinity in the outflowing water in the cave.

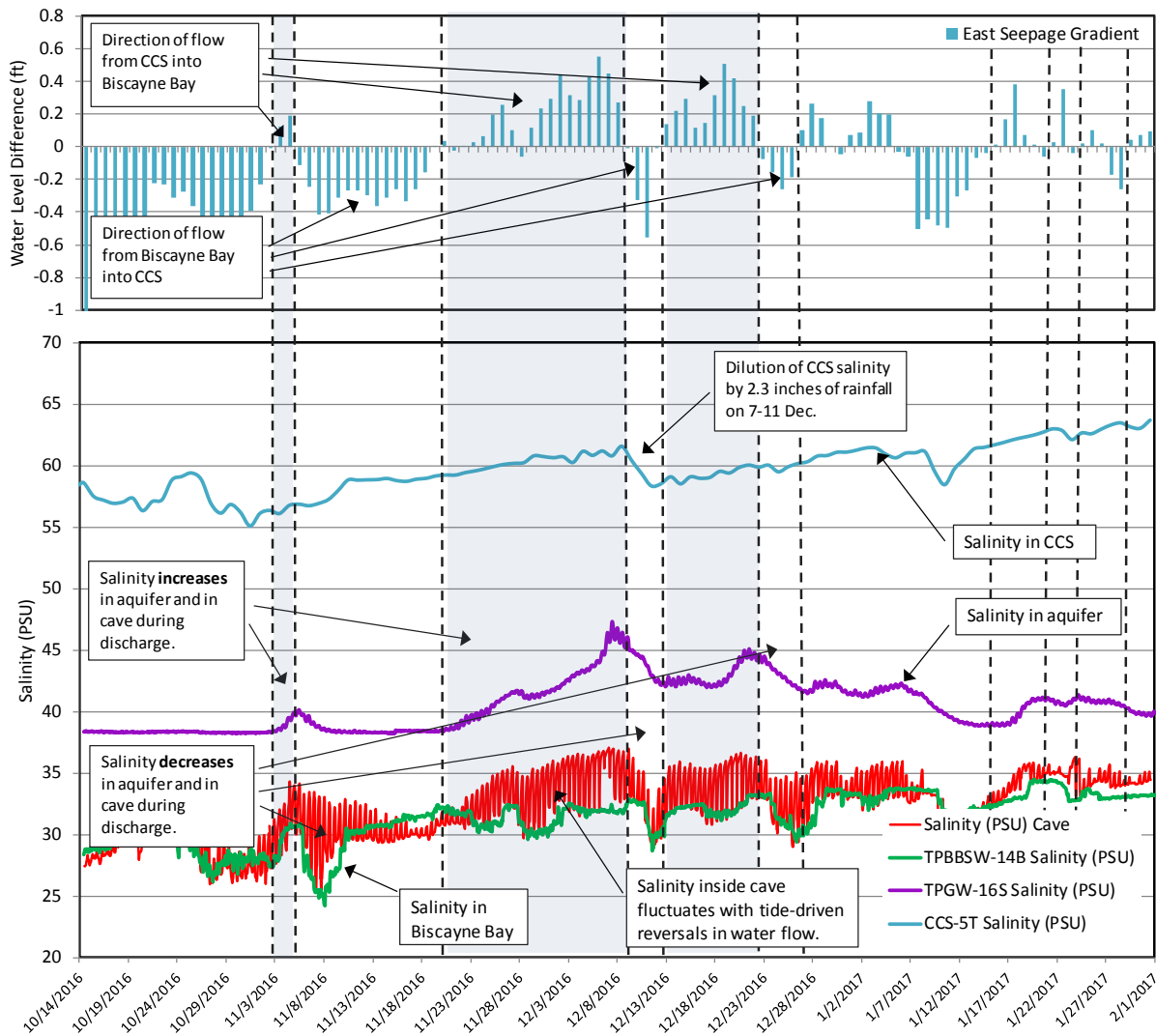
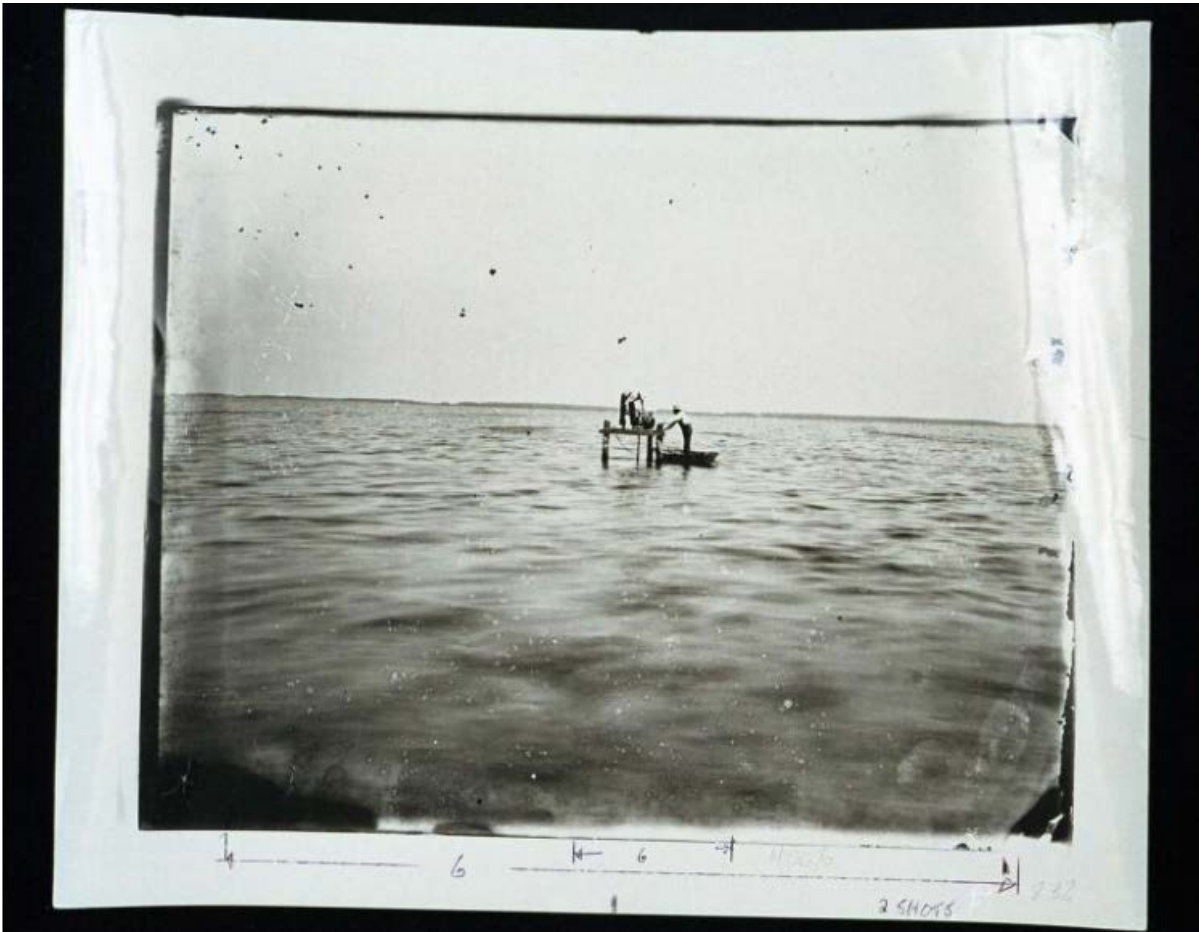
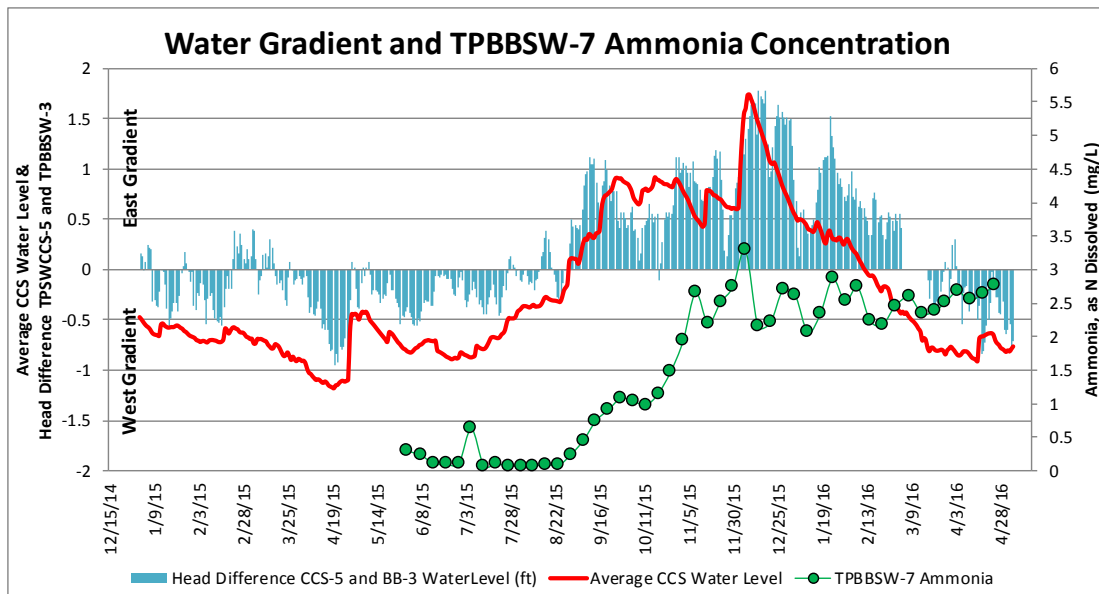


Figure 5: Groundwater discharging through cavities in the limestone Biscayne aquifer fed freshwater springs under Biscayne Bay that were used as a source of freshwater in the late 19th century. (Photo credit: Freshwater springs in Biscayne Bay, ca. 1890, Munroe, Ralph, 1851-1933)⁴²



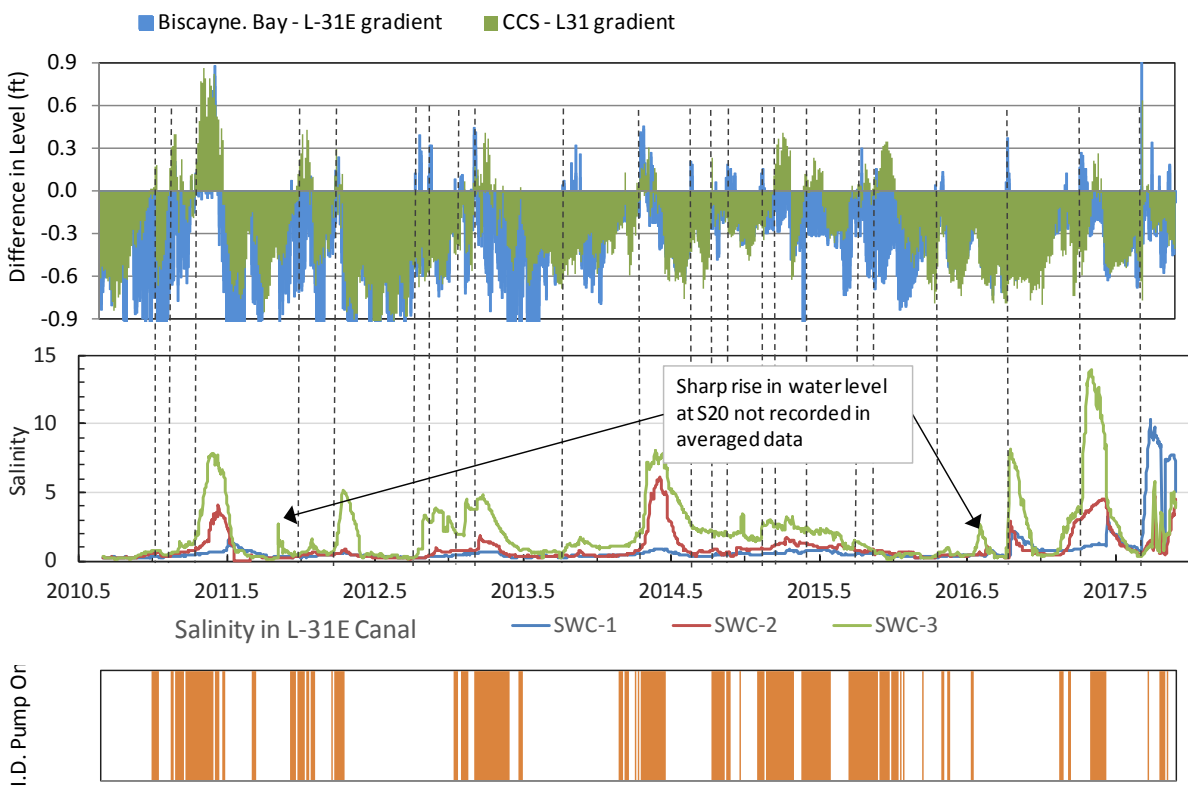
⁴² Online: <http://dpanther.fiu.edu/sobek/RM00010005/00001>; accessed 14 May 2018

Figure 6: The high-water event in 2015/2016 (CCS water level shown in red) corresponded with an extended period of discharge from the CCS into Biscayne Bay through the aquifer. Positive values of the hydraulic gradient, measured as the difference in daily average water levels in the CCS (TPSWCCS-5) and in Biscayne Bay (TPSWBB-3), correspond with flow from the CCS into Biscayne Bay. The rise in ammonia concentrations measured in Biscayne Bay water (at TPBBSW-7) follows the classic pattern of a breakthrough curve for the discharge of a plume of contaminant moving in groundwater.⁴³



⁴³ This figure is taken from a spreadsheet obtained from Miami-Dade DERM. The author of the spreadsheet is indicated as Sara Mechtensimer. A LinkedIn profile for Sara Mechtensimer identifies her as an employee of FPL. [accessed 25 May 2017].

Figure 7: Salinity measured in the L-31E canal (middle panel) rises in response to intermittent groundwater discharge from the CCS and Biscayne Bay. Discharge is inferred from periods in which the hydraulic gradients are favorable for flow from the CCS and Biscayne Bay toward the L-31E canal (upper panel). The hydraulic gradients are calculated as the difference between daily average water levels in the CCS and the canal and between the tailwater and headwater levels at the S20 structure.⁴⁴ Positive values for the hydraulic gradients indicate flow is from the CCS or Biscayne Bay toward the L-31E canal. In the two instances in which a spike in salinity does not correspond to a positive hydraulic gradient, inspection of instantaneous water level data from the S20 structure confirms the short-term occurrence of a positive gradient not captured in the daily average data. Pumping from the Interceptor Ditch (ID; bottom panel) can contribute to the inflow of saline water into the canal by inducing vertical movement of the boundary between fresh and salt water in the aquifer.



⁴⁴ The hydraulic heads are uncorrected for density differences. The difference in density between the saline water in the CCS and the (mostly) freshwater in the L-31E favors flow from the CCS toward the L-31E canal when the water levels are equal. The error introduced by neglecting the effect of density differences in calculating hydraulic head for flow toward the L-31E canal is in failing to identify conditions for flow toward the L-31E when they exist.

Figure 8: Daily values of the components of the CCS water budget measured by FPL's monitoring program: evaporation, rainfall, other inflow.

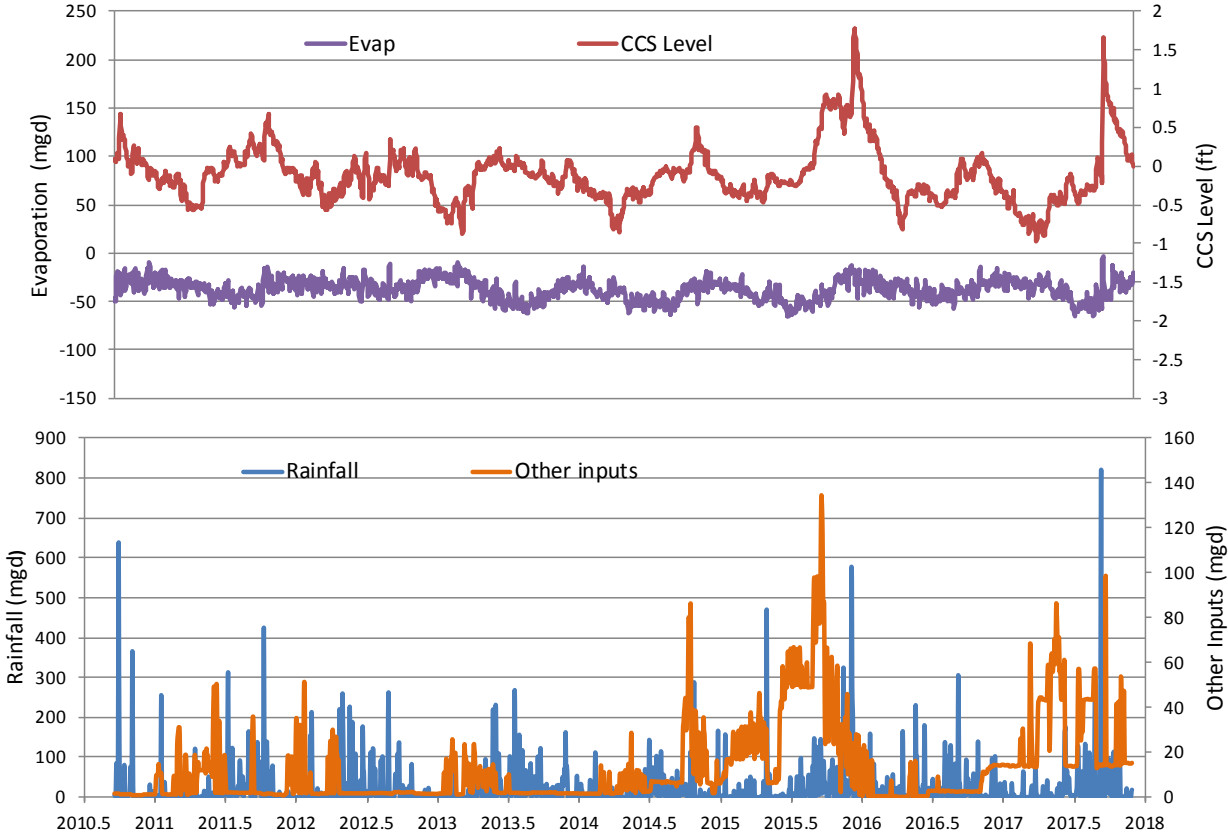


Figure 9: During Hurricane Irma, surface flooding from storm surge (inset) and rainfall during Hurricane Irma storm added about 3 billion gallons to the volume of the CCS. Rainfall accounted for 2 billion gallons of this increase, and flooding by storm surge accounted for the remaining 1 billion gallons.

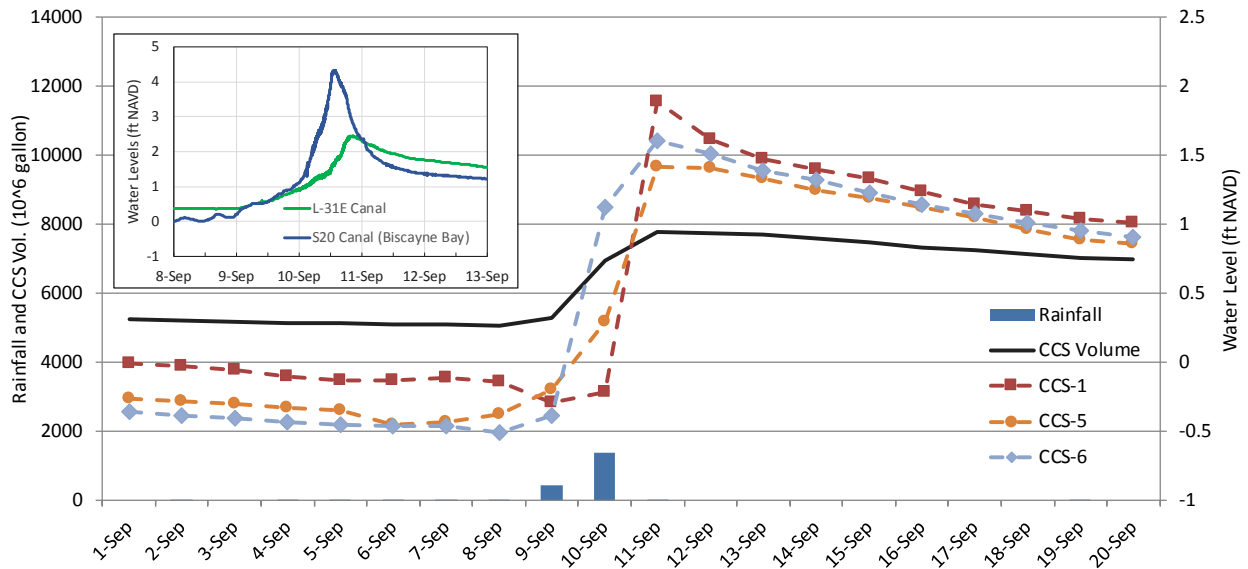


Figure 10: Upper panel: computed daily net groundwater flow into the aquifer (mgd). Positive values of net flow indicate flux into the aquifer. Negative values of net flow indicate flux into the CCS. Middle panel: monthly average groundwater flow (mgd) into the aquifer through the bottom of the CCS, computed by FPL as part of its regular monitoring and reporting on conditions in and around the CCS. Lower panel: daily inflow from “other sources.” Inflow from other sources includes the water pumped out of the ID, inputs from various sources for “freshening activities” and relatively much smaller inputs from plant blowdown. Water inputs for the purpose of freshening first occurred in the last half of 2014, and they occur regularly under “current operations,” defined as beginning in 2015.

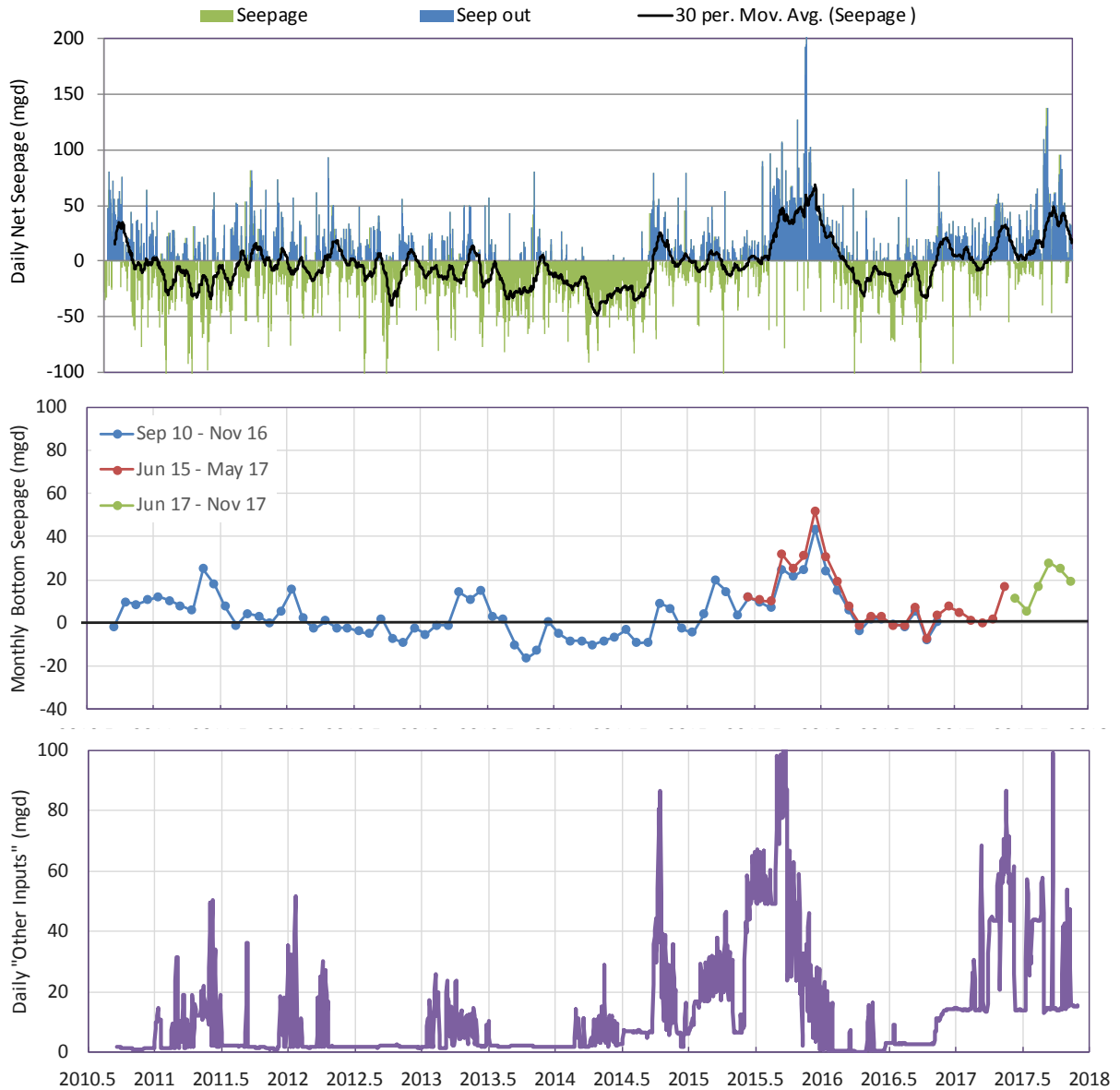


Exhibit B: Curriculum Vitae

William K. Nuttle, Ph.D, P.Eng

11 Craig Street
Ottawa, Ontario
Canada K1S 4B6
wknuttle@gmail.com

Profile

William K. Nuttle has 25 years of experience working with water managers, engineers, Earth scientists and ecologists in planning eco-hydrology research and applying the results of this research to ecosystem restoration and management of natural resources. Prior to joining the University of Maryland he coordinated ecosystem research programs directed at supporting large-scale ecosystem restoration activities and resource management in South Florida and Louisiana. He was director of the Everglades Department for the South Florida Water Management District in 2000-2001, and prior to that he served as Executive Officer for the Florida Bay Science Program. Dr. Nuttle received his M.S. and Ph.D. (1986) degrees in civil engineering from the Massachusetts Institute of Technology and his BSCE from the University of Maryland. He has previously worked as an expert on water and salt budgets for the Turkey Point Power Plant cooling canals for the South Florida Water Management District, and as an expert witness in Florida Division of Administrative Hearing cases.

Education

1986 PhD, Civil Engineering, Massachusetts Institute of Technology, 1986
1982 MS, Civil Engineering, Massachusetts Institute of Technology, 1982
1980 BS, Civil Engineering, University of Maryland, 1980

Career Summary

1986 - Consultant in Environmental Science, Hydrology, and Water Resources
2013 - Science Integrator, Integration and Application Network, Center for
 Environmental Science, University of Maryland
2009 - 2012 Executive Officer, South Florida Marine and Estuarine Goal Setting for
 South Florida (MARES) Project
2000 - 2001 Director, Everglades Department, Division of Watershed Research and
 Planning, South Florida Water Management District
1998 - 2000 Executive Officer, Science Program for Florida Bay and Adjacent Marine
 Systems
1997 Lecturer, Environmental Science Program, Carleton University, Ottawa,
 Ontario
1991 - 1993 Associate, Rawson Academy of Aquatic Science, Ottawa, Ontario
1990 - 1991 Assistant Professor (Research), Memorial University of Newfoundland
1986 - 1989 Assistant Professor, University of Virginia

Scientific Publications (last 10 years)

- 2014 J.S. Ault, S.G. Smith, J.A. Browder, W. Nuttle, E.C. Franklin, J. Luo, G.T. DiNardo, J.A. Bohnsack, Indicators for assessing the ecological dynamics and sustainability of southern Florida's coral reef and coastal fisheries, *Ecological Indicators*, Volume 44, September 2014, Pages 164-172, ISSN 1470-160X, <http://dx.doi.org/10.1016/j.ecolind.2014.04.013>.
(<http://www.sciencedirect.com/science/article/pii/S1470160X14001435>)
- 2014 Pamela J. Fletcher, Christopher R. Kelble, William K. Nuttle, Gregory A. Kiker, Using the integrated ecosystem assessment framework to build consensus and transfer information to managers, *Ecological Indicators*, Volume 44, September 2014, Pages 11-25, ISSN 1470-160X, <http://dx.doi.org/10.1016/j.ecolind.2014.03.024>.
(<http://www.sciencedirect.com/science/article/pii/S1470160X14001265>)
- 2014 Grace Johns, Donna J. Lee, Vernon (Bob) Leeworthy, Joseph Boyer, William Nuttle, Developing economic indices to assess the human dimensions of the South Florida coastal marine ecosystem services, *Ecological Indicators*, Volume 44, September 2014, Pages 69-80, ISSN 1470-160X, <http://dx.doi.org/10.1016/j.ecolind.2014.04.014>.
(<http://www.sciencedirect.com/science/article/pii/S1470160X14001447>)
- 2013 Kelble CR, Loomis DK, Lovelace S, Nuttle WK, Ortner PB, Fletcher P, Cook GS, Lorenz JJ, Boyer JN. The EBM-DPSER Conceptual Model: Integrating Ecosystem Services into the DPSIR Framework. *PLOS One* 8 (8):e70766. doi:10.1371/journal.pone.0070766
- 2010 Lookingbill, T., T.J.B. Carruthers, J.M. Testa, W.K. Nuttle, and G. Shenk. Chapter 9: Environmental Models, in: Longstaff, B.J. and others (eds), *Integrating and Applying Science: A Practical Handbook for Effective Coastal Ecosystem Assessment*. IAN Press, Cambridge, MD.
- 2008 Habib, E., B.F. Larson, W.K. Nuttle, V.H.Rivera-Monroy, B.R. Nelson, E.A. Meselhe, R.R. Twilley. Effect of rainfall spatial variability and sampling on salinity prediction in an estuarine system. *Journal of Hydrology* 350:56-67.

Technical Reports (last 10 years)

- 2015 Nuttle W., America's Watershed Initiative Report Card for the Mississippi River Methods: report on data sources, calculations, additional discussion. [online: <http://americaswater.wpengine.com/wp-content/uploads/2015/12/Mississippi-River-Report-Card-Methods-v10.1.pdf>; accessed 1 May 2017]
- 2015 Nuttle, W.K. Review of CCS Water and Salt Budgets Reported in the 2014 FPL Turkey Point Pre-Uprate Report and Supporting Data. Prepared for the South Florida Water Management District, 8 June 2015.
- 2013 Nuttle, W.K., and P.J. Fletcher (eds.). Integrated conceptual ecosystem model development for the Florida Keys/Dry Tortugas coastal marine ecosystem. NOAA Technical Memorandum, OAR-AOML-101 and NOS-NCCOS-161. Miami, Florida. 92 pp.
- 2013 Nuttle, W.K., and P.J. Fletcher (eds.). Integrated conceptual ecosystem model development for the Southwest Florida Shelf coastal marine ecosystem. NOAA

- Technical Memorandum, OAR-AOML-102 and NOS-NCCOS-162. Miami, Florida. 108 pp.
- 2013 Nuttle, W.K., and P.J. Fletcher (eds.). Integrated conceptual ecosystem model development for the Southeast Florida Coast coastal marine ecosystem. NOAA Technical Memorandum, OAR-AOML-103 and NOS-NCCOS-163. Miami, Florida. 125 pp.
- 2013 Nuttle, W.K. Review of CCS Water and Salt Budgets Reported in the 2012 FPL Turkey Point Pre-Uprate Report and Supporting Data. Prepared for the South Florida Water Management District, 5 April 2013.
- 2012 Day, J. and others. Answering 10 Fundamental Questions About the Mississippi River Delta. Mississippi River Delta Science and Engineering Special Team, National Audubon Society.
- 2010 Marshall, F., and W. Nuttle. Development of Nutrient Load Estimates and Implementation of the Biscayne Bay Nutrient Box Model. Final Report prepared by Cetacean Logic Foundation, Inc. for Florida International University Subcontract No. 205500521-01.
- 2008 Marshall, F., W. Nuttle, and B. Cosby, 2008. Biscayne Bay Freshwater Budget and the Relationship of Inflow to Salinity. Project report submitted to South Florida Water Management District by Environmental Consulting and Technology, Inc., New Smyrna Beach, FL.
- 2008 Nuttle, W.K, F.H. Sklar, A.B. Owens, M. D. Justic, W. Kim, E. Melancon, J. Pahl, D. Reed, K. Rose, M. Schexnayder, G. Steyer, J. Visser and R. Twilley. 2008. Conceptual Ecological Model for River Diversions into Barataria Basin, Louisiana, Chapter 7. In, R.R. Twilley (ed.), Coastal Louisiana Ecosystem Assessment & Restoration (CLEAR) Program: A tool to support coastal restoration. Volume IV. Final Report to Department of Natural Resources, Coastal Restoration Division, Baton Rouge, LA.
- 2008 Habib,E., W.K. Nuttle, V.H. Rivera-Monroy, and N. Nasrollahi. An Uncertainty Analysis framework for the CLEAR Ecosystem Model: Using Subprovince 1 as Test Domain and Skill assessment, Chapter 12. In, R.R. Twilley (ed.), Coastal Louisiana Ecosystem Assessment & Restoration (CLEAR) Program: A tool to support coastal restoration. Volume IV. Final Report to Department of Natural Resources, Coastal Restoration Division, Baton Rouge, LA.

UNITED STATES DISTRICT COURT
SOUTHERN DISTRICT COURT OF FLORIDA
Miami Division

Case No.: 1:16-cv-23017-DPG

SOUTHERN ALLIANCE FOR CLEAN ENERGY
TROPICAL AUDUBON SOCIETY INCORPORATED,
and FRIENDS OF THE EVERGLADES, INC.,

Plaintiffs,

v.

FLORIDA POWER & LIGHT COMPANY,

Defendant.

EXPERT REPORT OF JAMES FOURQUAREAN, Ph.D. (Miami)

I have been retained by the Plaintiffs in this matter to offer expert testimony. Pursuant to Fed. R. Civ. P. 26(a)(2)(B), the following is my written report. I have attached a C.V. with my qualifications and publications as Attachment 1 to the report. A list of all other cases in which, during the previous 4 years, I have testified as an expert at trial or by deposition is attached as Attachment 2. I am being paid an hourly rate of \$175 for my work in this case.

My opinions are based on the data on seagrass distribution, nutrient availability and water quality of both surface water and groundwater available to me as of May 14, 2018. I will continue to search for new data to inform my opinions as set forth below.

OPINIONS

1. The seagrass beds of Biscayne Bay and the rest of south Florida require very low nutrient loading to survive. In essence, seagrasses are killed and replaced by fast-growing, noxious seaweed if nutrient delivery is increased. Nutrient delivery can be increased either by increasing the concentration of nutrients in discharges, OR by increasing the volume of water containing nutrients, even at very low concentrations that would pass drinking water quality standards over a long period of time.

All plants, including seagrasses, require light, water, and mineral nutrients, such as phosphorus and nitrogen, to grow. The required supply of nutrients for any plant population to grow is a function of the plants relative growth rate. Plants that grow quickly require high rates of nutrient supply, while plants that grow more slowly require a lower rate of supply. As a consequence, rapidly-growing plants are found where nutrient supplies are high, and slow-growing plants where nutrient supplies are low. High nutrient supplies are not necessarily bad for slow-growing plants, but at high nutrient supply rates fast growing plants can overgrow and shade out the slow growers.

In general, the size of a plant is a good indicator of its relative growth rate, with smaller plants having higher growth rates. In seagrass beds in Biscayne Bay, the fastest growing plants are the single-celled algae that live either in the water, in the sediments, or attached to hard surfaces, such as seagrass leaves. Filamentous algae that grow on surfaces grow slightly slower, followed by more complex macroalgae, like the fleshy and calcareous seaweeds. Seagrasses grow even slower. Different species of seagrass have different growth rates and nutrient requirements. The narrow-bladed species widgeon grass (*Ruppia maritima*) and shoal weed (*Halodule wrightii*) grow faster than the spaghetti-like manatee grass (*Syringodium filiforme*) which in turn has a faster growth rate, and therefore higher nutrient requirements, than turtle grass (*Thalassia testudinum*). It quite common in south Florida, that nutrient supplies can be so low as to constrain the growth of even the slowest growing species (Fourqurean and Rutten 2003).

Evidence to support the relationship between growth rate and nutrient requirement come from both the distribution of seagrasses around natural nutrient “hot spots” in south Florida (Powell et al 1991) and from fertilization experiments (Armitage et al 2011, Ferdie and Fourqurean 2004). For example, the natural state of eastern Florida Bay is very low nutrient availability. However, on some of the mangrove islands in Florida Bay, there are large colonies of wading birds that hunt for food around the bay (Figure 1). Those birds roost and nest on the islands, and bring food home to feed their young. Both adults and young defecate on the islands, causing natural point sources of nutrient supplies around these small islands. In response to this point source, nutrient availability is very high within a few meters of the islands and decreases with distance away from the mangrove shoreline. In response to this gradient, there are concentric halos of different plants growing on the bottom. Closest to the island where nutrient pollution is greatest, there is only a coating of microalgae covering the sediments. Further away from the island there is a macroalgae zone, followed by a halo of dense widgeon grass, a halo of dense shoal weed, then a zone of mixed shoal grass and dense turtle grass. Farther away still, outside the zone of influence of nutrients from the bird colony, turtle grass declines in density to very sparse coverage.

Fertilization experiments have confirmed that a change in nutrient supply first leads to a change in the density, and then the species composition, of seagrass beds in south Florida (Fourqurean et al 1995). In Florida Bay, fertilizing sparse turtle grass beds with phosphorus first results in an increase in the density of turtle grass; however, once shoal grass becomes established in the

fertilized patches, it rapidly displaces the turtle grass (Figure 2). Less controlled experiments illustrate how the seagrass beds of the Florida Keys changed as the Keys became developed. Early developments relied on cesspools or septic tanks for wastewater “treatment.” Neither provide nutrient removal in the rocky limestone substrate of the Keys. Thus, wastewater and stormwater nutrients emanating from the shoreline development resulted in the growth of lush seagrass beds immediately off shore of Key Largo (Figure 3). This observation could be interpreted as a “good” thing because seagrass growth and coverage expanded. However, data from other observations and experiments temper this optimism.

A model has been developed to illustrate how normally low-nutrient seagrass beds of south Florida will change as nutrient availability changes (Fourqurean and Rutten 2003, Figure 4). The model shows that seagrass beds composed of abundant turtle grass, the slowest-growing species, become lush with increased nutrient conditions. But, as nutrient supply continues to increase, the species composition gradually changes as faster-growing species replace the slower-growing ones. At the highest nutrient levels, seagrasses are replaced by seaweeds and microalgae. Loss of the seagrass community will result in a dramatic change in community structure and function. Animal species dependent on seagrass for food and shelter (e.g., speckled trout, redfish, bonefish and tarpon) are replaced by less desirable species (e.g., jellyfish). The model predicts that the relative abundance of benthic plants at a site is an indicator of the current rate of nutrient supply. Changes in the relative abundance from slow-growing to fast-growing species at any site indicates an increase in nutrient supply.

2. The seagrasses along the coastline of the Cooling Canal System (CCS) existed for thousands of years in a nutrient-limited state, which means any addition of new nutrients changes the balance of these ecosystems. Increased nutrients harm the ecosystem by increasing the rates of primary production by marine plants. Increase in growth rates means that faster-growing, noxious marine plants, like macroalgae (seaweeds) and microscopic algae and photosynthetic bacteria, overgrow and outcompete seagrasses and corals for light, leading to the losses of corals and seagrasses.

The density and species composition of the seagrasses of southern Biscayne Bay are controlled by the availability of phosphorus. The water column in southern Biscayne Bay has very low concentrations of dissolved phosphorus, and the grand mean TN:TP ratios (ie, the ration of moles of nitrogen to the moles of phosphorus) of the water in southern Biscayne Bay average 177.9 (Caccia and Boyer 2005). When TN:TP of oceanic water is above 16 it indicates that the availability of phosphorus limits the growth of plankton (Redfield 1958). Seagrasses are more complex than phytoplankton, so that the critical ratio determining whether N or P limits plant growth for seagrasses is 30 (Fourqurean and Rutten 20013). The N:P of Turtle Grass (*Thalassia testudinum*) collected in the vicinity of Turkey Point was 88.6 in 2013, a clear indication of phosphorus limitation (Dewsbury, 2014). Fertilization experiments (Armitage et al 2011, Ferdie

and Fourqurean 2004) clearly show that phosphorus fertilization of turtle grass with N:P > 80 first leads to an increase in density of turtle grass, then a replacement of turtle grass by faster-growing seagrasses, followed by a loss of seagrasses as P loading continues.

3. Around the world, there are many nutrients that can limit noxious plant growth, but most often, the nutrients that limit this growth are either nitrogen or phosphorus. In south Biscayne Bay, phosphorus is limiting to phytoplankton and macroalgae. This means that addition of phosphorus will upset the ecological balance of seagrass beds as has been exhibited in Northern Biscayne Bay and Florida Bay. Upsetting the balance of populations of aquatic flora and fauna by nutrient addition is a violation of Florida surface water quality standards.

As set forth in F.A.C. 62-302.520(48)(b), Nutrients, “In no case shall nutrient concentrations of a body of water be altered so as to cause an imbalance in natural populations of aquatic flora or fauna.” Although there are numeric nutrient criteria for Biscayne Bay, F.A.C. 62-302.532(h), the narrative criterion still applies. F.A.C. 62-302(48)(a) states, “Man-induced nutrient enrichment (total nitrogen or total phosphorus) shall be considered degradation in relation to the provisions of Rules 62-302.300, 62-302.700, and 62-4.242, F.A.C.” Because Biscayne Bay is Outstanding Florida Waters under 62-302.700, man-induced nutrient enrichment from the FPL CCS is considered degradation, which is prohibited.

4. Current seagrass species composition and abundance data collected by ongoing seagrass monitoring programs show that Turtle Grass biomass offshore from the CCS is unusually dense compared to other areas in southern Biscayne Bay, likely as a consequence of increased P availability in the region.

Seagrass density data collected around Turkey Point in the late 1960's-early 1970's describe a system with very sparse turtle grass interspersed with a few dense patches more than a few hundred meters offshore (Zieman 1972). In addition, long-time fisherman report that the dense Turtle Grass flats they fished further offshore near the Arsenicker Keys in the early 1970's are now devoid of seagrasses, likely because of continued P addition. In my opinion, there is an imbalance in the seagrass meadows of southern Biscayne Bay in the vicinity of the CCS, likely caused by increased P discharged from the CCS. A preliminary review of seagrass abundance (% cover) data collected in Biscayne Bay since the mid 1980's and statements from keen observers responsible for these and other monitoring programs suggest seagrasses in the nearshore vicinity of the CCS and TP facility are denser than elsewhere in Biscayne bay. I will be collecting and analyzing any and all data not available to me at this time to better understand these preliminary statement and observations.

5. The nearshore seagrass beds are incredibly efficient at removing P from the water column and storing P at vanishingly small concentrations. In fact, even 30 feet from large point-sources of P in Florida Bay, it is not possible to measure increases in P concentrations in the water column because it has all been captured by the seagrass communities. This P capture causes increased plant growth and ecosystem imbalances. This imbalance first leads to an actual increase in the abundance of seagrass, but rapidly it causes a change in species composition, first to faster-growing seagrasses, then to seaweeds, then to microscopic algae.
6. Groundwater discharges along the coast of southern Biscayne Bay contain elevated concentrations of phosphorus, so that any process that causes groundwater discharge to the local seagrasses will supply the limiting nutrient that upsets the balance of the ecosystem.

P concentrations in the deeper canals offshore of the CCS and in caves offshore of Turkey Point are 10-20 times higher than the median concentrations (0.03 μM) of inorganic phosphorus in Biscayne Bay waters (Caccia and Boyer 2005).

7. The geology underlying the CCS and the adjacent seagrass meadows is based on limestone, which is made of calcium carbonate minerals. Calcium carbonate minerals strongly absorb orthophosphate onto their surfaces. But, respiration by plants, animals and bacteria dissolve calcium carbonate minerals, releasing the orthophosphate absorbed to the surfaces. During normal conditions, south Florida ecosystems are incredibly efficient at holding on to captured phosphorus— so much so that the impacts caused by adding P to seagrass beds in south Florida for even short periods can still be measured 30 years after the P additions. On the other hand, bacteria cause added N captured by south Florida ecosystems to be rapidly transformed and removed from those ecosystems. Bacterial processes transform oxidized inorganic nitrogen species and organic nitrogen into ammonium. Other bacterial processes lead to the loss of inorganic nitrogen (ammonium, nitrate and nitrites) from the system as nitrous oxide and dinitrogen gas. These facts result in P additions causing permanent and cumulative imbalances in nearshore marine waters of the Keys while N additions cause imbalances that can be corrected by the cessation of N addition.

Inorganic phosphorus strongly sorbs onto limestone minerals, retarding the transport of phosphorus through the limestone aquifer. However, the binding of phosphate to those minerals is a function of both the salinity of the groundwater (Price et al 2010) as well as the oxidation state of that groundwater (Flower et al 2017a). Both large increases and decreases in the salinity can desorb the phosphate, and make it mobile in the groundwater. The seawater of Biscayne Bay and the fresh groundwater of the Biscayne Aquifer are both supersaturated with respect to

limestone minerals, and therefore they will not liberate phosphate immobilized on limestone in the groundwater, but calcite will dissolve, and phosphorus will be released, where these two waters mix (Wigley and Plummer 1976). Hence, mixing of saltwater and freshwater in the aquifer can liberate phosphorus and transport it to the surface. This phenomenon explains the plant biomass and productivity increases along the coast of south Florida where brackish groundwater discharges (Price et al 2006). Further, injection of salty groundwater into freshwater aquifers through saltwater intrusion drives phosphorus release from that bedrock (Flower et al 2017b).

When saline and fresh groundwater mix in south Florida sources mix, they create a brackish water solution that dissolves calcium carbonate minerals, releasing orthophosphate stored on the surfaces of the limestone particles.

When this P-laden water reaches the surface, it will be captured by the ecosystem and cause an imbalance because it will be used by the ecosystem resulting in the growth of noxious plants (algae) which outcompete the seagrasses.

The operations of the CCS create saline water that infiltrates the groundwater and is transported and discharged under the seagrass

It is my opinion that operation of the CCS has 1) carried phosphorus-polluted groundwater to near-shore surface waters through the highly porous bedrock and 2) has dissolved carbonates in that bedrock, releasing additional phosphorus that had been incorporated into that rock. As this phosphorus reaches the seagrass meadows offshore in Biscayne Bay, it will continue to degrade the ecosystem and cause an imbalance and change the nature of the surrounding marine environment.

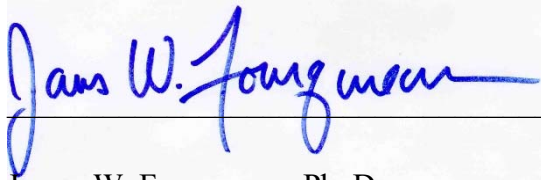
8. An imbalance of the seagrasses that form the near-shore habitat near the CCS in Biscayne Bay and provide the food at the base of the food chain harms the fish and wildlife that use these habitats and therefore effects fishing, recreational activities such as bird watching and other activities based on that habitat change and eventual loss.

Salinity and the abundance and species composition of Biscayne Bay's seagrass beds interact to control the types and numbers of animals that live in the area (Santos et al 2018, Zink et al. 2017). For example, Biscayne Bay's fish populations reflect the salinity regime along the shoreline, with lower salinity sites having fewer fish like bluestriped grunt, schoolmaster snapper and sailors choice, and higher densities of fishes like killifishes, than higher-salinity sites (Serafy

et al 2003). Salinity variability can be as important as mean salinity along this coastline in influencing fish communities (Machemer et al 2014).

I submitted this report on May 14, 2018.

Signed:

A handwritten signature in blue ink that reads "James W. Fourqurean". The signature is written in a cursive style and is positioned above a horizontal line.

James W. Fourqurean, Ph. D.

LITERATURE CITED

Armitage, A. R., T. A. Frankovich, and J. W. Fourqurean. 2011. Long-term effects of adding nutrients to an oligotrophic coastal environment. *Ecosystems* **14**:430-444.

Caccia, V. G., and J. N. Boyer. 2005. Spatial patterning of water quality in Biscayne Bay, Florida as a function of land use and water management. *Marine Pollution Bulletin* **50**:1416-1429.

Dewsbury, B. M. 2014. The ecology and economics of seagrass community structure. P..D Dissertation, Florida International University. 168 pp.

Ferdie, M., and J. W. Fourqurean. 2004. Responses of seagrass communities to fertilization along a gradient of relative availability of nitrogen and phosphorus in a carbonate environment. *Limnology and Oceanography* **49**:2082-2094.

Flower, H., M. Rains, D. Lewis, and J. Z. Zhang. 2017a. Rapid and Intense Phosphate Desorption Kinetics When Saltwater Intrudes into Carbonate Rock. *Estuaries and Coasts* **40**:1301-1313.

Flower, H., M. Rains, D. Lewis, J. Z. Zhang, and R. Price. 2017b. Saltwater intrusion as potential driver of phosphorus release from limestone bedrock in a coastal aquifer. *Estuarine Coastal and Shelf Science* **184**:166-176.

Fourqurean, J. W., and L. M. Rutten. 2003. Competing goals of spatial and temporal resolution: monitoring seagrass communities on a regional scale. Pages 257-288 *in* D. E. Busch and J. C. Trexler, editors. *Monitoring ecosystem initiatives: interdisciplinary approaches for evaluating ecoregional initiatives*. Island Press, Washington, D. C.

Fourqurean, J. W., G. V. N. Powell, W. J. Kenworthy, and J. C. Zieman. 1995. The effects of long-term manipulation of nutrient supply on competition between the seagrasses *Thalassia testudinum* and *Halodule wrightii* in Florida Bay. *Oikos* **72**:349-358.

Kruczynski, W. L. and P. J. Fletcher. *Tropical Connections: South Florida's marine environment*. IAN press, Cabridge Md, 474 pages.

Machemer, E. G. P., J. F. Walter, J. E. Serafy, and D. W. Kerstetter. 2012. Importance of mangrove shorelines for rainbow parrotfish I: habitat suitability modeling in a subtropical bay. *Aquatic Biology* **15**:87-98.

Powell, G. V. N., J. W. Fourqurean, W. J. Kenworthy, and J. C. Zieman. 1991. Bird colonies cause seagrass enrichment in a subtropical estuary: observational and experimental evidence. *Estuarine, Coastal and Shelf Science* **32**:567-579.

Price, R. M., M. R. Savabi, J. L. Jolicoeur, and S. Roy. 2010. Adsorption and desorption of phosphate on limestone in experiments simulating seawater intrusion. *Applied Geochemistry* **25**:1085-1091.

Price, R. M., P. K. Swart, and J. W. Fourqurean. 2006. Coastal groundwater discharge - an additional source of phosphorus for the oligotrophic wetlands of the Everglades. *Hydrobiologia* **569**:23-36.

Redfield, A. C. 1958. The biological control of chemical factors in the environment. *American Scientist* **46**:205-221.

Santos, R. O., D. Lirman, S. J. Pittman, and J. E. Serafy. 2018. Spatial patterns of seagrasses and salinity regimes interact to structure marine faunal assemblages in a subtropical bay. *Marine Ecology Progress Series* **594**:21-38.

Serafy, J. E., C. H. Faunce, and J. J. Lorenz. 2003. Mangrove shoreline fishes of Biscayne Bay, Florida. *Bulletin of Marine Science* **72**:161-180.

Wigley, T.M.L., and Plummer, L. N. 1976, Mixing of carbonate waters: *Geochimica et Cosmochimica Acta*, **40**:989-995.

Zink, I. C., J. A. Browder, D. Lirman, and J. E. Serafy. 2017. Review of salinity effects on abundance, growth, and survival of nearshore life stages of pink shrimp (*Farfantepenaeus duorarum*). *Ecological Indicators* **81**:1-17.

Zieman, J. C. 1972. Origin of circular beds of *Thalassia* (Spermatophyta: hydrocharitaceae) in south Biscayne Bay, Florida, and their relationship to mangrove hammocks. *Bulletin of Marine Science* **22**:559-574.

QUALIFICATIONS

My resume is attached and contains my qualifications and a list of all publications that I have authored.

PRIOR TESTIMONY

During the past 4 years, I have participated in the following cases:
(1 deposition and 1 administrative hearing)

STATE OF FLORIDA
DIVISION OF ADMINISTRATIVE HEARINGS
MIKE LAUDICINA; DON
DEMARIA; CUDJOE GARDENS
PROPERTY OWNERS ASSOC.
INC.; AND SUGARLOAF
SHORES PROPERTY OWNERS
ASSOC., INC.,
Petitioners,
vs.
FLORIDA KEYS AQUADUCT
AUTHORITY AND DEPARTMENT
OF ENVIRONMENTAL
PROTECTION,
Respondents.
Case No. 15-1233

I gave deposition in this case on October 14, 2015 at Veritext Legal Solutions, 2 South Biscayne Blvd., Suite 2250, Miami, FL 33131

STATE OF FLORIDA
DIVISION OF ADMINISTRATIVE
HEARINGS
LAST STAND (PROTECT KEY
WEST AND THE FLORIDA
KEYS, b/d/a LAST STAND, AND
GEORGE HALLORAN,
Petitioners,
vs.
KET WEST RESORT UTILITIES
CORPORATION, AND STATE OF
FLORIDA DEPARTMENT OF
ENVIRONMENTAL PROTECTION,
Respondents
Case No. 14-5302

_____/
The final hearing in this matter was held on April 21-May 1, 2015 at the Freeman Justice Center, Conference Room A, 302 Fleming Street, Key West, Florida, before Cathy M. Sellers, an Administrative Law Judge of the Division of Administrative Hearings (“DOAH”).

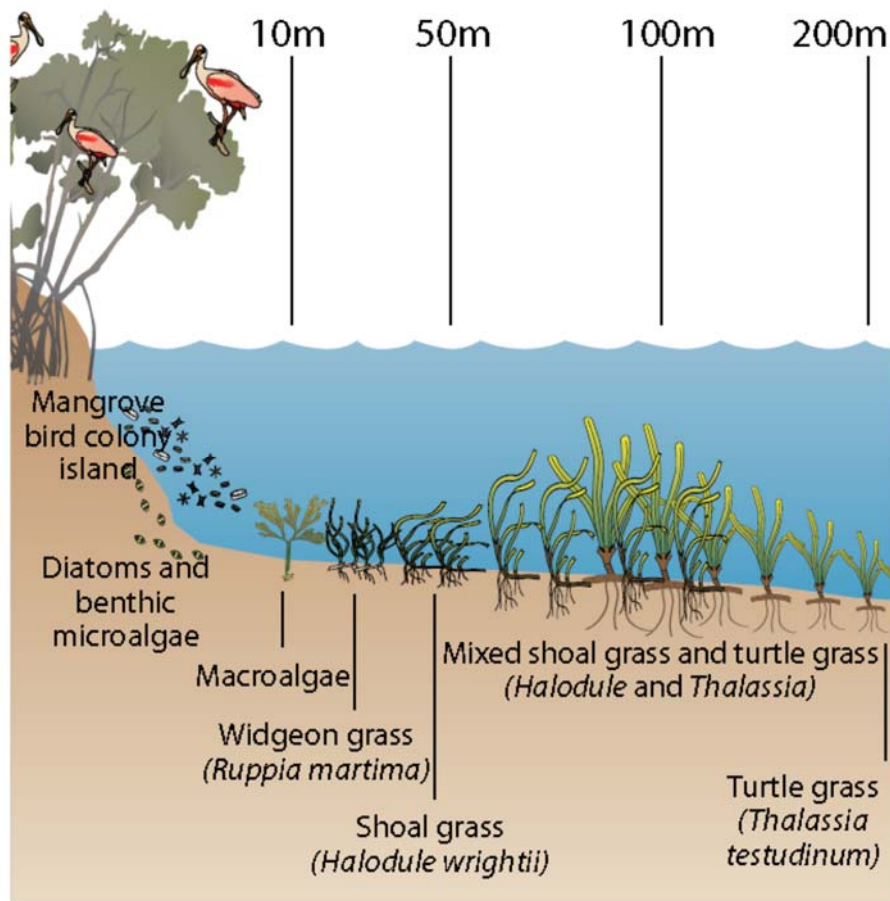


Figure 1. Islands with large bird colonies in Florida Bay are natural nutrient sources that cause zonation of the benthic habitat, with fast-growing microalgae dominant near the nutrient source and slow-growing turtle grass dominant far from the nutrient supply. See Powell et al 1991. Figure reproduced from Kryczynski and Fletcher 2012, page 276.

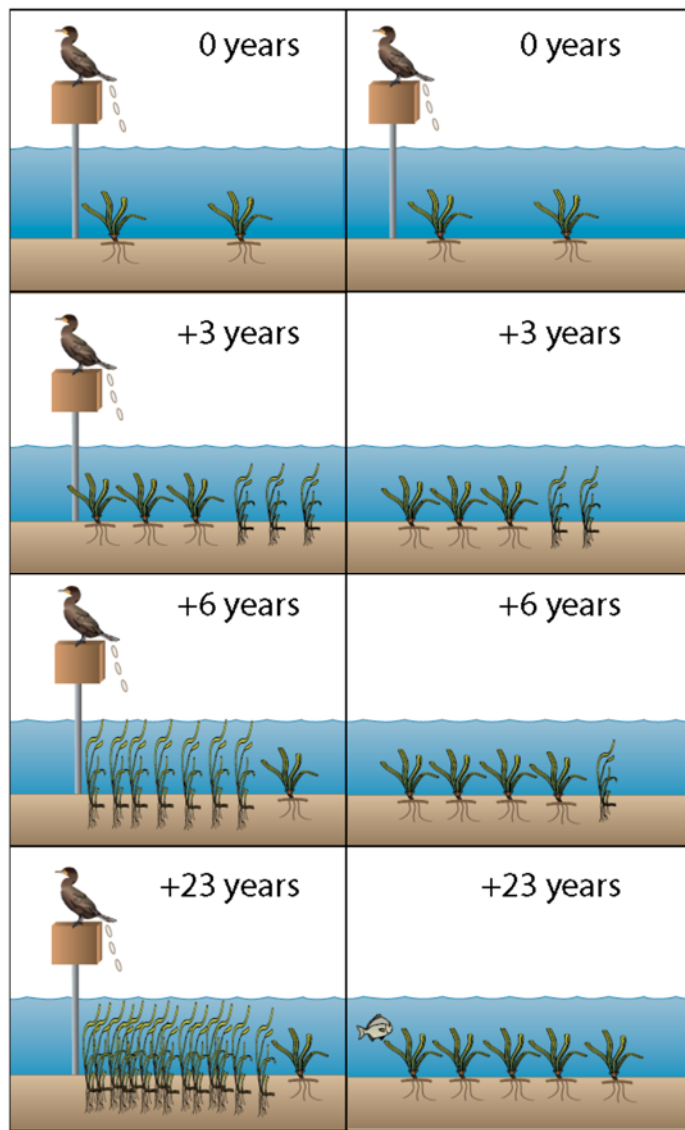


Figure 2. Artificial bird perches have been used to study the effects of nutrient additions to nutrient-limited seagrass beds in south Florida (Fourqurean et al 1995). Fertilization initially leads to more turtle grass, but that turtle grass is replaced by faster-growing shoal weed (left column). Short term fertilization has impacts that last for decades (right column). Figure reproduced from Kryczynski and Fletcher 2012, page 276.

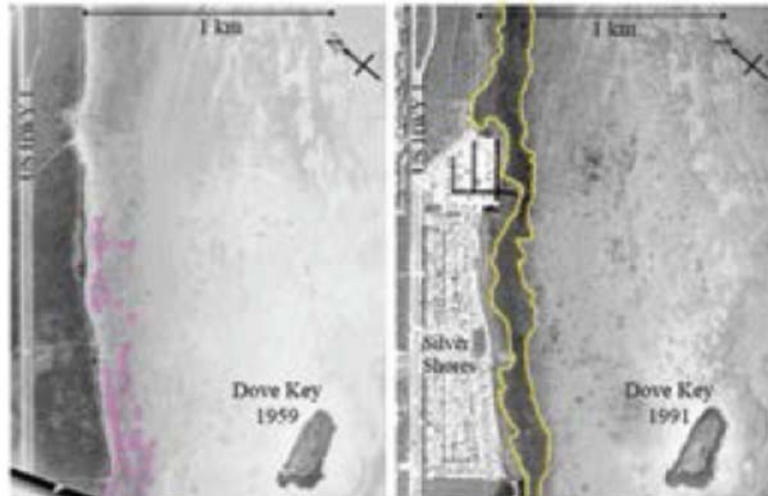


Figure 3. Seagrass distribution along the shoreline of Key Largo near Dove Key in 1959 (left) and 1991 (right). Prior to development, seagrass coverage was sparse along the shoreline. However, by 1991 seagrass coverage and density increased substantially along the shoreline in response to nutrients emanating from development. Figure reproduced from Kryczynski and Fletcher 2012, page 277.

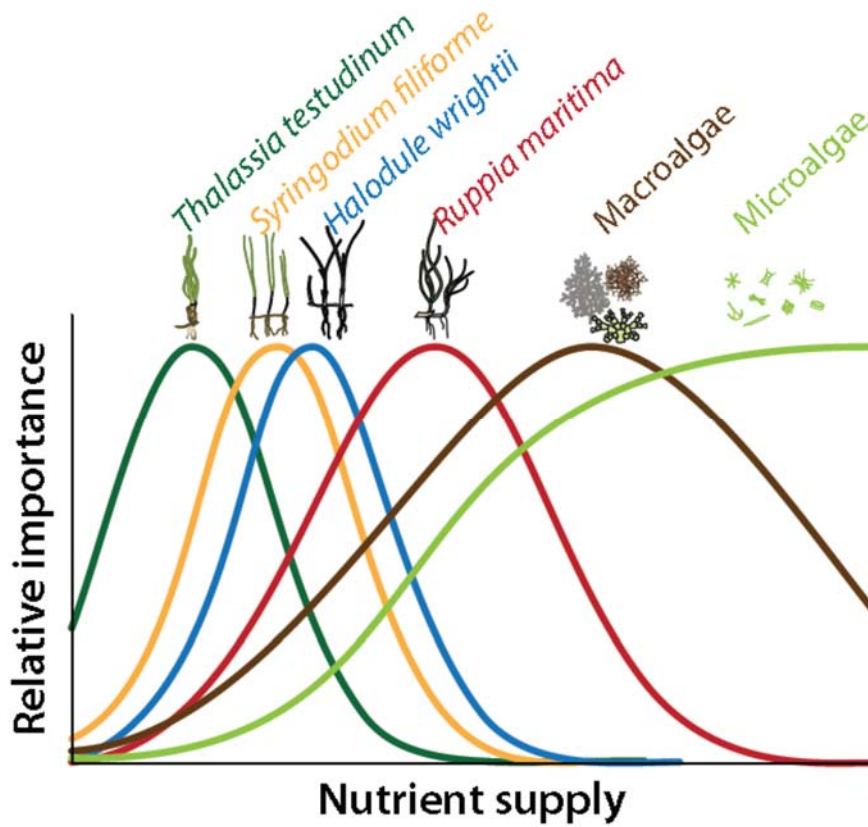


Figure 4. This model describes how the dominant organisms from shallow Biscayne Bay change with addition of nutrients. Nutrient supply can increase either with an increase in concentration OR and increase in volume of nutrient sources. This figure is based on Fourqurean and Rutten (2003) and is reproduced from Kryczynski and Fletcher 2012, page 276.

Curriculum Vitae

James W. Fourqurean, Ph.D.

17641 SW 75th Ave
Palmetto Bay, FL 33157

Profile

James Fourqurean is a marine and estuarine ecologist with a special interest in benthic plant communities and nutrient biogeochemistry. He received his undergraduate and graduate training in the Department of Environmental Sciences at the University of Virginia, where he became familiar with the Chesapeake Bay and its benthic communities. He developed a love of tropical ecosystems while doing his dissertation research in Florida Bay. After a post doc at San Francisco State studying planktonic processes in Tomales Bay, California, he was recruited to return to south Florida to join a new research group at the newest research university in the country, Florida International University. He has at FIU since 1993, where he is now Professor of Biological Sciences and the Director of the Center for Coastal Oceans Research in the Institute for Water and Environment. For the past three decades, his main research areas have been in the seagrass environments of south Florida, but he has also worked in coastal environments around the Gulf of Mexico, in Australia, Indonesia, Mexico, Panama, Bahamas, Bermuda, the United Arab Emirate and the western Mediterranean. He is the lead scientist and overall manager of FIU's Aquarius Reef Base, the world's only saturation diving habitat and laboratory for research, education and outreach. He has served as the Principal Investigator of over \$25M in grants and contracts at FIU, and published 127 papers in the refereed scientific literature and 13 book chapters. Seven graduate students have received PhD degrees working under his direction, along with 15 MS students. His global leadership in coastal oceans research was recently recognized when he was elected President of the Coastal and Estuarine Research Federation, the world's leading body of scientists who study coastal issues.

Education

Ph.D. 1992 University of Virginia, Department of Environmental Sciences
M.S. 1987 University of Virginia, Department of Environmental Sciences
B.A. 1983 University of Virginia, Depts of Biology and Environmental Sciences

Career Summary

2006- Professor, Department of Biological Sciences, Florida International University
2017 - President-elect, Coastal and Estuarine Research Federation
2014 - Adjunct Professor, School of Plant Biology, University of Western Australia
2014 Visiting Research Fellow, Oceans Institute, University of Western Australia
2012- Director, Center for Coastal Oceans Research, Institute of Water and Environment, Florida International University

- 2012- Director, Center for Coastal Oceans Research, Institute of Water and Environment, Florida International University
- 2012- Visiting Research Fellow, Oceans Institute, University of Western Australia
- 2002 - 2006 Chair, Department of Biological Sciences, Florida International University
- 2001 - 2002 Visiting Professor, Institut Mediterrani d'Estudis Avançats, CSIC-Universitat des Illes Balears, Esporles, Mallorca, Spain
- 1998 - 2006 Associate Professor
- 1993 - 1998 Assistant Professor, Department of Biological Sciences and Southeast Environmental Research Center, Florida International University
- 1992 Postdoctoral research associate, San Francisco State University
- 1983 - 1992 Graduate research assistant, University of Virginia. J.C. Zieman, advisor.
- 1983 - 1987 Research biologist, National Audubon Society

Scientific Publications

Scientific Journals

- 127. Bonthond, G., D.G. Merselis, K.E. Dougan, T. Graff, W. Todd, J.W. Fourqurean and M. Rodriguez-Lanetty. 2018. Inter-domain microbial diversity within the coral holobiont *Siderastrea siderea* from two depth habitats. Peer J 6:e4323.
- 126. Arias-Ortiz, A., O. Serrano, P.S. Lavery, G.A. Kendrick, P. Masqué, U. Mueller, A. Esteban, M. Rozaimi, J. W. Fourqurean, N. Marbà, M.A. Mateo, K. Murray, M. Rule, C.M. Duarte. 2018. A marine heat wave drives massive losses from the world's largest seagrass carbon stocks. Nature Climate Change DOI:# 10.1038/s41558-018-0096-y
- 125. Burgett, C.M., D.A. Burkholder, K.A. Coates, V.L. Fourqurean, W. J. Kenworthy, S.A. Manuel, M.E. Outerbridge and J.W. Fourqurean. 2018. Ontogenetic diet shifts of green sea turtles (*Chelonia mydas*) in a mid-ocean developmental habitat. Marine Biology 165:33.
- 124. Campbell, J.E. and J.W. Fourqurean. In Press. Does nutrient availability regulate seagrass response to elevated CO₂? Ecosystems.
- 123. Lovelock, C.E., J.W. Fourqurean and J.T. Morris. 2017. Modelled CO₂ emissions from coastal wetland transitions to other land uses: mangrove forests, tidal marshes and seagrass ecosystems. Frontiers in Marine Science 4:123
- 122. Howard, J.L., J.C. Creed, M.V.P. Aguiar and J.W. Fourqurean. 2018. CO₂ released by carbonate sediment production in some coastal areas may offset the benefits of seagrass "blue carbon" storage. Limnology and Oceanography 63(1):160-172.
- 121. Sweatman, J., C.A. Layman and J.W. Fourqurean. 2017. Habitat fragmentation has some impacts on aspects of ecosystem functioning in a sub-tropical seagrass bed. Marine Environmental Research 126:95-108.
- 120. Nowicki, R.J., J.A. Thomson, D.A. Burkholder, J.W. Fourqurean and M.R. Heithaus. 2017. Predicting seagrass recovery trajectories and their implications following an extreme climate event. Marine Ecology-Progress Series. 567:70-93.

119. Schile, L.M., J.B. Kauffman, S. Crooks, J.W. Fourqurean, J. Glavin and J.P. Megonigal. 2017. Limits on carbon sequestration in arid blue carbon ecosystems. *Ecological Applications* 27(3):859-874.
118. Frankovich, T.A., D. T. Rudnick and J.W. Fourqurean. 2017. Light attenuation in estuarine mangrove lakes. *Estuarine, Coastal and Shelf Science*. 184:191-201.
117. McDonald, A.M., P. Prado, K.L. Heck, Jr, J.W. Fourqurean, T.A. Frankovich, K.H. Dunton and J. Cebrian. 2016. Seagrass growth, reproductive, and morphological plasticity across environmental gradients over a large spatial scale. *Aquatic Botany* 134:87-96.
116. Bessey, C., M.R. Heithaus, J.W. Fourqurean, K.R. Gastrich, and D.A. Burkholder. 2016. The importance of teleost grazers on seagrass composition in a subtropical ecosystem with abundant populations of megagrazers and predators. *Marine Ecology – Progress Series* 553:81-92.
115. Howard, J.L., A. Perez, C.C. Lopes** and J.W. Fourqurean. 2016. Fertilization changes seagrass community structure but not blue carbon storage: results from a 30-year field experiment. *Estuaries and Coasts* 39:1422-1434.
114. Dewsbury, B.M., M. Bhat and J.W. Fourqurean. 2016. A review of economic valuations of seagrass ecosystems. *Ecosystem Services* 18:68-77.
113. Armitage, A.R and J.W. Fourqurean. 2016. Carbon storage in seagrass soils: long-term nutrient history exceeds the effects of near-term nutrient enrichment. *Biogeosciences* 13:313-321.
112. Catano, L., M. Rojas, R. Malossi, J. Peters, M. Heithaus, J.W. Fourqurean, D. Burkepile. 2016. Reefscapes of fear: predation risk and reef heterogeneity interact to shape herbivore foraging behavior. *Journal of Animal Ecology* 85:146-156.
111. Alongi, D.M., D. Murdiyarto, J.W. Fourqurean, J.B. Kauffman, A. Hutahaean, S. Crooks, C.E. Lovelock, J. Howard, D. Herr, M. Fortes, E. Pidgeon, and T. Wagey. 2016. Indonesia's blue carbon: A globally significant and vulnerable sink for seagrass and mangrove carbon. *Wetlands Ecology and Management* 24:3-13.
110. Bourque, A.S., J.W. Fourqurean and W.J. Kenworthy. 2015. The impacts of physical disturbance on ecosystem structure in subtropical seagrass meadows. *Marine Ecology Progress Series* 540:27-41.
109. Atwood, T.B., R.M. Connolly, E.G. Ritchie, C.E. Lovelock, M.R. Heithaus, G.C. Hays, J.W. Fourqurean and P.I. Macreadie. 2015. Predators help protect carbon stocks in blue carbon ecosystems. *Nature Climate Change* 5:1038-1045
108. Fourqurean, J.W., S.A. Manuel, K.A. Coates, W.J. Kenworthy and J.N. Boyer. 2015. Water quality, isoscapes and stoichioscapes of seagrasses indicate general P limitation and unique N cycling in shallow water benthos of Bermuda. *Biogeosciences* 12:6235-6249

107. Gaiser, E.E., E.P. Anderson, E. Castañeda-Moya, L. Collado-Vides, J.W. Fourqurean, M.R. Heithaus, R. Jaffé, D. Lagomasino, N.J. Oehm, R.M. Price, V.H. Rivera-Monroy, R. Roy Chowdhury, T.G. Troxler. 2015. New perspectives on an iconic landscape from comparative international long-term ecological research. *Ecosphere* 6(10):181.
106. Mazarrasa, I., N. Marbà, C.E. Lovelock, O. Serrano, P. Lavery, J.W. Fourqurean, H. Kennedy, M.A. Mateo, D. Krause-Jensen, A.D.L. Steven and C.M. Duarte. 2015. Seagrass meadows as globally significant carbonate reservoir. *Biogeosciences* 12:4993-5003.
105. Dewsbury, B.M., S. Koptur and J.W. Fourqurean. 2015. Ecosystem responses to prescribed fire along a chronosequence in a subtropical pine rockland habitat. *Caribbean Naturalist* 24:1-12.
104. Bourque, A.S., R. Vega-Thurber and J.W. Fourqurean. 2015. Microbial community structure and dynamics in restored subtropical seagrass soils. *Aquatic Microbial Ecology* 74:43-57.
103. Campbell, J.E., E.A. Lacey, R.A. Decker, S. Crooks and J.W. Fourqurean. 2015. Carbon storage in seagrass beds of the Arabian Gulf. *Estuaries and Coasts* 38:242–251.
102. Thomson, J.A., D.A. Burkholder, M.R. Heithaus, J.W. Fourqurean, M.W. Fraser, J. Statton and G.A. Kendrick. 2015. Extreme temperatures, foundation species and abrupt shifts in ecosystems. *Global Change Biology* 21:1463-1474.
101. Lacey, E.A., L. Collado-Vides and J.W. Fourqurean. 2014. Morphological and physiological responses of seagrasses to grazers and their role as patch abandonment cues. *Revista de Biología Tropical* 62(4):1535-1548.
100. Bourque, A.S. and J.W. Fourqurean. 2014. Effects of common seagrass restoration methods on ecosystem structure in subtropical seagrass meadows. *Marine Environmental Research* 97:67-78.
99. Heithaus, M.R., T. Alcovero, R. Arthur, D.A. Burkholder, K.A. Coates, M.J.A. Christianen, N. Kelkar, S.A. Manuel, A.J. Wirsing, W.J. Kenworthy and J.W. Fourqurean. 2014. Seagrasses in the age of sea turtle conservation and shark overfishing. *Frontiers in Marine Science* 1:28.
98. Campbell, J.E. and J.W. Fourqurean. 2014. Ocean acidification outweighs nutrient effects in structuring seagrass epiphyte communities. *Journal of Ecology* 102(3):730-737.
97. Troxler, T.G., E. Gaiser, J. Barr, J.D. Fuentes, R. Jaffe, D.L. Childers, L. Collado-Vides, V.H. Rivera-Monroy, E. Castaneda-Moya, W. Anderson, R. Chambers, M.L. Chen, C. Coronado-Molina, S.E. Davis, V. Engel, C. Fitz, J. Fourqurean, T. Frankovich, J. Kominoski, C. Madden, S.L. Malone, S.F. Oberbauer, P. Olivas, J. Richards, C. Saunders, J. Schedlbauer, L.J. Scinto, F. Sklar, T. Smith, J.M. Smoak, G. Starr, R.R. Twilley, and K. Whelan. 2013. Integrated carbon budget

- models for the Everglades terrestrial-oceanic gradient: Current Status and Needs for Inter-Site Comparisons. *Oceanography* 26:98-107.
96. Manuel, S.M., K.A. Coates, W.J. Kenworthy and J.W. Fourqurean. 2013. Tropical species at the northern limit of their range: composition and distribution in Bermuda's benthic habitats in relation to depth and light availability. *Marine Environmental Research* 89:63-75.
95. Bourque, A.S., and J.W. Fourqurean. 2013. Variability in herbivory in subtropical seagrass ecosystems and implications for seagrass transplanting. *Journal of Experimental Marine Biology and Ecology* 445:29-37.
94. Burkholder, D.A., M.R. Heithaus, J.W. Fourqurean, A. Wirsing and L.M. Dill. 2013. Patterns of top-down control of a seagrass ecosystem: could a roving top predator induce a behavior-mediated trophic cascade? *Journal of Animal Ecology* 82(6): 1192–1202.
93. Campbell, J.E. and J.W. Fourqurean. 2013. Effects of in situ CO₂ enrichment on the structural and chemical characteristics of the seagrass *Thalassia testudinum*. *Marine Biology* 160(6):1465-1475.
92. Campbell, J.E. and J.W. Fourqurean. 2013. Mechanisms of bicarbonate use influence photosynthetic CO₂ sensitivity of tropical seagrasses. *Limnology and Oceanography* 58(3): 839-848.
91. Lacey, E.A., J.W. Fourqurean and L. Collado-Vides. 2013. Increased algal dominance despite presence of *Diadema antillarum* populations on a Caribbean coral reef. *Bulletin of Marine Science* 89(2):603-620.
90. Burkholder, D.A., J.W. Fourqurean and M.R. Heithaus. 2013. Spatial pattern in stoichiometry indicates both N-limited and P-limited regions of an iconic P-limited subtropical bay. *Marine Ecology – Progress Series* 472:101-115.
89. Baggett, L.P., K.L. Heck, Jr., T.A. Frankovich, A.R. Armitage and J.W. Fourqurean. 2013. Stoichiometry, growth, and fecundity responses to nutrient enrichment by invertebrate grazers in sub-tropical turtlegrass (*Thalassia testudinum*) meadows. *Marine Biology* 160:169-180.
88. Fourqurean, J.W., G.A. Kendrick, L.S. Collins, R.M. Chambers and M.A. Vanderklift. 2012. Carbon and nutrient storage in subtropical seagrass meadows: examples from Florida Bay and Shark Bay. *Marine and Freshwater Research* 63:967-983.
87. [Kendrick](#) G.A., J.W. Fourqurean, M.W. Fraser, M.R. Heithaus, G. Jackson, K. Friedman and D. Hallac. 2012. Science behind management of Shark Bay and Florida Bay, two P-limited subtropical systems with different climatology and human pressures. *Marine and Freshwater Research* 63:941-951.
86. Fraser, M.W., G.A. Kendrick, P.F. Grierson, J.W. Fourqurean, M.A. Vanderklift and D.I. Walker. 2012. Nutrient status of seagrasses cannot be inferred from system-scale distribution of phosphorus in Shark Bay, Western Australia. *Marine and Freshwater Research* 63:1015-1026.

85. Frankovich, T.A., J. Barr, D. Morrison and J.W. Fourqurean. 2012. Differential importance of water quality parameters and temporal patterns of submerged aquatic vegetation (SAV) cover in adjacent sub-estuaries distinguished by alternate regimes of phytoplankton and SAV dominance. *Marine and Freshwater Research* 63:1005-1014.
84. Burkholder, D.A., M.R. Heithaus, and J.W. Fourqurean. 2012. Feeding preferences of herbivores in a relatively pristine subtropical seagrass ecosystem. *Marine and Freshwater Research* 63:1051-1058.
83. Price, R.M., G. Skrzypek, P.F. Grierson, P.K. Swart, and J.W. Fourqurean. 2012. The use of stable isotopes of oxygen and hydrogen in identifying water exchange of in two hypersaline estuaries with different hydrologic regimes. *Marine and Freshwater Research* 63:952-966.
82. Cawley, K.M., Y. Ding*, J.W. Fourqurean and R. Jaffé. 2012. Characterizing the sources and fate of dissolved organic matter in Shark Bay, Australia: A preliminary study using optical properties and stable carbon isotopes. *Marine and Freshwater Research* 63:1098-1107.
81. Belicka, L.L., D. Burkholder, J.W. Fourqurean, M.R. Heithaus, S.A. Macko and R. Jaffé. 2012. Stable isotope and fatty acid biomarkers of seagrass, epiphytic, and algal organic matter to consumers in a nearly pristine seagrass ecosystem. Australia. *Marine and Freshwater Research* 63:1085-1097
80. Pendleton, L., D.C. Donato, B.C. Murray, S. Crooks, W.A. Jenkins, S. Sifleet, C. Craft, J. W. Fourqurean, B. Kauffman, N. Marbà, P. Megonigal, E. Pidgeon, V. Bilbao-Bastidam, R. Ullman, and D. Gordon. 2012. Estimating global "blue carbon" emissions from conversion and degradation of vegetated coastal ecosystems. *PLoS ONE* 7(9):e43542.
79. Fourqurean, J.W., Duarte, C.M., Kennedy, H., Marbà, N., Holmer, M., Mateo, M.A., Apostolaki, E.T., Kendrick, G.A., Krause-Jensen, D., McGlathery, K.J., and O. Serrano. 2012. Seagrass ecosystems as a globally significant carbon stock. *Nature Geoscience* 5:505–509.
78. Campbell, J.E., L.A. Yarbro and J.W. Fourqurean. 2012. Negative relationships between the nutrient and carbohydrate content of the seagrass *Thalassia testudinum*. *Aquatic Botany* 99:56-60.
77. Hitchcock, G.L., J.W. Fourqurean, J. Drake, R.N. Mead and C.A. Heil. 2012. Brevetoxin persistence in sediments and seagrass epiphytes of east Florida coastal waters. *Harmful Algae* 13:89-94
76. Burkholder, D.A., M.R. Heithaus, J.A. Thomson and J.W. Fourqurean. 2011. Diversity in trophic interactions of green sea turtles (*Chelonia mydas*) on a relatively pristine coastal seagrass foraging ground. *Marine Ecology Progress Series* 439: 277–293.

75. Armitage, A.R., T.A. Frankovich and J.W. Fourqurean. 2011. Long term effects of adding nutrients to an oligotrophic coastal environment. *Ecosystems* 14:430–444.
74. Herbert, D.A., W.B. Perry, B.J. Cosby and J.W. Fourqurean. 2011. Projected reorganization of Florida Bay seagrass communities in response to increased freshwater delivery from the Everglades. *Estuaries and Coasts* 34:973-992.
73. Frankovich, T.A., D. Morrison and J.W. Fourqurean. 2011. Benthic macrophyte distribution and abundance in estuarine mangrove lakes: Relationships to environmental variables. *Estuaries and Coasts* 34(1):20-31.
72. Campbell, J.E. and J.W. Fourqurean. 2011. Novel methodology for in situ carbon dioxide enrichment of benthic ecosystems. *Limnology and Oceanography Methods* 9:97–109.
71. Duarte, C.M., N. Marbà, E. Gacia, J.W. Fourqurean, J. Beggins, C. Barrón, E.T. Apostolaki. 2010. Seagrass community metabolism: assessing the carbon sink capacity of seagrass meadows. *Global Biogeochemical Cycles* 24: GB4032.
70. Kennedy, H., J. Beggins, C. M. Duarte, J.W. Fourqurean, M. Holmer, N. Marbà, and J. J. Middelburg. 2010. Seagrass sediments as a global carbon sink: isotopic constraints. *Global Biogeochemical Cycles* 24: GB4026.
69. Fourqurean, J.W., S. Manuel, K.A. Coates, W.J. Kenworthy and S.R. Smith. 2010. Effects of excluding sea turtle herbivores from a seagrass bed: overgrazing may have led to loss of seagrass meadows in Bermuda. *Marine Ecology Progress Series* 419:223-232.
68. Fourqurean, J.W., M.F. Muth and J.N. Boyer. 2010. Epiphyte loads on seagrasses and microphytobenthos abundance are not reliable indicators of nutrient availability in coastal ecosystems. *Marine Pollution Bulletin* 60:971-983.
67. Dewsbury, B.M. and J.W. Fourqurean. 2010. Artificial reefs concentrate nutrients and alter benthic community structure in an oligotrophic, subtropical estuary. *Bulletin of Marine Science* 86(4): 813-828.
66. Baggett, L.P., K.L. Heck, Jr., T.A. Frankovich, A.R. Armitage and J.W. Fourqurean. 2010. Nutrient enrichment, grazer identity and their effects on epiphytic algal assemblages: field experiments in sub-tropical turtlegrass (*Thalassia testudinum*) meadows. *Marine Ecology - Progress Series* 406:33-45.
65. Fourqurean, J.W., T.J Smith III, J. Possley, T. M. Collins, D. Lee and S. Namoff. 2010. Are mangroves in the tropical Atlantic ripe for invasion? Exotic mangrove trees in the forests of south Florida. *Biological Invasions* 12:2509-2522.
64. Armitage, A.R. and J.W. Fourqurean. 2009. Stable isotopes reveal complex changes in trophic relationships following nutrient addition in a coastal marine ecosystem. *Estuaries and Coasts* 32:1152–1164.
63. Waycott, M., C.M. Duarte, T.J.B. Carruthers, R.J. Orth, W.C. Dennison, S. Olyarnik, A. Calladine, J.W. Fourqurean, K.L. Heck, Jr., A.R. Hughes, G. Kendrick, W.J.

- Kenworthy, F.T. Short and S.L. Williams. 2009. Accelerating loss of seagrasses across the globe threatens coastal ecosystems. *Proceedings of the National Academies of Science USA* 106(3):12377-12381.
62. Campbell, J.E. and J.W. Fourqurean. 2009. Interspecific variation in the elemental and stable isotopic content of seagrasses in South Florida. *Marine Ecology - Progress Series* 387:109-123.
61. Frankovich, T.A., A.R. Armitage, A.H. Wachnicka, E.E. Gaiser and J.W. Fourqurean. 2009. Nutrient effects on seagrass epiphyte community structure in Florida Bay. *Journal of Phycology* 45:1010-1020.
60. Madden, C.J., D.T. Rudnick, A.A. McDonald, K.M. Cunniff, J.W. Fourqurean. 2009. Ecological indicators for assessing and communicating seagrass status and trends in Florida Bay. *Ecological Indicators* 9S:S68-S82.
59. Herbert, D.A. and J.W. Fourqurean. 2009. Phosphorus availability and salinity control productivity and demography of the seagrass *Thalassia testudinum* in Florida Bay. *Estuaries and Coasts* 32(1):188-201.
58. Fourqurean, J.W., C.M. Duarte, M.D. Kershaw and S.T. Threlkeld. 2008. *Estuaries and Coasts* as an outlet for research in coastal ecosystems: a bibliometric study. *Estuaries and Coasts* 31(3):469-476. (*Invited editorial*)
57. Herbert, D.A. and J.W. Fourqurean. 2008. Ecosystem structure and function still altered two decades after short-term fertilization of a seagrass meadow. *Ecosystems* 11: 688–700.
56. Ruiz-Halpern, S., S.A. Macko and J.W. Fourqurean. 2008. The effects of manipulation of sedimentary iron and organic matter on sediment biogeochemistry and seagrasses in a subtropical carbonate environment. *Biogeochemistry* 87:113-126.
55. Fourqurean, J.W., N. Marbà, C.M. Duarte, E. Diaz-Almela, and S. Ruiz-Halpern*, 2007. Spatial and temporal variation in the elemental and stable isotopic content of the seagrasses *Posidonia oceanica* and *Cymodocea nodosa* from the Illes Balears, Spain. *Marine Biology* 151:219-232.
54. Heithaus, M.R., A. Frid, A.J. Wirsing, L.M. Dill, J.W. Fourqurean, D. Burkholder, J. Thomson and L. Bejder. 2007. State-dependent risk-taking by green sea turtles mediates top-down effects of tiger shark intimidation in a marine ecosystem. *Journal of Animal Ecology* 76(5):837-844.
53. Collado-Vides, L., V.G. Caccia, J.N. Boyer and J.W. Fourqurean. 2007. Distribution and trends in macroalgal components of tropical seagrass communities in relation to water quality. *Estuarine Coastal and Shelf Science* 73:680-694
52. Murdoch, T.J.T. , A.F. Glasspool, M. Outerbridge, J. Ward, S. Manuel, J. Gray, A. Nash, K. A. Coates, J. Pitt, J.W. Fourqurean, P.A. Barnes, M. Vierros., K. Holzer, and S.R. Smith. 2007. Large-scale decline of offshore seagrass meadows in Bermuda. *Marine Ecology Progress Series* 339:123-130.

51. Peterson, B.J., C.M. Chester, F.J. Jochem and J.W. Fourqurean. 2006. Potential role of the sponge community in controlling phytoplankton blooms in Florida Bay. *Marine Ecology Progress Series* 328:93-103.
50. Orth, R.J., T.J.B. Carruthers, W.C. Dennison, C.M. Duarte, J.W. Fourqurean, K.L. Heck, Jr., R. Hughes, G. Kendrick, W.J. Kenworthy, S. Olyarnik, F.T. Short, M. Waycott and S.L. Williams. 2006. A global crisis for seagrass ecosystems. *BioScience* 56(12):987-996.
49. Armitage, A.R and J.W. Fourqurean. 2006. The short-term influence of herbivory near patch reefs varies between seagrass species. *Journal of Experimental Marine Biology and Ecology* 339:65-74;
48. Johnson, M.W., K.L. Heck, Jr., J.W. Fourqurean. 2006. Nutrient content of seagrasses and epiphytes in the northern Gulf of Mexico: evidence of phosphorus and nitrogen limitation. *Aquatic Botany* 85(2):103-111
47. Price, R.M., P.K. Swart and J.W. Fourqurean. 2006. Coastal groundwater discharge – an additional source of phosphorus for the oligotrophic wetlands of the Everglades. *Hydrobiologia* 569:23-36.
46. Gil, M., A.R. Armitage, and J.W. Fourqurean. 2006. Nutrients increase epifaunal abundance and shift species composition in a subtropical seagrass bed. *Hydrobiologia* 569:437-447;
45. Armitage, A.R., T.A. Frankovich and J.W. Fourqurean. 2006. Variable responses within epiphytic and benthic microalgal communities to nutrient enrichment. *Hydrobiologia* 569:423-435;
44. Carruthers, T.J.B., P.A.G. Barnes, G.E. Jacome and J.W. Fourqurean. 2005. Lagoon scale processes in a coastally influenced Caribbean system: implications for the seagrass *Thalassia testudinum*. *Caribbean Journal of Science* 41(3):441-455
43. Fourqurean, J.W. S.P. Escorcia, W.T. Anderson and J.C. Zieman. 2005. Spatial and seasonal variability in elemental content, $\delta^{13}\text{C}$ and $\delta^{15}\text{N}$ of *Thalassia testudinum* from south Florida. *Estuaries* 28(3):447-461
42. Armitage, A.R., Frankovich, T.A., Heck, K.L. Jr., Fourqurean, J.W. 2005. Complexity in the response of benthic primary producers within a seagrass community to nutrient enrichment. *Estuaries* 28(3):422-434
41. Romero, L.M., T.J. Smith, III., and J.W. Fourqurean. 2005. Changes in mass and nutrient content of wood during decomposition in a South Florida mangrove forest. *Journal of Ecology* 93(3):618-631;
40. Collado-Vides, L., L.M. Rutten and J.W. Fourqurean. 2005. Spatiotemporal variation of the abundance of calcareous green macroalgae in the Florida Keys: A study of synchrony within a macroalgal functional-form group. *Journal of Phycology* 41(4):742-752

39. Borum, J., O. Pedersen, T. M. Greve, T. A. Frankovich, J. C. Zieman, J. W. Fourqurean and C. J. Madden. 2005. The potential role of plant oxygen and sulphide dynamics in die-off events of the tropical seagrass, *Thalassia testudinum*. *Journal of Ecology* 93(1):148-158;
38. Fourqurean, J. W. and L. M. Rutten*. 2004. The impact of Hurricane Georges on soft-bottom, backreef communities: site- and species-specific effects in south Florida seagrass beds. *Bulletin of Marine Science* 75(2):239-257.
37. Ferdie, M. and J.W. Fourqurean. 2004. Responses of seagrass communities to fertilization along a gradient of relative availability of nitrogen and phosphorus in a carbonate environment. *Limnology and Oceanography* 49(6):2082-2094.
36. Zieman, J.C., J.W. Fourqurean and T.A. Frankovich. 2004. Reply to B.E. Lapointe and P.J. Barile (2004). Comment on J.C. Zieman, J.W. Fourqurean and T.A. Frankovich, 1999. Seagrass die-off in Florida Bay: Long-term trends in abundance and growth of turtlegrass, *Thalassia testudinum*. *Estuaries* 27(1):165-172.
35. Fourqurean, J.W. and J.E. Schrlau. 2003. Changes in nutrient content and stable isotope ratios of C and N during decomposition of seagrasses and mangrove leaves along a nutrient availability gradient in Florida Bay. *Chemistry and Ecology* 19(5):373-390.
34. Fourqurean, J.W., N. Marbà and C.M. Duarte. 2003. Elucidating seagrass population dynamics: theory, constraints and practice. *Limnology and Oceanography* 48(5):2070-2074.
33. Fourqurean, J.W., J.N. Boyer, M.J. Durako, L.N. Hefty, and B.J. Peterson. 2003. Forecasting the response of seagrass distribution to changing water quality: statistical models from monitoring data. *Ecological Applications* 13(2): 474–489.
32. Anderson, W.T. and J.W. Fourqurean. 2003. Intra- and interannual variability in seagrass carbon and nitrogen stable isotopes from south Florida, a preliminary study. *Organic Geochemistry* 34(2):185-194.
31. Peterson, B.J., C. D. Rose, L.M. Rutten and J.W. Fourqurean. 2002. Disturbance and recovery following catastrophic grazing: studies of a successional chronosequence in a seagrass bed. *Oikos* 97:361-370.
30. Fourqurean, J. W. and J. C. Zieman. 2002. Nutrient content of the seagrass *Thalassia testudinum* reveals regional patterns of relative availability of nitrogen and phosphorus in the Florida Keys USA. *Biogeochemistry* 61:229-245.
29. Fourqurean, J.W. and Y. Cai. 2001. Arsenic and phosphorus in seagrass leaves from the Gulf of Mexico. *Aquatic Botany* 71:247-258.
28. Peterson, B.J. and J.W. Fourqurean. 2001. Large-scale patterns in seagrass (*Thalassia testudinum*) demographics in south Florida. *Limnology and Oceanography* 46(5):1077-1090.

27. Chambers, R.M., J. W. Fourqurean, S.A. Macko and R. Hoppenot. 2001. Biogeochemical effects of iron availability on primary producers in a shallow marine carbonate environment. *Limnology and Oceanography* 46(6):1278-1286.
26. Fourqurean, J.W., A. Willsie, C.D. Rose* and L.M. Rutten*. 2001. Spatial and temporal pattern in seagrass community composition and productivity in south Florida. *Marine Biology* 138:341-354.
25. Davis, B.C. and J.W. Fourqurean. 2001. Competition between the tropical alga, *Halimeda incrassata*, and the seagrass, *Thalassia testudinum*. *Aquatic Botany* 71(3):217-232.
24. Cai, Y., M. Georgiadis and J.W. Fourqurean. 2000. Determination of arsenic in seagrass using inductively coupled plasma mass spectrometry. *Spectrochimica Acta, Part B: Atomic Spectroscopy* 55:1411-1422.
23. Nuttle, W.K., J.W. Fourqurean, B.J. Cosby, J.C. Zieman, and M.B. Robblee. 2000. Influence of net freshwater supply on salinity in Florida Bay. *Water Resources Research* 36(7):1805-1822.
22. Fourqurean, J.W. and M. B. Robblee. 1999. Florida Bay: a history of recent ecological changes. *Estuaries* 22(2B):345-357.
21. Corbett, D. R., J. Chanton, W. Burnett, K. Dillon, C. Rutkowski and J.W. Fourqurean. 1999. Patterns of groundwater discharge into Florida Bay. *Limnology and Oceanography* 44(4):1045-1055.
20. Rose, C.D., W.C. Sharp, W.J. Kenworthy, J.H. Hunt, W.G. Lyons, E.J. Prager, J.F. Valentine, M.O. Hall, P. Whitfield, and J.W. Fourqurean. 1999. Sea urchin overgrazing of a large seagrass bed in outer Florida Bay. *Marine Ecology Progress Series* 190:211-222.
19. Zieman, J.C., J.W. Fourqurean and T.A. Frankovich. 1999. Seagrass dieoff in Florida Bay: long term trends in abundance and productivity of turtlegrass, *Thalassia testudinum*. *Estuaries* 22(2B):460-470.
18. Boyer, J.N., J.W. Fourqurean and R.D. Jones. 1999. Temporal trends in water chemistry of Florida Bay (1989-1997). *Estuaries* 22(2B):417-430.
17. Hall, M.O., M.D. Durako, J.W. Fourqurean and J.C. Zieman. 1999. Decadal scale changes in seagrass distribution and abundance in Florida Bay. *Estuaries* 22(2B):445-459.
16. Frankovich, T.A. and J.W. Fourqurean. 1997. Seagrass epiphyte loads along a nutrient availability gradient, Florida Bay, FL, USA. *Marine Ecology - Progress Series* 159:37-50.
15. Fourqurean, J.W., T.O. Moore, B. Fry, and J.T. Hollibaugh. 1997. Spatial and temporal variation in C:N:P ratios, $\delta^{15}\text{N}$, and $\delta^{13}\text{C}$ of eelgrass (*Zostera marina* L.) as indicators of ecosystem processes, Tomales Bay, CA, USA. *Marine Ecology - Progress Series* 157:147-157.

14. Boyer, J.N., J.W. Fourqurean, and R.D. Jones. 1997. Spatial trends in water chemistry of Florida Bay and Whitewater Bay: Zones of similar influence. *Estuaries* 20(4):743-758
13. Fourqurean, J.W., K.L. Webb, J.T. Hollibaugh and S.V. Smith. 1997. Contributions of the plankton community to ecosystem respiration, Tomales Bay, California. *Estuarine, Coastal and Shelf Science*. 44:493-505.
12. Chambers, R.M., J.W. Fourqurean, J.T. Hollibaugh and S.M. Vink. 1995. Importance of terrestrially-derived, particulate phosphorus to P dynamics in a west coast estuary. *Estuaries*. 18(3):518-526.
11. Fourqurean, J.W., G.V.N. Powell, W.J. Kenworthy and J.C. Zieman. 1995. The effects of long-term manipulation of nutrient supply on competition between the seagrasses *Thalassia testudinum* and *Halodule wrightii* in Florida Bay. *Oikos* 72:349-358.
10. Zieman, J.C., R. Davis, J.W. Fourqurean and M.B. Robblee. 1994. The role of climate in the Florida Bay seagrass dieoff. *Bulletin of Marine Science* 54(3):1088.
9. Fourqurean, J.W., R.D. Jones and J.C. Zieman. 1993. Processes influencing water column nutrient characteristics and phosphorus limitation of phytoplankton biomass in Florida Bay, FL, USA: Inferences from spatial distributions. *Estuarine, Coastal and Shelf Science*. 36:295-314.
8. Fourqurean, J.W., J.C. Zieman and G.V.N. Powell. 1992. Relationships between porewater nutrients and seagrasses in a subtropical carbonate environment. *Marine Biology* 114:57-65.
7. Fourqurean, J.W., J.C. Zieman and G.V.N. Powell. 1992. Phosphorus limitation of primary production in Florida Bay: evidence from the C:N:P ratios of the dominant seagrass *Thalassia testudinum*. *Limnology and Oceanography* 37(1):162-171
6. Chambers, R.M. and J.W. Fourqurean. 1991. Alternative criteria for assessing nutrient limitation of a wetland macrophyte (*Peltandra virginica* (L.) Kunth. *Aquatic Botany* 40:305-320.
5. Fourqurean, J.W. and J.C. Zieman. 1991. Photosynthesis, respiration and the whole plant carbon budget of the seagrass *Thalassia testudinum*. *Marine Ecology - Progress Series* 69(1-2):161-170.
4. Powell, G.V.N, J.W. Fourqurean, W.J. Kenworthy and J.C. Zieman. 1991. Bird colonies cause seagrass enrichment in a subtropical estuary: observational and experimental evidence. *Estuarine, Coastal and Shelf Science* 32(6):567-579.
3. Robblee, M.B., T.R. Barber, P.R. Carlson, M.J. Durako, J.W. Fourqurean, L.K. Muehlstein, D. Porter, L.A. Yarbro, R.T. Zieman and J.C. Zieman. 1991. Mass mortality of the tropical seagrass *Thalassia testudinum* in Florida Bay (USA). *Marine Ecology - Progress Series* 71:297-299.

2. Powell, G.V.N., W.J. Kenworthy and J.W. Fourqurean. 1989. Experimental evidence for nutrient limitation of seagrass growth in a tropical estuary with restricted circulation. *Bulletin of Marine Science* 44(1):324-340.
1. Zieman, J.C., J.W. Fourqurean and R.L. Iverson. 1989. Distribution, abundance and productivity of seagrasses and macroalgae in Florida Bay. *Bulletin of Marine Science* 44(1):292-311.

Book Chapters

13. Troxler, T., G. Starr, J.N. Boyer, J.D. Fuentes, R. Jaffe, S.L. Malone, J.G. Barr, S.E. Davis, L. Collado-Vides, J.L. Breithaupt, A.K. Saha, R.M. Chambers, C.J. Madden, J.M. Smoak, J.W. Fourqurean, G. Koch, J. Kominoski, L.J. Scinto, S. Oberbauer, V.H. Rivera-Monroy, E. Castañeda-Moya, N.O. Schulte, S.P. Charles, J.H. Richards, D.T. Rudnick, K.R.T. Whelan. (In Press). Chapter 6: Carbon Cycles in the Florida Coastal Everglades Social-Ecological System across scales. In Childers, D.L., E.E. Gaiser, L.A. Ogden (eds.) *The Coastal Everglades: The Dynamics of Social-Ecological Transformation in the South Florida Landscape*. Oxford University Press.
12. Lirman, D., J.S. Ault, J.W. Fourqurean and J.J. Lorenz. In Press. The Coastal Marine Ecosystem of South Florida, United States. In: Sheppard, C. (ed) *World Seas: An Environmental Evaluation*. Elsevier Press
11. Schile, L., J.B. Kauffman, S. Crooks, J. Fourqurean, J. Campbell, B. Dougherty, J. Glavan and J.P. Megonigal. In Press. Carbon Sequestration in Arid Blue Carbon Ecosystems – a case study from the United Arab Emirates. In: Windham-Myers, L., Crooks, S. and T. Troxler (eds.) *A Blue Carbon Primer: The state of coastal wetlands carbon science, practice and policy*. CRC Press
10. Lovelock, C.E., D. A. Friess, J. B. Kauffman and J.W. Fourqurean. In Press. Human impacts on blue carbon ecosystems. In: Windham-Myers, L., Crooks, S. and T. Troxler (eds.) *A Blue Carbon Primer: The state of coastal wetlands carbon science, practice and policy*. CRC Press
9. Kennedy, H., J.W. Fourqurean and S. Papadimitriou. In press. The CaCO₃ Cycle in Seagrass Meadows. In: Windham-Myers, L., Crooks, S. and T. Troxler (eds.) *A Blue Carbon Primer: The state of coastal wetlands carbon science, practice and policy*. CRC Press
8. Nowicki, R.J., J.W. Fourqurean and M.R. Heithaus. In press. The role of consumers in structuring seagrass communities: direct and indirect mechanisms. In: Larkum, A.W.D. and G. Kendrick (eds) *Biology of Seagrasses: an Australian perspective*.
7. Fourqurean, J.W., B. Johnson, J.B. Kauffman, H. Kennedy, C. Lovelock, N. Saintilan, D.M. Alongi, M. Cifuentes, M. Copertino, S. Crooks, C. Duarte, M. Fortes, J. Howard, A. Hutahaean, J. Kairo, N. Marbà, J. Morris, D. Murdiyarsa, E. Pidgeon, P. Ralph, O. Serrano. 2014. Field Sampling of Vegetative Carbon Pools in

- Coastal Ecosystems. Pp. 67-108 in Howard, J., S. Hoyt, K. Isensee, E. Pidgeon and M. Telszewski, eds. Coastal Blue Carbon: methods for assessing carbon stocks and emissions factors in mangroves, tidal salt marshes, and seagrass meadows. Conservation International, Intergovernmental Oceanographic Commission of UNESCO, International Union for Conservation of Nature. Arlington, Virginia, USA. 181 pp.
6. Fourqurean, J.W., B. Johnson, J.B. Kauffman, H. Kennedy, C. Lovelock, D.M. Alongi, M. Cifuentes, M. Copertino, S. Crooks, C. Duarte, M. Fortes, J. Howard, A. Hutahaean, J. Kairo, N. Marbà, J. Morris, D. Murdiyarso, E. Pidgeon, P. Ralph, N. Saintilan, O. Serrano. 2014. Field Sampling of Soil Carbon Pools in Coastal Ecosystems. Pp. 39-66 in Howard, J., S. Hoyt, K. Isensee, E. Pidgeon and M. Telszewski, eds. Coastal Blue Carbon: methods for assessing carbon stocks and emissions factors in mangroves, tidal salt marshes, and seagrass meadows. Conservation International, Intergovernmental Oceanographic Commission of UNESCO, International Union for Conservation of Nature. Arlington, Virginia, USA. 181 pp.
 5. Fourqurean, J.W., B. Johnson, J.B. Kauffman, H. Kennedy, I. Emmer, J. Howard, E. Pidgeon, O. Serrano. 2014. Conceptualizing the Project and Developing a Field Measurement Plan. Pp 25-38 in Howard, J., S. Hoyt, K. Isensee, E. Pidgeon and M. Telszewski, eds. Coastal Blue Carbon: methods for assessing carbon stocks and emissions factors in mangroves, tidal salt marshes, and seagrass meadows. Conservation International, Intergovernmental Oceanographic Commission of UNESCO, International Union for Conservation of Nature. Arlington, Virginia, USA. 181 pp.
 4. Coates, K.A., J.W. Fourqurean, W.J. Kenworthy, A. Logan, S.A. Manuel and S.R. Smith. 2013. Introduction to Bermuda geology, oceanography and climate. Pp 115-133 In: Sheppard, C. (Ed) Coral Reefs of the World – Volume 4: Coral Reefs of the UK overseas territories. Springer, Dordrecht. 336pp. ISBN: 978-94-007-5964-0
 3. Duarte, C.M., J.W. Fourqurean, D. Krause-Jensen and B. Olesen. 2005. Dynamics of seagrass stability and change. Pp. 271-294 In Larkum, A.W.D., Orth, R.J., and C.M. Duarte. Seagrasses: Biology, ecology and conservation. Springer. DOI: 10.1007/978-1-4020-2983-7_11
 2. Fourqurean, J.W. and L.M. Ruttén*. 2003. Competing goals of spatial and temporal resolution: monitoring seagrass communities on a regional scale. Pp 257-288 in: Busch, D. E. and J.C. Trexler, eds. Monitoring ecosystems: interdisciplinary approaches for evaluating ecoregional initiatives. Island Press, Washington, D. C. 447 pp.
 1. Fourqurean, J.W., M.D. Durako, M.O. Hall and L.N. Hefty. 2002. Seagrass distribution in south Florida: a multi-agency coordinated monitoring program. Pp

497-522 in: Porter, J.W. and K.G. Porter, eds. The Everglades, Florida Bay, and the coral reefs of the Florida Keys. CRC Press LLC, Boca Raton. 1000pp.

Technical Reports

- Howard, J., Hoyt, S., Isensee, K., Telszewski, M., Pidgeon, E. (eds.) (2014). Coastal Blue Carbon: Methods for assessing carbon stocks and emissions factors in mangroves, tidal salt marshes, and seagrasses. Conservation International, Intergovernmental Oceanographic Commission of UNESCO, International Union for Conservation of Nature. Arlington, Virginia, USA. 180pp. JWF - Lead Author
- Harlem, P. W., J. N. Boyer, H. O. Briceño, J. W. Fourqurean, P. R. Gardinali, R. Jaffé, J. F. Meeder and M. S. Ross. 2012. Assessment of natural resource conditions in and adjacent to Biscayne National Park. Natural Resource Report NPS/BISC/NRR—2012/598. National Park Service, Fort Collins, Colorado.
- Fourqurean, J. W. 2012. The south Florida marine ecosystem contains the largest documented seagrass bed on the planet. pp. 263-264 in Kruczinsky, W. L. and P. J. Fletcher. Tropical Connections: South Florida's marine environment. IAN Press, Cambridge MD. 451 pp.
- Fourqurean, J. W. 2012. Seagrasses are very productive. pp. 265-266 in Kruczinsky, W. L. and P. J. Fletcher. Tropical Connections: South Florida's marine environment. IAN Press, Cambridge MD. 451 pp.
- Fourqurean, J. W. 2012. Seagrasses are sentinels of water quality. pp. 274-276 in Kruczinsky, W. L. and P. J. Fletcher. Tropical Connections: South Florida's marine environment. IAN Press, Cambridge MD. 451 pp.
- Fourqurean, J. W. 2012. As nutrients change, so do plant species. pp. 277-279 in Kruczinsky, W. L. and P. J. Fletcher. Tropical Connections: South Florida's marine environment. IAN Press, Cambridge MD. 451 pp.
- Kruczynski, W.L., M.B. Robblee and J.W. Fourqurean. 2012. The ecological character of Florida Bay responds to both changing climate and man's activities. pp. 120-122 in Kruczinsky, W. L. and P. J. Fletcher. Tropical Connections: South Florida's marine environment. IAN Press, Cambridge MD. 451 pp.
- Kenworthy, J., S. Manuel, J. Fourqurean, K. Coates and M. Outerbridge. 2011. Bermuda Triangle: Seagrass, green turtles and conservation. Seagrass Watch Magazine 44:16-18
- Kershaw, M., J. Fourqurean and C.M. Duarte. 2007. Bibliometric data show *Estuaries and Coasts* is a great venue for publishing your research. Estuarine Research Federation Newsletter 33(1):6-7.
- Bricker, S., G. Matlock, J. Snider, A. Mason, M. Alber, W. Boynton, D. Brock, G. Brush, D. Chestnut, U. Claussen, W. Dennison, E. Dettmann, D. Dunn, J. Ferreira, D. Flemer, P. Fong, J. Fourqurean, J. Hameedi, D. Hernandez, D. Hoover, D. Johnston, S. Jones, K. Kamer, R. Kelty, D. Keeley, R. Langan, J. Latimer, D.

- Lipton, R. Magnien, T. Malone, G. Morrison, J. Newton, J. Pennock, N. Rabalais, D. Scheurer, J. Sharp, D. Smith, S. Smith, P. Tester, R. Thom, D. Trueblood, R. Van Dolah. 2004. National Estuarine Eutrophication Assessment Update: Workshop summary and recommendations for development of a long-term monitoring and assessment program. Proceedings of a workshop September 4-5 2002, Patuxent Wildlife Research Refuge, Laurel, Maryland. National Oceanic and Atmospheric Administration, National Ocean Service, National Centers for Coastal Ocean Science. Silver Spring, MD. 19 pp. Available at: <http://www.eutro.org/publications.aspx>
- Fourqurean, J. W. 2002. Seagrass ecology (Marten A. Hemminga and Carlos M. Duarte). *Limnology and Oceanography* 47(2):611. [Book Review]
- Durako, M.J., J.W. Fourqurean and 9 others. 1994. Seagrass die-off in Florida Bay. In: Douglas, J. (ed.) Proceedings of the Gulf of Mexico Symposium. U.S.E.P.A., Tarpon Springs, FL. pp. 14-15.
- Fourqurean, J.W. 1992. The roles of resource availability and competition in structuring seagrass communities of Florida Bay. Ph.D. Dissertation, Department of Environmental Sciences, University of Virginia. 280 pp.
- Fourqurean, J.W. and J.C. Zieman. 1991. Photosynthesis, respiration and whole plant carbon budgets of *Thalassia testudinum*, *Halodule wrightii* and *Syringodium filiforme*. pp 59-70 in Kenworthy, W.J. and D.E. Haurert (eds.). The light requirements of seagrasses: proceedings of a workshop to examine the capability of water quality criteria, standards and monitoring programs to protect seagrasses. NOAA Technical Memorandum NMFS-SEFC-287.
- Continental Shelf Associates. 1991. A comparison of marine productivity among outer continental shelf planning areas. Supplement - An evaluation of benthic habitat primary productivity. Final Report, U.S. Department of the Interior, Minerals Management Service OCS Study MMM 91-0001, Contract #14-35-0001-30487, Herndon, VA. 244 pp + appendix.
- Fourqurean, J.W. 1987. Photosynthetic response to temperature and salinity variation in three subtropical seagrasses. MS Thesis, Department of Environmental Sciences, University of Virginia. 80 pp.
- Zieman, J.C. and J.W. Fourqurean. 1985. The distribution and abundance of benthic vegetation in Florida Bay, Florida. Final report, USNPS South Florida Research Center, Everglades National Park. Contract CX5280-2-2204.